

**MASARYK UNIVERSITY
FACULTY OF SCIENCE**

Ph.D. Dissertation

BRNO 2014

MAREK SKARKA



MASARYK UNIVERSITY
FACULTY OF SCIENCE

DEPARTMENT OF THEORETICAL PHYSICS AND ASTROPHYSICS



Characteristics of RR Lyrae type stars

Ph.D. Dissertation

Marek Skarka

Supervisor: Doc. RNDr. Miloslav Zejda, Ph.D. Brno 2014

Bibliographic Entry

Author: Marek Skarka
Faculty of Science, Masaryk University
Department of Theoretical Physics and Astrophysics

Title of Thesis: Characteristics of RR Lyrae type stars

Degree Programme: Physics

Field of Study: Theoretical Physics and Astrophysics

Supervisor: Doc. RNDr. Miloslav Zejda, Ph.D.
Faculty of Science, Masaryk University
Department of Theoretical Physics and Astrophysics

Academic Year: 2014/2015

Number of Pages: 18 + 120

Keywords: RR Lyr, TV Boo, Blažko effect, photometry, Hertzsprung-Russel diagram, ASAS, SuperWASP

Bibliografický záznam

Autor: Marek Skarka
Přírodovědecká fakulta, Masarykova univerzita
Ústav teoretické fyziky a astrofyziky

Název práce: Charakteristiky pulsujících hvězd typu RR Lyrae

Studijní program: Fyzika

Studijní obor: Teoretická fyzika a astrofyzika

Vedoucí práce: Doc. RNDr. Miloslav Zejda, Ph.D.
Přírodovědecká fakulta, Masarykova univerzita
Ústav teoretické fyziky a astrofyziky

Akademický rok: 2014/2015

Počet stran: 18 + 120

Klíčová slova: RR Lyr, TV Boo, Blažkův jev, fotometrie, Hertzsprungův-Russelův diagram, ASAS, SuperWASP

Abstract

In this thesis I focus on the Blažko effect in RR Lyrae type stars and on its manifestations. A large part of this work is devoted to the examination of differences between modulated and ordinary RR Lyrae stars of the ab type. After two introductory chapters results of studies of RRab stars are presented.

After three years of observing the RRc star TV Boo at Masaryk University Observatory in Brno, it was found that this star has a higher metallicity than previously thought and that it could show long term light curve changes similar to the four-year cycle of RR Lyrae itself. Analysis of high density SuperWASP data revealed that TV Boo undergoes parallel modulation with two components with periods of 9.737 d and 21.4 d. At the time of publication it was the first such known object.

Due to a lack of precise multicolour observations of RR Lyrae type stars, a new project, called the *Czech RR Lyrae stars observation project*, was founded in a collaboration with amateur astronomers. The main goal is to obtain precise observations in BVR_cI_c passbands for many tens of stars, create an atlas of RR Lyrae stars' light curves, revise their ephemerides, and determine light curve parameters. These data would also be useful in statistical studies. The first results comprising the discovery of the Blažko effect in three stars are presented.

For the facilitation of the work on RR Lyrae stars with the Blažko effect an on-line, regularly updated BlaSGalF database was created. In its first hard-copy version from the end of 2012, the list contained 242 stars that show modulation. Currently, almost 340 stars are given in this database. From the analysis of the data in this list it is evident that the vast majority of modulated RR Lyrae stars are of the RRab type, and that modulation periods of RRab and RRc stars depend differently on the basic pulsation period. In addition, BlaSGalF contains 32 stars which show parallel multiple modulation, and six objects with changing Blažko effect.

However, the most important parts of the thesis are devoted to the analysis of data for bright RRab Lyrae stars from the ASAS and SuperWASP surveys. Almost six hundred light curves were individually scanned, and after rejection of badly sampled or highly scattered light curves, they were carefully cleaned and analysed to properly identify possible modulation. This was done for 321 stars. It was found that the incidence rate of modulated stars in our sample is at least 31 % and that 12 % of them show parallel modulation. This is a surprisingly high percentage. In addition the majority of these multiple modulated targets show small integer ratio modulation periods. It was also shown that statistics based on the appearance of frequency spectra could be very misleading.

Once the modulation was properly identified, it was possible to compare light curve parameters and physical characteristics determined on the basis of Fourier coefficients for modulated and ordinary stars. After an additional rejection of stars in which modulation was not detected with certainty, the sample contained 268 stars. Light curve parameters from the SuperWASP survey were transformed to those from the ASAS using new calibrations. In addition, stars from the Galactic bulge, LMC, SMC and globular clusters were also used to extend our very limited sample. The comparison of Blažko and regular stars yielded many interesting results. We confirmed the previously known fact that modulated stars have smaller total amplitudes and longer rise times. It was

found that rise time could serve as a proper indicator of modulation, because over $RT = 0.24$ almost no regular star is observed.

We constructed several diagrams showing correlations between various light curve parameters. For example, in the plot where Fourier coefficient R_{31} is plotted against R_{21} stars show a strong metallicity correlation. When Fourier phases ϕ_{21} and ϕ_{31} of field and globular cluster stars were compared with the parameters of stars in the LMC, SMC and Galactic bulge, it was found that they differ. Except that this means that empirical relations are limited to galactic stars only, this could also point to different physical parameters of stars in LMC, SMC and Galactic bulge.

Although we observed a slight preference of Blažko stars for shorter periods and lower metallicity, no conclusive result was obtained regarding this question. Blažko stars were found to be slightly less (about 0.03 mag) faint than ordinary stars. Although similar behaviour was observed in M5, this finding also needs independent confirmation. No colour dependence of modulated stars was noticed in our analysis. Nevertheless, when T_{ef} was plotted versus extinction free index $(B - V)_0$, an interesting split appeared. Short-period stars with high metallicity were found to have about 180 K higher temperature than their low metallicity counterparts. This split was also observed in the $(B - V)_0$ vs. pulsation period diagram.

Abstrakt

V této práci se zabývám Blažkovým jevem a jeho projevy u hvězd typu RR Lyrae. Valná část práce je věnována studiu odlišností mezi hvězdami typu RRab se stabilními křivkami a hvězdami modulovanými. Za dvěma úvodními kapitolami následují kapitoly prezentující výsledky mé práce.

Na základě fotometrických dat napozorovaných během tří let na observatoři Přírodovědecké fakulty Masarykovy univerzity v Brně bylo zjištěno, že hvězda TV Boo (typ RRc) má značně vyšší metalicitu, než se dříve uvádělo a že pravděpodobně vykazuje dlouhodobé změny světelné křivky, které se podobají čtyřletému cyklu u samotné hvězdy RR Lyrae. Dále byla analyzována data pro TV Boo z přehlídky SuperWASP, která odhalila paralelní modulaci světelné křivky s dvěma komponentami s periodami 9.373 d a 21.5 d. V době publikace těchto výsledků byla TV Boo první známou hvězdou s takovýmto chováním.

Protože je obecně nedostatek kvalitních fotometrických dat v různých fotometrických barvách, byl založen projekt *Czech RR Lyrae observational project*, který funguje ve spolupráci s amatérskými astronomy. Hlavním cílem této přehlídky je získat kvalitní pozorování ve filtrech BVR_cI_c pro mnoho desítek hvězd a vytvořit tak atlas světelných křivek. Tato data budou dále užitečná pro revizi světelných elementů, k určení parametrů křivek a pro různé statistické studie. Prvními výsledky projektu jsou objevy Blažkova jevu u tří hvězd.

Pro zjednodušení práce na hvězdách typu RR Lyrae s Blažkovým jevem byla vytvořena pravidelně aktualizovaná online databáze BLASGALF. Její první verze z konce roku 2012 obsahovala 242 hvězd s Blažkovým jevem. V současnosti je v ní uvedeno téměř 340 hvězd. Z analýzy dat v této databázi vyplývá, že Blažkův jev postihuje zejména hvězdy typu RRab, a že hvězdy typu RRab a RRc mají rozdílné chování modulačních period v závislosti na pulzační periodě. BLASGALF také obsahuje 32 hvězd, které vykazují známky vícenásobné modulace, a šest hvězd se změnou Blažkova jevu.

Nicméně, hlavní části práce jsou věnovány analýze dat pro jasné hvězdy typu RRab, které mají data dostupná v přehlídkách SuperWASP a ASAS. Bylo individuálně kontrolováno téměř 600 světelných křivek, ze kterých bylo, po vyřazení hvězd se špatně pokrytými či výrazně zašumělými křivkami, vybráno 321 hvězd, jejichž data byla pečlivě vyčištěna a dále analyzována tak, aby byly odhaleny případné projevy Blažkova jevu. Bylo zjištěno, že nejméně 31 % hvězd z tohoto vzorku je modulovaných a že 12 % ze všech těchto hvězd vykazuje vícenásobnou modulaci, což je překvapivě vysoké číslo. Navíc, většina hvězd s paralelním Blažkovým jevem měla poměr modulačních period v poměru malých celých čísel. Konečně bylo také ukázáno, že běžně užívané statistiky založené na vzledu frekvenčního spektra mohou být velmi zavádějící.

Ve chvíli, kdy byly identifikovány hvězdy s modulací, bylo možno srovnat parametry světelných křivek a fyzikální vlastnosti určené na základě Fourierových koeficientů stabilních hvězd a hvězd s Blažkovým jevem. Po dalším vyřazení několika hvězd, u kterých nebyla jistota, že jsou stabilní (modulované), obsahoval celkový soubor 268 hvězd. Parametry křivek z přehlídky SuperWASP byly transformovány na parametry z přehlídky ASAS s použitím nových převodních vztahů. Jako rozšíření našeho velmi malého souboru hvězd posloužila dostupná data pro několik tisíc hvězd z galaktické výdutě, Velkého a Malého Magelanova mračna a z kulových hvězdokup.

Bylo zjištěno mnoho zajímavých skutečností. Mimo jiné bylo potvrzeno, že modulované hvězdy mají menší celkové světelné změny a delší vzestup z minima do maxima. Dále bylo zjištěno, že tento parametr, tzv. rise time (RT), může sloužit jako dobrý ukazatel na modulaci, protože mezi hvězdami s $RT > 0.24$ se vyskytují téměř výhradně hvězdy s Blažkovým jevem.

Bylo zkonstruováno několik diagramů ukazujících závislosti mezi různými parametry světelných křivek. Například, pokud vyneseme poměr Fourierových amplitud R_{31} jako funkci R_{21} , je tato závislost silně korelována s metalicitou. Srovnáním Fourierových fází ϕ_{21} a ϕ_{31} hvězd galaktického pole a kulových hvězdokup s fázemi hvězd nacházejících se v galaktické výduti a Velkém a Malém Magellanově mračnu, jsme zjistili, že se liší. Kromě toho, že to znamená omezenou platnost známých empirických vztahů pouze pro hvězdy galaktického pole a kulových hvězdokup, také to může poukazovat na rozdílné fyzikální parametry pro hvězdy v těchto hvězdných systémech.

Ačkoli naše analýza naznačovala, že hvězdy s Blažkovým jevem mají lehce kratší periody a nižší metalicitu, přesvědčivý důkaz nebyl nalezen. Podobná situace panuje i v případě absolutních hvězdných velikostí ve filtru V - zjistili jsme, že modulované hvězdy jsou asi o 0.03 magnitudy slabší. Přesto, že něco podobného bylo pozorováno v kulové hvězdokupě M5, také tento fakt vyžaduje další nezávislé potvrzení. V rámci naší studie nebyla pozorována jakákoliv závislost hvězd s Blažkovým jevem na barvě (teplotě). Nicméně, po vynesení teploty T_{ef} v závislosti na nezčernalém barevném indexu $(B - V)_0$ jsme pozorovali zajímavé rozštěpení této závislosti. Krátkoperiodické hvězdy s vysokou metalicitou mají asi o 180 K vyšší teplotu, než ostatní hvězdy. Podobné rozštěpení se také objevuje v grafu, kde je vynesena index $(B - V)_0$ v závislosti na pulzační periodě.

Acknowledgements

I realize that this is probably the most difficult part of a thesis to write. There are many people to whom I am very grateful for their support during my PhD studies. Hopefully I will not forget to mention some.

Without a doubt the most important person during my studies was my scientific advisor Miloslav Zejda. He introduced the real scientific world to me, and opened the doors to many amazing places such as the observatory at Sutherland and La Silla. He was always willing to listen to me and to assist me whenever needed. He inspired, supported and motivated me during difficult times. Thank you Milos!

However, I am also grateful to my other teachers and colleagues. In particular I would like to thank my friends Lenka, Klárka, Petr and Jirka who provided comfort and contributed towards making my studies enjoyable. Especially Jirka deserves my special thanks. We grew closer in the last two years and experienced many fruitful discussions which resulted in close cooperation between us.

I would like to express my gratitude to Stephanus de Villiers for his help with language corrections, and for his patience with my English.

One person deserves special attention. It is my charming wife Helena. Without her I would not have been here writing these words. She has been my guardian angel since we met seven years ago. Thinking about my travels and stays abroad, and many tens of nights that I spent at MUO or the Observatory and Planetarium in Brno, I admire her and thank her for her tolerance and patience. Thank you my Sun.

Finally I thank my parents for supporting me in anything I liked, and my close friends and my mates from the band who were able to take my mind off the daily concerns. Thank you all!

This research made use of NASA's Astrophysics Data System Bibliographic Services. All work was financed by projects GD205/08/H005, GAP 209/12/0217, LG12001, and Masaryk University grants MUNI/A/0968/2009, MUNI/A/0735/2012 and MUNI/A/0773/2013.

Contents

Introduction	xvii
Chapter 1. A brief overview of RR Lyrae type stars	1
1.1 Historical remarks	1
1.2 Basic characteristics	2
1.2.1 Pulsational properties	2
1.2.2 Evolution of RR Lyrae type stars	6
1.3 Connection between light curve characteristics and physical parameters	11
1.3.1 Characteristics of RR Lyrae star light curves	11
1.3.2 Amplitudes, periods and metallicity - the Oosterhoff problem	14
1.3.3 Empirical relations	16
Chapter 2. The Blažko effect	21
2.1 An introduction of the Blažko effect	21
2.2 Mathematical description of Blažko modulation. Manifestation of the modulation in the frequency spectra	22
2.2.1 Amplitude modulation	24
2.2.2 Frequency modulation	27
2.2.3 Phase modulation	28
2.2.4 Combined modulation	29
2.3 Observed properties of Blažko stars	30
2.3.1 Frequency spectra of real Blažko stars	30
2.3.2 The length of the Blažko cycle	33
2.3.3 Amplitude of the modulation	35
2.4 Incidence rate of Blažko stars	36
2.5 The difference between Blažko and non-modulated stars	37
2.6 Explanation of the Blažko effect	39
Chapter 3. Observational efforts on RR Lyrae type stars	43
3.1 The first known double modulated RRc star TV Boo	43
3.1.1 Observation and data reduction	44
3.1.2 Frequency analysis	44
3.1.3 Physical parameters	51
3.2 The Czech observational project	52
3.2.1 Motivation and description of the project	52
3.2.2 A new Blažko star CN Cam	53

3.2.3	CzeV283 Aql, CzeV397 Her - two new Blažko stars	56
Chapter 4.	Characteristics of RRab stars from the ASAS and SuperWASP surveys . .	61
4.1	The BlaSGalF database	61
4.2	Study of the Blažko effect based on data from ASAS and SuperWASP surveys . . .	66
4.2.1	The surveys and data characteristics	66
4.2.2	Sample selection and data cleaning	67
4.2.3	Methods of searching for the Blažko effect	69
4.2.4	Blažko stars from ASAS	72
4.2.5	Blažko stars from SuperWASP	78
4.2.6	Statistics of the Blažko variables in the ASAS and SuperWASP sample	82
4.3	Characteristics of bright ab-type RR Lyrae stars from the ASAS and SuperWASP surveys	83
4.3.1	Data sets	83
4.3.2	Physical parameters determination	86
4.3.3	Light-curve properties of regular and modulated RRab stars	87
4.3.4	Discussion on physical parameters	95
	Summary and conclusions	103
	References	107
	List of publications	117
	List of abbreviations	120

Introduction

RR Lyrae stars constitute one of the most important classes of variable stars. It is not only due to their applications in stellar astrophysics (e.g. pulsation and evolution modelling), but also in other fields of astronomy. Since they are old, evolved stars in the helium-core-burning stadium, they are very useful in studying population II stars. Their light curves are very characteristic with relatively high amplitudes and therefore easily detectable and distinguishable from other types of variable stars. Since RR Lyraes occupy the instability region of the horizontal branch, they are relatively luminous with similar radiative output of all class members. All these characteristics, together with their relatively common occurrence, predestine RR Lyraes as a very efficient tool for distance determination, as well as for an estimation of galaxy evolution and mapping of the distribution and kinematics of population II stars. They can also serve as metallicity tracers of evolved stars.

During the last few decades, and mainly during the golden era of space missions and large sky surveys of the last few years, our knowledge of RR Lyrae type stars has increased significantly. Nevertheless, there are many problems that are still unresolved. One of these mysteries represents the often pronounced Blažko effect, which causes long term changes in the light-curve shape of a large fraction of RR Lyrae stars (up to 50 %), and which probably also occurs in Cepheids. While modulation of the light curve is a quite common phenomenon that also occurs in other pulsating variables such as e.g. δ Sct stars, the physics behind this modulation might be of a different nature than in RR Lyraes. Unresolved questions about the Blažko effect involve both those related to its nature and mechanism as well those about its incidence rate among RR Lyrae stars, or why some stars show modulation and others do not.

A variety of models were proposed to explain the Blažko behaviour, but almost all failed at least partially. Fortunately, recent discoveries (e.g. uncovering of period doubling, high-order resonances etc.) increase the chance for successful modelling of the Blažko effect in the near future. This thesis deals with the latter mentioned group of problems. It focuses on the discussion of the proportional representation of Blažko stars and on the comparison of Blažko and ordinary RR Lyraes based on photometric data. Although a few studies have been done that are mainly focused on the metallicity dependence of the Blažko effect, a comprehensive study has been missing.

The whole text of the thesis is divided into five main parts. The first chapter deals with RR Lyraes stars in general. Their historical background, basic physical and pulsation characteristics, sorting into subclasses and other related topics are briefly discussed in the first few sections. In the early eighties of the 20th century it was found that the shapes of light curves of Cepheids and RR Lyrae stars coincide with their physical properties and so-called Fourier coefficients were introduced to describe their light changes. These parameters were then connected with physical characteristics via empirical calibrations mainly in the nineties. Especially Hungarian astronomers excelled in this field. Using this simple method, scientists obtained a powerful instrument to get information about these stars via easily and widely accessible photometry. Since many such calibrations based on various light curve parameters were defined, we briefly discuss their application and choose some of them to be used later in chapter 4 of this thesis.

Chapter 2 is devoted to the Blažko effect itself. As its manifestations cover a wide range of periods and amplitudes, its basic attributes, mathematical description, as well as its demonstration in frequency spectra, are discussed in detail. We also comment on the incidence rate and characteristics of Blažko stars in various stellar systems, i.e. in our Galaxy, in globular clusters, in the LMC or in other nearby stellar systems. One part of this chapter is dedicated to a comparison of characteristics of ordinary and Blažko stars. We also briefly describe models explaining the one century old Blažko enigma.

The third chapter deals with original observational efforts on RR Lyrae stars. The detailed study of an RRc star, TV Boo, is presented in sec. 3.1. Based on SuperWASP data and three-years' observations at Masaryk University Observatory, TV Boo was found to be the first known example of a modulated RRc stars with parallel modulation with two components. The second modulation component significantly changes over time. It is shown that the photometric metallicity of TV Boo is probably much higher than previously thought. The remaining part of chapter 3 is devoted to the *Czech RR Lyrae observation project*, which was established in cooperation with amateur astronomers to obtain high quality photometry. The first results of this expanding project (e.g. discovery of a new Blažko star CN Cam) are described in detail.

To enhance and update the statistics for field Blažko stars, the database BLASGALF is introduced in the first part of chapter 4. This regularly updated, on-line database contains 338 RR Lyrae stars showing the Blažko effect (August 2014). The rest of this chapter is dedicated to analyses of bright field RRab Lyrae stars observed by the ASAS and SuperWASP surveys. These investigations originated from a sample of 321 stars with well defined light curves. An individual approach was applied to each light curve and its Fourier transform to properly identify the Blažko effect. In addition, this approach allowed us to avoid contamination of Blažko stars in the stable sample. We show that the incidence rate of Blažko stars is much higher than proposed in previous studies based on ASAS data. It is also shown that statistics based on frequency spectra examination of such data are highly unreliable. This study revealed several stars which show parallel modulation with the ratio of modulation periods in small integers.

The last part of chapter 4 deals with a comparison between Blažko and regularly changing stars based on photometric data from the mentioned surveys. Fourier parameters of SuperWASP light curves were calibrated to ASAS parameters to get a homogeneous sample. Subsequently empirical relations were used to get the physical characteristics of stars. Many diagrams describing interrelations between various combinations of Fourier parameters were constructed to see whether they differ for ordinary and modulated stars. In addition, light curve parameters and physical characteristics of field stars were complemented with data for stars in globular clusters, the LMC, SMC, and Galactic bulge.

The last part of this work summarises all results.

Chapter 1

A brief overview of RR Lyrae type stars

Together with technological progress, all human activities experienced an extraordinary boom in the twentieth century. Astronomy was no exception.

Although the pulsation behaviour of RR Lyraes has been a challenging topic in stellar pulsation theory, RR Lyrae research introduced them as a very powerful tool in various fields in astrophysics. Due to their relatively large and well defined luminosity they are used as distance indicators not only in our Milky Way Galaxy, but also in extragalactic scales. Their advanced stage of evolution makes them ideally suited for the analysis of old-population stars and allow astronomers to use them as metallicity tracers. They are also useful in investigation of the dynamical evolution of the Galaxy.

These very few, but most important examples, illustrate the importance of RR Lyrae stars in modern astronomy. Besides discussing their basic physical properties, light curve characteristics and empirical relations are briefly surveyed in this chapter.

1.1 Historical remarks

The first representatives of a very broad RR Lyrae type subclass, comprising about 44 thousands known members in our Galaxy (Watson et al., 2006) and more than 24 000 stars in the Large Magellanic Cloud (Soszyński et al., 2009), were discovered at the end of 19th century in globular clusters. Observations of these old stellar structures revealed an extraordinary number of new variable stars (Pickering & Bailey, 1895). Many of them were of previously unknown type showing similar periods and light curves. Due to their location, Bailey & Leland (1899) called them *Cluster variables*.

It did not take long before the first cluster-variable star was identified in the Galactic field¹ in the constellation Lyra by W. P. Fleming (Pickering, 1901). This 7-8-magnitude star acquired the designation RR Lyrae, and later, in 1948, it became the eponym of cluster variables at the meeting of Commission 27 of the International Astronomical Union held in Zurich.

Cluster variables were also often referred to as “short-period” cepheids because of the similarity of their light and radial-velocity curves. Besides considering RR Lyrae variables as extreme cases of cepheids, binary (“Antalgot” group) and other theories were considered as plausible explanations for their light changes at the beginning of the twentieth century (Kiess, 1912). Shapley (1916) summarized the then available knowledges about RR Lyr itself, and supported pulsation theory for its light changes rather than the binary explanation (Shapley, 1914). In addition, general properties like periods, spatial distribution, or appearance in globular clusters, indicated that RR Lyrae stars

¹Actually, the first known variable of this type, U Lep, was identified by Kapteyn (1890).

constitute a separate group of variables, which does not belong to cepheids. Currently pulsation theory (Eddington, 1926) is considered as a definite explanation for light changes of RR Lyrae stars.

Shapley (1916) in his work also reported about the period and light-curve-shape change of RR Lyr. However, he was not the first to notice such behaviour – S. N. Blažko (1907) found that the period of RW Dra could not be fitted with a constant value only a few years earlier. The phenomenon was thus named after this Russian astronomer, *The Blažko effect*. For a long time this still not-fully explained phenomenon was known to manifest in only several example stars. However, recently this behaviour has become very important, because it seems that up to 50 % of all RR Lyrae stars show some sort of modulation (e.g. Jurcsik et al., 2009).

1.2 Basic characteristics

Variables of RR Lyrae type are usually defined as radially pulsating stars of spectral types from A to F with periods from about 0.2 to one day. Light changes in V passband have usually amplitudes from several tenths of a magnitude up to more than one magnitude.

Table 1.1: Basic physical characteristics of RR Lyrae type stars according to Smith (1995).

Period	0.2-1.1 days
$\langle M_v \rangle$	$+0.6 \pm 0.2$ mag
$\langle T_{\text{eff}} \rangle$	7400 – 6100 K
$\langle \log g \rangle$	2.3 – 3
[Fe/H]	0.0 – –2.5
Mass	$\approx 0.7 M_{\odot}$
Radius	$\approx 4-6 R_{\odot}$

In tab. 1.1, which comes from a classical review by Smith (1995), rough values and limits of the basic physical characteristics are summarized. Some of these parameters will be discussed in detail later.

1.2.1 Pulsational properties

Basic principles of stellar pulsations

Stellar pulsation theory supposes that effects connected with changes in opacity are responsible for the pulsation of RR Lyrae type stars. According to pioneering work of Eddington (1926), there should exist some layer (Eddington's valve) with special properties inside the star, which drives pulsations.

Material in this region should be able to absorb energy during contraction, become opaque, and push up the above layers. Subsequently, during expansion, it should release trapped energy more quickly than the surrounding material. Problem was that 'normal' stellar gas behaves contrary to these assumptions.

Opacity κ of stellar material follows the Rosseland mean opacity relation

$$\kappa = \kappa_0 \rho^n T^{-s}, \quad (1.1)$$

where κ_0 is a constant, ρ is density, and T is temperature. For the gas in the stellar envelope where no important element is undergoing ionisation, subscript n is about 1, and s approximately equals 3.5. Therefore an increase in temperature leads to a decrease in opacity.

Fortunately, regions with partially ionized hydrogen and helium were identified to be efficiently able to drive stellar pulsations (Zhevakin, 1953; Baker & Kippenhahn, 1962; King & Cox, 1968). In pulsations of RR Lyrae variables and cepheids helium partial ionized zone plays a crucial role. The temperature in this region does not increase as quickly as in surrounding regions during contraction ($s < 3.5$), because energy is used to ionize the elements. As a result, the opacity of material in this zone increases with increasing temperature. Radiation pressure is then able to push the layer

upwards. During expansion recombination happens, the rate of temperature decrease in the layer is slower than in its surroundings, opacity decreases, the layer falls back, and the cycle repeats. Because this mechanism reflects changes in opacity, it was called the κ -mechanism.

Since the temperature in a partial ionization zone increases more slowly during contraction than in adjacent layers, the heat has a tendency to flow into this region. Because the ratio of specific heats C_P and C_V decreases, material in the driving zone is able to absorb more energy. This process, called the γ -mechanism, further reinforces the kappa mechanism (Cox et al., 1966).

Instability strip and basic pulsation period

The location of the partial ionization zone inside a star determines whether the star starts to pulsate or not. The helium partial ionization zone is found at temperatures about $3 - 6 \times 10^4$ K, which means that, depending on particular stellar parameters, it is located at various depths. When the zone is too deep (cool stars), it experiences high damping, and it has a too small amplitude for driving the pulsation. In addition, in cool stars convection influences and suppresses the pulsations. On the other hand, in hot stars, the zone is very close to the surface and has a too small mass to sufficiently drive pulsation. These limits define the boundaries of the so called *instability strip* (hereafter IS). In the Hertzsprung-Russel diagram (hereafter HRD, fig. 1.1) it propagates almost vertically from the regions of giant, luminous stars (cepheids) through the RR Lyrae region at the Horizontal Branch (hereafter HB) to the Main sequence, where δ Sct stars are located.

The exact boundaries of the IS of the HB are subject to discussion, because it depends on particular stellar parameters. However, rough limits can be approximately given as $3.75 < \log T_{\text{eff}} < 3.9$ (Lee & Demarque, 1990; Sandage, 1990). A different shape of the theoretical IS can be seen in fig. 1.2.

The basic pulsation period P of a star located in the IS roughly depends on its mean density ρ as

$$P\sqrt{\rho} = Q, \quad (1.2)$$

which was first introduced by Ritter (1879). In this relation Q is a ‘‘pulsation constant’’, which slowly varies with stellar properties, and with internal structure of the star. For the fundamental

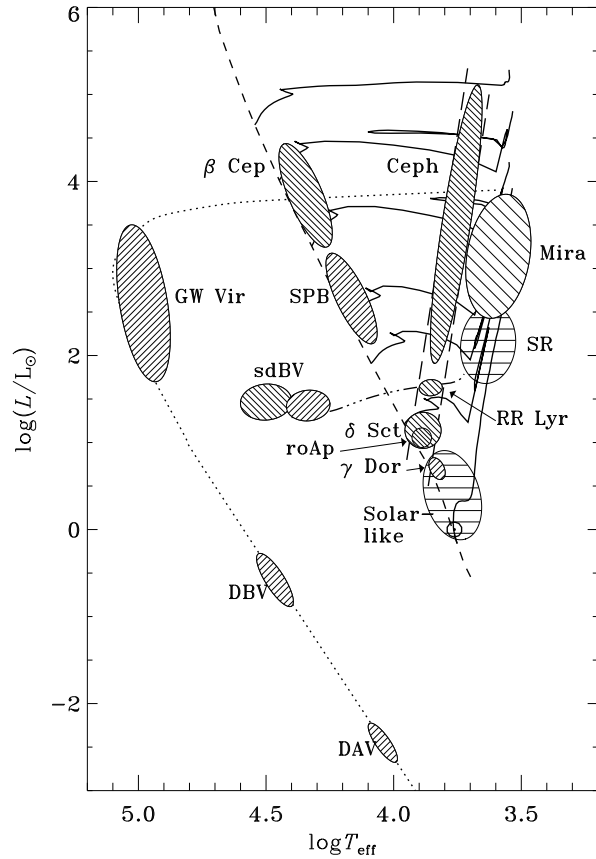


Figure 1.1: Hertzsprung-Russel diagram with basic types of pulsating stars (Metcalf et al., 2004).

mode of a homogeneous star with uniform density the value of Q is

$$Q = \frac{2\pi}{\sqrt{\frac{4}{3}\pi G(3\gamma - 4)}}, \quad (1.3)$$

where G is the gravitational constant and γ is the adiabatic exponent

$$\gamma = \left(\frac{d \ln p}{d \ln \rho} \right)_{\text{ad}}, \quad (1.4)$$

which is assumed to be constant throughout the star. When ρ is in solar units and P in days in eq. 1.2, for ideal gas ($\gamma = 5/3$) the pulsation constant is 0.116. For a more realistic distribution of density $Q \in (0.03, 0.06)$, for RR Lyrae stars Q is typically 0.04. Equations 1.2 and 1.3 are results of a simplified, but very illustrative one-zone linear model, when pulsations are assumed to be adiabatic. Nevertheless, relation 1.2 works very well.

RR Lyrae pulsation types

The location of the driving layer also determines in which mode the star will pulsate. RR Lyrae stars closer to the red edge of the IS pulsate in the fundamental radial mode. This means that all layers of the star move in the same direction, and that a pulsation node in the center of the star does not move. These stars are usually marked as RRab stars (Bailey, 1902). RR Lyraes closer to the blue edge of the IS pulsate in the first overtone mode (RRc). In this subclass of RR Lyraes, there is a nodal sphere in the interior of a star which does not undergo pulsation movements, except for the center. Therefore, RRab stars have longer periods and larger amplitudes than RRc Lyrae stars.

Labelling RR Lyrae stars as RRab and RRc comes from Bailey (1902), who categorized them on the basis of their light curve shape at the beginning of the twentieth century. The connection between the shape and the pulsation mode was recognized by Schwarzschild (1940), who linked the RRab type to fundamental radial pulsators (marked by Alcock et al. (2000) as RR0), and RRc to the first overtone radial pulsators (after Alcock et al. (2000) RR1).

There are also RR Lyraes which pulsate in the second overtone mode (designed as RRe or RR2). Stars which pulsate simultaneously in the fundamental and in the first overtone modes are marked as RRd or RR01. Recent observations showed that RR Lyrae stars can pulsate even in other combinations of radial modes (RR12, RR02, Olech & Moskalik, 2009; Moskalik et al., 2013). Especially in Blažko stars, signs of higher radial overtones were observed (Benkő et al., 2014). In fig. 1.2 there are regions where a particular subtype of the RR Lyrae class can lie. There are two special zones, so called “hysteresis zones”, where the star can pulsate in two ways depending on the direction of its evolution (see sec. 1.2.2).

The observational differences between basic subtypes of the RR Lyrae class should be apparent from fig. 1.3. RRab stars have strongly asymmetric light curves with a steep rise to maximum light and a slow decrease to minimum. RRc Lyraes, on the other hand, have an almost sinusoidal light curve shape, often with a double maximum. The first maximum, which is a consequence of a shock-wave generated by the κ -mechanism, usually have a lower amplitude, and it is called ‘hump’ (Gillet & Crowe, 1988). This behaviour is also observed to a lower extent in some RRab stars around phase 0.9, but it is not as pronounced as in RRc stars. In some RRab stars a ‘bump’ is also observed just before minimum light. In this case it would be the consequence of the collision of the upper atmospheric layers with deeper ones during the infall phase (Gillet & Crowe, 1988).

Since RRd stars pulsate simultaneously in the fundamental and in the first radial overtone, their light curves are influenced by the interaction between the pulsation modes. In the bottom panel of fig. 1.3 the light curve of an example RRd star is decomposed into pulsation modes.

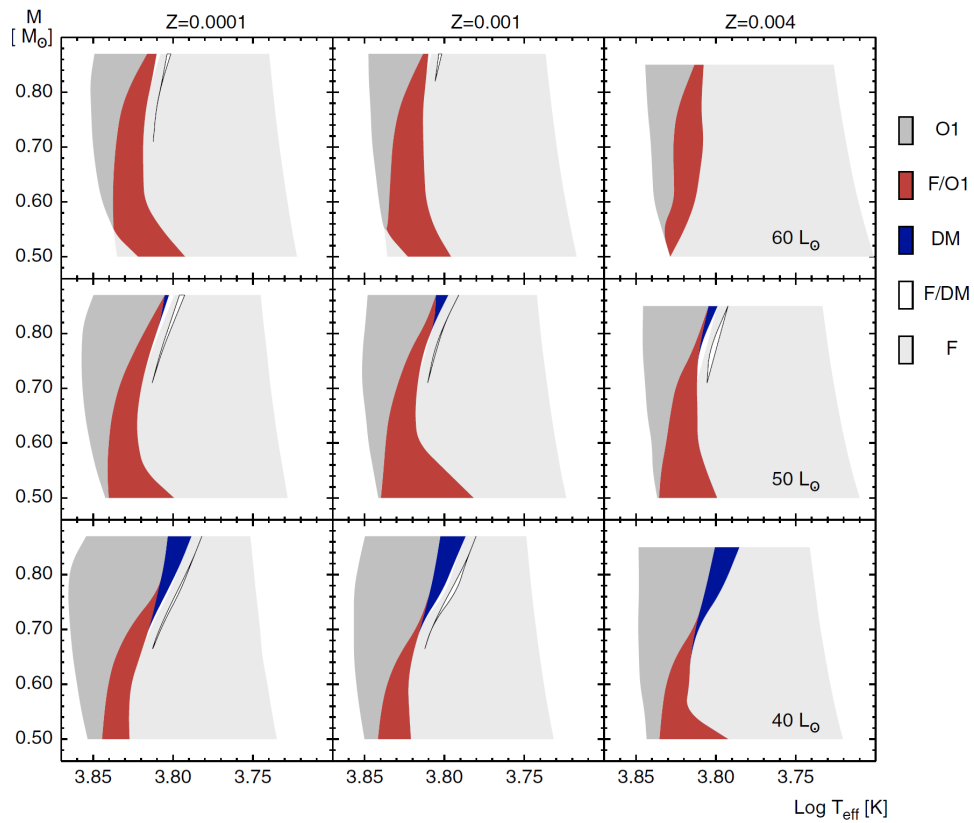


Figure 1.2: Theoretical IS and mode-selection maps for stars with different luminosity and metallicity (taken from Szabó et al., 2004). In this figure, F=RR0, O1=RR1, DM=RR01. For the sake of clarity, the F/DM (RR0/RR01) hysteresis zone is shifted 100 K to the right.

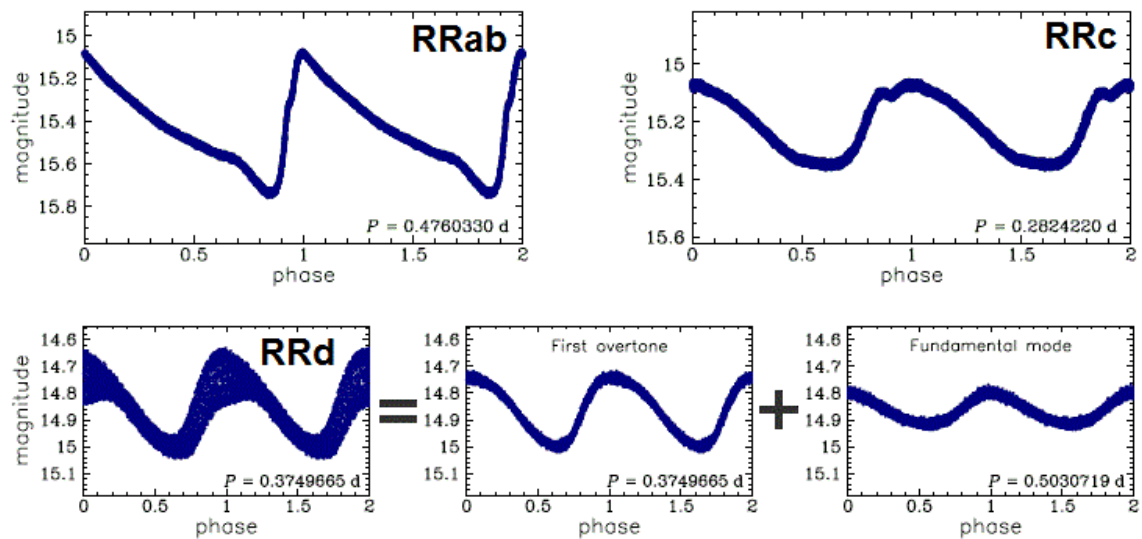


Figure 1.3: Basic Bailey’s types of RR Lyrae variables. Fundamental mode (RRab) stars are shown in the top left panel, RRc are in the top right panel. In the bottom panel the light curve of an RRd star, which is decomposed to the fundamental and the first overtone mode is shown. Figure is taken from http://ogle.astrouw.edu.pl/atlas/RR_Lyr.html.

Recently, based on ultra-precise photometric measurements, which were produced by space telescopes and large-scale surveys, it was discovered that higher radial modes and resonances between them can play an important role in RR Lyrae stars (see e.g. Benkő et al., 2010; Guggenberger et al., 2012; Moskalik, 2014). These resonances typically occur in RRc stars and in modulated RRab stars (Benkő et al., 2010; Moskalik et al., 2013). RR Lyrae variables also recently turned out to be possible non-radial pulsators (e.g. Olech et al., 1999; Chadid et al., 2010; Guggenberger et al., 2012; Buchler & Kolláth, 2011; Moskalik et al., 2013; Moskalik, 2014). This means that, in addition to radial modes described by pulsation number n ($n = 0$ for fundamental mode, $n = 1$ for the first overtone radial mode, etc.), there are nodal circles on the surface of a star, which are described by two pulsation numbers l (number of all circles), and $m \in \langle -l, 0, l \rangle$, which gives information about nodes going through the poles. Because nonradial modes have much lower amplitudes than radial ones, they were discovered only very recently.

1.2.2 Evolution of RR Lyrae type stars

As already mentioned, RR Lyraes occur where the IS crosses the HB in HRD. This location means that they are in the late stadium of their lives. Stellar evolution and pulsation theory predict their masses to be lower than the mass of the Sun. Therefore, they have to be products of stars with a similar or slightly lower main sequence mass than the mass of our Sun. Stars with significantly lower masses (under $0.8 M_{\odot}$) did not have enough time to evolve to this stadium, and more massive stars have higher luminosities at this life-phase than RR Lyrae variables. Of course, the evolution of a particular star depends on many factors, e.g. on chemical composition.

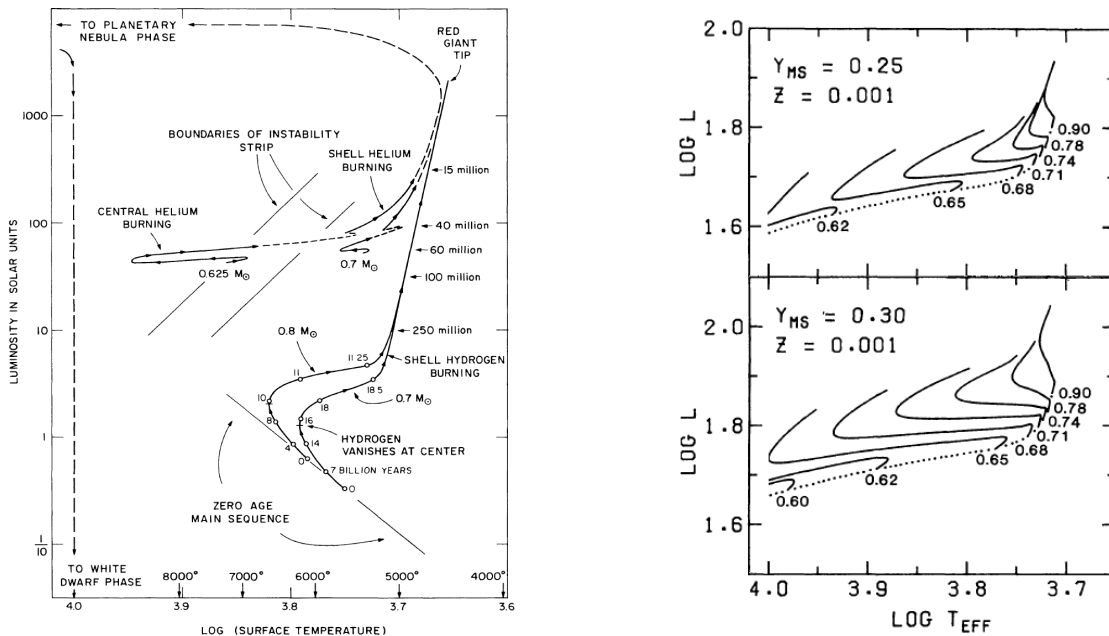


Figure 1.4: Theoretical evolutionary tracks for 0.7 and $0.8 M_{\odot}$ stars with $Z = 0.001$ and $Y = 0.3$ from Iben (1971) (left panel), and on the right panel an example of evolutionary tracks of HB stars with various masses for the same Z , but for $Y = 0.25$ (top right panel) and $Y = 0.3$ (bottom right panel) from Sweigart (1987).

On the left panel of fig. 1.4, theoretical evolutionary tracks are schematically displayed for low-metal stars with low masses according to Iben (1971). The iron-to-hydrogen content of the

shown stars is $Z = 0.001$, which, according to the relation from Cassisi et al. (2004)

$$[\text{Fe}/\text{H}] = \log Z - 1.7 \quad (1.5)$$

corresponds to metallicity $[\text{Fe}/\text{H}] \approx -1.3$. The helium abundance of the depicted RR Lyraes is $Y = 0.3$.

Stars leave the main sequence after exhaustion of hydrogen in their cores. Subsequently, as the helium core contracts and heats, the star increases its luminosity due to the fusion of hydrogen to helium in a shell surrounding the core. The star climbs to the red giant branch (RGB) in this phase. Since the temperature inside the core is insufficient for fusion of helium atoms to heavier elements, the helium core becomes electron degenerate.

As a product of hydrogen fusion, helium settles in the core, which becomes more massive, and its temperature increases to a certain point when the temperature is sufficiently high to initiate helium burning via the 3α process (in HRD red giant tip). The electron degeneracy is explosively removed at this moment in a so called helium flash, and the star proceeds to the *Zero-age horizontal branch* (hereafter ZAHB). At this point the mass distribution inside the star is highly unequal - a very tiny core of the size of 5 earth radii comprising about $0.5 M_{\odot}$ is surrounded by a very sparse envelope (see e.g. Christy, 1966). Stars spend about 10^8 years (Pietrinferni et al., 2004) at the HB, but the specific life-time depends on the mass of the star, and also on its chemical composition (lower metallicity means a shorter HB life, Cassisi et al., 2004).

Typical masses of HB stars are from about 0.5 to $0.8 M_{\odot}$. This means that stars have to lose some material before settling on the HB, mainly during their RGB phase. This loss can be about $0.2 M_{\odot}$ (Reimers, 1975). Pietrinferni et al. (2006) assumed in their evolutionary models that RR Lyrae progenitors are stars with RGB masses (which are roughly equal to main sequence masses) about $0.8 M_{\odot}$ for low-metal stars, and about $1.0 M_{\odot}$ for stars with higher metallicity. In the left panel of fig. 1.4, there are evolutionary tracks of ZAHB stars with masses 0.625 and $0.7 M_{\odot}$, while there are HB evolutionary tracks of stars with various masses shown on the right panel of this figure. If the star crosses the IS during its evolution on HB, it starts to pulsate as an RR Lyrae star. From fig. 1.4 it is seen that only HB stars with special characteristics become ZAHB RR Lyrae pulsators. It is also obvious that it takes about 19 Gyr for $0.7 M_{\odot}$ star to become an HB star. Therefore, we can currently observe only stars at the HB, which had mass higher than about $\sim 0.8 M_{\odot}$ at the main sequence.

At the HB stars gain their energy from helium burning in their cores and hydrogen burning in surrounding shell. After exhaustion of helium in their cores, stars begin to increase their luminosity climbing to the asymptotic giant branch (similarly to when hydrogen was depleted in the core after the main sequence evolution). No additional nuclear reactions occur in the core of a low-mass star, because of its insufficient mass. Therefore, after disposing an envelope, it ends its life as a white dwarf.

Structure of the IS - characteristics of RR Lyrae variables

In the previous section we saw that the position of a star on the HB depends on its total mass. Nevertheless, not only this parameter, but also the mass of the helium core, and metal and helium abundances are very important parameters.

The influence of various core-masses is demonstrated in the left panel of fig. 1.5, where theoretical evolutionary tracks of stars with $Y = 0.3$ and $Z = 10^{-3}$ are shown (Iben, 1971). Models with higher core masses have the ZAHB shifted to a higher luminosity.

The right panels of figures 1.4 and 1.5 show the consequences of different helium abundances illustrated on theoretical models from Sweigart (1987). Stars with the same total mass are cooler

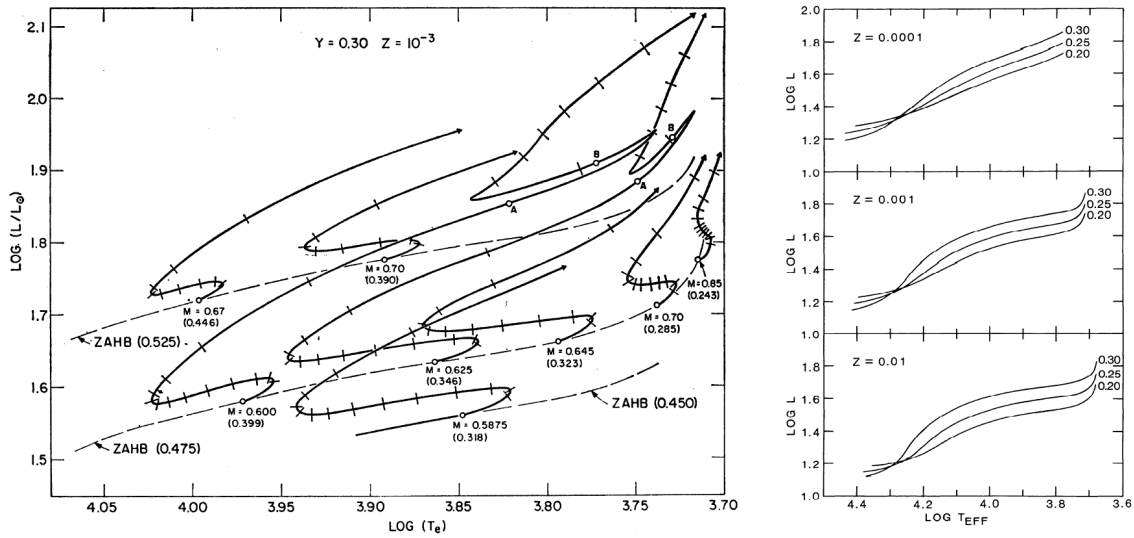


Figure 1.5: Theoretical evolutionary tracks of stars with various total and core mass (left panel, from Iben, 1971) and luminosity dependence of ZAHB for different Y and Z (Sweigart, 1987).

(redder) when Y is higher. For a given Z more helium-abundant stars at the ZAHB are more luminous. Observational efforts made on globular clusters (GCs) resulted in the range of helium abundance of approximately $0.24 < Y < 0.34$ (see e.g. the review in Mucciarelli et al., 2014)².

Theoretical models (fig. 1.6), as well as observational results, showed that more metal-poor RR Lyraes are more luminous than metal-rich stars (see e.g. Lee et al., 1990; Sandage & Cacciari, 1990). Except for this initial disposition, RR Lyraes also change their luminosity during their evolution - after leaving the ZAHB their luminosity increases for almost all post-ZAHB evolution (fig. 1.4, 1.5). Therefore, more evolved stars are generally more luminous than stars on the ZAHB. Apparently, the location of a particular RR Lyrae at the HB represents a very complex problem influenced by many factors.

When characteristics of RR Lyraes in two different stellar systems (e.g. globular clusters) are compared, we can assume that all stars in a particular system have a similar chemical composition and a similar evolution stage³. Thus, a system with more evolved RR Lyraes will show its HB shifted to higher luminosities, when compared to another system with less evolved RR Lyrae variables. This means that HB stars with the lowest metallicity (which are the oldest) will be more luminous due to its low metallicity, and, in addition, also due to their advanced evolutionary stage. For example, the shift in luminosities between the HB of GC M15 ($[\text{Fe}/\text{H}] = -2.4$) and M3

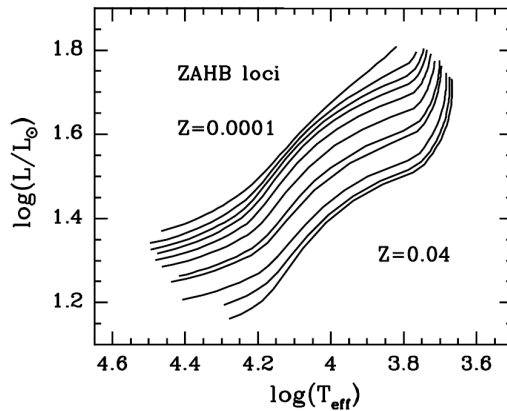


Figure 1.6: Theoretical ZAHBs with different metal content (Pietrinferni et al., 2006).

²The best initial solar abundances obtained by theoretical modelling by Pietrinferni et al. (2004) are $Y_{\odot} = 0.2734$ and $Z_{\odot} = 0.0198$.

³Recently, it seems that various stellar populations can be present in particular GC (e.g. Alonso-García et al., 2013).

($[\text{Fe}/\text{H}] = -1.5$, both from Kraft & Ivans, 2003) was found to be $\Delta L = 0.09$ (Sandage et al., 1981).

As the star evolves, it also moves in HRD horizontally and it can cross the IS more than once (depending on its position on ZAHB). Due to changes in internal composition, and probably also due to mass loss (Koopmann et al., 1994), the star changes its size, density, and surface temperature during its HB phase. As a consequence, the luminosity and pulsation period also changes. These changes can be continuous, but they can also occur suddenly.

Evolution models predict that stars first evolve slowly blueward, and then rapidly redward at higher luminosity (e.g. Lee & Demarque, 1990; Pietrinferni et al., 2004), as shown in the left panel of fig. 1.5. The rate of these changes is no faster than about $\beta = dP/dt = -0.02$ days/Myr when moving blueward. When evolving from higher to lower temperatures, changes can be as high as $\beta = 0.3$ d/Myr. On average, when analysing e.g. GCs, β should be about zero or slightly higher, which was confirmed by observations (e.g. Lee et al., 1990; Jurcsik et al., 2012; Szeidl et al., 2011). Large positive β of stars in some GCs (on average) are due to their evolution redward across the IS towards the asymptotic giant branch.

The situation with average period changes in globular clusters is nicely shown in fig. 1.7, where β is plotted against HB type introduced in Lee (1989) to describe HB morphology through the $(B - R)/(B + V + R)$ parameter, where B , V , and R are the numbers of blue HB stars (bluer than the fundamental blue edge), RR Lyraes, and red HB stars, respectively⁴. It is seen that theory roughly resembles observations.

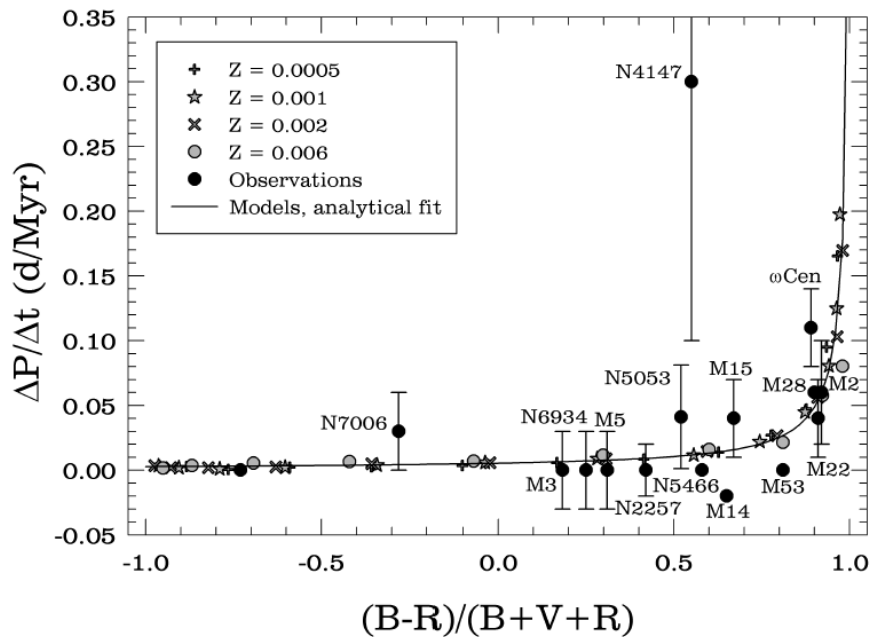


Figure 1.7: Evolutionary changes of pulsation period as a function of HB type. The solid line represents theoretical period changes, while points show average period changes observed in several GCs. Taken from Smith (2013).

Nevertheless, there are many stars, which do not show any change in period, and, on the other hand, there are RR Lyrae variables, which show larger period-changes than evolution theory can explain. These stars are thought to be either pre-HB stars (largest negative β) or stars which are close to their HB life (largest positive β). It is worth noting that these large changes could

⁴In other sections B , V , and R mean photometric filters.

possibly be the consequences of binarity in some cases, which only mimic as changes in period when analysing $O - C$ diagrams with a limited time span.

Some stars also show both positive and negative abrupt changes (e.g. RR Gem and XZ Cyg, Sódor et al., 2007; Bezdenezhnyi, 1988). These changes, which can not be explained through slow HB evolution, are relatively common among Blažko stars (for example Jurcsik et al., 2012; Le Borgne et al., 2007, and others). Sweigart & Renzini (1979) suggested that these abrupt period changes result from discrete mixing events in the semiconvective zone of an RR Lyrae star, while Stothers (1980) proposed that hydromagnetic effects might be responsible for the observed changes. Nevertheless, a final solution for this behaviour remains unclear.

Depending on the particular location inside the IS, an RR Lyrae star can pulsate in several ways. As already discussed in sec. 1.2.1 the radial mode of pulsation of the vast majority of RR Lyrae stars can be either fundamental, first overtone, second overtone or double-mode with simultaneous fundamental and first overtone pulsation⁵. A star can even change its pulsation mode, for example from fundamental to the first overtone and vice versa, when evolving through the IS.

In fig. 1.2, where mode-selection maps are shown, there are coloured regions, which represent the location of different pulsation state of a particular star. There are also two so called hysteresis regions, where stars can pulsate in two different modes depending on the direction of their evolution. These hysteresis regions were firstly introduced by van Albada & Baker (1973). The mode of pulsation of an RR0 star, which evolves blueward and enters the RR0/RR1 hysteresis region, remains fundamental till it reaches the blue edge of this area. When an RR1 star evolves redward, and crosses the RR0/RR1 hysteresis area, it holds its first overtone mode till the red edge of the hysteresis region is reached. A similar situation holds for fundamental/double-mode hysteresis region. Theoretical evolutionary tracks for four different masses from Demarque et al. (2000) are plotted together with a mode-selection map in fig. 1.8 (Szabó et al., 2004).

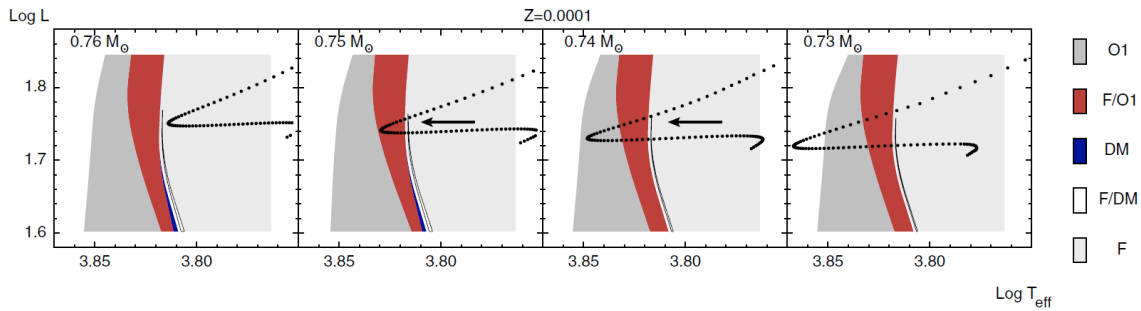


Figure 1.8: Evolutionary tracks through the IS for $Z = 0.0001$ -stars with different masses plotted over mode-selection maps (taken from Szabó et al., 2004). Labels are the same as in fig. 1.2. For the sake of clarity, the F/DM (RR0/RR01) hysteresis zone is shifted 100 K to the right.

There are some indications that the mode-switching can possibly play an important role in the nature of the Blažko effect. Goranskij et al. (2010) and Jurcsik et al. (2012) reported on V79 in GC M3, which shares the properties of both the double mode and the Blažko phenomenon. Switching from double mode to the fundamental mode was recently observed in OGLE-BLG-RRLYR-12245 (Soszyński et al., 2014).

⁵Benkő et al. (2014) found that some RRab Blažko stars can pulsate in fundamental and second overtone simultaneously.

1.3 Connection between light curve characteristics and physical parameters

Some physical parameters are best determined from high-dispersion spectroscopy. Unfortunately spectroscopic measurements of RR Lyrae variables are available only for several tens or maximally few hundreds of RR Lyraes, because it is very time-consuming and often impractical. Contrary to spectroscopy, obtaining light curves is a relatively easy task even for amateur astronomers with appropriate CCD equipment, and, in addition, photometry can be done in large-scale surveys, which enables exploring overall characteristics in a statistical way. Therefore, it would be of great benefit to have some method for physical parameters determination that is based only on photometric measurements.

A necessary assumption in all attempts based on photometric characteristics is that the shape of an RR Lyrae light curve reflects its basic physical properties. Many on-going efforts have been made to estimate physical parameters through the light curves. In particular, pulsation periods, mean magnitudes, colours, and quantities that characterize the shapes of the light curves (e.g. amplitudes, rise times, Fourier coefficients) have been used. In addition non-linear convective pulsation models were calculated to describe light curves recently. All these efforts would not have been possible without large samples of stars with precise photometric light curves (e.g. Lub, 1977) and with spectroscopic measurements (e.g. Layden, 1994; Suntzeff et al., 1994).

1.3.1 Characteristics of RR Lyrae star light curves

The two most important parameters defining the basic light-curve shape are the *total amplitude* A_{tot} of observed light changes, which is defined simply as the difference between maximum and minimum magnitude, and the *rise time* RT , which defines the degree of asymmetry of a light curve. Alternatively, RT carries information about the part of a cycle from minimum to maximum light and reads as

$$RT = \frac{T_{\text{max}} - T_{\text{min}}}{P}. \quad (1.6)$$

Total amplitudes of RR Lyrae variables range from about 0.3 to 2 mag in some extreme cases. From many analyses (e.g. Nemeč et al., 2011), it was found that stars with large A_{tot} have a low RT . Therefore, RR Lyraes with the most skewed light curves have the shortest RT and largest A_{tot} . According to its definition (eq. 1.6) a symmetric light curve will have $RT = 0.5$. RRab stars usually have rise times between 0.1 and 0.3, RRc stars can have an $RT > 0.4$. For both RRab and RRc stars, shorter-period RR Lyraes have lower RT s and larger amplitudes (Sandage, 1981).

Both parameters are not constant in the case of multi-mode stars and in stars which experience modulation. In some modulated stars the changes can be so drastic that in a specific part of the modulation cycle the star appears like a stable stars with no light changes. For example, V445 Lyr mimics as a non-variable object during its minimum Blažko phase (Guggenberger et al., 2012).

Fourier parameters

A complex approach for light curve description is through Fourier decomposition techniques. Using these methods, light changes of a star are fitted with a Fourier series of the form

$$m(t) = A_0 + \sum_{i=1}^n A_i \sin \left(2\pi i \frac{(t-t_0)}{P} + \phi_i \right), \quad (1.7)$$

where n is the degree of the harmonic polynomial, t_0 is a time of maximum light and P is the basic pulsation period. The shape of the light curve can then be quantified using amplitudes ratios R_{i1} and phase differences ϕ_{i1} defined as

$$R_{i1} = A_i/A_1, \quad (1.8)$$

$$\phi_{i1} = \phi_i - i\phi_1. \quad (1.9)$$

These coefficients, which were introduced in early eighties of the 20th century by Simon & Lee (1981), can be used as physical-parameter indicators (as we will see later in sec. 1.3.3). Because different types of variables, and types of RR Lyraes, have different Fourier coefficients, they also serve as variable-type indicators. This is demonstrated in fig. 1.9, where Fourier coefficients are used for defining different types of RR Lyrae stars in the Galactic bulge (GB, Soszyński et al., 2011).

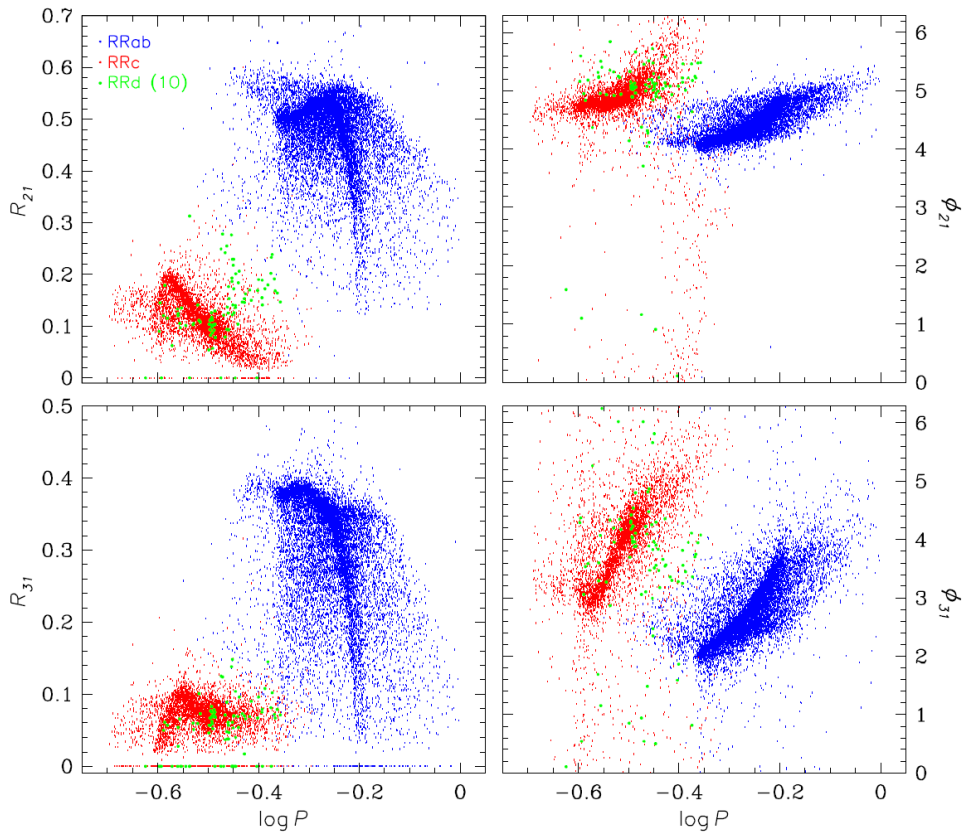


Figure 1.9: Diagrams utilizing Fourier coefficients for defining different types of RR Lyrae stars in the GB observed in the OGLE survey (figure is taken from Soszyński et al., 2011). Apparently, RRc stars are well separated from RRab stars in all plots.

In empirical relations the most widely used coefficients are usually those with $i = 2$ and $i = 3$. Some authors use the cosine instead of sine form of eq. 1.7. Transformation from sine to cosine coefficient terms is through

$$\phi_{21}^s = \phi_{21}^c - \frac{\pi}{2}, \quad (1.10)$$

$$\phi_{31}^s = \phi_{31}^c - \pi, \quad (1.11)$$

where subscript 's' relates to sine, and 'c' to cosine terms.

How to determine the appropriate degree of the fit N is still an open question. The standard deviation of the residuals of the fit is not an optimal indicator of the quality of the model, because the higher the value of N , the lower the standard deviation of residuals. In high-order models applied on scattered data, noise can be fitted instead of fitting real light changes. Usually $N \in (4; 15)$. The larger number is needed when the skewness is greatest (shortest RT), and when bumps, or other anomalies are present. Indeed, in the excellent high-precision space data from the *Kepler* satellite, perhaps 50-100 terms would be needed to obtain residuals showing normally distributed white noise (Nemec et al., 2011). The best way for estimating N in common ground-based data is to maintain visual inspection and choose the model with the lowest N which sufficiently describes the light changes.

After several manual experiments on data from *the All sky automated survey, ASAS* (e.g. Pojmanski, 1997, 2002), Kovács (2005) found an empirical formula for determining a suitable degree of the fit, which should avoid overfitting light curves that are noisy or badly sampled, and underfitting those with low noise. Kovács defined parameter

$$m^* = \text{INT} \left(\frac{A_1 \sqrt{n}}{10\sigma} \right), \quad (1.12)$$

where A_1 is the Fourier amplitude at the main frequency component, n is the number of data points and σ is the standard deviation of the residuals between the data and the fit. The number of terms in fitting formula is then chosen according to m^* : $N = 4$ for $m^* < 4$, $N = m^*$ for $m^* \in \langle 4; 10 \rangle$ and $N = 10$ for $m^* > 10$.

Fourier coefficients are not independent, but they correlate among themselves by dependences, which can be expressed with linear equations (tables 6 and 2 in Jurcsik & Kovács, 1996; Kovács & Kanbur, 1998). This is a consequence of the finite number of physical parameters which each Fourier parameter depends on. It has an important consequence that there is the possibility to use various combinations of coefficients for determination the same physical parameter. Correlations between some of the Fourier coefficients are shown in fig. 1.10. The most evident is a linear dependence between ϕ_{21} and ϕ_{31} .

Jurcsik & Kovács (1996) introduced a light-curve quality indicator D_m , which is estimated using differences D_F between observed F_{obs} and predicted Fourier parameters F_{calc} (calculated from other observed parameters). The equation for D_m reads as

$$D_F = |F_{\text{obs}} - F_{\text{calc}}| / \sigma_F. \quad (1.13)$$

In this formula σ_F is the respective standard deviation for each formulae, which is given by the authors. Parameter D_m is then defined as the maximum of the deviation parameters $\{D_F\}$. Jurcsik & Kovács (1996) found that Blažko stars never have $D_m < 3$ in any phase of their modulation cycle. Therefore they proposed D_m as an indicator of modulation. They also suggest to be cautious when determining metallicity through their relation in stars with $D_m > 3$. Later it was found that D_m gives information about the quality of the data and coverage of the light curve rather than about modulation. Cacciari et al. (2005) found that D_m is effectively unable to distinguish between Blažko and non-Blažko stars down to $D_m \geq 2$.

1.3.2 Amplitudes, periods and metallicity - the Oosterhoff problem

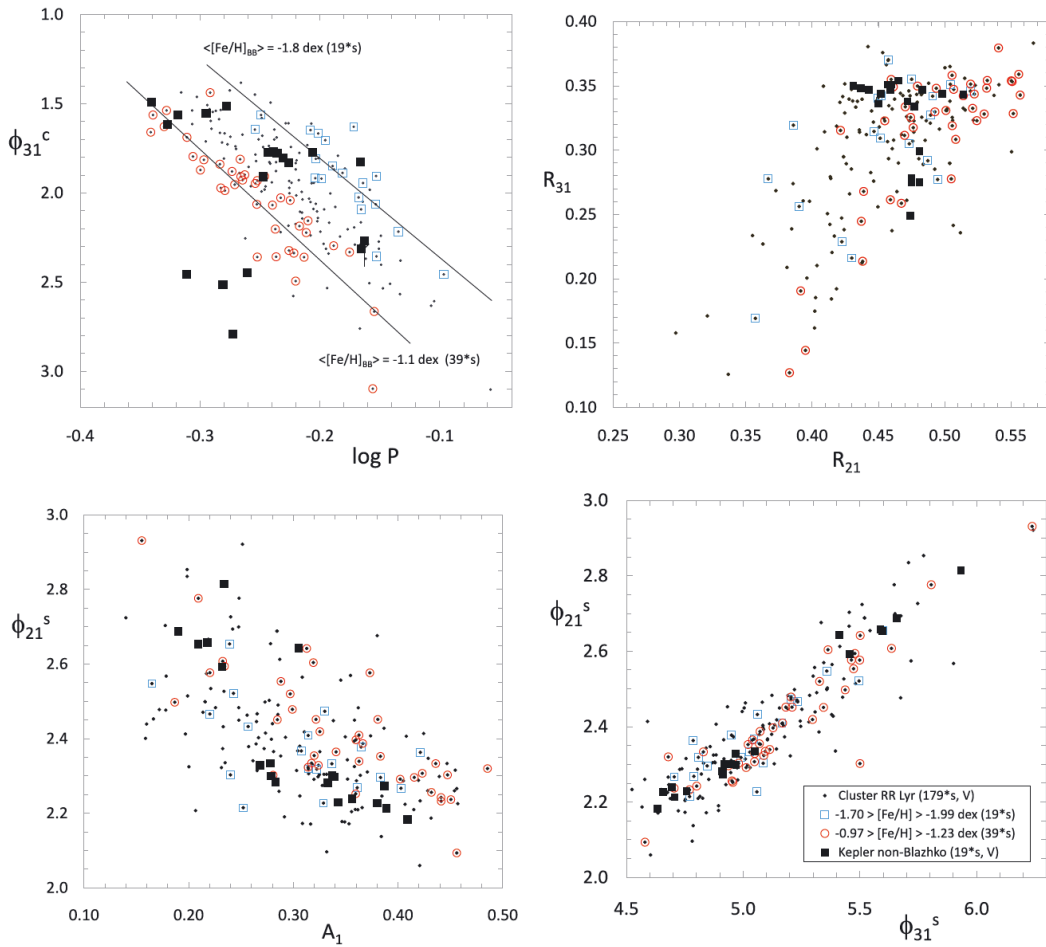


Figure 1.10: Example of some interrelations between Fourier coefficients of GC stars and stars in a *Kepler* field taken from (Nemec et al., 2011).

Already from Bailey's pioneering studies on GCs at the beginning of 20th century it became obvious that basic characteristics of RR Lyrae variables differ from GC to GC. Oosterhoff (1939, 1944) pointed out that some globular clusters have different populations of RRab and RRC stars, and that the average periods of these two subclasses systematically differ. The first group, now known as Oosterhoff type I clusters (OoI), contains less than 20 % RRC stars with mean period $\langle P_c \rangle = 0.32 \text{ d}$. RRab stars in this group have $\langle P_{ab} \rangle = 0.55 \text{ d}$. For example, GCs M3 and M5 belong to OoI. The second group (OoII, for example M15 and ω Centauri), contains more than 40 % RRC stars with $\langle P_c \rangle = 0.37 \text{ d}$, and RRab stars with $\langle P_{ab} \rangle = 0.64 \text{ d}$.

The differences between Oosterhoff's groups are well pronounced in period-amplitude ($P - A$) diagrams (now called the Bailey diagram, fig. 1.11), where OoII stars have longer periods than OoI stars at the same amplitude. Later it was found that Oosterhoff's groups roughly follow their metal abundances. Usually, stars belonging to OoII group are more metal-poor than those from OoI group. Thus, galactic GCs are sharply separated in (mean) period-metallicity diagrams (fig. 1.12). Unfortunately, this is not a general property of all known GCs.

GC M2 has a similar metallicity as M3, but it belongs to OoII, while M3 belongs to OoI (Lee & Carney, 1999). NGC 6388 and NGC 6441 were identified to show the OoII type period-amplitude

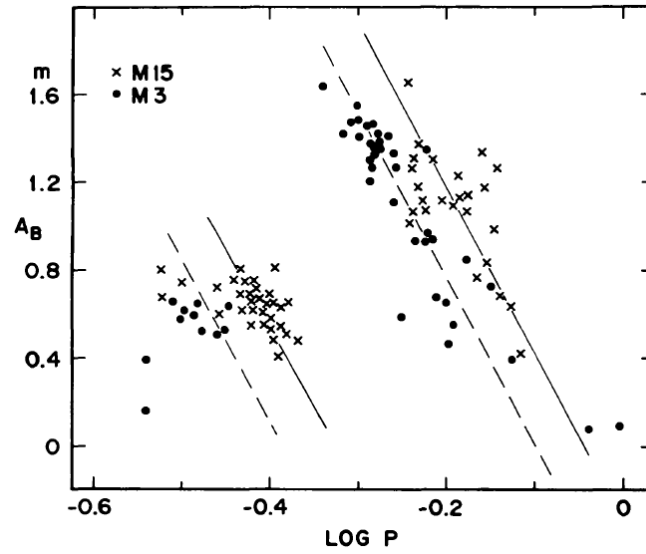


Figure 1.11: Period-amplitude diagram of GC M15 (crosses) and M3 (circles). It is seen that stars from M3 (OoI) have at the same amplitude shorter period than stars in M15 (OoII) (Sandage et al., 1981).

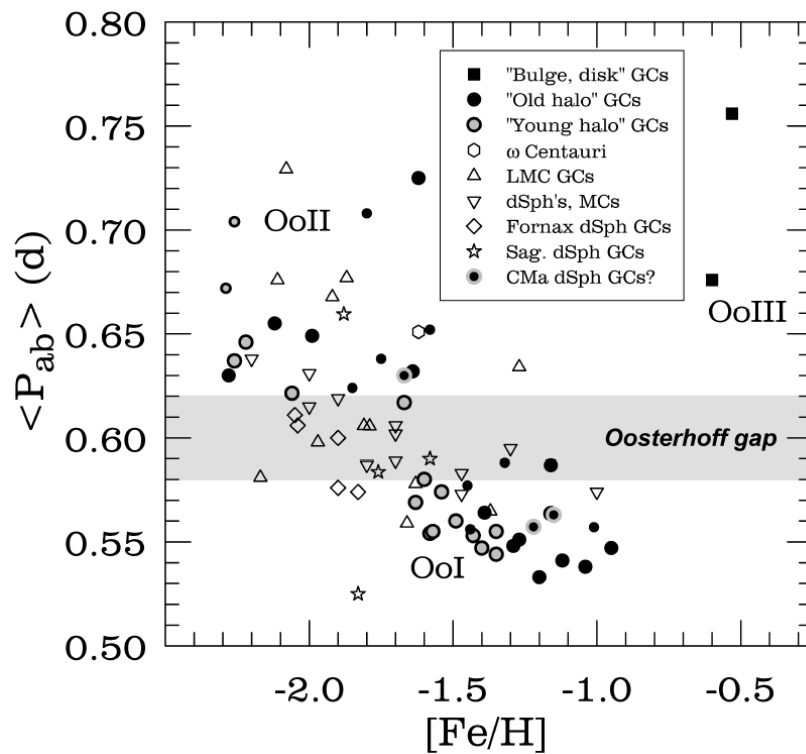


Figure 1.12: Mean period of RRab type stars located in various stellar systems as a function of metallicity. Figure is taken from Smith et al. (2011).

diagram, but they have very high metallicity not corresponding to OoII group (see reviews of Catelan, 2009; Smith et al., 2011). Therefore they were classified as a new Oosterhoff group OoIII. In addition, dwarf spheroidal (dSph) satellite galaxies of the Milky Way, as well as their globular clusters, fall preferentially on the Oosterhoff gap region - they form the Oosterhoff intermediate group (see fig. 1.12, Catelan, 2009; Smith et al., 2011).

Concerning Galactic field stars, the Oosterhoff dichotomy is also observed. Although the difference in the $P - A$ diagram between OoI and OoII groups is not so pronounced as in the case of GCs, it is still well apparent among close RR Lyraes (< 4 kpc, Szczygieł et al., 2009), as well as in more distant regions between 4 and 20 kpc from the Sun (Miceli et al., 2008). This is strong evidence against the built-up theory of the Galactic halo through the accretion of smaller fragments (e.g. Searle & Zinn, 1978), because if this were true, no Oosterhoff dichotomy would be observed.

Miceli et al. (2008) and Szczygieł et al. (2009) found that the majority of RR Lyraes in the Galactic field belong to OoI, and that they are concentrated close to the plane of the Galaxy. This should not be surprising considering the fact that OoI stars are more metal-abundant than OoII stars. In addition, Szczygieł et al. (2009) and McNamara & Barnes (2014) identified a new group of OoI metal-rich, short-period stars which in the period-amplitude diagram locate to the left from the OoI stars.

The nature of the Oosterhoff dichotomy is still a problem to be solved. The most popular explanation deals with the hysteresis zones mentioned in sec. 1.2.2 (van Albada & Baker, 1973). It is known that OoII stars are metal-poorer than OoI stars which has some implications. Firstly, OoII stars are more luminous and hotter by 270 K than OoI stars (OoI: $M_V = 0.61$, OoII: $M_V = 0.43$, McNamara & Barnes, 2014). Lee & Carney (1999) proposed OoII stars to be about 2-3 Gyr older than OoI stars, which not only implies a different formation time, but that the origin of different Oosterhoff groups might differ. As shown with Oosterhoff intermediate stars and GC M2 vs. M3, the Oosterhoff dichotomy is not simply metallicity-dependent, but the evolutionary effects probably play a crucial role.

1.3.3 Empirical relations

From the discussion in previous sections it should be apparent that all physical parameters correlate with measurable quantities, as was assumed. The first attempts to determine physical parameters involved period shifts between RR Lyraes in M3 and others GCs (Sandage, 1981; Sandage et al., 1981). They utilized amplitudes in their relationships, and in addition found that RT correlates with period.

Research papers on RR Lyraes using Fourier decomposition started appearing at the same time as Sandage's with the studies of N. R. Simon. After defining the method in the study of cepheids (Simon & Lee, 1981), Simon & Teays (1982) analysed the behaviour of low-order Fourier coefficients of 70 field RR Lyraes. They found a weak dependence of these coefficients on period. When they plotted Fourier coefficients against period, they found that this approach provides a very efficient tool for resolving RRc stars from RRab type (see fig. 1.9).

Two years later, Petersen (1984) investigated RR Lyrae variables in GC ω Cen using photographic measurements from Martin (1938). He found even more pronounced progressions of coefficients against period. He also discussed the scatter of these dependences and attributed them to different physical properties of particular members of this cluster. Mainly ϕ_{21} and ϕ_{31} versus period were well defined for RRc stars and turned out to be unambiguously correlated. This was significant progress towards linking Fourier coefficients with physical parameters.

After Simon (1988) discovered that ϕ_{21} decreases with decreasing metallicity for field RRab stars with $P < 0.575$ d, Kovács & Zsoldos (1995) established second-order polynomial metallicity dependences of 2-4 Fourier parameters and period. Precise photometric measurements of field

and GC stars allowed Kovács & Jurcsik (1996) to determine a relation for absolute V -magnitude as a function of period, A_1 and ϕ_{31} . In the same year, Jurcsik & Kovács (1996) published that a linear correlation exists between metallicity, period and Fourier phase parameter ϕ_{31} . Two years later, Jurcsik (1998) presented a large set of relations for various physical parameters based on Fourier coefficients employing atmospheric and HB models. These calibrations were subsequently refined many times, or new relations were defined (e.g. Kovács & Walker, 2001; Sandage, 2004, and others).

Fourier-decomposition techniques are applicable to both regular and modulated stars when the light curve is sufficiently dense, and uniformly covered without any preference to any modulation phase (e.g. Alcock et al., 2003; Jurcsik et al., 2009; Smolec, 2005). Nemec et al. (2013) recommend determining $[\text{Fe}/\text{H}]$ as an average during the Blažko cycle, which gives slightly better results, rather than to use a mean light-curve fit.

Although semi-empirical calibrations were defined for both RRab and RRc stars, we will exclusively give relations for RRab stars in the text to follow.

Metallicity

The first papers on metallicity determination dealt with period shift in the $P-A$ diagram of globular clusters. M3 served as reference for the comparison of other GCs. Sandage et al. (1981) found $\Delta \log P = -0.112 \Delta \log Z$, i.e. they confirmed that the period increases with metal content. As previously discussed in sec. 1.3.2, period-shift is not only metallicity dependent, and therefore only usable as a rough estimation when it is impossible to determine metallicity in other ways.

One of the most popular and most widely used calibrations for metallicity estimation is that of Jurcsik & Kovács (1996), which employs the period and phase coefficient ϕ_{31}

$$[\text{Fe}/\text{H}] = -5.038 - 5.394P + 1.345\phi_{31}. \quad (1.14)$$

Because of the 2π ambiguity it is necessary to use a value of $\phi_{31} > \pi$. This relation, based on a large sample of stars, which was also tested on GCs, gives about 0.3 dex higher predictions at the low abundance level (Jurcsik & Kovács, 1996; Nemec, 2004; Smolec, 2005). The standard deviation of the estimated abundance can be calculated using the relation from Jurcsik & Kovács (1996)

$$\sigma_{[\text{Fe}/\text{H}]}^2 = 1.809\sigma_{\phi_{31}}^2 + 2K_{12}P + 2K_{13}\phi_{31} + 2K_{23}P\phi_{31} + K_{11} + K_{22}P^2 + K_{33}\phi_{31}^2, \quad (1.15)$$

where the coefficients have the following values

$$\begin{aligned} K_{11} &= 0.08910, & K_{22} &= 0.02529, & K_{33} &= 0.00374 \\ K_{12} &= 0.00116, & K_{13} &= -0.01753, & K_{23} &= -0.00289. \end{aligned} \quad (1.16)$$

The other calibration, which uses P and ϕ_{31} is the one of Sandage (2004)

$$[\text{Fe}/\text{H}] = -6.025 - 7.012 \log P + 1.411\phi_{31}. \quad (1.17)$$

Sandage (2004) also defined other relations using amplitude and rise time (his eq. 6 and 7). However, Jurcsik & Kovács (1996) found that $P - \phi_{31} - [\text{Fe}/\text{H}]$ gives a tighter correlation between calculated and observed metallicity than other combinations of Fourier coefficients (fig. 1.13).

The metallicity in eq. 1.14 is on Carretta & Gratton (1997) scale (we will denote the metallicity using this scale as $[\text{Fe}/\text{H}]_{\text{CG}}$), while eq. 1.17 is on the Zinn & West (1984) scale ($[\text{Fe}/\text{H}]_{\text{ZW}}$). The transformation between these two scales is through the calibration of Sandage (2004)

$$[\text{Fe}/\text{H}]_{\text{ZW}} = 1.05 - 0.2[\text{Fe}/\text{H}]_{\text{CG}}. \quad (1.18)$$

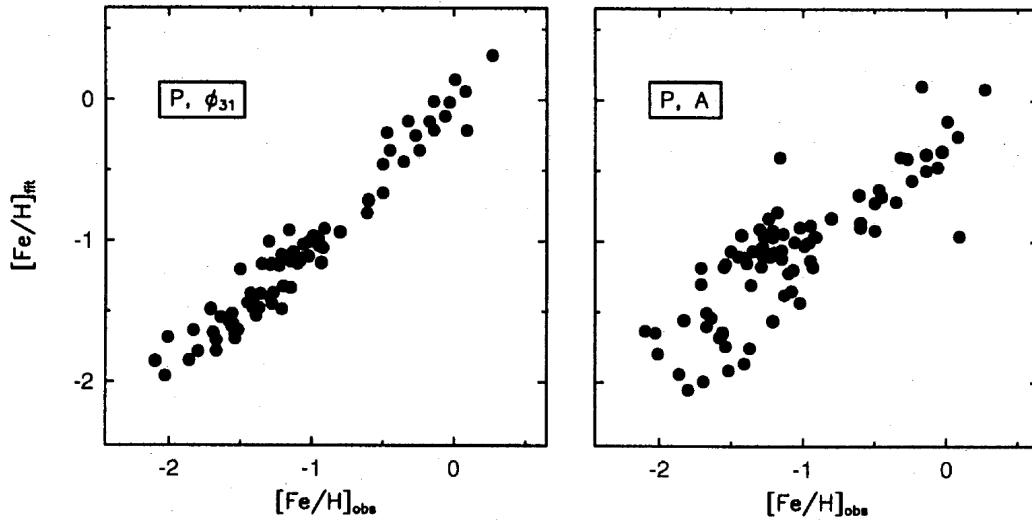


Figure 1.13: Demonstration that the relation based on P and ϕ_{31} is more appropriate for metallicity determination than the $P - A - [\text{Fe}/\text{H}]$ relation (Jurcsik & Kovács, 1996).

Recently, based on ultra-precise measurements and new spectroscopy, Nemeč et al. (2013) found a new, nonlinear $P - \phi_{31} - [\text{Fe}/\text{H}]$ relation, which gives better results than the linear calibration from eq. 1.14.

Absolute magnitude and luminosity

Although the luminosity of RR Lyrae stars depends on many factors, a general linear correlation with metallicity is observed. This is well illustrated in $L - [\text{Fe}/\text{H}]$ relation in fig. 1.14, where these secondary effects cause broadening of the dependence (different period and luminosity at the same metallicity). Jurcsik (1998) introduced such linear correlation

$$\log L = 1.464 - 0.106[\text{Fe}/\text{H}]_{\text{CG}}. \quad (1.19)$$

Theoretical ZAHB models for fundamental blue edge predict $\frac{d \log L}{d \log Z} \sim -0.08$ (Sweigart, 1987; Dorman, 1993), which correlates well with the slope at constant temperature in other relation from Jurcsik (1998)

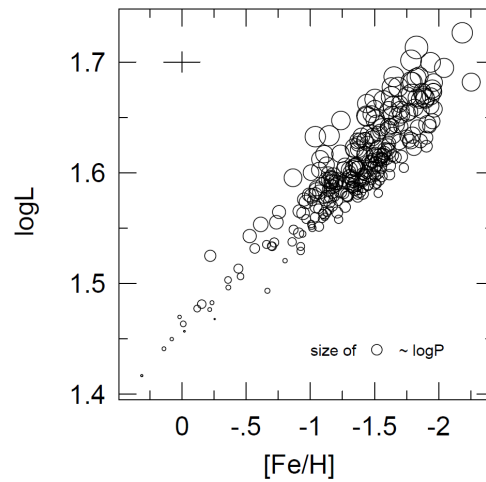


Figure 1.14: Linear correlation between luminosity and $[\text{Fe}/\text{H}]$ (Jurcsik, 1998).

$$\log L = 10.260 - 0.062[\text{Fe}/\text{H}]_{\text{CG}} - 2.294 \log T_{\text{eff}}. \quad (1.20)$$

Both Jurcsik's calibrations proceed from the pulsation equation 1.2. Sandage (2006) used stellar evolutionary models and published a quadratic metallicity-dependence of luminosity

$$\log L = 1.245 - 0.451[\text{Fe}/\text{H}]_{\text{ZW}} - 0.097[\text{Fe}/\text{H}]_{\text{ZW}}^2. \quad (1.21)$$

Unfortunately, pulsation-based calibrations give slightly lower results than those which are based on stellar evolution models (see discussion in Nemeč et al., 2011). It is still unclear which calibrations are correct.

Luminosity is directly linked with absolute magnitude. Therefore similar, metallicity-dependent relations can also be expected for absolute magnitude. For example, Bono et al. (2007) published a quadratic calibration for field stars with the entire metallicity range from $[\text{Fe}/\text{H}]_{\text{ZW}} = -2.5$ to 0.0 dex

$$M_V = 1.19 + 0.50[\text{Fe}/\text{H}]_{\text{ZW}} + 0.09[\text{Fe}/\text{H}]_{\text{ZW}}^2. \quad (1.22)$$

Only one year later, Catelan & Cortés (2008) argued that revised values for the trigonometric parallax and reddening of RR Lyr imply a brighter luminosity scale for RR Lyrae stars and give following equation:

$$M_V = 0.23[\text{Fe}/\text{H}]_{\text{ZW}} + 0.984. \quad (1.23)$$

This relation gives, according to Nemeč et al. (2011), results that are about 0.15 brighter than that of eq. 1.22.

Kovács & Jurcsik (1996) established a relation derived from the then actual Baade-Wesseling results, which includes Fourier parameters determined directly from light-curve shape

$$M_V = 1.221 - 1.396P - 0.477A_1 + 0.103\phi_{31}. \quad (1.24)$$

This equation turned out to give about 0.2 mag fainter magnitudes than the more recent calibration of Catelan & Cortés (2008), eq. 1.23.

When determining absolute magnitude, it is also possible to utilize the period shift in the $P - A$ diagram. Sandage et al. (1981) compared the period shift of various GCs using M3 as a reference and found that $\Delta M = 3\Delta \log P$.

Dereddened colours, effective temperature

In her large set of relations, Jurcsik (1998) shows that the mean $(B - V)_0$ depends on the pulsation period and Fourier amplitude A_1 in a following way:

$$(B - V)_0 = 0.308 + 0.163P - 0.187A_1. \quad (1.25)$$

Nemeč et al. (2011) found that this equation gives the same results as the calibration of Kovács & Walker (2001):

$$(B - V)_0 = 0.189 \log P - 0.313A_1 + 0.293A_3 + 0.460. \quad (1.26)$$

Effective temperature can be calculated e.g. via a relation of Sandage (2006)

$$\log T_{\text{eff}} = -0.380(B - V)_0 + 0.0144[\text{Fe}/\text{H}]_{\text{ZW}} + 3.960, \quad (1.27)$$

or through the calibration from Kovács & Walker (2001), which is recommended by Nemeč et al. (2011)

$$\log T_{\text{ef}} = 3.884 + 0.3219(B - V)_0 + 0.0167 \log g + 0.007[\text{Fe}/\text{H}]_{\text{CG}}, \quad (1.28)$$

where $\log g$ is the surface gravity. The calibration for this quantity comes from Jurcsik (1998) and reads as follows:

$$\log g = 2.473 - 1.226 \log P. \quad (1.29)$$

Mass

Similarly to other physical parameters, a linear metallicity dependence of mass was found based on pulsation as well as on evolution models. Photometric mass can then be estimated through the dependence from Jurcsik (1998)

$$\log \mathcal{M} = -0.328 - 0.062[\text{Fe}/\text{H}]_{\text{CG}}, \quad (1.30)$$

with standard error of the regression $\sigma = 0.019$. Bono et al. (2007) offers another possible relation

$$\log \mathcal{M} = -0.265 - 0.063[\text{Fe}/\text{H}]_{\text{ZW}}. \quad (1.31)$$

This calibration is based on theoretical HB models of Pietrinferni et al. (2004, 2006).

Chapter 2

The Blažko effect

Together with the Oosterhoff problem, the Blažko effect represents the most puzzling, still unsolved mystery in RR Lyrae stars. Research in this phenomenon experienced tremendous progress over the three last decades. Especially thanks to observations from space the true diversity in all conceivable manifestations of the Blažko modulation was revealed in the last few years. The following pages of this work are devoted to summarizing the current knowledge about the Blažko effect and its characteristics. A mathematical description of the modulation is presented, and manifestations of the effect in frequency spectra are described in detail. In addition, Blažko periods and amplitudes, incidence rate of modulated stars, and models for the Blažko effect are discussed.

2.1 An introduction of the Blažko effect

The discovery of the irregularity of the light changes of RR Lyrae type stars dates back to the beginning of the 20th century. The Russian astronomer S. N. Blažko (1907) was the first to report on the periodic changes in the timing of maximum light for the star RW Dra which, in fact, was the discovery of the phase modulation. A few years later, Shapley (1916) noticed the different heights of observed maxima in the prototype star RR Lyrae itself, revealing the amplitude modulation. Therefore, the phenomenon was named after S. N. Blažko, and it has been defined as regular, long-term cyclic changes in amplitude and/or phase of the light curve over many decades since its discovery.

However, recent findings showed that both types of modulation are always present in modulated stars (Benkő et al., 2010). In some cases modulation is so huge that the light variations can even cease in particular Blažko phases. In addition, it was found that the Blažko effect might change its characteristics over the long time scales (e.g. in RR Lyr or XZ Cyg Le Borgne et al., 2014; LaCluyzé et al., 2004). In several examples multiple modulation was revealed (e.g. CZ Lac, V445 Lyr, Sódor et al., 2011; Guggenberger et al., 2012). It is clear that the description of the Blažko effect is not trivial and represents a very complex problem.

The modulation similar to the Blažko effect does not affect only RR Lyrae variables, but also representatives of other types of pulsating stars. Especially double mode cepheids in the LMC, which pulsate simultaneously in the first and second radial overtone, show long-term periodic amplitude modulation typically with periods longer than 700 d. The incidence rate of such modulated cepheids is at least 20 %, but can be as high as 35 % (Moskalik, 2014). The only galactic cepheid currently known to unambiguously show the Blažko effect is V473 Lyr which pulsate in the second overtone mode and undergoes modulation with a period of 14.5 year (Molnár & Szabados, 2014). However, Blažko modulation plays the most important role among RR Lyrae stars, because it seems that about a half of RRab Lyraes might show modulation (for details see sec. 2.4).

An example of an artificial light curve¹ of a hypothetical star which undergoes simultaneous simple sinusoidal amplitude and frequency modulation is shown in fig. 2.1. The model is constructed on the basis of a real mean light curve of an ordinary star, WY Ant, observed in the SuperWASP survey (*Super Wide Angle Search for Planets*, Pollacco et al., 2006; Butters et al., 2010). In this model the period of the modulation is arbitrary chosen as 20 d, which is clearly seen from the shape of the envelope in the top left panel. The two bottom panels show what the situation looks like in different parts of the Blažko cycle. The solid black line shows simple amplitude modulation, while the blue points represent the situation when both types of modulation are present. For a comparison between regular and modulated light curve the data are phased with the basic pulsation period in the top right panel (the non-modulated signal is shown by the solid black line).

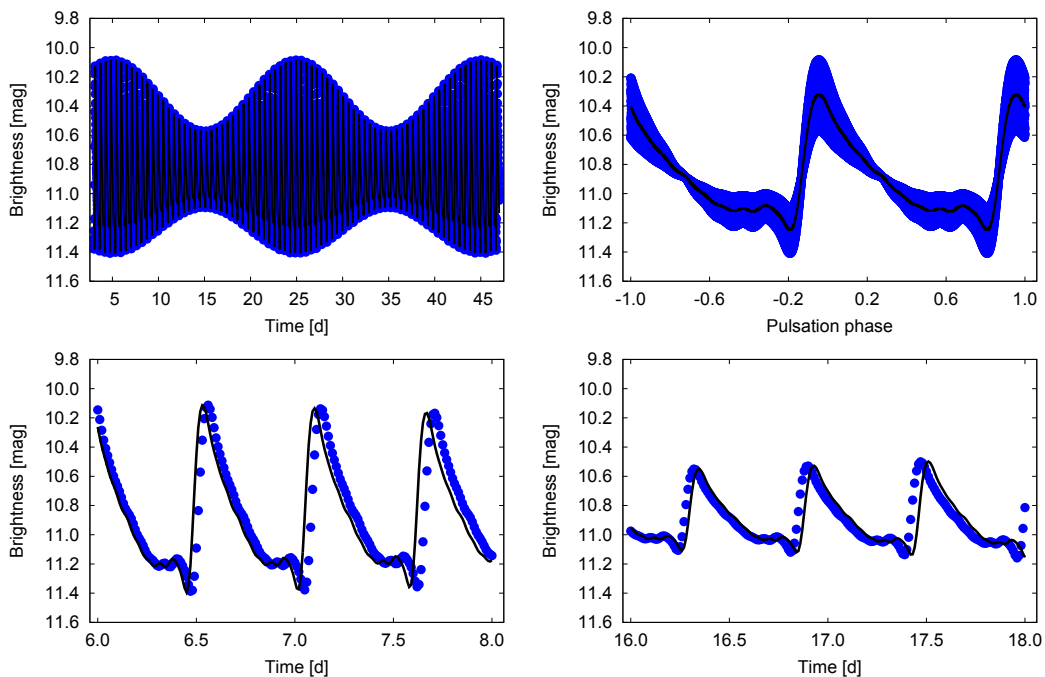


Figure 2.1: An artificial light curve demonstrating amplitude and frequency modulation. The solid line in the top right panel shows the light curve of a non-modulated carrier. In others panels, the solid black line represents the situation when only amplitude modulation is present, while the blue circles show the situation when both amplitude and frequency modulation influence the light curve.

2.2 Mathematical description of Blažko modulation. Manifestation of the modulation in the frequency spectra

Except for changes in the shape of the light curve, the modulation manifests itself as a characteristic pattern in the frequency spectra. This represents a very powerful and unambiguous tool for the identification of the modulation of the stars.

¹constructed according to methods described in the next section.

It is well known that light curves of non-modulated RR Lyrae stars can be described as the sum of goniometric functions, *i.e.* with eq. 1.7, which we modify to

$$m(t) = A_0 + \sum_{i=1}^n A_i \sin[2\pi i f_0 t + \phi_i], \quad (2.1)$$

where f_0 represents the basic pulsation frequency.

Logically, the Fourier amplitude spectrum will then show peaks at $k f_0$, as shown in fig. 2.2. In this figure the detail plots the $n = 10$ model of an ordinary star, WY Ant. The time span of the model light curve is 100 d with a time resolution of 0.01 d. The basic pulsation frequency $f_0 = 1.7411257$ c/d and its harmonics form the only structures in the Fourier amplitude spectrum.

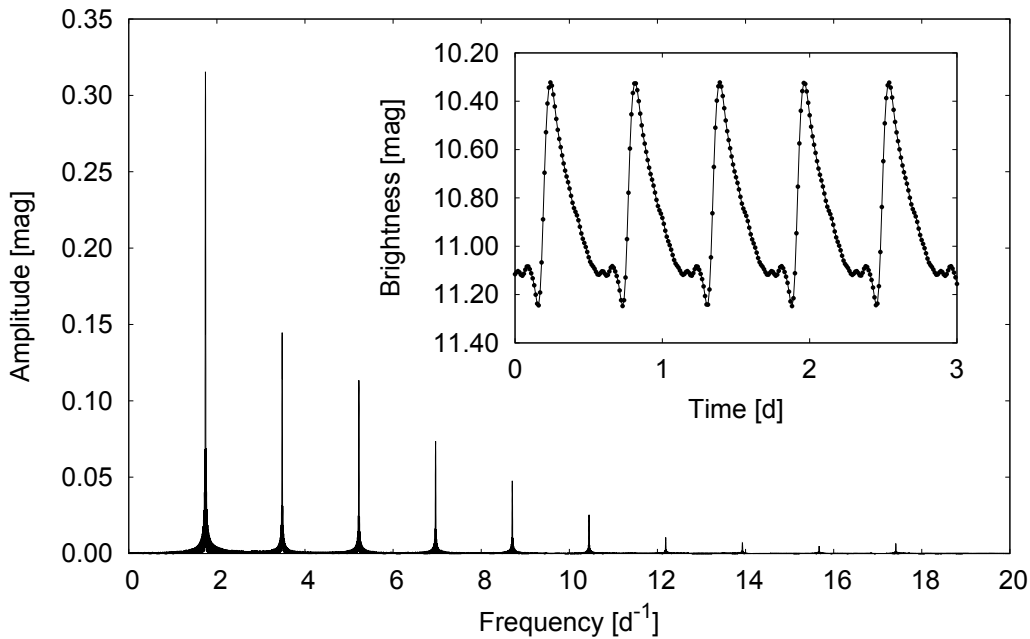


Figure 2.2: Fourier amplitude spectrum of the model of WY Ant comprising ten sine components. The light curve model is plotted in detail.

Starting with the paper by Szeidl & Jurcsik (2009), methods that involve mathematical modelling of the Blažko effect as a modulated signal, were introduced. More recently, Benkő et al. (2011) published an excellent and comprehensive review in which they gave a general, analytical formalism for the description of Blažko RR Lyrae light curves. The approach which they used, is based on the theory of electronic signal transmission. They considered a monoperiodic RR Lyrae light curve to be the carrier wave, and modulated its amplitude, frequency and phase. With their approach they were able to explain numerous light-curve characteristics and complicated envelopes as well as the properties of the frequency spectra. A free account of their paper is given as a brief introduction to the problem. Equations and the majority of figures in sec. 2.2 are taken from this paper. The style of the other plots of frequency spectra in this section was inspired by the figures in Benkő et al. (2011).

2.2.1 Amplitude modulation

The signal $c(t)$, which should be modulated, could be simple sinusoidal, but also a complex periodic function. For simplicity, let us consider the carrier to be a sinusoid with amplitude U_c

$$c(t) = U_c \sin(2\pi f_c t + \phi_c). \quad (2.2)$$

An amplitude modulated signal can be easily created by adding some periodic signal $U_m(t)$ to the carrier amplitude

$$U_{AM}(t) = [U_c + U_m(t)] \sin(2\pi f_c t + \phi_c) = \left[1 + \frac{U_m(t)}{U_c} \right] c(t). \quad (2.3)$$

When we substitute the carrier wave $c(t)$ with a non-modulated RR Lyrae star (eq. 2.1) (neglecting A_0), and assume a sinusoidal dependence $U_m(t) = a_m \sin(2\pi f_m t + \phi_m)$ with the modulation frequency f_m and amplitude of the modulation a_m , we get the simplest possible amplitude modulation which can be expressed as:

$$m_{AM}(t) = [1 + h \sin(2\pi f_m t + \phi_m)] \left[a_0 + \sum_{i=1}^n A_i \sin 2\pi i f_0 t + \phi_i \right], \quad (2.4)$$

where $h = a_m/U_c$ and a_0 is a non-zero constant which is usually some hundredths of a magnitude in RR Lyrae stars. Note that a_0 differs from the zero-point of the light curve A_0 . It is mathematically obligatory, otherwise the Fourier sum would not comprise a complete set of functions. Physically it represents the difference between the magnitude and intensity means, because the average of the transformed light curve (from fluxes to magnitudes) differs from zero. Equation 2.4 can be transformed to more illustrative form

$$m_{AM}(t) = a_0 + h a_0 \sin(2\pi f_m t + \phi_m) + \sum_{j=1}^n a_j \sin(2\pi j f_0 t + \phi_j) + \frac{h}{2} \sum_{j=1}^n a_j \left\{ \sin [2\pi(j f_0 - f_m)t + \phi_j^-] + \sin [2\pi(j f_0 + f_m)t + \phi_j^+] \right\}, \quad (2.5)$$

where $\phi_j^+ = \phi_j - \phi_m + \pi/2$, $\phi_j^- = \phi_j - \phi_m - \pi/2$. When $a_m < a_0$, the resulting modulation will be symmetrical around an average value. For $a_m > a_0$ this symmetry is broken, but the coincidence of maxima and minima of the envelope remain unchanged, and, in addition, the average brightness varies with f_m during the modulation cycle.

The constant $h = a_m/U_c$ defines the strength of the modulation. When the modulation is very strong, *i.e.* when $h > 1$, the amplitude of the light curve and its shape undergo heavy changes. Thus, in some modulation phases the light changes can be negligible with a very unusual shape. This resembles the behaviour of V445 Lyr (Guggenberger et al., 2012) mentioned in sec. 1.3. Samples of light curves for various mixtures of a_m , a_0 , and h can be found in Benkő et al. (2011).

The characteristics of a Fourier amplitude spectrum (plotted in fig. 2.3) of a pure amplitude-modulated star are obvious from the equation 2.5. It consists of the spectrum of a non-modulated star (third term) and two equidistant side peaks around each harmonic (the last term). Finally, the second term in eq. 2.5, which causes the changes in average variations, produces the modulation peak at f_m . The side peaks have always the same amplitude for a simple sinusoidal amplitude modulation $A(j f_0 \pm f_m) \sim a_j h/2$.

The analysed example illustrates the simplest possible amplitude modulation. However, modulation can be very complex. Firstly, the modulation function can be considered as an arbitrary

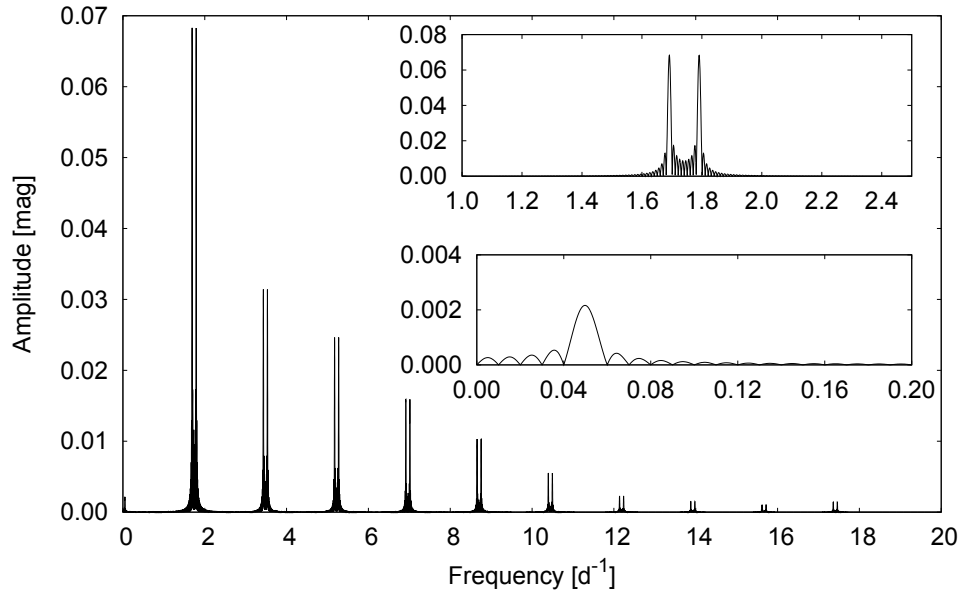


Figure 2.3: Fourier amplitude spectrum of the model of WY Ant with additional amplitude modulation ($f_m = 0.05$ d, $\phi_m = 0^\circ$, $a_0 = 0.005$, $h = 0.43$) after prewhitening with the basic pulsation components. The top detail shows the vicinity of f_0 , while the bottom insert shows the modulation peak.

periodic signal represented by a Fourier sum with a constant frequency. Light changes of a star with such modulation can be expressed analogically to eq. 2.5 as

$$m_{AM} = \sum_{p=0}^q \sum_{j=0}^n \frac{a_p^A}{2} a_j \sin \left[2\pi(jf_0 \pm pf_m)t + \phi_{jp}^\pm \right], \quad (2.6)$$

where $\phi_{jp}^+ = \phi_j + \phi_p - \pi/2$, $\phi_{jp}^- = \phi_j + \phi_p + \pi/2$. The index p represents the number of modulation components. The amplitudes a_p^A are defined as a ratio of the particular amplitudes of the modulation components and the amplitude of a non-modulated signal a_p/U_c . The envelopes of stars with non-sinusoidal modulation are asymmetric, and the shape of a particular envelope depends on the actual values of a_p^A and ϕ_p .

The examples of synthetic light curves constructed on the basis of a two-term sum of the modulation signal are in fig. 2.4. Evidently, maxima and minima of the envelopes appear at the same Blažko phase as in the previous sinusoidal case. The frequency spectrum of a star with non-sinusoidal modulation is, after prewhitening with the main pulsation components, dominated by equidistant side peaks around jf_0 . The number of additional peaks on each side of jf_0 corresponds with the number of components of the modulation. In addition, the harmonic components of the modulation frequency pf_m appear in the low-frequency part of the Fourier amplitude spectrum (the bottom insert in fig. 2.5) in the case of non-sinusoidal modulation. Amplitudes of the side peaks meet $A(jf_0 \pm pf_m)/A_{jf_0} \sim a_p^A$. Since the amplitude a_p^A belongs to both side peaks, the frequency pattern around jf_0 is symmetric (fig. 2.5).

So far only modulations with one modulation frequency have been discussed. However, nothing prevents a multiperiodic modulation in RR Lyraes. In that case the modulation signal would be a sum of signals with different modulation frequencies. This will result in several sets of side peaks creating unevenly spaced multiplets around jf_0 and in additional peaks in the low-frequency range. Linear combinations of the modulation frequencies also appear in the parallel modulation. The envelopes of the light curves of multiple modulated stars will undergo beating phenomena

like those shown in fig. 2.6. The left panel plots a light curve when the ratio of the modulation frequencies is 9:10, while the right panel shows a light curve with a resonance of 4:3.

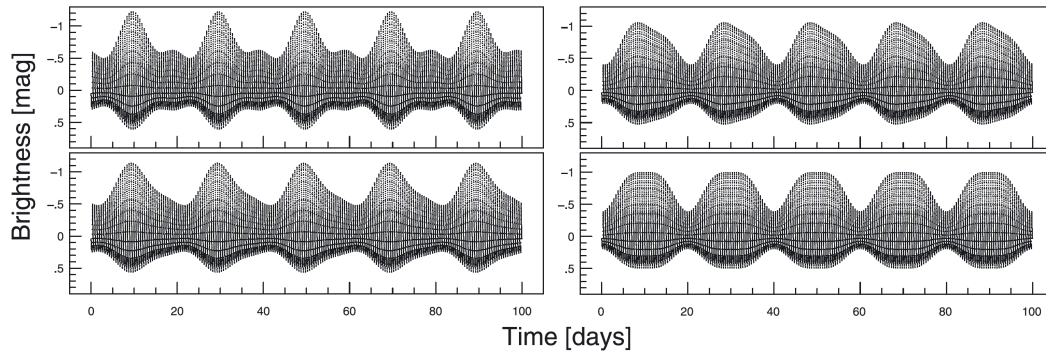


Figure 2.4: Examples of synthetic light curves of non-sinusoidal AM signals (taken from Benkő et al., 2011).

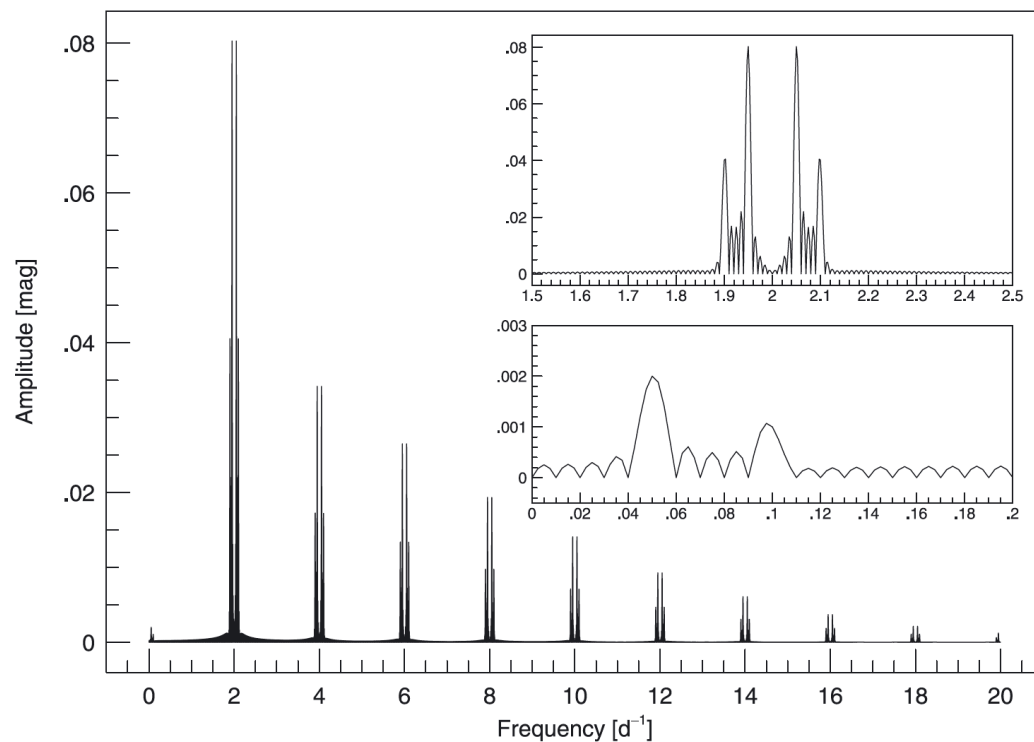


Figure 2.5: Fourier amplitude spectrum of the synthetic non-sinusoidal AM light curve after prewhitening with main pulsation frequency components $jf_0 = 2c/d$. Inserts are zooms around f_0 (top), and the modulation frequency $f_m = 0.05 \text{ d}^{-1}$ (bottom), respectively. Figure is taken from Benkő et al. (2011).

Continuing with generalizing amplitude modulation, all previously discussed types of AM can be present simultaneously and combined in various ways. In addition, the modulation itself can be modulated creating an AM cascade. All these features could influence the appearance of the Fourier amplitude spectra making them very complex and difficult to interpret.

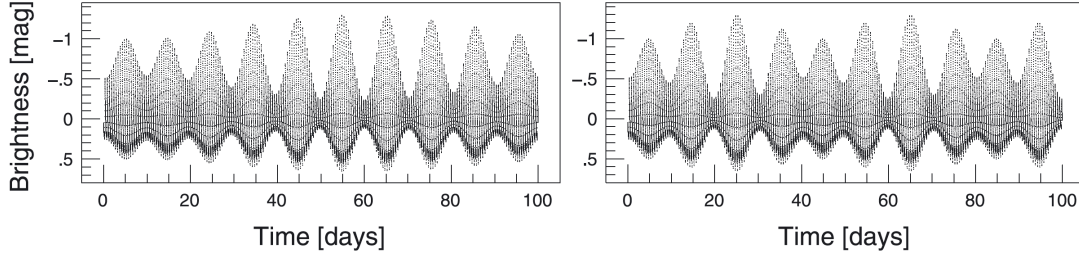


Figure 2.6: Synthetic light curves calculated with two independent sinusoidal AM modulations by Benkő et al. (2011).

2.2.2 Frequency modulation

Analogue to AM, a frequency-modulated signal can be created by adding some modulation signal $m_m(t)$ to a constant frequency:

$$m_{\text{FM}}(t) = a_0 + \sum_{j=1}^n a_j \sin \{ 2\pi j [f_0 + m_m(t)]t + \phi_j \}. \quad (2.7)$$

When the modulation signal is simple sinusoidal, this formula becomes

$$m_{\text{FM}}(t) = a_0 + \sum_{j=1}^n a_j \sin [2\pi j f_0 t + j a^{\text{F}} \sin(2\pi f_m t + \phi^{\text{F}}) + \phi_j], \quad (2.8)$$

where $a^{\text{F}} = a_m/f_m$, $\phi^{\text{F}} = \phi_m + \pi/2$. The amplitude of the signal is determined by the Fourier amplitudes a_j of the carrier wave. Thus no amplitude changes are present. Equation 2.8 can be further transformed using relations for trigonometrical and Bessel functions to:

$$m_{\text{FM}}(t) = a_0 + \sum_{j=1}^n \sum_{k=-\infty}^{\infty} a_j J_k(j a^{\text{F}}) \sin [2\pi(j f_0 + k f_m)t + k \phi^{\text{F}} + \phi_j], \quad (2.9)$$

where $J_k(j a^{\text{F}})$ is the Bessel function of the first kind with integer order k for the value of $j a^{\text{F}}$. The Fourier amplitude spectrum of FM consists of carrier components at $j f_0$ and symmetrically placed side peaks separated by f_m , while no peak at f_m is observed in the case of pure FM.

The amplitudes follow the Bessel functions. When j increases, the amplitude of the carrier decreases while the amplitude of the side peaks increase. As a consequence, the amplitude of side peaks can be higher than the peaks produced by the carrier at higher j . In addition, more side peaks around the higher order harmonics are observed, because the argument of the Bessel functions depends on the order of harmonics j . The side peaks $j f_0 \pm k f_m$ at the two sides have the same amplitude. All formerly noted features are well demonstrated in fig. 2.7, where the Fourier amplitude spectrum of a synthetic light curve is shown.

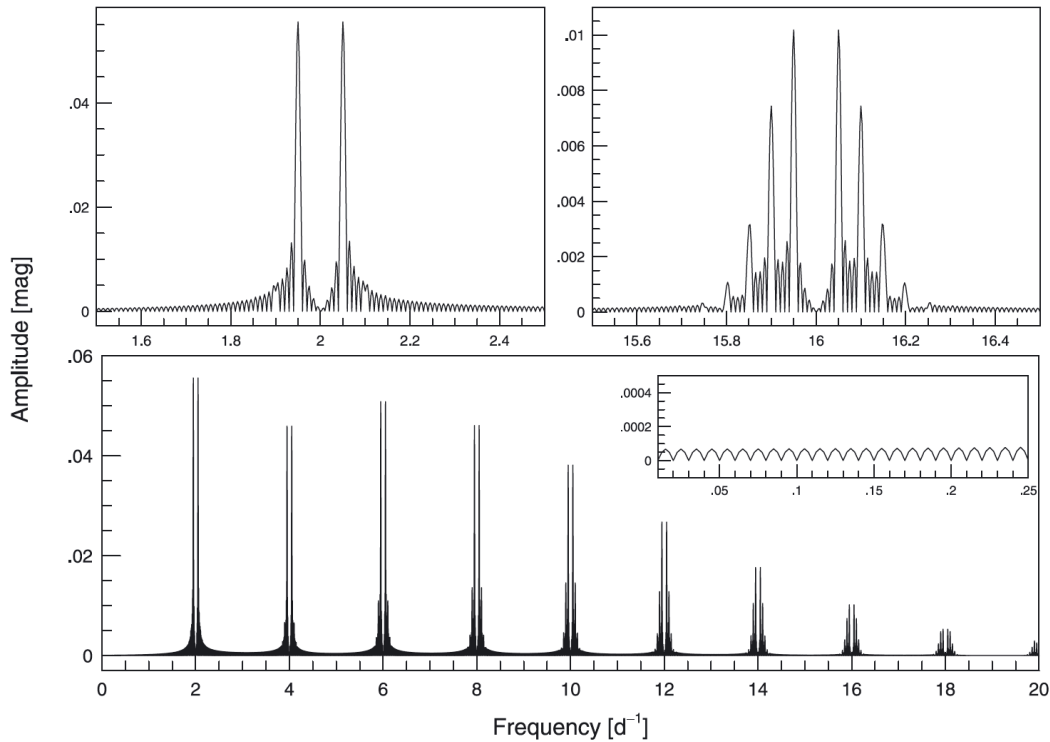


Figure 2.7: Fourier amplitude spectrum of a synthetic sinusoidal FM light curve after prewhitening with the main pulsation frequency components $jf_0 = 2$ c/d (Benkő et al., 2011). Top panels are zooms around f_0 (top left), $8f_0$ (top right panel). The insert in the bottom panel demonstrates that in the case of FM the modulation peak is missing in the low-frequency range.

Of course, there is no restriction for the complexity of FM from a mathematical point of view. As in the case of AM, it could be non-sinusoidal, compound, combined, and even the modulation itself can be modulated. This results in a very complex Fourier amplitude spectrum with forests of peaks around jf_0 which can have different amplitudes at the two sides.

2.2.3 Phase modulation

The last possibility to create a modulated signal is to let phase to be modulated. In such a case, assuming that the modulation function $m_m(t)$ does not contain any time variation, the basic equation of PM reads as

$$m_{\text{PM}}(t) = a_0 + \sum_{j=1}^n a_j \sin[2\pi j f_0 t + m_m(t) + \phi_j]. \quad (2.10)$$

The problem with PM is that there is no chance of distinguishing between FM and PM phenomena purely on the basis of their measured signals without knowledge of whether it is FM or PM. When eq. 2.10 is expressed as eq. 2.9, the arguments of Bessel functions are independent of the harmonic order j . Therefore, in PM the number of the side peaks does not increase with increasing j as opposed to FM.

2.2.4 Combined modulation

Although there are several reports on stars with pure amplitude and pure frequency modulation, it is very likely, depending on the detection limit, that in all Blažko stars AM is always accompanied by FM with the same frequency. A general formula for combined AM+FM modulation can be expressed as

$$m_{\text{Comb}}(t) = [1 + m_m(t)]m_{\text{FM}}(t), \quad (2.11)$$

where $m_{\text{FM}}(t)$ represents the general FM function (eq. 2.7). It is obvious that the Fourier amplitude spectrum should show traces of both AM and FM. An example of a synthetic light curve of a star with single sinusoidal AM and FM with $f_m = 0.05$ d is shown in fig. 2.1. The carrier of the model is based on the light curve of WY Ant. Parameters of the modulation are: $f_m = 0.05$ d, $\phi_m = 0^\circ$, $a_0 = 0.005$, $h = 0.43$, $a^F = 0.6$, the relative phase between AM and FM was set to 90° . This model has (after prewhitening with jf_0) a frequency spectrum shown in fig. 2.8.

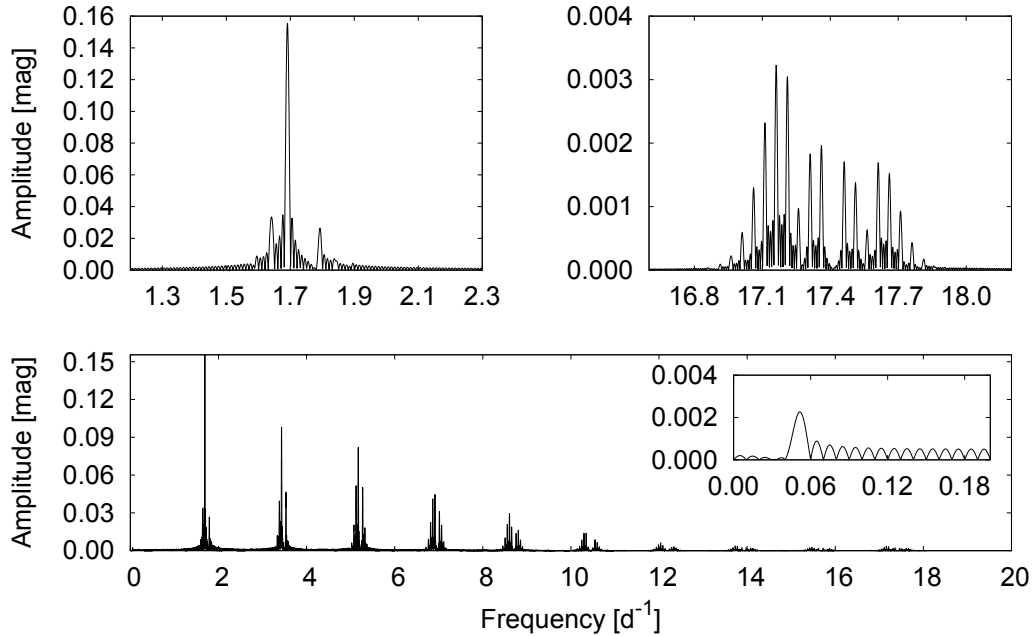


Figure 2.8: Frequency spectrum of a synthetic light curve of a star with combined AM+FM sinusoidal modulation after prewhitening with the main pulsation frequency $f_0 = 1.7411257$ c/d. The top panels are zooms around f_0 (the left), $10f_0$ (the right). The insert in the bottom panel shows the vicinity around the modulation frequency $f_m = 0.05$ d $^{-1}$.

Due to the AM component of the modulation, a peak at f_m is present (the insert of the bottom panel). The vicinity of f_0 and $10f_0$ is shown in the top left panel and in the top right panel respectively. The increase in the number of side peaks is a consequence of the FM component. It is easily seen that the multiplets are asymmetrical with regard to their amplitudes. This is the result of the phase difference between AM and FM, which is 90° in our case. When the phase difference is $0 < \Delta\phi = \phi_m^A - \phi_m^F < 180^\circ$ the side peaks with higher amplitudes are on the left-hand side of jf_0 . The maximum difference between amplitudes of left- and right-hand side peaks appears at $\Delta\phi = 90^\circ$, when the right peak can disappear², while symmetrical amplitudes are observed at

²An additional condition for disappearing of the peak is that $ja^F = hl$, where $l = 0, 1, 2, \dots$

$\Delta\phi = 0^\circ$ and $\Delta\phi = 180^\circ$. On the other hand, when $\Delta\phi \in (180, 360)^\circ$, peaks to the left from the basic pulsation frequency and its harmonics have smaller amplitudes than the right-hand side peaks with the maximum amplitude-difference at $\Delta\phi = 270^\circ$.

These findings result from the relation for the power difference of the amplitudes of l th side peaks at the j th harmonics, where the AM–FM phase difference ϕ_m is present:

$$A^2(jf_0 + lf_m) - A^2(jf_0 - lf_m) = -4 \frac{hl}{ja^F} a_j^2 J_l^2(ja^F) \sin \phi_m. \quad (2.12)$$

The relative strength of AM and FM can be investigated using maximum brightness versus maximum phase diagrams. For simple sinusoidal AM and FM the diagram form ellipses with axes of the size of h and a^F . Then, obviously, for $a^F = h$ the diagram is a circle. The inclination of the semi-major axis to the vertical horizontal position is given by the phase difference between AM and FM. Only at $l\pi/2$ the inclination is 0° . Phase difference also defines the direction of motion in maximum brightness versus maximum phase diagram. If $\Delta\phi \in (180, 360)^\circ$ it is anticlockwise, while if $\Delta\phi \in (0, 180)^\circ$ it is clockwise.

All efforts made in this section were performed to get some solid background for the interpretation of the Fourier amplitude spectra of real, observed RR Lyrae stars, and to show the possible diversity and complexity of the Blažko effect.

2.3 Observed properties of Blažko stars

2.3.1 Frequency spectra of real Blažko stars

As already noted, recent observing efforts showed that Blažko stars are always amplitude and frequency modulated simultaneously. Thus, their frequency spectra should contain multiplets with equidistant spacing around the basic pulsation frequency and its harmonics. Also the peak in the low-frequency range, which is a product of the amplitude modulation itself, is expected to be present in the Fourier amplitude spectra. A Fourier transform of signals from stars with a non-sinusoidal, composed modulation, or with changing period will be very complicated. In addition, analysis of high-precision data gathered from space telescopes revealed the presence of low-amplitude peaks at millimag range connected with radial overtones and period doubling (e.g. Kolenberg et al., 2010; Szabó et al., 2010; Kolláth et al., 2011; Molnár et al., 2014b; Benkő et al., 2014).

Nevertheless, the frequency spectra of ground-based observations significantly differ from that of the model with single modulation illustrated above, and differ from the space-based measurements as well. Fig. 2.9 clearly demonstrates these differences. The left panels show ground based data of RR Lyr and their Fourier transform, while the right panels show the data and corresponding Fourier amplitude spectrum based on data from the *Kepler* telescope.

The main problems with ground-based observations are gaps in observations and the lower precision of such measurements. Single-site observations also suffer from various aliases. This makes the frequency spectra noisy and complicate the identification of important peaks (the bottom panel of fig. 2.9). Especially gaps and phase-coverage of the data influence the frequency spectra substantially. For example, Jurcsik et al. (2005b) reported on the difference in appearance of the frequency spectrum, and different amplitudes of the side peaks when analysing datasets with the same time span, but with different coverage.

This problem is demonstrated by means of a Blažko star SS CVn in fig. 2.10. Both panels show the Fourier amplitude spectrum in the vicinity of $f_0 = 2.08978$ c/d (the red dashed line) after prewhitening with this frequency and its detectable harmonics. The left panel is based on

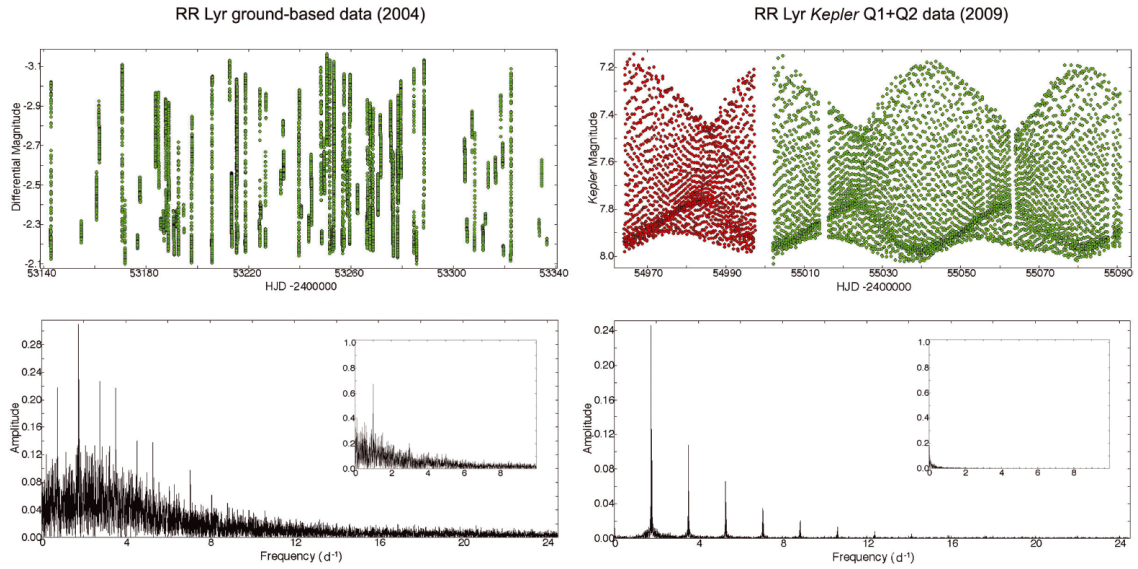


Figure 2.9: Comparison of the multi-site (six observatories) ground-based data (the left panels) and data from the *Kepler* (the right panels) of the prototype star RR Lyr. The high noise level and aliases resulting from the gaps in observations and incomplete phase coverage are clearly apparent in the bottom left panel. Figure is taken from Kolenberg et al. (2011).

low-cadence, low-quality NSVS measurements *Northern sky variability survey* (Wozniak et al., 2004) with time span 1 year (210 points), while the right panel shows spectrum of high-cadence SuperWASP data (8800 points in three years) which, on the other hand, suffer from large gaps (for more details about SuperWASP data characteristics see sec. 4.2). It can be seen that the left peak has the same amplitude in both surveys, while the right peak from SuperWASP data is almost twice as big as in NSVS.

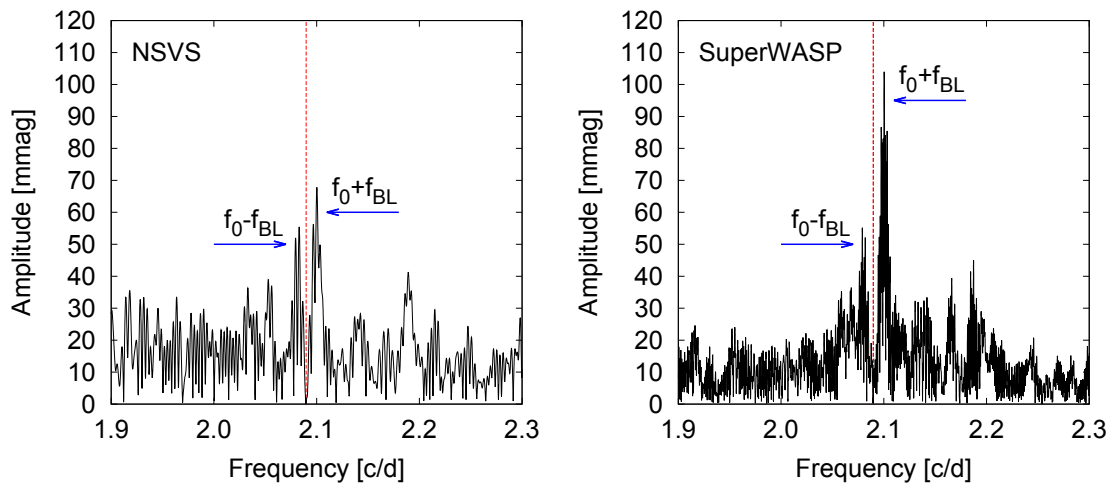


Figure 2.10: The vicinity of the position of f_0 is indicated by the vertical red dashed line in the Fourier amplitude spectra of SS CVn after prewhitening this frequency and its harmonics. The left and right panel is based on NSVS and SuperWASP data respectively.

All these issues could prevent peaks of low amplitude from being detected and could lead to a misinterpretation of the type of modulation (single, parallel, etc.). For example, a highly asymmetric triplet can mimic as a doublet when the low amplitude peak vanishes in noise, a modulation peak at low-frequency range is undetectable etc. High-quality data requirements were probably the reason why structures with more than two side peaks were revealed only recently. The first quintuplet was identified by Hurta et al. (2008) in RV UMa. Jurcsik et al. (2008) found a sextuplet in the frequency spectrum of MW Lyr, while Chadid et al. (2010) detected even eighth order multiplet frequencies in the Fourier amplitude transformation of *CoRoT* data of V1127 Aql. Before these discoveries it seemed that the majority of Blažko stars show doublets in their spectra (studies of RR Lyraes in the LMC and GB by Alcock et al., 2003; Moskalik & Poretti, 2003).

Alcock et al. (2003) introduced the classification of Blažko RRab stars on the basis of their frequency spectra as RR0-BL1 (one close frequency component to jf_0), RR0-BL2 (two close symmetric frequency components to jf_0), RR0- ν M (several close components), RR0-PC (stars with period change with close side peaks which can not be resolved). However, this classification become obsolete in the era of longer observational data sets and more precise space measurements.

For the characterisation of the asymmetry of triplets we could either use the power amplitude difference (eq. 2.12) or asymmetry parameter Q_A ³ defined by (Alcock et al., 2003) as

$$Q_A = \frac{A_+ - A_-}{A_+ + A_-}, \quad (2.13)$$

where A_+ and A_- are the amplitudes of modulation peaks to the right and to the left from jf_0 , respectively. From the definition, $Q_A > 0$ when $A_+ > A_-$. Alcock et al. (2003) found that 74 % of all Blažko stars that they studied have the peak with larger amplitude to the right of f_0 . Moskalik & Poretti (2003) who investigated GB stars obtained a similar result (80 %). This tells us that, according to sec. 2.2.4, in the majority of modulated RR Lyrae stars the phase difference between amplitude and phase modulation is between 180 and 360°. This could possibly be a general property of RRab stars.

Concerning RRc stars in the LMC, the situation is the opposite. Alcock et al. (2000) found that 63 % of modulated RRc stars have $A_- > A_+$. Nevertheless, due to many factors that could influence the appearance of Fourier amplitude spectra, one has to be very careful when interpreting the information on the asymmetry of the triplet in the case of low quality, badly sampled, ground-base data with large gaps as it was demonstrated in fig. 2.10.

The deviation of equidistant spacing can be examined using

$$\delta f = f_+ + f_- - 2f_0. \quad (2.14)$$

Subscripts '+' and '-' relate to the peak with higher and lower frequency than f_0 , respectively. In stars observed from the ground with a non-equidistant triplet it is probable that their modulation actually has two components with $f_{m1} = f_+ - f_0$ and $f_{m2} = f_0 - f_-$, and that their mirror frequencies remain hidden in noise.

Multiperiodic modulation has been reported in several cases so far. For example, LaCluyzé et al. (2004) detected two periods in the modulation of XZ Cyg, Sódor et al. (2006) identified two modulation components in UZ UMa, and CZ Lac appeared to be a star with two modulation periods, which are in a 4:3 resonance (Sódor et al., 2011). Very recently, Benkő et al. (2014) analysed complete data sets available from the *Kepler* space telescope, and found that 12 out of 15 Blažko stars studied show a parallel modulation. In addition, they found that the ratio between the primary and secondary modulation is almost always very close to the ratios of small integer numbers. This clearly indicates that multiple modulation is rather more common than rare.

³Do not confuse this parameter with pulsation constant defined in sec. 1.2.1.

2.3.2 The length of the Blažko cycle

Usually, periods of the Blažko effect given in literature range from a few days to a few thousands of days. However, the upper limit is very unclear, because it is very difficult to distinguish between continuous period change and long-term Blažko effect when examining time-limited data sets.

Among RRab stars, SS Cnc and AE PsA has the shortest known modulation period of 5.3 d (Jurcsik et al., 2006) and 5.78 d (Szczygiel & Fabrycky, 2007), respectively. V1645 Sgr occurs in the long-period tail of the distribution. This star has $P_{BL} = 1331$ d (Szczygiel & Fabrycky, 2007). However, most modulated RRab stars have Blažko periods between 30 and 70 d, as shown in fig.

2.11, where the distribution of the length of the Blažko cycle of RRab stars from the LMC is shown. This dependence is highly asymmetric with a steep increase and a slow decline towards longer modulation periods.

The distribution of the Blažko period P_{BL} versus the main pulsation period P for galactic Blažko stars is shown in fig. 2.12 giving a nice comparison of the distribution of modulation periods for RRab and RRC Lyraes stars (taken from Szczygiel & Fabrycky, 2007). RRab stars show an almost homogeneous transition from short to long periods, while RRC stars exhibit a strongly bipolar distribution with preference for short periods of about 10 d and long periods with a condensation around 1500 d. Between 20 d and 300 d no modulated galactic RRC stars are observed.

No clear correlation between pulsation period and the length of the modulation cycle is known so far. However, Jurcsik et al. (2005a) examined a large sample of 894 single-modulated RR Lyrae stars which are located in various stellar systems including e.g. the LMC, Galactic bulge

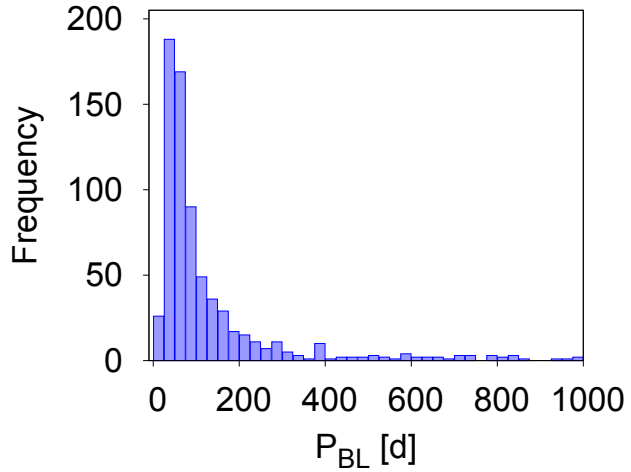


Figure 2.11: Blažko period distribution of RRab stars in the LMC from MACHO survey (Alcock et al., 2003).

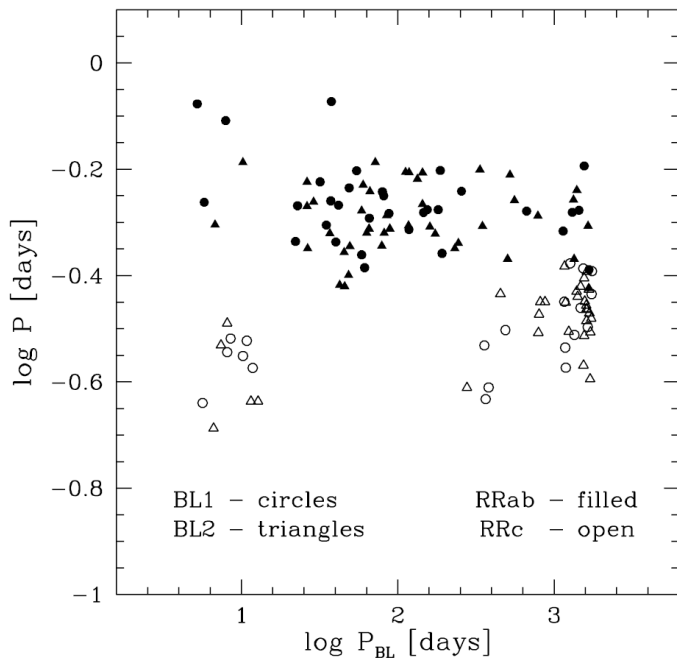


Figure 2.12: The distribution of galactic modulated RR Lyrae stars taken from Szczygiel & Fabrycky (2007).

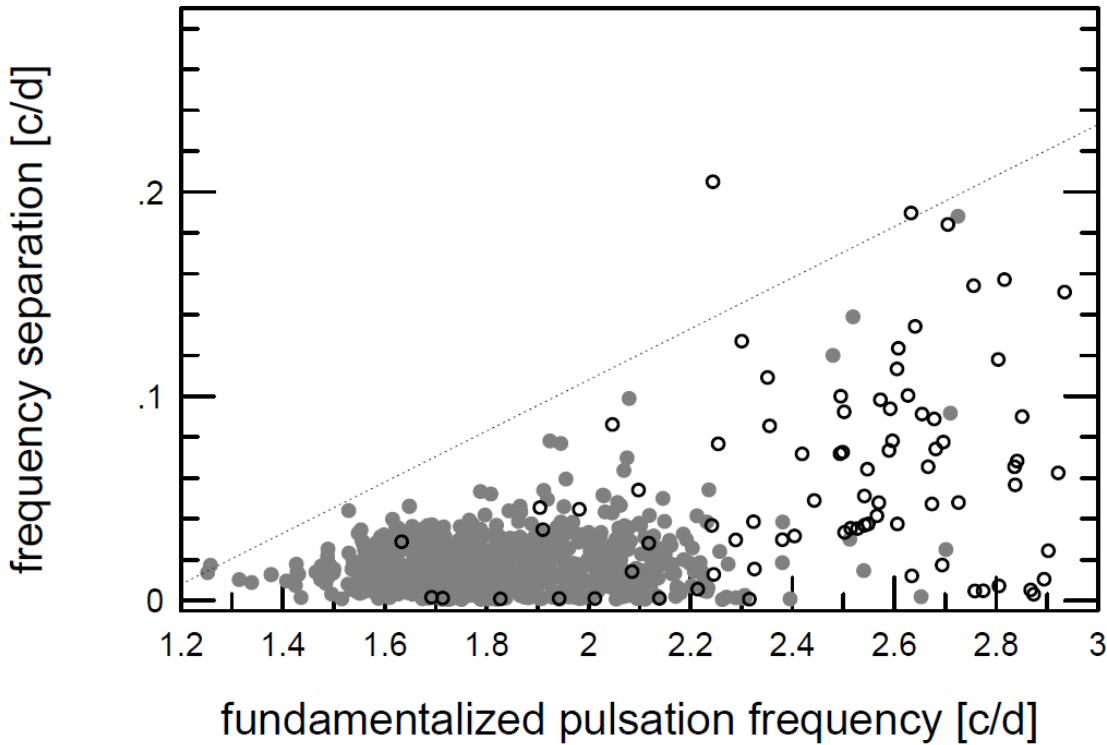


Figure 2.13: The frequency separation versus pulsation period for 894 stars studied by Jurcsik et al. (2005a). The dashed line represents the dependence from eq. 2.15. Open and filled circles represent RRc and RRab stars, respectively.

and GCs. They found that the possible maximum value of the modulation frequency depends linearly on the pulsation frequency f_0 as

$$\text{MAX}(f_{\text{mod}}) = 0.125f_0 - 0.142. \quad (2.15)$$

In other words, short period variables ($P < 0.4$ d) could have a modulation period as short as some days, while longer period variables ($P < 0.6$ d) always exhibit modulation with P_{BL} longer than 20 days (fig. 2.13). They linked this behaviour with the surface rotation velocity. However, this is probably a secondary effect, because there are evidences that the length of the cycle is primarily not a consequence of the rotation of the star (see sec. 2.6).

Due to frequency modulation the basic pulsation period of Blažko stars changes during the modulation. The best way to estimate the strength of such changes is through $O - C$ diagrams. Period-changes during the modulation cycle can be almost undetectable in some cases (e.g. KIC 11125706, Nemeč et al., 2013), but they can be very strong with an amplitude of more than 0.1 d, which is the case with V445 Lyr (Guggenberger et al., 2012).

In some cases the Blažko effect can be unstable over long time scales. RR Lyrae itself undergoes a 4-year long cycle during which the modulation characteristics change. Detre & Szeidl (1973) reported that in June 1971 the amplitude of modulation was almost undetectable, while in April 1972 maximum amplitude was observed again. Currently the rate of changes in modulation period is of about 2% from 38.4 to 39.2 days (Kolenberg et al., 2014). In addition, during the twentieth century the length of the modulation cycle of RR Lyr irregularly changed between about 41 d and 38 d (e.g. Kolenberg et al., 2006, 2011; Le Borgne et al., 2014). Stothers (1980) connected

the long-term changes with the cycles analogous to the 11-year Solar cycle. However, observations have not confirmed this assumption. In some stars almost complete disappearing of the modulation was also reported (e.g. in RRc star GSC 02626-00896, Groebel, 2013).

The changes in the modulation period are usually accompanied with changes in the basic pulsation period. These variations can be parallel (lengthening of P_{BL} results in lengthening of the basic pulsation period) or antiparallel at different times. Except for an eponym RR Lyr, a simultaneous change of the Blažko and pulsation period was also observed in other stars, e.g. in XZ Cyg (LaCluyzé et al., 2004), XZ Dra (Jurcsik et al., 2002), or in RV UMa (Hurta et al., 2008).

2.3.3 Amplitude of the modulation

The change in amplitude of the light curve of a Blažko star is the most evident manifestation of the modulation. The observed range is very wide. Although it is usually about a few tenths of a magnitude, it can be as small as a few hundredths of a magnitude, and therefore almost undetectable in low quality data. On the other hand, it can dominate the phase light curve with changes up to more than one half of a magnitude. For example, the total amplitude of the modulation of KIC11125706 is only about 0.01 mag (Benkő et al., 2014), while V445 Lyr shows one of the largest known amplitudes of modulation with the amplitude of about 0.6 mag (Guggenberger et al., 2012; Benkő et al., 2014).

Is there any connection between pulsation frequency and the modulation amplitude? Firstly, the modulation amplitude has to be defined which is not at all straightforward. For example, when the modulation is not pure amplitude modulation, the amplitude of the variation in the height of maxima may significantly underestimate the real strength of the modulation. One approach to estimate the modulation amplitude is to sum the Fourier amplitudes. This was what Jurcsik et al. (2005c) performed. They summed the amplitude of the first four modulation components for several hundreds of stars and plotted it against the pulsation frequency (fig. 2.14). A result of their study was that the possible largest value of the modulation amplitudes increases towards longer pulsation frequencies. Nevertheless, as they warned, their finding could be somewhat unreliable due to using only the Fourier amplitude sum of the first four modulation components, while the sum of all the detectable modulation components in their data gave significantly higher results. Also the amplitude of the maximum brightness variation was higher.

Benkő et al. (2014) plotted the Blažko period vs. amplitude of the AM frequency of the Fourier transform of modulated stars in the *Kepler* field of view. Their plot indicates a slight increase of amplitude with increasing modulation period. Nevertheless, they could not rule out that this behaviour might only be the effect of a small sample. Therefore, the correlation of the modulation amplitude with the periods of RR Lyrae stars remains unclear.

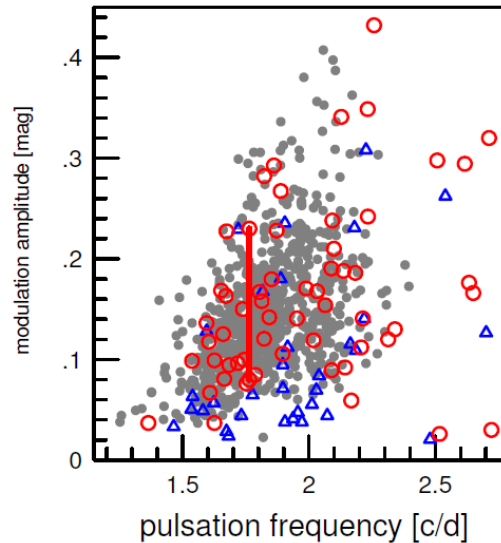


Figure 2.14: Modulation amplitude plotted vs. pulsation frequency (taken from Jurcsik et al., 2005c). Circles are for Galactic field stars, triangles for stars in the Galactic bulge, and grey dots represent RR Lyrae stars from the LMC.

2.4 Incidence rate of Blažko stars

Thanks to the currently available precise measurements it seems that the estimation of the fraction of modulated stars among RRab variables converges to about a half. However, this is not a general property, because the incidence rate differs in different stellar systems, and on data sets that various authors use. For RRc stars the fraction of modulated stars presented in literature is from 5 to 40 % depending on the particular stellar system.

One of the first reliable estimations of the fraction of field RRab stars was given by Szeidl (1976). His percentage was 15 – 20 %. However, twelve years later it was 20 – 30 % (Szeidl, 1988). Both estimates are from studies based on relatively small samples of stars, but with relatively precise measurements. Contrary to these findings, results from large scale sky surveys from the beginning of the new millennium showed a significant drop in these statistics. Based on the ASAS data Szczygiel & Fabrycky (2007) found only 5.1 % of field RRab stars to be modulated, while Kinemuchi et al. (2006) obtained a slightly lower result on the basis of NSVS data (4.3 %).

Nevertheless, recent findings indicate that the true incidence rate is probably much higher. Starting in 2004, the Hungarian group around J. Jurcsik and B. Szeidl began to collect accurate, extended, multicolour light curves of northern fundamental mode RR Lyraes. This project, called *The Konkoly Blažko survey*, led to the discovery of many interesting and important results (e.g. Sódor, 2007; Sódor et al., 2012; Jurcsik et al., 2009, and references therein). Within the scope of this survey, which was dedicated to the monitoring bright RR Lyraes (up to 14 mag in minimum light), it was found that the incidence rate is surprisingly high. About 47 % of RRab stars with $P < 0.5$ d, and about 43 % in the sample without period limitation, were found to be modulated.

A similar result was obtained with ultra-precise measurements gathered using the *Kepler* space telescope. Kolenberg et al. (2010) reported that at least 40 % of RR Lyraes monitored by *Kepler* undergo modulation. A year-later study by Benkő et al. (2011) showed the incidence rate as 48 % based on *Kepler* data. Szabó et al. (2014) found that 60 % of RRab stars observed by CoRoT space telescope show modulation. However, this could be observational bias since only 10 RRab stars are present in this field.

Outside our Galaxy the incidences of modulated stars are heterogeneous. In addition, the given percentages changed significantly during recent years. For example, Alcock et al. (2003) studied stars in the LMC from the MACHO survey, and found the incidence rate of RRab Lyraes with side peaks close to the main pulsation frequency as 11.9 % (731 of 6158 stars). Six years later, Soszyński et al. (2009) found in their analysis of OGLE data of 17 693 stars in the LMC that about 1/5 of this RRab sample show modulation. Concerning LMC RRc and RRe stars, close frequency peaks were identified in 6 % and in 23 % respectively (Soszyński et al., 2003). In 2009 it was 19 % and 25 % (Soszyński et al., 2009). The most recent results on RR Lyraes in the Galactic bulge report on at least 30 % of RRab and 8 % of RRc with modulated light curves (Soszyński et al., 2011). In the SMC the fraction of the Blažko stars is about 22 % for RRab stars and 16 % for RRc pulsators (Soszyński et al., 2010), respectively.

In GCs the ratio of modulated to regular stars differs. For example, in M3 50 % RRab Lyraes have Blažko unstable light curves (Jurcsik et al., 2012), 60 % of RRab stars are modulated in M5 Jurcsik et al. (2011)⁴, while Arellano Ferro et al. (2012) detected modulation in 11 out of 24 RRab, and in 23 out of 31 RRc Lyraes, which brings incidence rates of 46 % and 74 % for RRab and RRc stars in M53, respectively.

⁴No modulated RRc star was observed in M5.

For a better arrangement, recent incidence rates for RRab stars in various stellar systems are listed in Tab. 2.1. All given examples clearly illustrate the importance of high-quality data with a large time span to properly identify modulation and its properties.

Table 2.1: The fraction of modulated RRab stars in various stellar system.

Galactic field	47 %	Jurcsik et al. (2009)
Galactic field	48 %	Benkő et al. (2011)
LMC	20 %	Soszyński et al. (2009)
SMC	22 %	Soszyński et al. (2010)
Galactic Bulge	30 %	Soszyński et al. (2011)

2.5 The difference between Blažko and non-modulated stars

Due to modulation it can be expected that Blažko RR Lyraes should have smaller average total amplitudes than regular stars. This is precisely what Szeidl (1988) observed. He found that the maximum amplitude of modulated stars resembles the amplitude of non-modulated RR Lyraes. In other phases of the modulation the amplitude was lower than for regular stars.

Concerning the shape of light changes, the mean light curves of Blažko stars are generally less skewed than those of ordinary stars. This means that larger rise times and lower values of higher order Fourier amplitudes can be expected in modulated stars. This assumption was confirmed by Alcock et al. (2003) who compared Fourier parameters ϕ_{i1} of Blažko and single-periodic stars in the LMC. In addition they found that Fourier phases of Blažko and regular stars are almost comparable in average. This result has an important implication. It provides, due to no, or very slight difference between phases, the possibility to use period-phase-metallicity relations also for modulated stars.

A still fully unanswered question is whether there is any difference in periods of Blažko and non-Blažko stars. From many analyses it seems that modulated stars generally could prefer shorter periods than ordinary RR Lyraes. For example, when we compare the average pulsation period of Blažko stars in the LMC from Alcock et al. (2003) with the average period of all RR Lyraes which are available in the OGLE database, we found that $P_{BL,avg} = 0.552$ d and $P_{All,avg} = 0.573$ d. Szczygiel & Fabrycky (2007) reveal that the number of field Blažko stars falls rapidly for pulsation periods longer than 0.65 d. Smolec (2005) noticed similar behaviour in his analysis of RR Lyrae stars in the LMC and GB. Although the distributions of stable and modulated stars in the GB look very similar, Blažko stars also have slightly lower periods in this galactic subsystem (Mizerski, 2003). Jurcsik et al. (2011) also reported that the average pulsation period of modulated stars in globular cluster M5 is about 0.04 d shorter than the mean period of the entire RRab sample. In addition, they noted that among stars with $P < 0.55$ d the incidence rate of Blažko stars is about 60 %. A recent detection of helium emission only in modulated stars, which all have short pulsation periods, could also indicate the short-period preference of Blažko variables (Gillet et al., 2013a). At this point it should be clear that modulated stars really have shorter periods.

The situation with different absolute magnitude of modulated RR Lyraes reported by some authors is not as clear as with periods. Alcock et al. (2003) found no difference for stars in the LMC, Arellano Ferro et al. (2012) observed the same in M53, while Jurcsik et al. (2011) reported on a slight tendency of modulated stars to be fainter by about 0.05 mag than their stable counterparts. Only further observations could put some light on this problem.

According to Jurcsik et al. (2011) RRab Lyraes in M5 are bluer than regular RR Lyraes. As a result of this finding they speculated that the Blažko effect may have an evolutionary connection with the mode switch from fundamental to overtone-mode pulsation. Also Arelano Ferro et al. (2012), who noted that Blažko RRc stars in M53 are redder than the regular RRc RR Lyraes, proposed an evolutionary nature of the Blažko modulation. Nevertheless, Blažko RRab Lyraes in M53 do not show any distinct colour preference. Gillet (2013b) constructed HRD with field RRab Lyraes with accurately determined parameters, and found clear evidence that Blažko stars are hotter than their ordinary counterparts (fig. 2.15). However, this result could be misleading, because of very few stars used. The temperature dependence of the Blažko effect is another controversy which needs to be resolved.

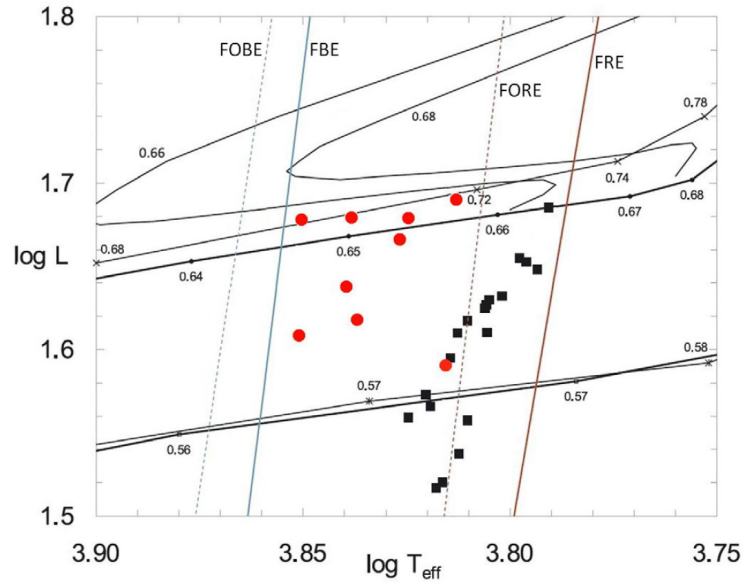


Figure 2.15: The Hertzsprung-Russell diagram of field RRab stars with accurate parameters (taken from Gillet, 2013b). Blažko stars (the red circles) are clearly separated from regular variables (the black squares) observed with *Kepler* telescope (Nemec et al., 2011).

The latest period-change statistics of field Blažko stars (based on GEOS collection of maximum timings) show that the majority of modulated stars show irregular period changes (Vandenbroere et al., 2014). Similar behaviour was observed in M3 (Jurcsik et al., 2012). Further, the rest of modulated stars from the Galactic field prefer increasing periods which would indicate late evolutionary stage with higher luminosity. This is contrary to finding of Jurcsik et al. (2011) that Blažko stars in M5 are slightly fainter than regular stars. In addition, the situation with modulated stars is exactly opposite for stars in M3 than for stars in Galactic field, because Jurcsik et al. (2012) found that Blažko stars prefer (except for irregular changes) period decrease. Therefore, behaviour in period changes is another controversy which needs solution.

The different incidence rates in different stellar systems directly raise a question whether the Blažko effect depends on metallicity. This represents one of the most quoted problems, which also has not been resolved yet. Szeidl (1976) divided the Blažko stars according to their spectroscopic metallicity, and found that a lower metallicity means a higher incidence rate of modulated stars. Moskalik & Poretti (2003) obtained the exact opposite result in their study of Galactic bulge stars using the comparison of Fourier phases ϕ_{i1} . Smolec (2005) proved the Blažko-metallicity dependence with a negative result through the analysis of RR Lyraes from the Galactic bulge and the LMC. Since the distribution of Blažko stars indicates a significant drop at long periods (stars with low metal content), it could be possible that modulated stars could indeed be missing in a low metallicity range.

2.6 Explanation of the Blažko effect

Recently, mainly due to results from space measurements, it seems that astronomers are close to solving the century old problem of the nature of the Blažko effect. However, the journey to this point has not been straightforward, and history has witnessed many false directions. Here is a brief survey of proposed models originated from various physical effects.

The first solution for the Blažko effect was provided by Kluyver (1936), who proposed the observed long time changes to be attributed to the interference between the fundamental and the second overtone mode. The idea of resonances of radial modes was well foresighted, and was revived and refined several decades later.

Some authors linked the modulation changes of Blažko stars with a binary nature. For example, Fitch (1967) assumed that in binary systems with close components the pulsation radial mode would be tidally modulated by the companion. Kinman & Carretta (1992) explained the modulation of AR Her as a consequence of a non-resolved pair of RRab and RRC stars with pulsation periods of 0.47 and 0.233 d. An alternative explanation of the behaviour of AR Her was provided by Borkowski (1980). In his model the modulation is a consequence of near-resonant double-mode pulsation involving the fundamental and the second or third radial overtone. The frequency ν of the additional mode would be a combination of a pulsation frequency ν_0 and Blažko frequency ν_{BL} expressed as $\nu = 2\nu_0 + \nu_{BL}$. However, Borkowski (1980) noted that in his 2:1 resonant model the mass of the star, determined from pulsation properties, would be unrealistically high. A similar solution was introduced by Moskalik (1986), who also proposed a 2:1 resonance between the fundamental and the damped third radial overtone. However, his model was not able to describe light variations of Blažko stars with long modulation periods and changes in modulation.

Nevertheless, the idea of resonances between radial modes was not rejected out of hand, and it has experienced a renaissance very recently. The reason for reviving the idea was the discovery of half integer frequencies (HIFs) in frequency spectra of modulated stars observed from space. These additional peaks, which appear around $f_0/2, 3f_0/2, 5f_0/2 \dots$, are products of the so called *period doubling* (PD), which causes alternating of the light curve shape. Especially changes in amplitude are most conspicuous. Such behaviour was observed in RV Tauri variables (Preston et al., 1963) and, for example, in the Mira star R Cyg (Kiss & Szatmáry, 2002). Moskalik & Buchler (1990) found PD connected with a 3:2 resonance between fundamental and the second overtone in their Cepheid models. Smolec et al. (2013) detected PD in a population II Cepheid of BL Her type, BLG184.7 133264, located in the Galactic bulge.

In Fig. 2.16 the PD is demonstrated using Blažko star V808 Cyg. The plots are based on more than 48 000 measurements from *Kepler* (taken from Benkő et al., 2014). In the top left panel the first part of the observations is plotted. It is seen that the modulation of V808 Cyg is highly non-sinusoidal (sharp triangle maxima of the Blažko cycle). In addition, data phased with the basic pulsation period are shown in the zoomed part of this panel. The area defined with a narrow rectangle in the top left panel is zoomed in the top right panel. The alternations of the height of maxima are easily seen. Finally, the part of frequency spectra after prewhitening with $jf_0 \pm f_{BL}$ up to $j = 10$ is plotted in the bottom panel. The spectrum is dominated by the side peaks $jf_0 \pm 2f_{BL}$ and HIFs which are labelled. For a better arrangement the positions of jf_0 are also marked by the dotted lines.

The reason why the PD was not revealed until recently is very simple. Since most RRab stars have periods of about half a day, the ground-base observation of a subsequent maximum is impossible because of its occurrence during daytime. In addition, the depths of these alternations change during the Blažko cycle and even from the modulation cycle to another in an almost random way, which results in a change of amplitude of HIFs.

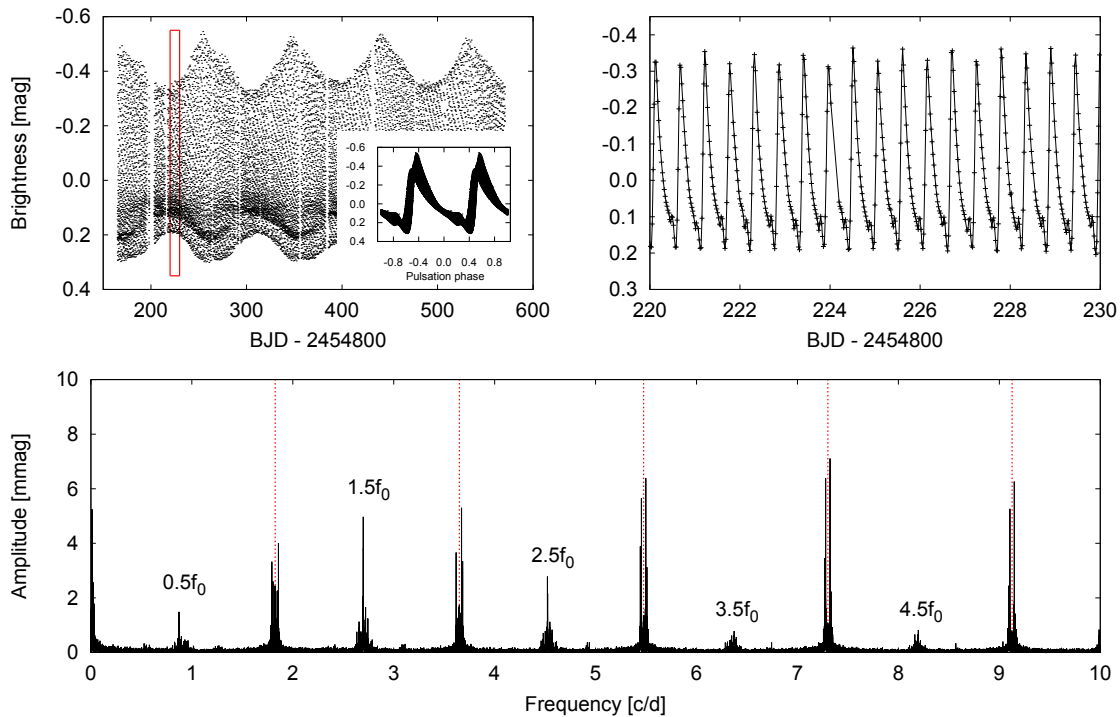


Figure 2.16: The plots in this figure are based on the *Kepler* data for V808 Cyg (after Benkő et al., 2014). The top left panel shows time series of the first part of measurements. A phased light curve is plotted in detail of this panel. The narrow rectangle delimits the area which is shown in the top right panel with a better resolution. The frequency spectrum after prewhitening with first ten triplets is shown in the bottom panel. The dotted red lines show the positions of jf_0 . Labels identify the position of HIFs.

Most, but not all of Blažko stars show PD. For example, an indication of PD was detected in 9 out of 15 modulated stars from the *Kepler* telescope (Benkő et al., 2014), and in four out of six stars from the *CoRoT* satellite (Szabó et al., 2014). Since this phenomenon is observed only in Blažko stars, it could be crucial for understanding the modulation in RR Lyraes. Therefore, Kolláth et al. (2011) performed a detailed hydrodynamic modelling, and confirmed the assumption of Szabó et al. (2010) that the fundamental pulsation mode can become destabilized by a 9:2 resonant interaction with the 9th (strange) overtone resulting in PD⁵. On the basis of the amplitude equation formalism, Buchler & Kolláth (2011) showed that the 9:2 resonance could not only be the cause of the PD, but also of the modulation. In addition, they also demonstrated that irregular amplitude modulations, that are often observed, can occur naturally as a result of the non-linear, resonant coupling between the fundamental and the 9th overtone over a broad range of physical parameters. Although this model is not perfect⁶, this explanation is currently considered as the most promising for unravelling the Blažko effect.

However, two alternative models appeared very recently. The first of them, the *Hybrid model* (Bryant, 2014a), deals with interactions between the fundamental mode and the first overtone which both have the same frequency. The fundamental mode is sinusoidal, while the first overtone, if excited to high amplitudes, drops in frequency and becomes highly non-sinusoidal. Bryant (2014a)

⁵Also other half-integer resonances with different overtones could be possible Kolláth et al. (2011).

⁶For example, Bryant (2014b) argued that the amplitudes of HIFs and basic pulsation components do not reflect the necessary rate of energy transfer between the fundamental and the 9th overtone, and that the fact that HIF at $3f_0/2$ has a higher amplitude than the HIF at $9f_0/2$ could rather indicate the presence of a 3:2 resonance than a 9:2 resonance (in such case the HIF at $9f_0/2$ would be $3 \times 3f_0/2$).

succeeded fairly well in fitting the *Kepler* light curve of RR Lyr when the additional contribution from the mode with $3f_0/2$ was included. He assumes this additional mode to possibly be a non-radial mode. Then the long-term change in modulation can be explained as a resonance between this mode and other close non-radial modes which could also be excited.

In his next paper, Bryant (2014b) expands and modifies the hybrid model concerning the near-resonant type of double-mode pulsation. In this model, two oscillations with slightly different frequencies gradually slip in phase producing a beat frequency. The first, non-sinusoidal component with frequency correlating with the pulsation frequency of the star f_0 is composed of two non-sinusoidal sub-components, while the second component with a frequency of $f_2 = f_0 + f_{BL}$ is sinusoidal. The author proposes that the fundamental and non-radial mode with $l = 1$ possibly can be involved in this model. Bryant (2014b) was able to reproduce many features observed in *Kepler* data of RR Lyr including the motion, disappearance and reappearance of the bump, and the upper and lower Blažko envelope functions. Although he gives some arguments against the 9:2 resonant model (note 5 at the previous page), his model also needs to be slightly improved, because it seems that it does not reproduce the PD. In addition, although the author gives some alternatives, the origin and the mechanism for generation of the sub-components of the first pulsation component are not fully explained.

Another recent model involved in the solution of the Blažko effect was introduced by Gillet (2013b). His explanation deals with interacting shock waves in the atmosphere producing the Blažko modulation. Since the involved physical mechanisms are non-linear, the Blažko process is expected to be unstable and irregular. In this *Shock wave model* both the fundamental and first overtone modes are excited. The author proposes that the 9:2 resonant model together with the interacting shock hypothesis could lead to the final solution of the Blažko enigma.

Just for completeness three other most promising models, which were rejected only recently by observations and theoretical modelling, have to be mentioned. The first two of them involve non-radial pulsations. They are: *Non-radial Resonant Rotator* (NRRP; e.g. Dziembowski & Mizerski, 2004) and *Magnetic Oblique Rotator/Pulsator* (MORP; Shibahashi, 2000). In NRRP it is assumed that the non-radial mode with $l = 1$ and $m = \pm 1$ is easily excited. The modulation is then the consequence of rotation. This model predicts symmetric triplets in the frequency spectra. The MORP model assumes that in strong dipole magnetic fields non-radial pulsations with $l = 2$ and $m = 0$ will be excited. When the magnetic axis is inclined to the rotational axis, modulation will be observed due to the rotation of the star. This model predicts symmetric quintuplets in frequency spectra. However, both models were ruled out, because none of them is able to explain higher order multiplets, asymmetric amplitudes of the side peaks, and irregularity in the Blažko cycle. Since no strong magnetic field in the order of 1 kG was observed in RR Lyraes (Chadid et al., 2004; Kolenberg & Bagnulo, 2009), the MORP model could survive no longer.

Stothers (2006, 2010) proposed a completely different mechanism from others which proceeds from the variable turbulent convection in outer stellar layers caused by cyclic changes in the magnetic field. Although this idea was very attractive from its stochastic nature possibly explaining the irregularities in pulsation and Blažko cycles observed in many variables, the convection model does not give any prediction of observable properties. In addition, Stothers neither gives any estimation of the strength of the magnetic field nor any detail about the interaction between the magnetic field, turbulent convection and pulsation.

Smolec et al. (2011) put Stothers' idea to the test through non-linear hydro modelling based on the Warsaw hydrocode (Smolec & Moskalik, 2008). They neglected the effects of magnetic field and only assumed the time-variable strength of the turbulent convection (described by a cyclic variation of the mixing length parameter α). With this simplified, but still very illustrative model, they were able to reproduce the modulation of the light curve of RR Lyr (based on *Kepler* data)

only with a huge, physically unrealistic modulation of α (in the order of $\pm 50\%$) over relatively short time scales of several tens of days.

Current models indicate that the Blažko effect could be caused by interaction between radial modes possibly further influenced by non-radial pulsations. Some hints, especially the position of Blažko variables in the HRD, suggests that evolutionary effects are responsible for the modulation of RR Lyraes.

Chapter 3

Observational efforts on RR Lyrae type stars

Special observational campaigns and observations devoted to particular object(s) are very valuable even in the era of space measurements and large sky surveys. With an individual approach an observer can allocate a great deal of observing time to carefully selected objects of interest. The main advantage of such observations is the ability to precisely manage the observations (exposure time, observing log, appropriate comparison star etc.). Large observing surveys usually measure only in one colour or are unfiltered, which is a significant disadvantage. On the other hand, measuring one single object can be very time consuming and gathering data for a reliable analysis can take up to several years. Nevertheless, efficiency of such an approach can be demonstrated, e.g. in a very successful project, *The Konkoly Blazhko Survey*. Within the scope of this project many crucial discoveries have been made.

In this chapter I focus on the analysis of observations of a star TV Boo, which appeared to be a star with compound modulation of the RRc type. At the end of 2012 it was the first RRc star known with double modulation. The remaining parts of this chapter are devoted to the first results of a Czech project, which was established in a cooperation with amateur observers.

3.1 The first known double modulated RRc star TV Boo

The variability of TV Boo ($\alpha = 14^{\text{h}}16^{\text{m}}36.58^{\text{s}}$, $\delta = +42^{\circ}21'35.69''$, J2000) was first reported by Gutnick & Prager (1926) who defined it as an RRc star with a period of 0.3124 d. The General Catalogue of Variable Stars (GCVS, Samus et al., 2012) gives the period $P = 0.3125609$ d and spectral type A7–F2. According to available literature this star is one of the most metal-poor RR Lyraes, e.g. Butler et al. (1982) gives $[\text{Fe}/\text{H}]_{\text{ZW}} = -2.5$.

TV Boo is one of a very few RRc stars with known Blažko effect. Its modulation has been known since 1965, when Detre (1965) found long term light curve changes with a period of 33.5 d. Almost ten years later Firmanjuk (1974) reported the Blažko effect with a period of 16.14 d. Finally, a more recent value of 10 days was found by Wils et al. (2006) who utilized data from NSVS. The discrepancies between published values of P_{BL} are obvious.

Since TV Boo is one of a very few known modulated RRc stars located in the Galactic field, in addition with a questionable value of its modulation period, it represented a very interesting object for possible detailed analysis. The proposed very low metallicity made TV Boo even more interesting. The location of TV Boo in the northern sky, its brightness between 11.2 to 11.9 mag together with a relatively short pulsation period of only 8 hours made it a promising object for the collection of enough data from the Czech Republic to solve the modulation-period ambiguity.

It is worth noting that the decision to observe TV Boo was made independently of the observing campaigns of the Blažko project (e.g. Kolenberg, 2005) and The Konkoly Blažko Survey.

3.1.1 Observation and data reduction

TV Bootis was observed on 23 nights during three seasons from 2009 to 2011 (for the complete observation log see tab. 3.1) with the 60cm Newtonian telescope of Masaryk University Observatory (MUO) in Brno, Czech Republic. This telescope equipped with a ST-8 CCD with a KAF-1600 chip provided a field of view of about $17.0' \times 11.3'$. Observations were carried out using a standard Johnson-Cousins set of filters $BV(R_c)$. In each passband more than 2000 data points were collected.

Table 3.1: Observation log.

Season	Time-span ($JD - 2450000$)	Number of nights	Number of hours	Number of data points		
				B	V	(R_c)
2009	4921 – 4971	8	50.9	1125	1173	1228
2010	5287 – 5377	3	9.5	-	307	356
2011	5614 – 5683	12	53.4	956	1180	1190
Total		23	113.8	2081	2660	2774

Table 3.2: MUO V data. The complete table is on the enclosed CD.

JDhel	V [mag]
2454921.515	11.201
2454921.516	11.204
...	...

The data reduction (dark frame and flat field corrections) and differential photometry were performed using the C-MUNIPACK package (Motl, 2009)¹ which is based on the DAOPHOT (Stetson, 1987). TYC 3038-955-1 and TYC 3038-1064-1 were used as comparison and check stars respectively. Although both stars are significantly redder than TV Boo itself (which could slightly affect the light curve and mainly colour indices), these stars

were chosen as comparisons because of the lack of other suitable stars in the vicinity of TV Boo. Standard deviations in the difference between the comparison and check stars were about 0.01 mag in all passbands. All the points were transformed to the standard magnitudes using standard stars in Landolt fields (Landolt, 1992). MUO V data are in fig. 3.1. The first two lines of these data are listed in tab. 3.2. The complete table is available as supporting information on the enclosed CD.

3.1.2 Frequency analysis

PERIOD04 (Lenz & Breger, 2004) was used as the main tool for frequency analysis. Because our measurements were not ideal for frequency analysis, we also searched for additional data. In 2010 the observations from the SuperWASP survey became available. These data were of better quality for frequency analysis than MUO data, because of the number of points (8914 measurements) and their time-span (205 nights, 1138 d). In addition we also analysed data from the NSVS which were of the worst quality. For the basic pulsation period determination PERSEA software (created by G. Maciejewski on the basis of Schwarzenberg-Czerny (1996) method) and a Matlab script based on the non-linear least square method were used for a comparison with PERIOD04. Within their errors all methods gave the same results.

¹<http://c-munipack.sourceforge.net/>

The maxima timings can be expressed as:

$$\text{HJD } T_{\text{max}} = 2454922.2334(2) + 0.3125615(7)E_{\text{puls}}. \quad (3.1)$$

Frequency analysis based on the MUO and SuperWASP datasets gave almost the same results. Except for data from NSVS, which showed only three frequencies (f_0 , $2f_0$ and $f_0 + f_{m1}$) in its frequency spectrum, all detected frequencies in MUO and SuperWASP datasets are listed in tab. 3.3. Semi-amplitudes, S/N ratios² for individual frequencies and their standard deviations (derived using the Monte Carlo simulation tool of Period04) are also given in this table.

Table 3.3: Frequencies found in MUO and SuperWASP data sets. The uncertainties in their final digits are given in parentheses.

Id	MUO			SuperWASP		
	Frequency c/d	A_V mag	S/N	Frequency c/d	A mag	S/N
f_0	3.1993740(8)	0.2620(3)	163.9	3.1993646(4)	0.2497(3)	326.0
$f_0 + f_{m1}$	3.302036(6)	0.0342(6)	21.5	3.302066(3)	0.0318(3)	42.0
$f_0 - f_{m1}$	3.09671(2)	0.0109(4)	6.8	3.09667(1)	0.0093(3)	11.9
$f_0 + f_{m2}$	3.244555(3)	0.0066(6)	4.1	3.24598(2)	0.0060(3)	7.9
$f_0 - f_{m2}$				3.15276(2)	0.0070(3)	9.1
$2f_0$	6.398748(4)	0.0730(5)	49.1	6.398738(2)	0.0729(3)	156.6
$2f_0 + f_{m1}$	6.50141(2)	0.0133(5)	9.0	6.50143(2)	0.0092(3)	19.9
$2f_0 - f_{m1}$	6.29609(3)	0.0072(5)	4.8	6.29603(2)	0.0069(3)	14.8
$2f_0 + f_{m2}$				6.44534(3)	0.0040(4)	8.7
$2f_0 - f_{m2}$				6.35212(4)	0.0026(3)	5.6
$3f_0$	9.59812(1)	0.0187(4)	14.8	9.598107(6)	0.0185(3)	43.6
$3f_0 + f_{m1}$	9.70078(3)	0.0102(4)	5.7	9.70080(1)	0.0077(3)	18.2
$3f_0 - f_{m1}$				9.49540(3)	0.0034(3)	8.0
$3f_0 + f_{m2}$				9.64471(5)	0.0024(3)	5.6
$4f_0$	12.79750(2)	0.0088(4)	9.1	12.79748(1)	0.0107(3)	29.3
$4f_0 + f_{m1}$	12.90016(4)	0.0051(4)	5.2	12.90020(3)	0.0032(3)	8.7
$4f_0 - f_{m1}$				12.69480(6)	0.0021(3)	5.7
$5f_0$	15.99687(2)	0.0090(4)	11.7	15.99685(1)	0.0079(3)	22.5
$5f_0 + f_{m1}$				16.09950(6)	0.0019(3)	5.6
$5f_0 + f_{m2}$				16.04341(7)	0.0016(3)	4.6
$6f_0$	19.19624(4)	0.0052(4)	7.7	19.19621(2)	0.0050(3)	15.4
$7f_0$	22.39562(5)	0.0037(4)	6.4	22.39558(3)	0.0032(3)	11.2
$8f_0$	25.59499(5)	0.0018(4)	4.6	25.59495(6)	0.0019(3)	6.9

Fourier amplitude spectra together with the spectral window resulting from the SuperWASP dataset are shown in fig. 3.2. The first two panels show a Fourier spectrum with the main pulsation frequency (a) and spectrum after removal of this frequency and its detectable harmonics (b). The

²We mention only peaks with $S/N > 4$, because this is a generally accepted limit to distinguish between frequency peaks due to pulsation and noise (Breger et al., 1993).

daily aliases dominate the frequency spectra, because the SuperWASP measurements are single-sided. The final residual spectrum, after prewhitening with all detected basic pulsation harmonics and their side peaks, is given in panel (d). There is no significant peak in the residual plot.

Eight harmonics of the main pulsation frequency were detected in both studied datasets. In the case of SuperWASP data, symmetric, but unequally spaced side peaks were identified around the basic pulsation frequency and its first harmonic. According to the discussion in sec. 2.2.4 it should indicate compound modulation with two parallel modulations. Side peaks with higher amplitudes relate to the main Blažko component with frequency $f_{m1} = 0.10269$ c/d (Blažko period $P_{BL} = 9.7374(54)$ d). Other detected side peaks with about five times lower amplitudes around f_0 correspond to the second modulation component with frequency $f_{m2} = 0.04661$ c/d (modulation period 21.5(2) d). Although complete quintuplets were detected only in f_0 and $2f_0$, side peaks of both modulation components were detectable up to $5f_0$. Only one component related to the second modulation frequency ($f_0 + f_{m2} = 3.244555$ c/d) was revealed in the MUO data set.

Except for LS Her, in which different types of side peaks were detected³, TV Boo is the first known RRc type star with the frequency structure described above, and, thus, also the first RRc star with known parallel modulation.

Maxima timings for the Blažko effect can be expressed as

$$\text{HJD } T_{\max\text{Blažko}} = 2454950.80(10) + 9.7374(54)E_{\text{Blažko}}. \quad (3.2)$$

From the amplitudes of the side peaks it is seen that $A(f_0 + f_{m1}) \approx 3A(f_0 - f_{m1})$ and $A(f_0 + f_{m2}) \approx 0.85A(f_0 - f_{m2})$. These amplitudes result in the asymmetry parameter (eq. 2.13) $Q_{Am1} = 0.55$ and $Q_{Am2} = -0.08$ for the first and second modulation component respectively. Since the modulation m_1 has much higher amplitude than m_2 , it will dominated the light changes. Since Q_{Am1} is positive, the direction of motion in the phase-amplitude diagram should be counter-clockwise (see fig. 3.4).

At the same time when our results were published, another study devoted to TV Boo was released independently. Hajdu et al. (2012) analysed their high-quality colour measurements with a time span of about four months (63 nights). Except for the two modulation components they found an additional peak at $f' = 3.0838$ c/d and two combination peaks corresponding to $f_0 + f'$ and $f_0 - f' - f_{m1}$. They speculated whether the peak f' relates to an additional modulation or an independent non-radial mode. Since they could not find a symmetric peak at $f_0 + f'$ they preferred the non-radial explanation of f' .

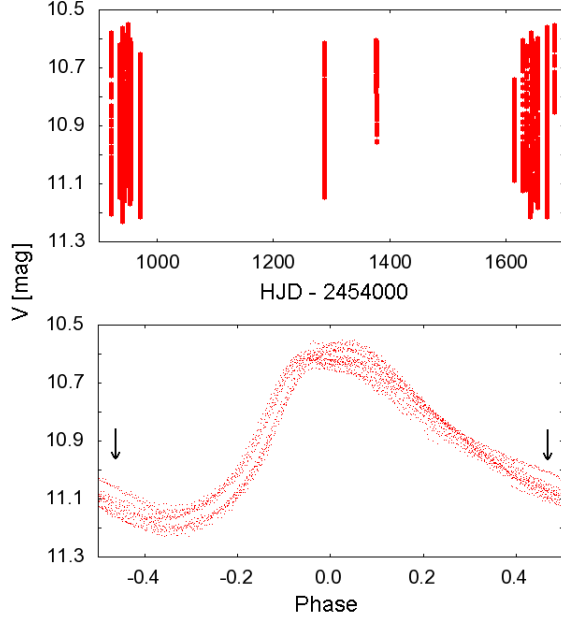


Figure 3.1: Standard V data gathered on MUO between seasons 2009 and 2011. In the bottom panel the data are phased according to eq. 3.1. The bump on the descending branch is marked by an arrow.

³A frequency structure with two triplets equidistantly spaced on both sides of the main pulsation frequency was detected in LS Her (Wils et al., 2008).

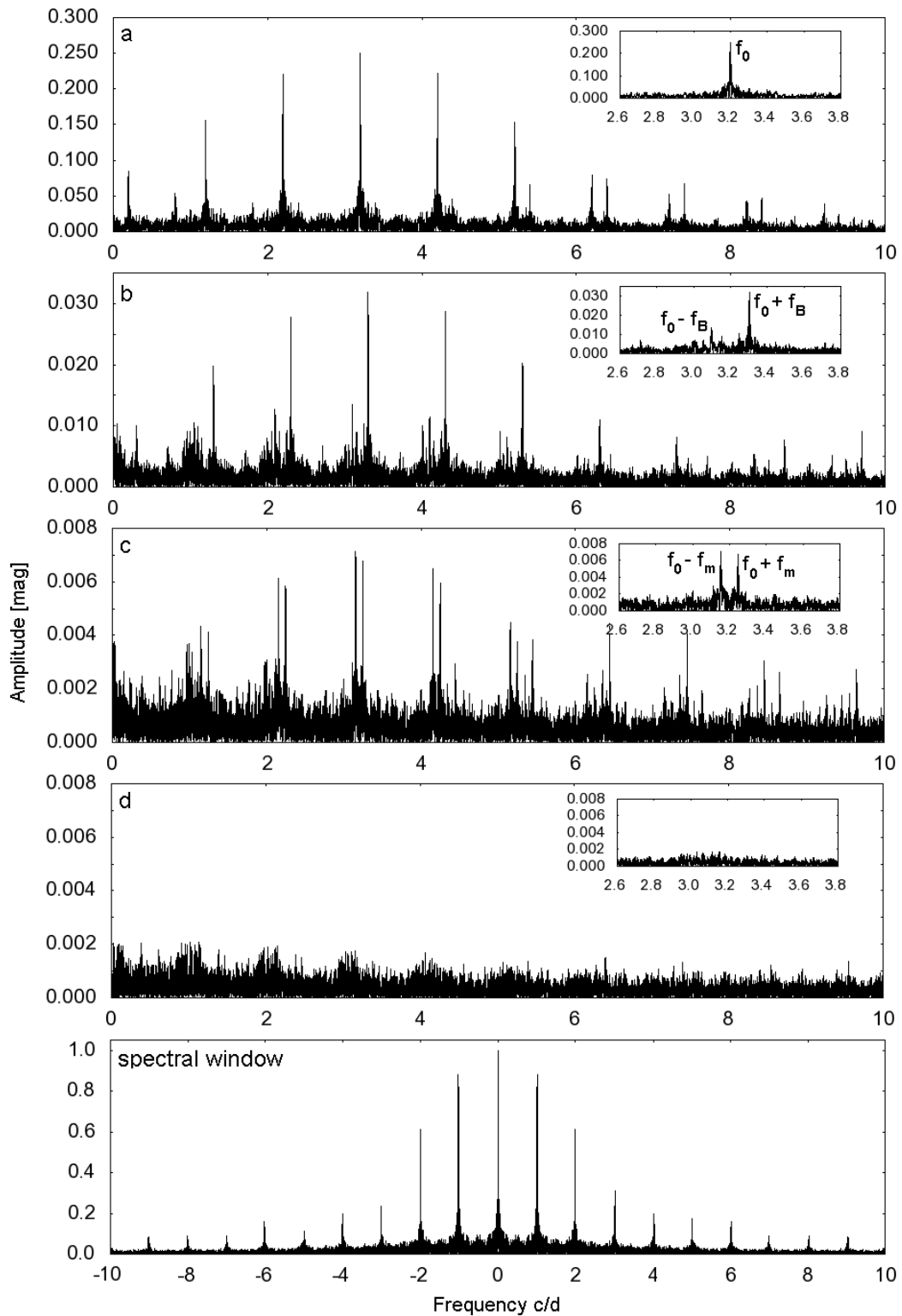


Figure 3.2: Frequency spectra of TV Boo based on SuperWASP data. The top panel shows the Fourier spectrum with the main pulsation frequency (the highest peak). Other noticeable peaks are daily aliases of the main pulsation frequency. The next two panels show prewhitened spectra after removal of the main pulsation frequency and its harmonics (panel b), after removal of the frequencies related to the Blazhko effect (panel c) and final residual spectra with all modulation frequencies removed (panel d). The vicinity of the main pulsation frequency with frequency identifications are provided as further detail in panels (a) to (d). The bottom panel shows the spectral window.

This paper brought our attention back to the SuperWASP data. We re-analysed the complete dataset. In addition the full dataset was divided according to gaps in observation into two comparable subsets (seasons 2004 and 2007) with a length of about 130 days. The middle part (season 2006) of the data was omitted due to the short time span of only 63 days and 570 points.

The reanalysis of the complete dataset as well as of the subsets showed the pulsation harmonics up to $10f_0$, and complete triplets of both modulation components up to the 4th order down to $S/N > 3.5$. The asymmetry parameter Q_A had an almost constant value in both subsets for the modulation component m1, while it differed for m2 - it was positive in 2004, while in 2007 it was negative. These changes in the m2 component could cause long-term changes in the strength of the overall modulation.

In the two subsets the low-frequency peak directly related to the first modulation component $f_{m1} = 0.1027$ c/d was also easily detectable. The suspicious peak f' at 3.084 c/d, with an amplitude of about 7 mmag, was found in all three datasets. In original analysis of the whole dataset, which showed many false peaks around $f = 1$ c/d generated by small shifts between observing seasons, f' was considered as some instrumental effect. Therefore it was previously ignored. No signs of combination peaks that were detected by Hajdu et al. (2012), or the side peak possibly related to the third modulation component, was observed in SuperWASP data.

In addition, we did not detect any sign of period doubling. Another puzzling effect seen in many RRC stars (and Cepheids) observed with high-precision photometry, is the presence of an additional frequency with a strangely repeating frequency ratio of 1.58–1.63 from star to star (see e.g. Moskalik, 2013). Again, no frequency peaks with the given ratio, or even close to this ratio, were identified in the datasets down to the level of residuals. It is worth noting that the detection of such frequency was complicated by the fact that in the area defined by the ratio, 1-day aliases of the main and modulation frequencies occurred. In any case, we could not confirm or disprove the presence of the frequency in the range of 1.58–1.63 f_0 .

Fig. 3.3 shows what the light curve looked like during one Blažko cycle between HJD 2454151 and 2454161. Each Blažko cycle affects the light curve shape uniquely in a given Blažko phase. Notice the change of light curve shape around maxima during the Blažko cycle.

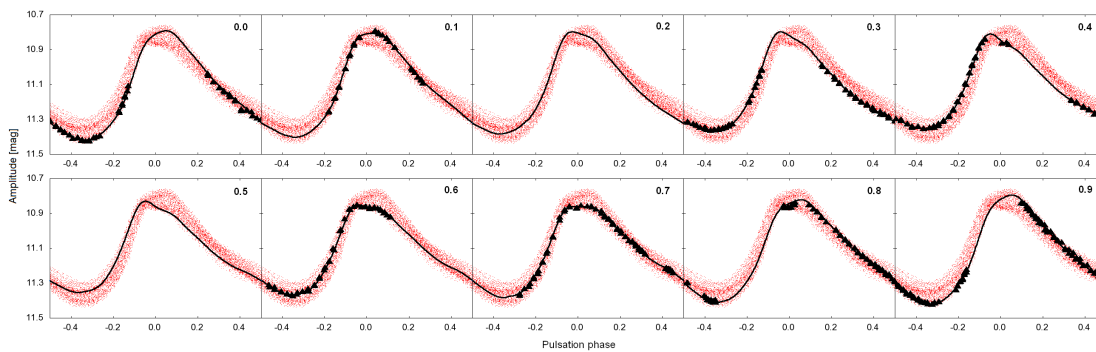


Figure 3.3: Light curve changes during one unique Blažko cycle between HJD 2454151 and 2454161. The model light curve based on frequencies in Table 3.3 is plotted as a continuous line. The corresponding Blažko phase is mentioned in the top right corner of each plot. The triangles show real SuperWASP data for the given Blažko phase in this unique time-span. All available SuperWASP data (plotted with dots) are shown for illustration to see the range of possible light changes.

Remarks on the period change during a Blažko cycle and possible long term features

Blažko RRC stars primarily show frequency modulation with only small amplitude modulation. In TV Boo the amplitude of the light curve modulation is only about 0.1 mag, and the maximum and minimum of the light changes are affected to a similar extent. Therefore the fuzziness of the light curve is uniform in all its parts (check fig. 3.1).

TV Boo, as a frequency modulated star with only small amplitude modulation, shows changes in pulsation period during the Blažko cycle. Changes in phase and amplitude of maximum light during three unique Blažko cycles between HJD 2454151 and 2454181 can be seen in fig. 3.4. Points in this plot represent maxima of our light curve model. Maxima from the first and third Blažko cycles create curves of almost the same shape, but the dependence based on points coming from the cycle between them differs. The phase-amplitude diagram is similar for a few consecutive Blažko cycles before it changes considerably. Bear in mind that the shape of the light curve is slowly changing over time due to the interaction between modulation components, the appearance of the phase-amplitude diagram is completely different after many Blažko cycles.

The amplitude of the period changes determined from maxima timings is about $0.13P_{\text{puls}}$, which is about 58 minutes. However, this value is strongly affected by the change of the light curve shape around maxima. Thus, a more realistic estimation of the magnitude of the phase modulation can be obtained by measuring the phase shift in the ascending branch. We measured the phase shift in a fixed SuperWASP magnitude 11.1 (approximately half of the light curve amplitude), and we obtained the strength of the period change during a Blažko cycle beginning at HJD 2454151 shown in fig. 3.3 as $0.046P_{\text{puls}}$, which is a little less than 21 minutes. This value is also slightly cycle-to-cycle dependent, but only in the order of $10^{-3}P_{\text{puls}}$.

An interesting feature was noticed in the shape of the descending branch in some minima of the Blažko cycles (they are not present in each Blažko cycle). In the MUO data a bump was detected in seasons 2010 and 2011, while it is invisible in the data gathered in 2009. Similarly, in the SuperWASP data from the season 2007 this behaviour was not unveiled, but there is a weak sign of a bump in the 2004 season (see fig. 3.5, middle panel).

These features could possibly be a demonstration of long-term changes known in a few other examples, e.g. in RR Lyrae itself with long changes lasting 4 years (Detre & Szeidl, 1973). We can not rule out a possible connection between the bump and a change in the m2 component. A first order estimation of such a period in TV Boo could be about 6 years. However this claim is based on the assumption that MUO V and SuperWASP light curves are of similar shape and amplitude. Of course, absence of the bump can be caused by the properties of the data itself - lack of data for such Blažko phases in studied datasets or the overlapping of data.

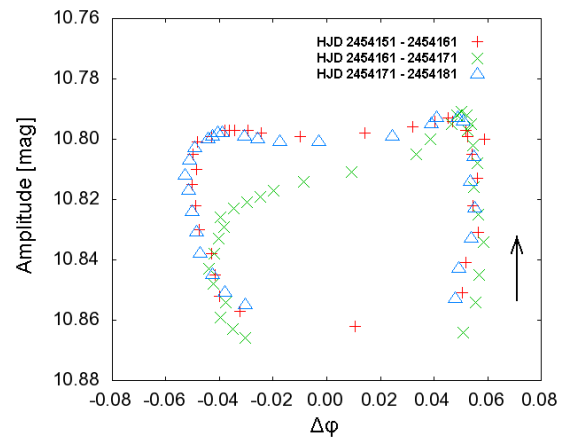


Figure 3.4: Phase-amplitude diagram in three Blažko consecutive cycles between HJD 2454151 and 2454181. The run of points is counterclockwise similarly as in majority of Blažko RRab stars.

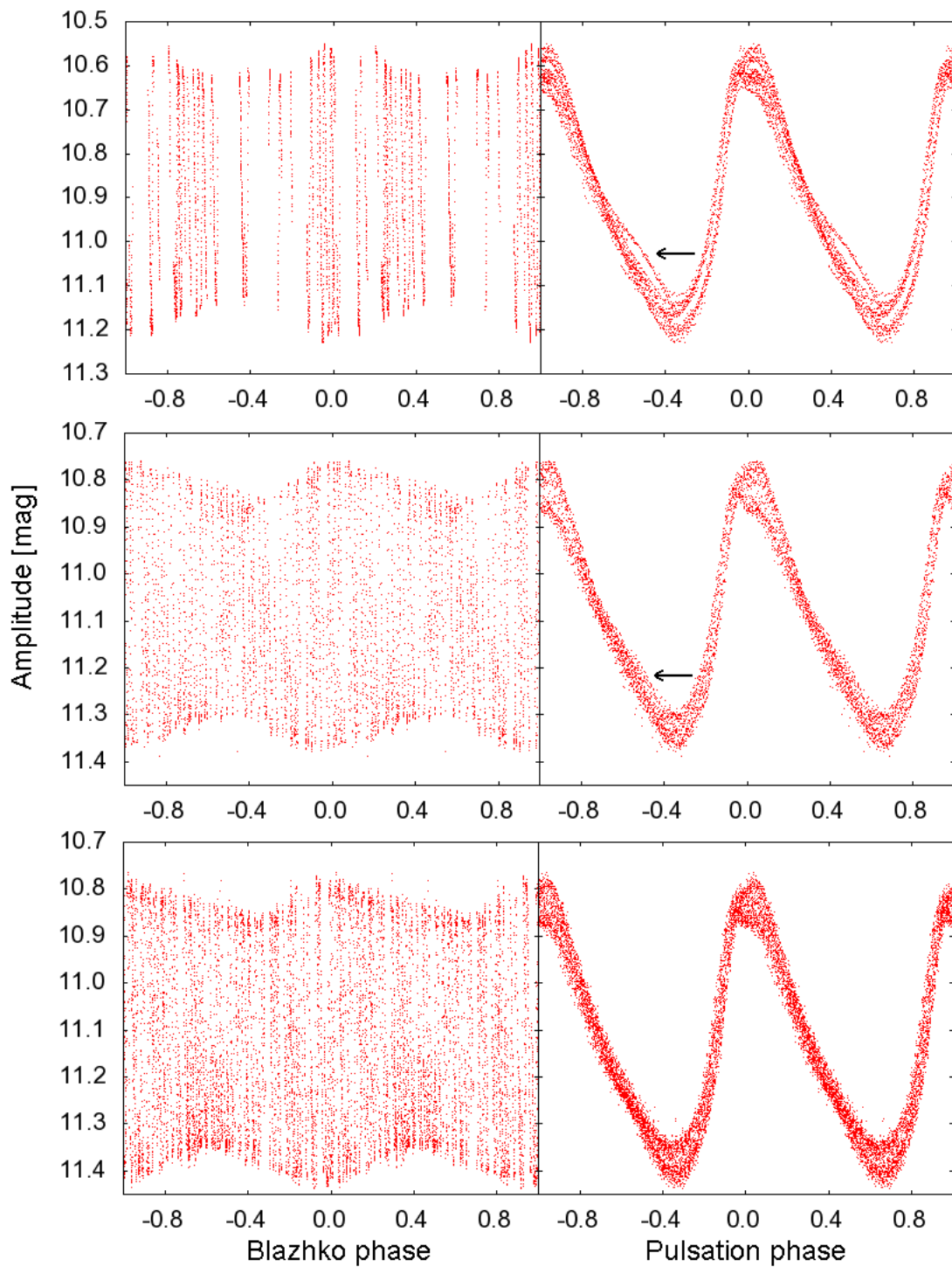


Figure 3.5: MUO V data (top panel), SuperWASP data from season 2004 (middle panel) and from season 2007 (bottom panel). Data folded with the Blazhko period are in the left panels, data phased with the main pulsation period are to the right. Note the bump on the descending branch of MUO data and SuperWASP data (indicated by an arrow).

3.1.3 Physical parameters

As for RRab stars (sec. 1.3.3), some empirical relations that utilize Fourier coefficients were also defined for RRC stars. We used the following calibrations for RRC stars presented by Simon & Clement (1993); Morgan et al. (2007); Kovács & Kanbur (1998):

$$[\text{Fe}/\text{H}]_{\text{ZW}} = 52.466P^2 - 30.075P + 0.131(\phi_{31}^c)^2 + 0.9825\phi_{31}^c - 4.198\phi_{31}^c P + 2.424 \quad (3.3)$$

$$M_V = 1.061 - 0.961P - 4.447A_4 - 0.044\phi_{21}^s \quad (3.4)$$

$$\log(L/L_\odot) = 2.41 + 1.04\log P - 0.058\phi_{31}^c \quad (3.5)$$

$$\log T_{\text{eff}} = 3.7746 - 0.1452\log P + 0.0056\phi_{21}^c \quad (3.6)$$

$$\log(\mathcal{M}/M_\odot) = 0.39 + 0.52\log P - 0.11\phi_{31}^c, \quad (3.7)$$

where ϕ_{ij}^c are coefficients based on cosine-term decomposition and ϕ_{ij}^s sine-term decomposition coefficients respectively (their interrelations give equations 1.10 and 1.11). The zero point in eq. 3.4 was decreased according to Cacciari et al. (2005) by 0.2 as opposed to the equation in Kovács & Kanbur (1998). Physical parameters resulting from eq. 3.3-3.7 based on the MUO V light-curve fit (fig. 3.6, tab. 3.4) are listed in tab. 3.5. The solution, and mainly parameter ϕ_{31} , is very sensitive to the coverage of the light curve. If we remove three nights when the bump was observed, ϕ_{31} decreases its value by about 0.04, which leads to a change in $[\text{Fe}/\text{H}]$ of about -0.4 dex. Since our light curve is not ideally covered in all Blažko phases, we suspect metallicity to be even slightly higher (in the order of hundredths) than the obtained value $[\text{Fe}/\text{H}]_{\text{ZW}} = -1.89$.

Table 3.4: Fourier parameters based on sine-term decomposition.

A_0	R_{21}	R_{31}	R_{41}	ϕ_{21}	ϕ_{31}	ϕ_{41}
mag	mag	mag	mag	rad	rad	rad
10.917	0.283	0.078	0.043	2.698	5.545	1.996

Table 3.5: Mean physical parameters of TV Boo.

$[\text{Fe}/\text{H}]$	-1.89 ± 0.14
T_{eff} [K]	7270 ± 50
M_V [mag]	0.59 ± 0.06
L [L_\odot]	56 ± 5
R [R_\odot]	4.8 ± 0.5
\mathcal{M} [M_\odot]	0.73 ± 0.04
r [pc]	1150 ± 30

This value differs by an order of a few tenths from the published values: $[\text{Fe}/\text{H}] = -2.5$ (Butler et al., 1982), $[\text{Fe}/\text{H}] = -2.22$ (Suntzeff et al., 1994), $[\text{Fe}/\text{H}] = -2.44$ (Fernley et al., 1998). These values came from the ΔS approach (Preston, 1959). Published values of ΔS vary between 8 (Preston, 1959) and 13.1 (Butler, 1975). Transforming them via eq. 3 in Suntzeff et al. (1994) we obtain a range of metallicities from -1.67 (Preston, 1959) to -2.44 (Butler, 1975). Solving ten light curves assuming one unique Blažko cycle as shown in fig. 3.3, we obtained metallicities between -1.68 and -2.0 . Therefore it seems that the determination of metallicity strongly depends on the Blažko phase.

Peña et al. (2009) observed TV Bootis and determined photometric physical parameters in the same way as we did. They proposed the metallicity of TV Boo to be $[Fe/H] = -2.04$. However, their measurements cover only one pulsation cycle. Thus we argue that our value is more reliable.

The errors of physical parameters were calculated according to errors of calibrations given in papers they were taken from. All parameters (except for metallicity) of TV Bootis in tab. 3.5 are almost the same as found in literature, especially with those listed in Peña et al. (2009). The value of the radius of the star is a rough estimation determined by solving the Stefan-Boltzmann equation for a black body. The estimated mass of TV Boo is quite high compared to RRab type stars, but it is just in the middle of the mass interval for RRC stars noted in Simon & Clement (1993). The distance r was determined using the distant modulus with extinction 0.024 mag in the V band⁴. This value is in excellent agreement with 1149 pc noted in Liu & Janes (1990).

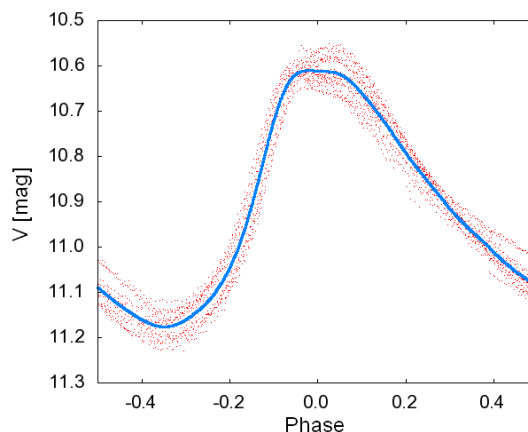


Figure 3.6: Phased MUO V light curve together with our sine-series fit. The data are plotted as points, the fit with continuous line.

3.2 The Czech observational project

In this section a new project dedicated for photometric measurements of RR Lyrae stars is introduced. The project was founded at the end of 2011 with the idea to monitor bright RR Lyraes with cooperation of amateur astronomers. The basic goal of *The Czech RR Lyrae Stars Observation Project* (hereafter CRRLSOP) is to obtain well-covered light curves in standard BVR_cI_c filters, which would be further analysed to determine ephemerides, periods, and light curve characteristics (amplitude, rising time, Fourier parameters). Originally, objects which were rarely observed were considered as primary targets. However, the preferences were loosened and extended gradually to monitoring of RR Lyraes in general (regular stars, modulated stars, stars without accurate measurements in sky surveys etc.).

The idea of the project was inspired by the great work of Lub (1977), who made an atlas of RR Lyrae light curves in the Walraven photometric system. Another great stimulation for our work were the Konkoly Blazhko Survey, which was operating for several years and provided a detailed study of many RR Lyrae stars, and *The Blazhko project* comprising few tens of observers utilizing both photometric and spectroscopic measurements (Kolenberg, 2005, 2007). Founding of the CRRLSOP was also stimulated by the study of TV Boo (sec. 3.1), which showed that relatively accurate data can be gathered even from the center of the town Brno using relatively small telescopes.

3.2.1 Motivation and description of the project

Since observing with one telescope is strongly limited by weather conditions and observing of RR Lyrae stars acquire a lot of observing time, the project involves participation of amateur as-

⁴taken from <http://ned.ipac.caltech.edu/forms/calculator.html>

tronomers with appropriate telescopes and CCD technique, who are members of the *Variable Star and Exoplanet Section of the Czech Astronomical Society*⁵. Similar cooperation between professional and amateur astronomers works in Bundesdeutsche Arbeitsgemeinschaft für Veränderliche Sterne e.V in Germany⁶ or in the international Groupe Europeen d'Observations Stellaires⁷ which manages the GEOS RR Lyrae database (Le Borgne et al., 2007)⁸. Although mainly Czech observers are interested in the CRRLSOP, of course, observers from other countries are warmly welcomed to join us as well.

The advantage of our conception is that we can observe many targets simultaneously, and produce more data than is possible with one telescope even with many observers. In 2012 our group comprised five members, in 2013 only three, and in 2014 seven interested observers (one from the southern hemisphere). We hope that this number will increase in years to come.

To be able to get data of sufficient quality, we decided to monitor only bright RR Lyrae stars which are brighter than about 12 mag at maximum light. This value is chosen to suit the telescopes that amateurs use, which are typically of the diameter between 20 and 30 cm. Another restriction is imposed by the location of the Czech Republic. We preferably choose targets with a declination of typically more than 20°, which are easily observable for a significant part of the year.

Each target is carefully selected to suit an observer's equipment and taking the observer's time constraints into account. This is crucial when deciding about the target type (regular or modulated star). Observers are briefed in detail about exposure times, about the field of view selection and time schedule for the measurements. All the observations are subsequently discussed. Each star is monitored uniquely by one observer to avoid merging data from different devices. We also put emphasis on the selection of comparison stars.

All the measurements gathered by observers are processed in the same way using the aperture photometry software C-MUNIPACK. Subsequently they are calibrated to the standard Johnson-Cousins system using standards in Landolt (1992) fields and in open clusters. The structure of the observations is as follows: stars which are expected to have a stable light curve are observed as long as the complete phase coverage require. All phases should be caught at least twice to achieve a higher density of data points. In addition, if weather permits, the star is observed two nights in a row followed by observation after one week, a few weeks and finally after a few months to verify the stability of the stellar pulsation. In the case of Blažko stars, the objects are monitored as often as possible to cover all Blažko phases. The time schedule of observations is, of course, not strictly given, because of weather or other unpredictable reasons. The examples of ongoing observations are in fig. 3.7.

The first results of the cooperation with amateur astronomers were the discovery that CN Cam shows the Blažko effect, and the discovery of two new modulated stars.

3.2.2 A new Blažko star CN Cam

CN Cam (= NSV 5256 = SAO1900 = BD+82 338 = GSC 04556-00251, J2000 11^h36^m11.8^s, +81°17'37.1"), found to be a variable by Strohmeier & Knigge (1961), was initially proposed to be an eclipsing binary. Based on a 12-night study, Campos-Cucarella et al. (1996) classified CN Cam as an RRab star and establish its period as 0.6214(1) d. Kinman et al. (2007) improved the period to 0.621445(2) d and determined the amplitude of the light changes to be 0.36 mag in *V* and 0.49 mag in *B*, Campos-Cucarella et al. (1996) gives 0.350(5) mag in *V* and 0.474(4) mag in *B*. Kinman et al. (2007) also estimated the metallicity of CN Cam using Fourier coefficients,

⁵<http://var2.astro.cz/EN/>

⁶<http://www.bav-astro.de/index.php?sprache=en>

⁷<http://http://geos.upv.es/>

⁸http://rr-lyr.irap.omp.eu/dbrr/dbrr-V1.0_0.php?en

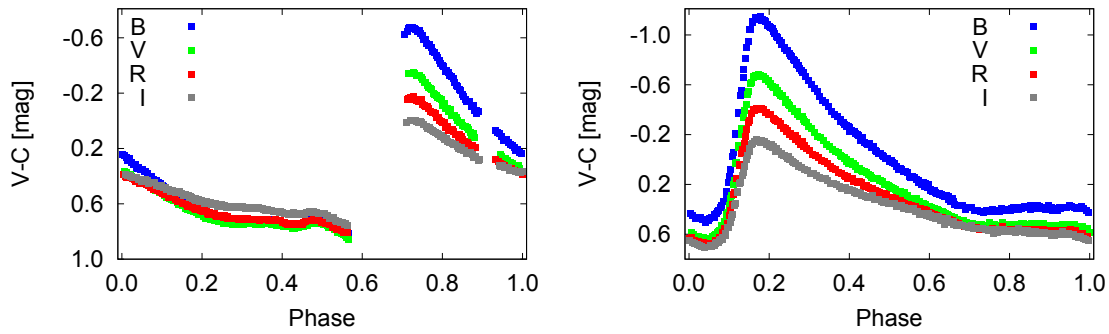


Figure 3.7: Light curves of BK Dra and VZ Her gathered with 35cm Schmidt-Cassegrain telescope in Brno, Czech Republic.

amplitude in V and rise time based on calibrations published by Sandage (2004). The values of metallicity that Kinman et al. (2007) obtained were about $[\text{Fe}/\text{H}] = -1.1$. They also derived the distance of CN Cam as 594 pc.

One of the most recent observations was performed by G. Maintz (2012). Between the years 2006 and 2012 she obtained seven maxima timings and improved the value of the period to 0.6214465(3) d. In none of these works the Blažko effect was noted.

CN Cam was observed in the BVR_cI_c passbands during 20 nights between the end of January and the end of June 2012. The journal of observations is in tab. 3.6. We obtained between 1341 and 1629 points in each filter (available as a supplement information on the enclosed CD). Observations were carried out at the Observatory and Planetarium of Johann Palisa in Ostrava using the 20cm Newtonian telescope which is equipped with a SBIG-ST8 XME camera. The data were reduced in the standard way and were transformed to the standard Johnson-Cousins magnitudes using stars in Landolt fields (Landolt 1992).

Table 3.6: Observation log and magnitude of the comparison star in different passbands.

Nights	Time-span [d]	B	V	R_c	I_c
20	186	1341	1498	1495	1629
brightness of the comparison star [mag]		10.62(9)	10.24(5)	10.01(5)	9.77(5)

Similarly to Campos-Cucarella et al. (1996) and Kinman et al. (2007), we used GSC 04556-00278 (= SAO1899 = BD+82 337, J2000 11 36 11.8, +81 17 37.1) as a comparison star and GSC 04556-00278 as a check star. According to the $J = 9.453(23)$ and $K = 9.248(22)$ magnitudes of the comparison star taken from the 2MASS All-Sky Catalog of Point Sources (Cutri et al., 2003) we got Johnson-Cousins magnitudes of the comparison star via the relations in Warner (2007) (given in tab. 3.6). Our $V = 10.24(5)$ magnitude of the comparison is nearly in the middle of the magnitudes given by Campos-Cucarella et al. (1996) and Kinman et al. (2007) (10.3 and 10.201(3) mag, respectively).

After performing the period analysis with PERIOD04 we found the following ephemeris:

$$\text{HJD } T_{\max} = 2455959.4707(1) + 0.621446(3)E_{\text{puls}}. \quad (3.8)$$

The times of maximum light were determined via polynomial fitting of the V -light curve (tab. 3.7). The value of the period is within the errorbars in agreement with the period determined by Maintz (2012).

Table 3.7: Times of maxima of CN Cam.

2455954.509	0.008
2455959.4710	0.0001
2455984.339	0.005
2456005.4588	0.0009
2456021.619	0.004
2456046.491	0.008
2456056.4158	0.0009
2456107.367	0.001
2456140.335	0.002

Frequency analysis with PERIOD04 revealed additional frequency peaks on the right-hand side of the basic pulsation frequency ($f_0 = 1.6091504(73)$ c/d) and its harmonics (jf_0 , where $j = 1, 2, 3, \dots$). In total we identified peaks related to the basic pulsation frequency up to $j = 8$ and right-hand side peaks corresponding to the modulation frequency $jf_0 + f_{BL}$ up to $j = 4$. The spacings of the side peaks were not equidistant, but they were slightly decreasing with rising j . The side peak with the highest amplitude was $f_0 + f_{BL} = 1.629877(61)$ c/d. Therefore we give the first rough estimation of the Blažko period of CN Cam

$P_{BL} = 48.25(14)$ d⁹. Data in the V filter phased with the modulation period are shown in fig. 3.9.

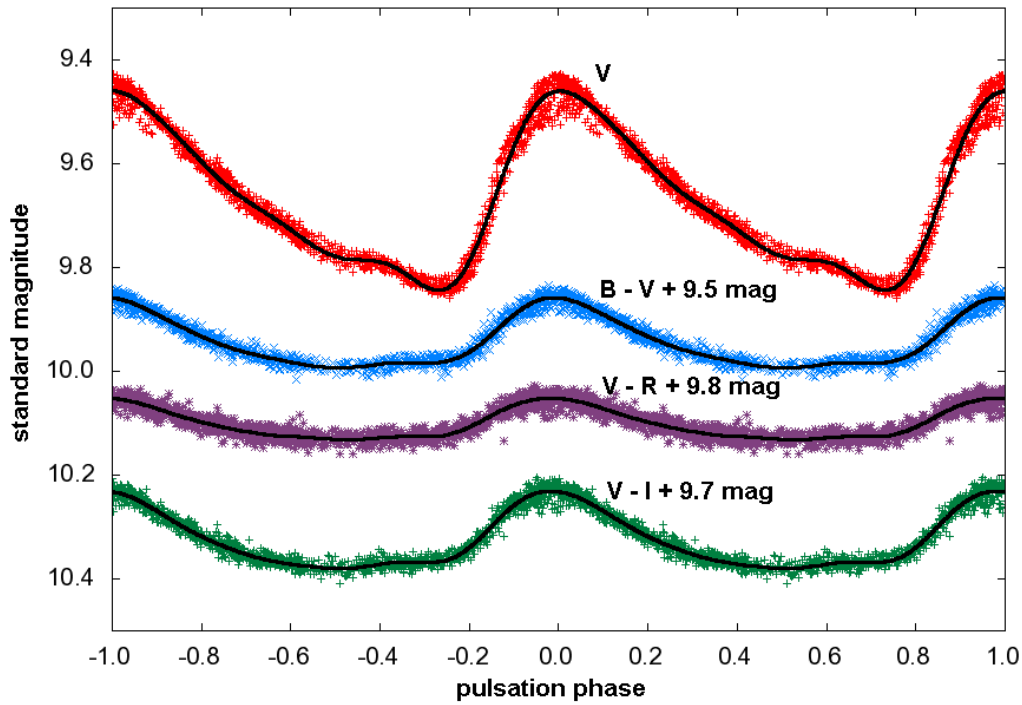


Figure 3.8: Calibrated data of CN Cam folded according to equation 3.8. The solid lines are the sine-series fit to the light curves.

Although the coverage of the light curves was not ideal, we fitted V , $B - V$, $V - R$ and $V - I$ data with sine series and got the approximations of the mean light curves (fig. 3.8). The degree of the fit was chosen using visual inspection. The analysis of the mean light curves allowed us to determine Fourier coefficients based on the sine-term decomposition of the V light curve, and it also allowed us to estimate mean colour indices, mean magnitudes (zero points), mean amplitudes and mean rise time during the Blažko cycle (tab. 3.8).

Subsequently we were able to estimate the metallicity of CN Cam using Fourier coefficients and pulsation period. Formula 1.14 gives (after transformation to ZW scale) $[Fe/H]_{ZW} = -1.15$ dex, which agrees well with the spectroscopic value $[Fe/H] = -1.2$ dex given in Kinman et al. (2007).

⁹All values of frequencies and periods in this paragraph are based on V data.

Table 3.8: Characteristics of the light curves and sine-term Fourier coefficients based on the V light curve fit. N is the degree of the fit, A_0 the mean magnitude. Phases ϕ_{ij} are in radians, Fourier combinations R_{ij} in mag.

	N	A_0 [mag]	max [mag]	amplitude [mag]	rise time
B	4	10.1168(7)	9.817(3)	0.510(4)	0.268(4)
V	4	9.6751(4)	9.460(2)	0.384(3)	0.272(4)
R_c	4	9.3703(4)	9.207(2)	0.313(3)	0.272(4)
I_c	4	9.0460(3)	8.925(2)	0.253(3)	0.282(4)
$B - V$	4	0.4456(4)	0.358(2)	0.130(4)	
$V - R$	5	0.3022(3)	0.252(4)	0.079(4)	
$V - I$	5	0.6262(9)	0.531(3)	0.149(4)	
ϕ_{21}	ϕ_{31}	ϕ_{41}	R_{21}	R_{31}	R_{41}
2.578(13)	5.567(28)	2.984(74)	0.365(5)	0.155(4)	0.054(4)

Following Kinman's study, who used calibrations from Sandage (2004), our parameters gave: $[\text{Fe}/\text{H}]_{\text{ZW}} = -1.15$ dex with Sandage's equation (3)¹⁰, -1.05 dex with his relation (6), and -1.00 dex with Sandage's equation (7) (with rise time 0.272). If we use the calibration of Clementini et al. (2003)

$$M_V = 0.214[\text{Fe}/\text{H}] + 0.86, \quad (3.9)$$

and assume our metallicity as $[\text{Fe}/\text{H}]_{\text{ZW}} = -1.15$ dex, we obtain $M_V = 0.61$ mag. The distance of CN Cam is therefore 608 pc.¹¹

Amplitudes and zero points of our mean light curves differ from the values given by Campos-Cucarella et al. (1996) and Kinman et al. (2007). Mainly our range in $(B - V)$ (0.358(2)-0.488(3)) is significantly higher than 0.26 – 0.38 mag (Campos-Cucarella et al., 1996) and 0.325 – 0.454 mag (K07). According to our $(B - V)$ range, CN Cam varies between spectral types F2 and F6. Our amplitude in B = 0.510(4) mag is also larger than 0.474(4) mag (Campos-Cucarella et al., 1996) and 0.49 mag (Kinman et al., 2007). Our metallicity estimation is slightly lower than Kinman et al. (2007) derived, but close to the spectroscopic value.

All the discrepancies are probably caused by the change in characteristics during the Blažko cycle which were not detected by Campos-Cucarella et al. (1996) or Kinman et al. (2007) probably due to small modulation amplitude, which is only about 0.09 mag in V and 0.11 mag in B . The slightly different magnitude of the comparison star that we used could also have played a small role. In addition, our mean light curves could differ from the 'true' mean light curves due to the non-uniform coverage of our data (our mean amplitudes of BVR_cI_c are probably slightly higher). For more reliable analysis more extended observations will be needed.

3.2.3 CzeV283 Aql, CzeV397 Her - two new Blažko stars

Variability of CzeV283 Aql=USNO-A2.0 0975-17144916 with celestial coordinates J2000 $\alpha = 19^{\text{h}}55^{\text{m}}38^{\text{s}}.1$, $\delta = +13^{\circ}43'22.4''$ and CzeV397 Her=USNO-A2.0 0975-11853460 (J2000 $\alpha = 18^{\text{h}}29^{\text{m}}43^{\text{s}}.3$, $\delta = +12^{\circ}06'39.2''$) were unveiled recently (in 2011 and 2012) in the framework of a private project, which deals with the searching for new variables in randomly chosen fields around

¹⁰to use this equation, ϕ_{31} from the tab. 3.8 has to be decreased of the parameter π .

¹¹with taking into account the extinction $E(B - V) = 0.047$ from Schlegel et al. (1998).

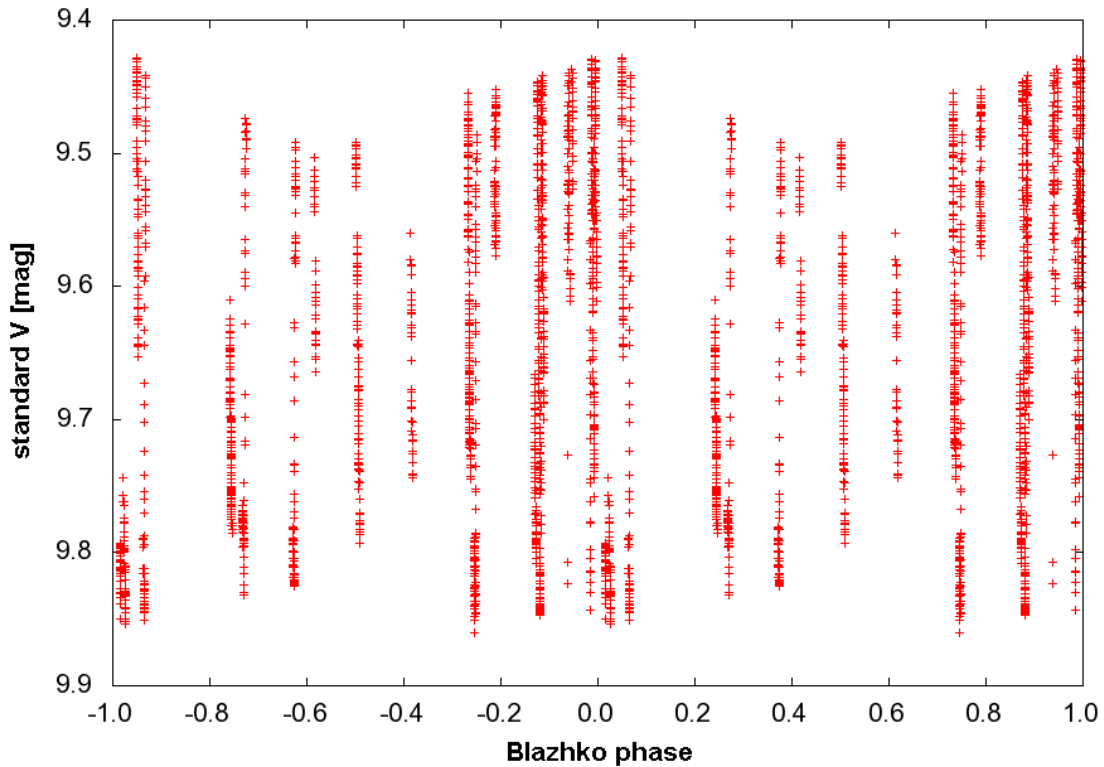


Figure 3.9: Standard V data of CN Cam phased with the period 48.25 d according to the epoch given in eq. 3.8.

known variables. This observation program resulted in the discovery of a few tens of new variables¹² among which some interesting cases occurred – e.g. a quadruple eclipsing binary system CzeV343 in the Auriga constellation (Cagaš & Pejcha, 2012).

The surroundings of V729 Aql and V1134 Her were observed during three seasons between 2011 and 2013 (see tab. 3.9 for the journal of observation) with a 10inch f/5.4 Newtonian telescope equipped with G4-16000 CCD camera¹³ (field of view 71'x71') at the private observatory in Zlín, Czech Republic. Since the aim of these measurements was searching for new variables, observations were carried out without filtering to gain the highest possible throughput.

Raw images, with exposure times of 240 and 180 seconds, were calibrated in the classical way using the CMUNIPACK software. USNO-A2.0 0975-17184388 (in CzeV283 Aql) and USNO-A2.0 0975-11774493 (in CzeV397 Her) were chosen as comparison stars. In total 910 measurements were gained for CzeV283 Aql in 19 nights with a time span of 413 d. In the case of CzeV397 Her it was a bit more: 1255 points in 22 nights with the total time span of 678 d. The relative precision of our photometry was about 0.05 mag.

The total observed amplitudes of the stars were estimated from the difference between maximum and minimum light as $\Delta = 0.93$ mag for CzeV283 Aql, and $\Delta = 0.67$ mag for CzeV397 Her, respectively.

Frequency analysis of our time series was performed with PERIOD04 to get the basic pulsation periods. Since we caught several maxima of both stars, we were able to determine their timings

¹² <http://www.bsobservatory.org/results.html>

¹³ Parameters of the detector can be found at <http://www.gxccd.com/>

through polynomial fitting (tab. 3.10). On the basis of our measurements we give

$$\text{HJD } T_{\max} = 2456222.3286(6) + 0.558488(2)E_{\text{puls}}, \quad (3.10)$$

for CzeV283 and

$$\text{HJD } T_{\max} = 2456132.3955(4) + 0.58664(3)E_{\text{puls}}, \quad (3.11)$$

for CzeV397.

Table 3.9: The journal of observations. The meaning of t is the duration of observation, N is the number of points and TS corresponds to the time span.

CzeV283 Aql			CzeV397 Her		
Night	t	N	Night	t	N
[HJD – 2450000]	[hours]		[HJD – 2450000]	[hours]	
5834	3.7	39	5830	1.6	27
5836	3.1	38	5835	3.1	43
5851	4.1	34	6095	3.0	26
5856	4.1	36	6101	1.1	19
5857	3.4	39	6102	2.7	47
5867	1.7	17	6121	3.6	64
5868	4.0	45	6131	4.3	69
5869	3.9	44	6132	3.8	66
5875	4.2	44	6145	1.5	22
5876	3.2	35	6152	3.6	64
6204	5.0	88	6153	2.4	41
6210	2.5	42	6155	4.2	68
6212	4.9	87	6157	3.1	56
6220	3.8	64	6158	4.5	75
6221	3.0	52	6159	4.3	75
6222	3.2	56	6180	4.7	79
6223	3.7	65	6181	2.8	40
6246	2.4	43	6483	4.2	66
6247	2.4	42	6494	5.1	89
			6495	4.8	85
			6507	4.1	72
			6508	4.0	62
Total					
$TS = 413$ d	66.3	910	$TS = 665$ d	68.4	1121

It was already obvious after a few nights that the light curves of both stars underwent changes (see phased light curves in the top panels of fig. 3.10 and close-ups in the bottom panel of the same figure), which is a sign of the Blažko effect. Unfortunately our data were too sparse for estimating the Blažko period. In the case of CzeV397 we identified a suspicious side peak near f_0 , which corresponds to a 38 day modulation period. This period gives a good phased light curve, but it needs to be confirmed through further observations.

Table 3.10: Maxima of stars.

CzeV283 Aql	CzeV397 Her
2455836.4148(8)	2456102.4842(4)
2455868.2524(9)	2456132.3955(4)
2456212.2797(5)	2456159.3754(3)
2456222.3286(6)	2456495.5320(14)
	2456508.4267(4)

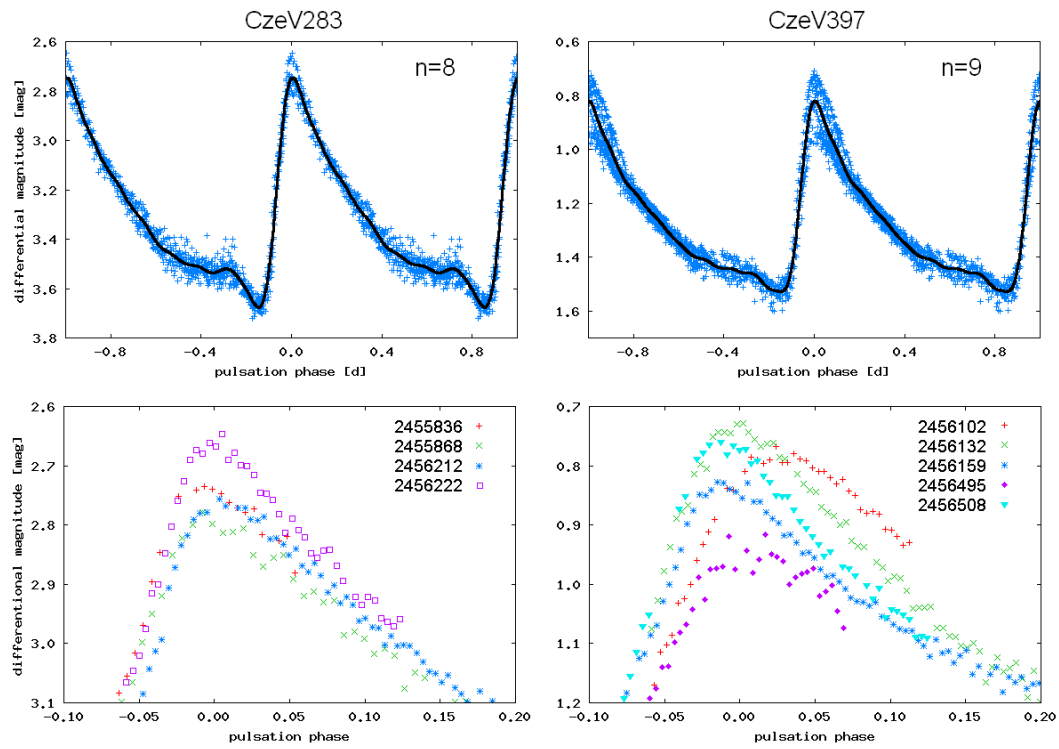


Figure 3.10: Data of CzeV283 and CzeV397 phased according to eq. 3.10 and 3.11 (top panels) and close-ups of the vicinities of the maxima of phased light curves in different nights. Change of the shape and amplitude in different nights is easily noticeable. The Solid lines represent the fit with the sum of sines.

Chapter 4

Characteristics of RRab stars from the ASAS and SuperWASP surveys

4.1 The BlaSGaLF database

Due to the heterogeneity in manifestations of the Blažko effect and current precise measurements, it is very difficult to manage the list of Blažko stars and keep it updated. Concerning globular clusters and stars in the LMC and other galaxies, this is an almost mission impossible. Nevertheless, some attempts have been presented.

The first list summarizing the then known field Blažko stars was the one by Szeidl (1988). This list, which was revised several times and complemented with stars observed mainly in a scope of sky surveys (Sódor & Jurcsik, 2005a; Sódor & Wils, 2005b; Wils et al., 2006), resulted in an on-line catalogue compiled by Nermin Deniz Ulus in 2008 as part of the website of the Blazhko project (Kolenberg, 2005, 2007)¹. This list contained 79 field stars and five stars from globular clusters. Large samples of modulated stars were published e.g. by Szczygiel & Fabrycky (2007, ASAS survey), Le Borgne et al. (2012), who utilized observations of ROTSE telescopes (Klotz et al., 2008), and by Benkő et al. (2010), who described Blažko RR Lyraes in the *Kepler* field. Due to ongoing progress in Blažko star research, all lists become outdated.

Therefore, it was of high importance to manage and maintain an on-line, regularly updated database which could provide observers with information about the modulation of a star. Such a list, which is based on catalogues and more than 70 papers, became available in 2013 with the initial hard-copy compilation of 242 stars. It was named the BlaSGaLF database, which is an acronym of *The Blažko Stars of the Galactic Field*. The on-line version of the catalogue can be found at <http://physics.muni.cz/~blasgalf/>.

Sample stars were divided into three categories according to their modulation type: stars with simple modulation (tab. 4.1, the complete table with references is available as supplementary material on CD or on-line at the project web page), RR Lyraes with multiple modulation (tab. 4.2) and a table with stars which change the length of their modulation period (tab. 4.3). It is worth noting that the latter two categories could overlap. The tables contain designation, coordinates, pulsation type (RRab, RRc), magnitude range, pulsation and modulation periods and references to the periods. The tables 4.1, 4.2, 4.3 contain stars from the BlaSGaLF actual in August 2014.

Coordinates and magnitude ranges are taken from the *Variable star index*, VSX (Watson et al., 2006)². If there is more than one available value of the Blažko period, then the value with the highest priority is given. The hierarchy of cited references is the following: values taken from

¹accessible at <https://www.univie.ac.at/tops/blazhko/Blazhkolist.html>

²Actual version can be found at <ftp://cdsarc.u-strasbg.fr/pub/cats/B/vsx/versions/>

Table 4.1: List of Blažko stars with one modulation period. References in the last column corresponds to those shown under link 'References' on the web page of the BlaSGalF database or in table 'References' which is on the enclosed CD.

Star	RA [^h ^m ^s]	DE [° ' "]	Type	Mag range	P_{Puls}	Modulation period	Reference
SW And	00 23 43.09	29 24 3.6	RRab	9.14 - 10.09	0.4422618	36.8	26
XY And	01 26 42.41	34 04 7.4	RRab	12.9 - 14.22	0.3987247	41.37	9
DM And	23 32 00.67	35 11 49.0	RRab	11.712 - 12.212	0.6304244	...	70
...

Table 4.2: Blažko stars with multiple modulations. References in the last column corresponds to those shown under link 'References' on the web page of the BlaSGalF database or in table 'References' which is on the enclosed CD.

Star	RA [^h ^m ^s]	DE [° ' "]	Type	Mag range	P_{Puls}	Modulation periods	Ref.
RS Boo	14 33 33.21	31 45 16.6	RRab	9.69 - 10.84	0.37733896	41.3, 62.5, 532.48	70, 23
TV Boo	14 16 36.58	42 21 35.7	RRc	10.57 - 11.23	0.3125615	9.737, 21.5	46
RW Cnc	09 19 6.04	29 03 55.7	RRab	10.7 - 12.6	0.547199	29.14, 21.9, 87	70, 26
RU Cet	01 00 40.30	-15 57 27.6	RRab	11.1 - 12.03	0.5862844	98.0, 24.3	70
RX Col	06 13 14.74	-37 15 0.6	RRab	12.32 - 12.95	0.59376	134.3, 79.7	70
SU Col	05 7 47.05	-33 51 54.5	RRab	11.32 - 13.33	0.4873552	65.22, 89.3, 29.5	70, 25
XZ Cyg	19 32 29.31	56 23 17.5	RRab	8.9 - 10.16	0.46659934	57.5, 41.6	20
V808 Cyg	19 45 39.07	39 30 54.8	RRab	15.3 - 16.6p	0.5478642	92.16, 1000	74
V2178 Cyg	19 40 6.99	38 58 20.4	RRab	15.5 - 17p	0.4869538	213, 167.5	64
KIC9973633	19 58 49.07	46 50 56.8	RRab	16.58 - 17.43k	0.51075	67.2, 27.17	74
RW Dra	16 35 31.60	57 50 23.2	RRab	11.05 - 12.08	0.442917	41.42, 72.6	70
V417 Dra	19 00 58.78	48 44 41.6	RRab	11.83 - 12.26	0.61322	40.21, 58.9	74
AG Her	16 40 32.85	40 37 06.1	RRab	11.99 - 13.24	0.6494465	79.69, 47.93	21
LS Her	16 02 3.79	17 28 50.4	RRc	11.04 - 11.53	0.230808	12.75, 109	21
IK Hya	12 04 47.27	-27 40 43.3	RRab	9.96 - 10.42	0.6503243	71.81 - 75.57, 1403	70
CZ Lac	22 19 30.76	51 28 14.8	RRab	10.77 - 11.26	0.432174	14.6, 18.6	30
RZ Lyr	18 43 37.88	32 47 54.0	RRab	10.6 - 12.03	0.51123	121, 30	11
V353 Lyr	18 52 1.78	45 18 31.4	RRab	16 - 17p	0.5568016	71.8, 132.2	74
V354 Lyr	18 52 50.27	41 33 49.4	RRab	15 - 16p	0.5616892	849, ?	74
V355 Lyr	18 53 25.83	43 09 16.2	RRab	13.8 - 15.3p	0.4737027	31.02, 16.24	74
V360 Lyr	19 01 58.53	46 26 45.7	RRab	15.5 - 16.5p	0.5575765	52.03, 21.07	74
V366 Lyr	19 09 40.65	46 17 18.1	RRab	15.5 - 16.5p	0.5270283	62.84, 29.29	74
V445 Lyr	18 58 25.59	41 35 48.6	RRab	15.3 - 17.3	0.5130907	54.83, 149.9	74
V450 Lyr	19 09 36.66	43 21 50.0	RRab	14.3 - 16.7p	0.5046198	123.8, 80.5	74
KIC7257008	18 47 27.41	42 49 52.7	RRab	16.13 - 16.95k	0.51177516	39.67, ζ 900	74
RY Oct	21 36 9.37	-77 18 13.5	RRab	11.46 - 12.46	0.5634476	217, 26.88	70
V784 Oph	17 35 25.19	7 45 21.1	RRab	11.952 - 12.898	0.6033557	24.51, 34.29	61
V872 Oph	17 55 17.81	8 13 42.9	RRab	14.7 - 15.8	0.45197319	13.5, 51.13	40
V1820 Ori	05 54 37.13	4 54 11.4	RRab	12.5 - 13.4	0.4790486	27.917, 34.72	47
AE Scl	01 07 25.81	-32 18 35.1	RRab	11.802 - 12.922	0.5501124	46.2, 104.7	70
UZ UMa	08 18 53.94	73 5 47.8	RRab	13.1.2015	0.4668413	26.7, 143	8
AM Vir	13 23 33.33	-16 39 57.9	RRab	11.16 - 11.85	0.61509	49.61, 141.9	70

detailed studies have the highest priority, data from surveys have lower priority, and the data based on *O-C* studies have the lowest priority. There are some exceptions, mainly if the data with should have higher priority were published before 1990 or if the data are of worse quality than values with lower priority. If the values of Blažko periods from literature differ by more than one day, then all available values are listed.

Table 4.3: Stars with changing Blažko period. References in the last column corresponds to those shown under link 'References' on the web page of the BlaSGaLF database or in table 'References' which is on the enclosed CD.

Star	RA [^h ^m ^s]	DE [° ' "]	Type	Mag range	P_{Puls}	Modulation period	Ref.
RZ CVn	13 45 03.11	32 39 16.5	RRab	10.88 - 11.92	0.5674325	29.6 - 33.36	70
XZ Dra	19 9 42.61	64 51 32.1	RRab	9.59 - 10.65	0.4764955	73 - 77	24
RR Lyr	19 25 27.91	42 47 3.7	RRab	7.06 - 8.12	0.566839	38.8 - 40.8	22
AD UMa	09 23 38.66	55 46 33.2	RRab	15 - 16.3	0.548315	35 - 40	26
RV UMa	13 33 18.09	53 59 14.6	RRab	9.81 - 11.3	0.46806	89.9 - 90.63	12
GSC02626-00896	18 09 30.34	32 45 13.5	RRc	12.9 - 13.4c	0.3227214	... - 26	76

If possible, the ASAS and other designations of the stars are transformed to GCVS names. Among others, this was the case for V1820 Ori, BB Lep, V339 Lup, MR Lib, V559 Hya, V552 Hya, V701 Pup, LR Eri, IY Eri, GW Cet, DZ Oct, V354 Vir, V419 Vir, V476 Vir, V551 Vir, OR Com, BT Sco, V1319 Sco, BT Ant, AD UMa, NS UMa, PP UMa, KV Cnc, AI Crt, and FR Psc, which were noted in Wils et al. (2006) and Szczygiel & Fabrycky (2007) in other forms.

The first version of the BLASGALF provided information about some peculiarity of particular objects. Stars with a Blažko period longer than 1000 d were marked by a colon in the second column. The same mark was used for stars that were only suspected of the Blažko effect or whose Blažko period has not been well determined. However, it was realized that almost all stars deserve to be marked as interesting objects. Consequently such mark is not used any more.

The current on-line version of the list (August 2014, fig. 4.1) contains 338 stars. The currency of data is guaranteed by daily scanning of new papers and by private communication with observers and authors. The list gives preference to bright RR Lyraes. Blažko stars identified in large surveys like LINEAR or CATALINA are omitted, because their lists were not published.

Except for providing a quick overview of the stars, BLASGALF offers the possibility to compile basic statistics for field Blažko variables. Currently the database contains the following:

- 283 RRab type stars (248 single modulated, 5 variables with changing Blažko period, 30 stars with multiple modulation period),
- 55 first overtone Blažko RR Lyraes (52 single modulated, 1 with changing Blažko period, 2 multi modulated),
- 6 stars that undergo modulation period changes,
- 32 stars that show a multiple Blažko effect.

In these statistics 25 new Blažko stars discovered in the ASAS and SuperWASP surveys (sec. 4.2) are already included. Fundamental mode RR Lyraes constitute 84 % of known field Blažko stars. About 10.5 % of them show a compound Blažko effect with more than one modulation period. This percentage is probably much higher, but appropriate data is needed for the discovery of additional modulation components (ultra-precise measurements indicate that about 80 % of modulated stars have compound modulation Benkő et al., 2014).

The distribution of modulation periods from the BLASGALF, plotted with respect to the basic pulsation period of stars, is in fig. 4.2. This plot, which is complemented with RRab stars from the

Known Blazhko stars in Galactic field

[Stars with one Blazhko period](#)

[Stars with changing Blazhko period](#)

[Stars with multiple Blazhko period](#)

[Sorted by RA](#)

[Sorted by Constellation](#)

[References to all resources](#)

[Description of the website and tables](#)

[Last modification: 18th August 2014](#)

The presented list contains 338 RR Lyrae type stars exhibiting the Blazhko effect.

Acknowledging us: If you have used this database in a paper then please add this citation: [Skarka, M. 2013, A&A, 549, A101](#)



Description of the website

This regularly updated website was created in an attempt to give an overall list of RR Lyraes which exhibit (or are suspected to exhibit) the Blazhko effect. This list is named **BlaSGaIF**, which is an abbreviation of Blazhko Stars of the Galactic Field. The tables contain only galactic Blazhko stars. Stars located in the galactic bulge or in globular clusters are not listed. Values given in tables come from available literature. Updating of the contents and values is based on regular checking of new publications. For each star the name, coordinates, type, magnitude range, pulsation period, Blazhko period and references are given.

Blazhko stars are divided into three groups according to the type of modulation. Just below the title you can find three links - stars with one Blazhko period ([sorted by RA](#) and [sorted by constellation](#), this table contains the majority of modulated RR Lyraes), [Stars with changing Blazhko period](#) (modulation period is not a constant) and [Stars with multiple Blazhko period](#) (table with stars with more than one modulation period).

Link [References to all resources](#) takes you to the list with publications from which the values were taken. Under [Last modification](#) you can find a description of the latest changes to tables and the website.

Description of the tables

Column 1	If possible, the GCVS name of the star is given. If the star has no GCVS name, another available designation is mentioned (ASAS, GSC, KIC etc.)
Column 2 - RA	Right ascension (epoch J2000.0) in the form of hours, minutes and seconds divided by spaces.
Column 3 - RA	Declination (epoch J2000.0) in the form of degrees, minutes and arcseconds divided by spaces.
Column 4 - Type	Type of RR Lyr - either RRab or RRc.
Column 5 - mag	Magnitude range in V. If noted, c means 'clear', R means Johnsons R filter, k kepler system, p photographic
Column 6 - P_{puls}	Basic pulsation period in days.
Column 7 - P_{bl}	Blazhko period in days.
Column 8 - Ref.	Reference for Blazhko period.

The same column description applies to the values in the tables with changing Blazhko period and with multiple Blazhko period.

Acknowledgements: We made use of NASA's Astrophysics Data System and the International Variable Star Index (VSX) database, operated at AAVSO, Cambridge, Massachusetts, USA. Work on the list has been supported by GACR project GD205/08/H005, MU MUNI/A/0968/2009, MUNI/A/0735/2012.

Contact: This database is managed by Marek Skarka. If you have more recent values or if you have any suggestions, please let me know: maska@physics.muni.cz

Figure 4.1: Current look of the on-line version of the BlaSGaIF database.

LMC (Alcock et al., 2003), resembles fig. 2.12. Although the preference for short and extremely long Blažko periods is still pronounced, the RRc dichotomy found by Szczygiel & Fabrycky (2007) has been broken - several RRc stars have periods in the order of hundreds of days.

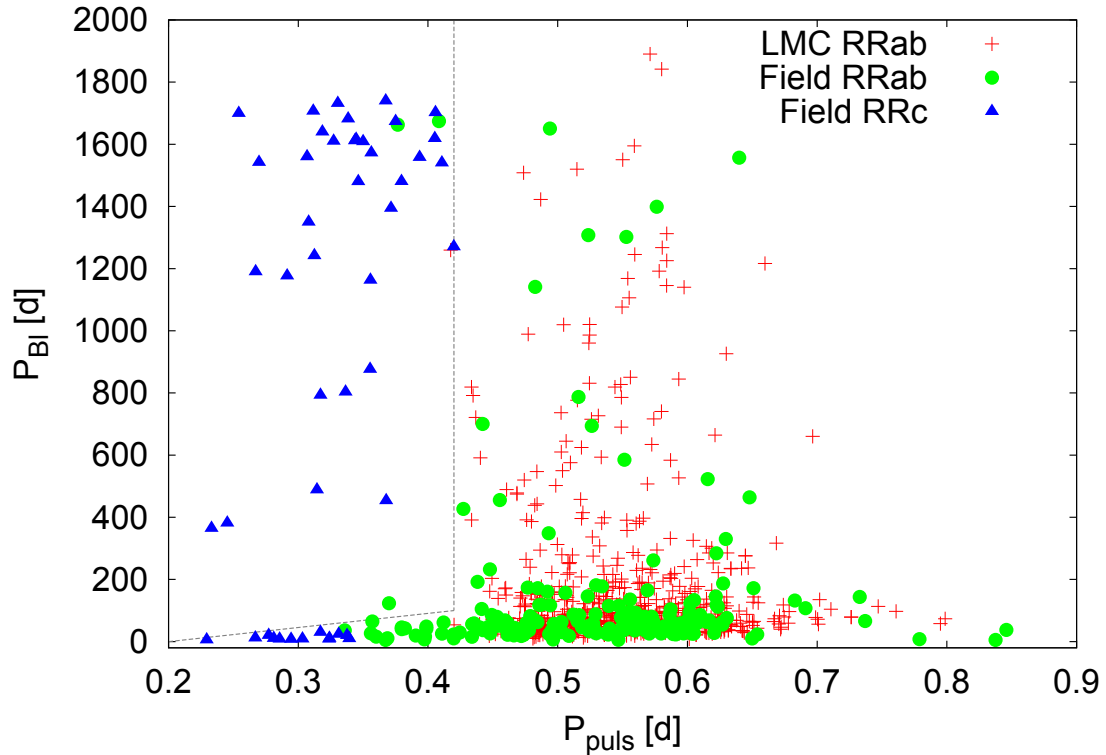


Figure 4.2: Distribution of modulation periods with respect to the basic pulsation period. For the sake of clarity HH Aqr, with modulation period of 3360 d, is not shown.

Fundamental mode stars are clearly separated from first overtone pulsators. It seems that the location of RRab stars is limited. Short period RRab Lyrae stars ($P_{\text{puls}} < 0.42$ d) are well below the line defined as $P_{\text{BI}} = -48 + 240P_{\text{puls}}$, *i.e.* they all have modulation periods shorter than 100 d. The only three exceptions are ASAS202746-2850.5 and ASAS054843-1627.0 with Blažko periods over 1600 d, and SS Tau with a 123-day modulation period. Stars with a pulsation period longer than 0.7 d have a similar behaviour: they all have modulation periods shorter than 200 d. The modulation period is generally shorter than 200 days between pulsation periods of 0.42 d and 0.7 days, but it can be as long as several hundreds or thousands of days. An interesting is a lack of modulated stars among short-period LMC stars.

We have a few future plans with the database. The most important improvements that should be available soon are links to the VSX (Watson et al., 2006) and GEOS databases (Le Borgne et al., 2007) for each star. Other intended changes relate to the organization of the website – sorting according to various characteristics, listing with regard to a particular constellation, a new section for stars currently only suspected of the Blažko effect etc. Other ideas are to extend the current information with light curves, amplitudes of the Blažko effect and with Fourier parameters. In addition, basic information about the Blažko effect might be provided on the website.

4.2 Study of the Blažko effect based on data from ASAS and SuperWASP surveys

Data from automatic sky surveys provide an invaluable opportunity for finding new variables and for long-term monitoring of the sky. The most extensive surveys of the Galactic field dealing with variable stars are without a doubt the Polish ASAS and SuperWASP managed by the University of Leicester.

Field RR Lyrae stars have been well studied by means of various automated surveys. Among others, Kinemuchi et al. (2006) and Wils et al. (2006) utilized data from NSVS, e.g. Kovács (2005) and Szczygieł et al. (2009) studied RR Lyraes based on ASAS data, and Drake et al. (2013) dealt with RR Lyraes measured in the CATALINA sky survey³. Large samples of Blažko RR Lyrae stars in galactic bulge were also studied in the framework of the MACHO and OGLE surveys (Soszyński et al., 2011; Moskalik & Poretti, 2003). Since the stars in the bulge are faint, and are not included in the ASAS or SuperWASP surveys, they were excluded from this study.

Concerning the Blažko effect in galactic RR Lyrae stars observed by automated surveys, several papers have been published so far. For example, Kovács (2005), Wils & Sódor (2005) (hereafter WS05), and Szczygieł & Fabrycky (2007) (hereafter SF07) studied stars observed by the ASAS survey. All these authors revealed many new Blažko variables. They also provided a list of these stars. An extensive study of the Blažko effect with *TAROT* telescopes (Klotz et al., 2008, 2009) is presented in the paper of Le Borgne et al. (2012). Another recent example of a comprehensive analysis of Blažko stars is the study of Bramich et al. (2014) on the data from the Qatar Exoplanet Survey (Alsubai et al., 2013). They detected modulation in 38 stars for the first time and determined modulation periods for 26 of them. However, in the case of SuperWASP, no comprehensive study of RR Lyraes has been performed yet. There are only very few studies on particular RR Lyraes, e.g. our work on TV Boo (sec. 3.1), or the study of GSC02626-00896 by Srdoc & Bernhard (2012), who revealed the Blažko effect in this star.

The goal of our work was to search for the presence of modulation and to describe its characteristics (modulation periods and multiplicity/irregularity of the modulation) based on ASAS and SuperWASP data. We applied the commonly used techniques of light curve and frequency spectra examination described in sec. 2.3.1 to complement and extend the list of known Blažko stars with bright RR Lyraes (up to 12.5 mag in maximum light). To be as precise as possible, we carefully cleaned and analysed each light curve and frequency spectrum individually.

4.2.1 The surveys and data characteristics

Both the ASAS and SuperWASP data are products of measurements with low-aperture telescopes (fig. 4.3). ASAS uses Johnson *V* and *I* filters, while SuperWASP telescopes are equipped with a broad-band filter (from 400 to 700 nm) (Pojmanski, 2001; Pollacco et al., 2006). Targets observed by both surveys are preferably located in the southern hemisphere, because ASAS measures only up to dec $+28^\circ$ and SuperWASP up to dec about $+60^\circ$. The typical scatter of data points is difficult to define, because it changes from target to target. In the case of ASAS it is from about 0.02 to 0.1 mag, while SuperWASP scatter extends from 0.007 to 0.04 mag for our sample stars. Also the time span and the distribution of the data differ for both surveys and various targets.

ASAS data typically cover a few years (up to year 2009) with point-to-point spacing between two and four days with only small gaps between observational seasons. Typical sampling of SuperWASP data points is between five and twelve minutes. Therefore SuperWASP data are generally

³<http://www.lpl.arizona.edu/css>



Figure 4.3: ASAS (the left panel) and SuperWASP (the right panel) telescopes. Figures taken from http://en.wikipedia.org/wiki/All_Sky_Automated_Survey and <http://www.superwasp.org/>.

more numerous and more dense than ASAS data, but they typically span only one or two seasons⁴ (except for table 4.8 see last columns in tables 4.4-4.9). These characteristics resulted in a typical Nyquist frequency from 0.17 to a few tens for ASAS and in 100 to more than 1000 c/d in the case of SuperWASP. For differences between ASAS and SuperWASP data see fig. 4.4, where data for RY Col are plotted with their spectral windows.

4.2.2 Sample selection and data cleaning

The basic set of stars originated in the GCVS catalog (Samus et al., 2012), which contains 512 stars of the RRab type brighter than 12.5 mag in maximum. This magnitude limit was chosen to analyse only stars with the best data quality – the scattering of data points for stars over 13 mag rapidly increases. The list extracted from GCVS was enhanced with 82 stars, which did not have a GCVS designation in 2012 and which were taken from SF07 and Szczygiel et al. (2009). There were data for 475 stars available in the ASAS database, and for 243 RR Lyrae stars in the SuperWASP archive. Data of 161 stars appeared in both the ASAS and SuperWASP archives. This means that a total of 557 stars remained for further analysis.

Unfortunately, data from automatic surveys are often very noisy and of bad quality. Therefore we first looked for ephemerides of the stars in the VSX to be able to construct phased light curves. This was done to quickly check the quality of the data. In many cases, the periods that we found were not current. Therefore we were forced to update and roughly estimate the actual pulsation period. For this purpose, as for all our other period analyses, PERIOD04 software was used.

In the case of the ASAS survey, only the best quality *V*-data (with flags A and B) were used. Following Kovács (2005), ASAS *V* magnitude was calculated as the weighted average of five values in different apertures using

$$V(t) = \frac{\sum_{i=1}^5 V_i(t) \sigma_i^{-2}(t)}{\sum_{i=1}^5 \sigma_i^{-2}(t)}. \quad (4.1)$$

Only light curves with more than 200 points from ASAS and with more than 1000 points from SuperWASP were left in the sample for further investigation.

⁴There are a few exceptions which cover three years.

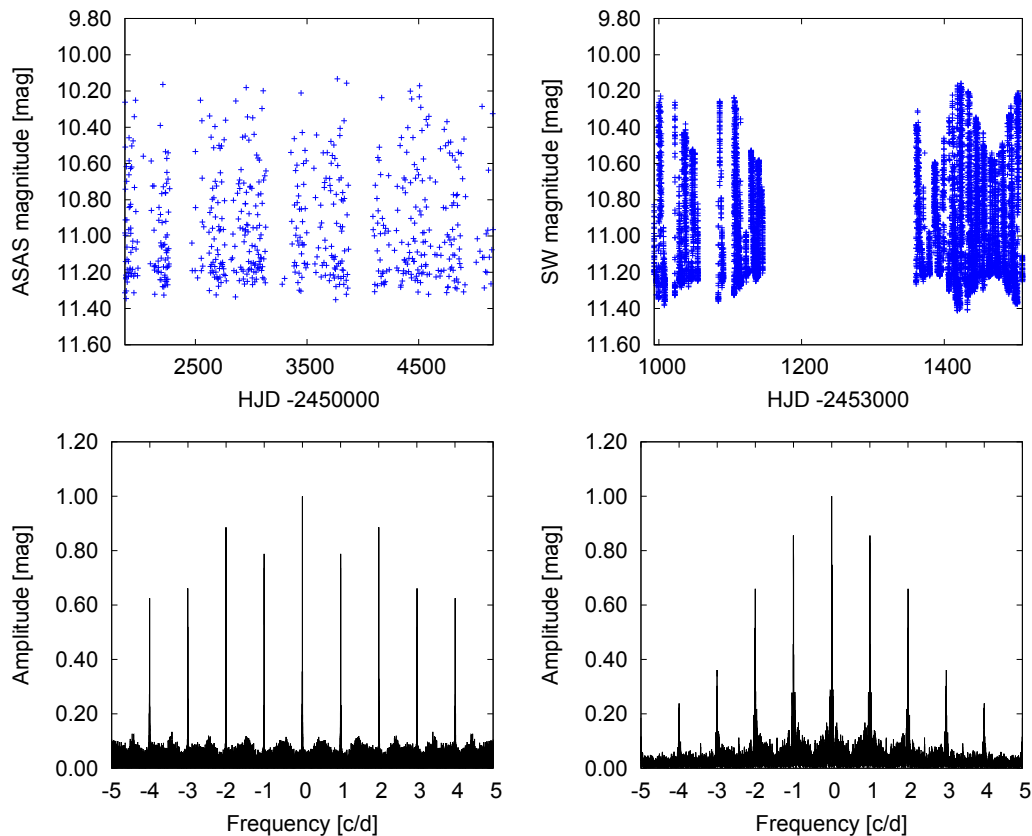


Figure 4.4: Differences between ASAS (left panels) and SuperWASP (right panels) data of RY Col together with their spectral windows (bottom panels). ASAS data are more or less uniformly distributed, while SuperWASP data show a large gap between observing seasons. Both spectral windows are dominated by strong daily aliases. Except these, SuperWASP data suffer from additional artefacts, namely from yearly aliases.

Once the phased light curves were prepared, we briefly evaluated them to immediately discard stars whose data, at a glance, were very noisy. The remaining light curves were then fitted with the sum of sines and points that were further away than 0.5 mag from the fit were automatically removed. This procedure guaranteed that real outliers were eliminated and points possibly scattered by the Blažko effect remained in the dataset. A careful visual examination of all light curves was then applied, and points which were unambiguously caused by noise were manually deleted. In the case of SuperWASP stars, we also visually scanned the time series night-by-night and removed outliers as well as entire noisy nights. Figure 4.5 shows steps in the cleaning process in the case of V559 Hya.

SuperWASP data often contained vertically shifted multiple points. This was the consequence of simultaneous imaging of the target by a few cameras. To avoid using such data, the information about the position of the star on the chip (fig. 4.6 bottom panels) was utilized. If the separation of the data from two cameras was impossible, each star with a vertical separation of points larger than 0.01 mag was discarded. This was for instance the case for DM And (fig. 4.6), which shows previously unknown modulation, and which was rejected from the sample.

Several targets from SuperWASP underwent vertical shifts of points taken in different seasons (as the third season of DM And, fig. 4.6). In such cases seasons were phased separately, and the light curves were fitted with the sum of sines to get zero points. Afterwards, the points from

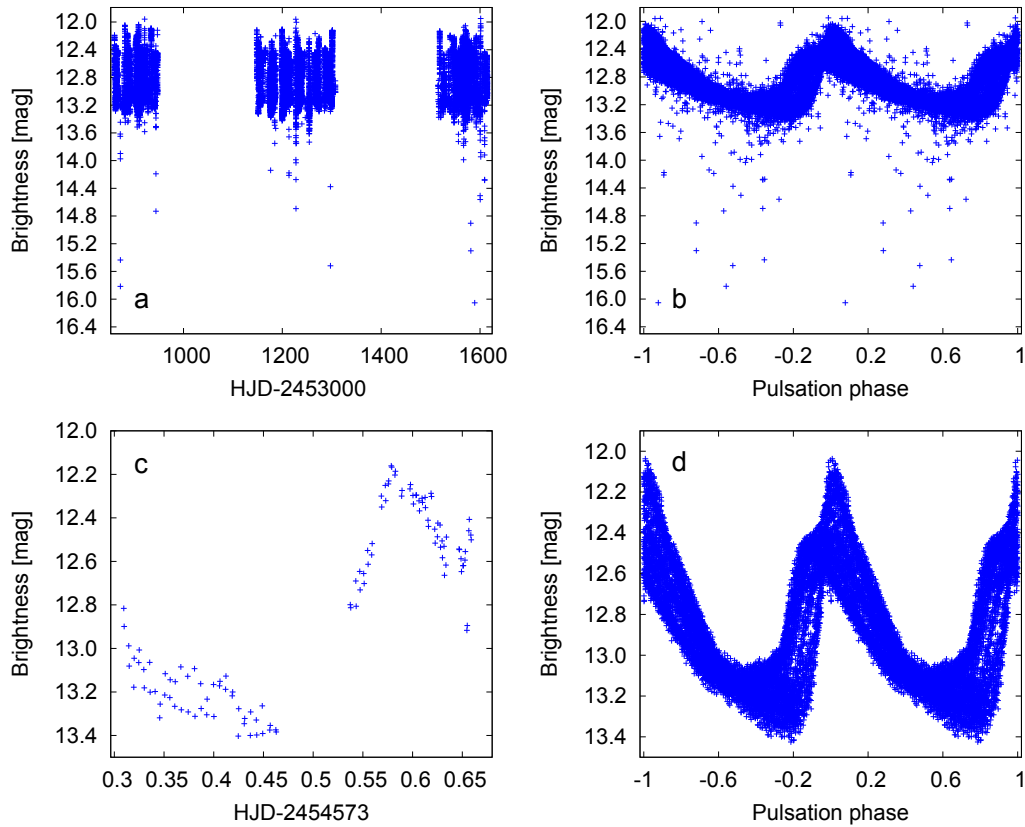


Figure 4.5: Steps in the cleaning process for V559 Hya. Panel 'a' shows raw SuperWASP data (in panel 'b' folded with the basic pulsation period), panel 'c' shows one of omitted nights that was discarded due to poor quality of the data, and finally panel 'd' plots cleaned data.

different seasons were shifted to fit one another. For example, this procedure was used in the case of U Tri, and magnitudes of the first part of the dataset were decreased by 0.09 mag. In some cases, when vertical shifts were present even in one season, we removed the whole season from the dataset. If all seasons underwent shifts, the star was discarded from the sample. Only 321 variables met all the above-mentioned criteria and were accepted for further analysis.

4.2.3 Methods of searching for the Blažko effect

Searching for the Blažko effect actually started during the cleaning process when phased light curves were examined. High-amplitude modulation was easily resolvable by a fleeting glance at the data. Our methods, inspired by methods used e.g. in Alcock et al. (2003), WS05, and Le Borgne et al. (2012), can be summarized in four points:

1. *Phased light curve visual examination* – visual inspection of the phased light curve to reveal a characteristic scattering around maximum light.
2. *Frequency spectra analysis with PERIOD04* – frequencies were fitted independently; i.e., we scanned for frequencies with the highest amplitude and subsequently subtracted them. This was done in the range of 0 – 30 c/d down to the signal-to-noise ratio (S/N) of the peaks higher than four⁵. We searched for the manifestation of the Blažko effect in the vicinity of

⁵This limit is usually used for plausible analysis (Breger et al., 1993).

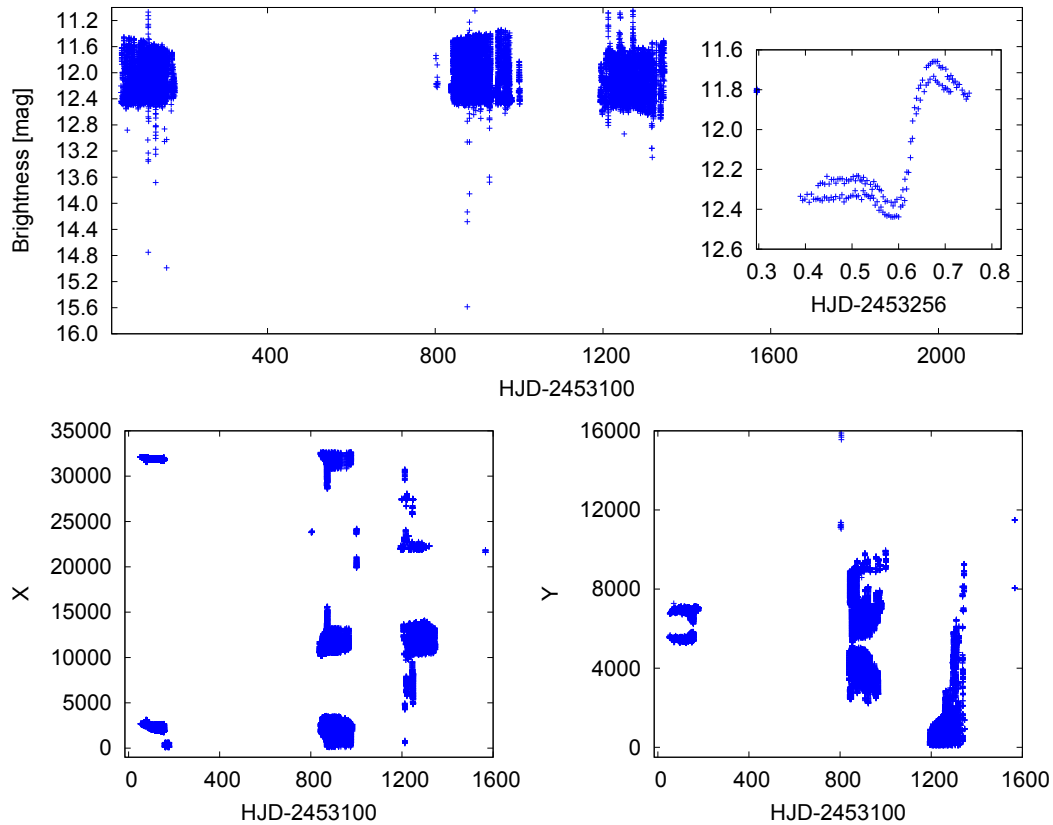


Figure 4.6: Illustration of difficulties in SuperWASP data processing in the case of DM And which was discarded from our sample. The upper panel shows raw data. The change in amplitude of this star caused by the Blažko effect is apparent. The detail shows the night of HJD 2453256, where the vertical shift between data coming from various cameras is demonstrated. The distribution of the positions of the star on the chip in x and y directions during the whole observation period are shown in the bottom part of this figure.

the main pulsation components, as well as for the presence of the Blažko peak itself (in the range of ~ 0.0001 to 0.2 c/d). All uncertainties were estimated using PERIOD04 tools.

3. *Checking of residuals* – In stars with only basic pulsation components in the frequency spectrum, residuals after prewhitening were visually inspected to see whether there were any typical inhomogeneities possibly caused by the Blažko effect.
4. *Magnitude-at-the-maximum-light vs. time-of-the-maximum series analysis* – this was done only for the SuperWASP sample, because ASAS light curves, with few exceptions, did not contain continuous time series to determine times and magnitudes of the maximums. For Mag_{\max} and T_{\max} determination, low-degree polynomial fitting (typically up to 5th order) was used. Only well defined maximums were fitted. In the next step, frequency analysis of such series was performed to search for a significant peak in the range of ~ 0.0001 to 0.2 c/d.

Each star was analysed individually without any automatic procedures (except for the removal of outliers and for prewhitening of the frequency spectra). We maintained permanent visual supervision of all steps to avoid omitting any possible sign of the Blažko effect. A candidate was marked as a Blažko star only if we were able to find the modulation period or if there was no doubt about the Blažko effect. Some exceptions, e.g. LS Boo, are discussed in sections 4.2.4 and 4.2.5.

As an example of the procedures used, the analysis of HH Tel (fig. 4.7) is demonstrated. This star was revealed to be a new Blažko star. Data from both surveys are plotted at the top in the first two columns of fig. 4.7. We can see a weak sign of the modulation around maximum light (especially in SuperWASP data). This indicated that the Blažko effect might be present. Frequency spectra analysis down to $S/N = 4$ unveiled only the main pulsation components. After prewhitening peaks that could possibly be caused by the Blažko effect ($f_0 \pm f_{BL}$) were identified, but they are of very low amplitude with $S/N \sim 3$ (fig. 4.7 two left bottom panels). No distinct peak in the range of ~ 0.0001 to 0.2 c/d was detected.

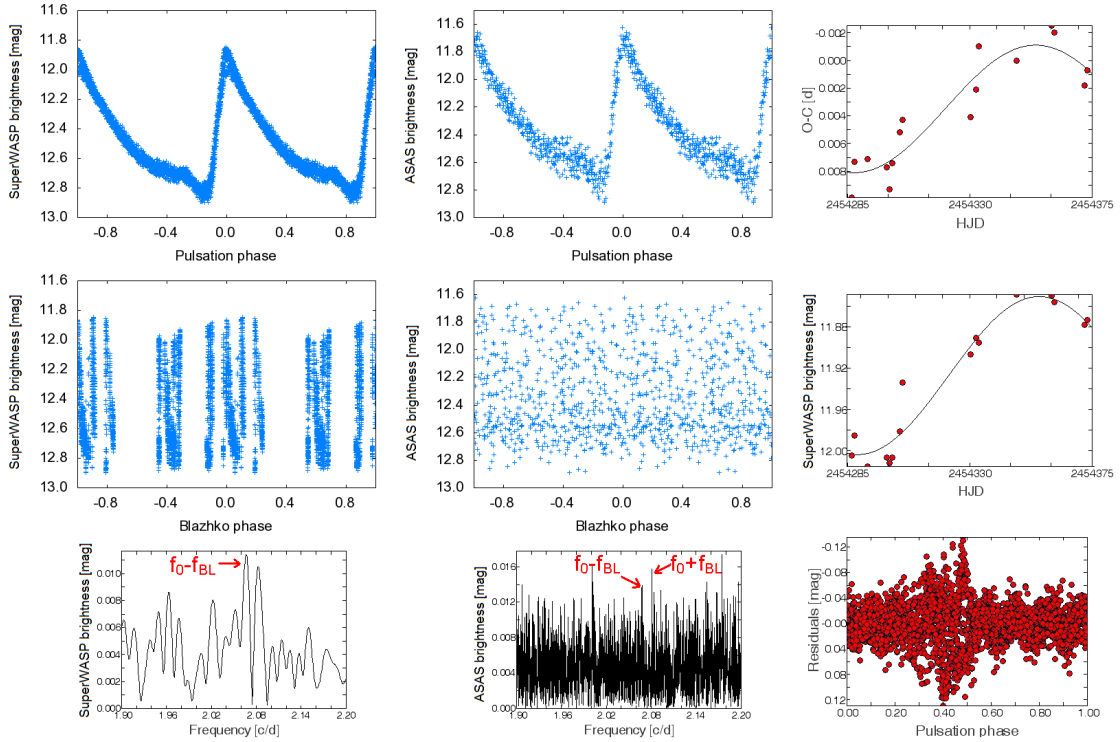


Figure 4.7: Analysis of HH Tel. The first column shows cleaned SuperWASP data folded on epoch 2454347.2643 with the main pulsation period $P = 0.4820925$ d (top panel) and with the Blažko period 133 d (middle panel). The frequency spectrum based on SuperWASP data in the vicinity of f_0 prewhitened with kf_0 is shown in the bottom panel in the first column. The second column displays the same as the first one, but for the ASAS data. The third column (based on SuperWASP data again) displays from the top changes in $O - C$ values, changes in maximum brightness, and residuals after prewhitening with the main pulsation components at the bottom (epoch is shifted by half a period for a better arrangement). For details see the text in section 4.2.3.

Consequently searching for additional peaks in the frequency spectra of the light curve yielded inconclusive results. However, the SuperWASP residuals (right bottom corner of fig. 4.7) showed a tell-tale characteristic of the Blažko effect: typically scattered points around the position corresponding to the ascending branch and maximum light.

The last step was to determine the modulation period. For this purpose the times (T_{\max}) and brightnesses of maximum light (Mag_{\max}) were used. Period analysis of such data directly revealed a modulation period of 133(9) d, while weak peaks identified in Fourier spectra of the light curves gave values 143(1) d and 123(5) d for ASAS and SuperWASP data, respectively. All values are very inaccurate, which is due to the limited time scale of SuperWASP data (only one Blažko cycle) and due to the inferior quality of ASAS data.

At that stage we were able to construct Blažko phased light curves (first two columns in the middle of fig. 4.7) to check for the correctness of the value we found. SuperWASP data showed a typical ‘Blazhko’ light curve, while there was no sign of modulation in the ASAS Blažko light curve⁶.

HH Tel was chosen intentionally to show that it is very problematic to decide the Blažko nature of this star based on ASAS data alone, while there is no doubt about the modulation in SuperWASP data. The example of HH Tel clearly shows that many Blažko stars could remain unveiled in the ASAS database.

4.2.4 Blažko stars from ASAS

Known Blažko stars

A review of 62 previously known Blažko stars included in our ASAS sample is given in Table 4.4. For comparison the values of Blažko periods found by WS05 and SF07 are also given (5th and 6th column). These are naturally very similar to ours, because we studied the same, but slightly more extended data. Therefore, with respect to periods, only a revision of the ASAS data was actually performed.

Epochs given in Table 4.4 are not times of maxima, which are usually given, but they are arbitrarily chosen to obtain Blažko-phased light curves, as well as the light curves phased with the main pulsation period, with the maximum around the zero phase. The amplitudes A_+ , A_- of the side peaks $f_{\pm} = f_0 \pm f_{BL}$ corresponding to the Blažko period P_{BL} are in the 7th and 8th columns, and their ratio (A_+/A_-) in the 9th column, respectively. All given Blažko periods in the study correspond to the side peak with the highest amplitude in the frequency spectrum. Label ‘ n ’ denotes the number of points used, and ‘ TS ’ their time span.

Eight of these stars (marked by an asterisk) showed additional peaks close to the basic pulsation components, which could possibly point to irregularity in modulation, period changes, or multiplicity of the modulation. The modulation periods for VX Aps, GS Hya, and AS Vir were estimated for the first time. The only equally spaced quintuplet was identified in RS Oct (fig. 4.8).

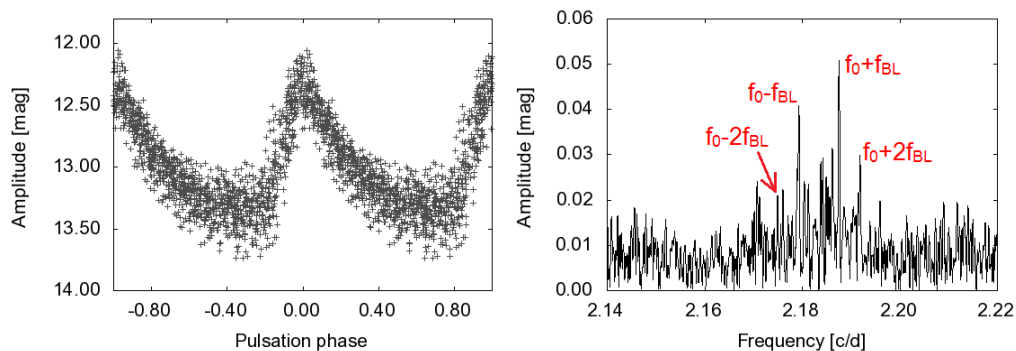


Figure 4.8: RS Oct, the only star in our ASAS sample that shows an equally spaced quintuplet.

Modulation of some known Blažko stars was not detectable in the ASAS sample. RZ Cet, RV Sex, V413 Oph, BB Vir, SW Cru, V Ind, and Z Mic were only presumed to show modulation with no amplitude or period of the modulation determined (Kovács, 2005; Samus et al., 2012; For et al., 2011; Jurcsik & Kovács, 1996). Either they are stable or their modulation is of low amplitude. In V672 Aql we found a possible Blažko period of 425.8 d, but the peak had $S/N < 4$ and the

⁶Compare with the light curve in fig. 4.11, where the ASAS data of HH Tel are phased with 143-day period and where the Blažko effect is apparent.

Table 4.4: Known Blažko stars from our ASAS sample

Star	Epoch HJD	P_{puls} [d]	P_{BL} [d]	WS05	SF07	A_{-} [mag]	A_{+} [mag]	A_{+}/A_{-}	n	TS [d]
BS Aps	2454527.8757	0.5825596(7)	46.53(7)			-	0.026	-	646	3210
VX Aps	2451981.7844	0.484663(2)	171.8(6)			0.024	0.039	1.60	647	3210
TY Aps	2452088.5376	0.501698(1)	108.6(2)			0.033	0.049	1.48	601	3208
V360 Aqr	2452168.6700	0.626946(3)	54.44(4)		54.52	-	0.097	-	413	3254
S Ara *	2454247.7025	0.451849(1)	49.51(5)	49.5	49.37	0.043	0.044	1.02	507	3175
TT Cnc	2454202.5461	0.563454(1)	88.8(2)			0.022	0.045	2.05	342	2546
RV Cap	2452002.1370	0.4477426(6)	232.3(5)		231.66	-	0.105	-	543	3117
Star 1	2452034.5590	0.526235(1)	694(10)		666.44	0.037	0.065	1.78	509	3245
BI Cen	2454932.6911	0.4531949(4)	79.45(9)		79.01	0.039	0.042	1.08	767	3179
RX Cet	2454666.8472	0.573741(1)	261.5(8)	256	255.5	0.058	-	-	397	3287
RV Cet	2452080.9219	0.6234136(8)	112.0(1)	112	112.05	0.025	0.040	1.60	394	3275
RX Col	2454751.8312	0.593749(3)	132.5(4)	130		-	0.043	-	675	3298
RY Col	2453854.5121	0.4788357(5)	82.12(7)	82	81.95	0.028	0.073	2.61	624	3298
WW CrA	2452514.1932	0.559490(1)	35.69(2)	35.5		0.039	0.025	0.64	530	3176
V413 CrA	2454508.8898	0.5893427(4)	60.5(2)		59.96	0.009	0.010	1.11	542	3158
X Crt	2453449.7158	0.732836(1)	143.8(3)	143		-	0.017	-	436	3296
VW Dor *	2454136.7779	0.5705770(7)	25.92(2)	25.9		0.014	-	-	667	3295
XY Eri	2452553.7594	0.554250(1)	50.11(5)	50		0.052	0.079	1.52	511	3287
LR Eri *	2453408.6223	0.602228(1)	123.5(6)	122		-	0.045	-	893	3296
Star 2	2453745.5476	0.62963274(9)	330(2)		335.29	0.033	0.050	1.51	683	3296
RX For	2452082.9124	0.5973129(8)	31.80(6)	31.8	31.81	-	0.061	-	517	3287
SS For	2451869.5957	0.4954329(4)	34.84(1)	34.8	34.88	0.026	0.064	2.51	501	3295
RT Gru	2452858.6870	0.512169(1)	86.94(8)			-	0.079	-	496	3256
DL Her	2453477.7851	0.591631(1)	34.66(4)			-	0.038	-	427	2396
BD Her	2453496.8160	0.473794(1)	21.68(1)			0.052	0.085	1.63	308	2417
GS Hya	2451998.7258	0.522829(1)	42.8(5)			0.051	-	-	453	3186
UU Hya	2453761.7195	0.5238652(9)	39.93(4)			0.042	-	-	349	3112
SV Hya	2452062.5225	0.4785476(3)	63.23(4)	63	63.29	0.022	0.028	1.27	877	3178
V552 Hya	2454931.6746	0.3987697(8)	48.53(3)	48.3		0.142	0.072	0.51	443	3177
V559 Hya *	2454199.5359	0.447944(2)	26.469(6)	26.6	26.5	0.076	0.135	1.78	454	3187
SZ Hya	2454258.5213	0.537225(1)	26.26(2)	26.3	26.3	0.076	0.080	1.05	543	3298
DD Hya	2454408.8593	0.5017706(6)	34.44(4)			0.036	0.027	0.75	634	3142
SZ Leo	2455012.4827	0.534080(9)	177.8(7)	179		0.091	0.062	0.61	339	2560
BB Lep	2452128.9235	0.5389127(9)	22.86(1)		22.84	0.039	0.041	1.05	567	3300
MR Lib	2453133.7052	0.540065(1)	41.85(3)	41.7	41.77	0.051	0.115	2.25	430	3172
PQ Lup	2453861.6802	0.581994(1)	48.77(3)	48.8	48.82	-	0.068	-	478	3189
V339 Lup	2453897.6107	0.6005772(7)	49.7(9)	49.5		0.014	0.029	2.07	526	3191
Star 3	2453428.6223	0.5501319(9)	37.2(2)		37	0.046	0.059	1.28	466	3186
UV Oct	2451976.8227	0.5425783(5)	144.6(2)	145	143.73	0.047	0.052	1.10	1292	3233
SS Oct	2453882.8524	0.6218497(4)	145.0(5)	145	144.12	0.020	0.021	1.05	1401	3297
RS Oct	2454255.6649	0.458007(1)	241(1)	244	244.2	0.045	0.058	1.29	1258	3295
DZ Oct	2453055.6301	0.4778589(6)	36.63(2)	36.8	36.79	0.066	0.047	1.40	1119	3294
V2709 Oph	2452454.6100	0.4613691(7)	22.18(1)	22.2	22.18	-	0.022	-	447	2944
FO Pav	2452947.5986	0.5514365(9)	585(6)	571	557.17	0.048	0.052	1.08	536	3272
BH Pav *	2452141.8540	0.4769604(5)	173.7(3)		173.7	0.061	-	-	1038	3161
BH Peg *	2452813.8617	0.640987(1)	175.7(7)			-	0.022	-	213	2346
ST Pic	2455105.8195	0.485744(1)	117.7(1)		117.9	0.011	-	-	660	3294
RY Psc	2452944.7300	0.529739(1)	153.3(5)		154.53	-	0.053	-	372	3279
X Ret *	2453823.5050	0.491995(2)	160.3(3)	161	160.64	0.039	0.052	1.33	1081	3273
V1645 Sgr*	2452141.9570	0.5529477(9)	1302(12)		1331.74	0.053	0.081	1.53	747	3271
V2239 Sgr	2452031.8445	0.4401917(8)	45.24(6)		45.39	0.040	0.051	1.26	386	3228
V494 Sco	2453656.5500	0.4272919(4)	426.8(8)	455		-	0.055	-	1532	3185
CD Vel	2453748.7247	0.5735082(6)	66.27(5)		66.35	-	0.022	-	610	3294
AF Vel	2453747.8076	0.5274129(4)	58.62(7)	59	58.68	0.036	0.040	1.11	1028	3180
V419 Vir	2452728.7022	0.5105245(8)	65.7(1)		65.69	0.041	0.042	1.02	413	3172
AS Vir *	2454631.5558	0.553412(1)	47.76(5)			-	0.055	-	420	3171
SV Vol	2454277.5415	0.6099111(8)	85.3(2)			0.031	-	-	1116	3300
Stars suspected of multiple modulation										
RU Cet	2452117.8386	0.5862853(7)	98.0(2), 24.2(3)			0.046	0.047	1.02	430	3287
SU Col	2453396.6813	0.4873555(6)	65.22(7), 89.3(2)		65.6, 89.2	0.056, 0.043	0.039, 0.031	1.43, 1.39	924	3295
IK Hya	2453085.8054	0.650321(3)	71.81(5), 1403(21)	72	71.79	0.038, 0.45	0.059, 0.060	1.55, 1.33	633	3177
RY Oct	2452987.6056	0.5634473(7)	217(1), 26.88(5)			-	0.054, 0.036	-	649	3274
AM Vir	2453432.873	0.6150856(6)	49.61(5), 141.9(4)	49.8		-	0.023, 0.020	-	456	3163

Star 1 denotes ASAS203420-2508.9, Star 2 ASAS032438-2334.7 and Star 3 ASAS062326+0005.8.

corresponding phase plot appears unconvincingly. The modulation of SS Cnc, BR Tau, RY Com, and U Cae was undetectable due to the limited precision of ASAS data. VX Her was studied by Wunder (1990), who gave its modulation period as 455.37 d and the amplitude of its $O - C$ changes as 0.013 d. No manifestation of modulation of VX Her was detected even in SuperWASP data. This could possibly be the consequence of ceasing Blažko effect.

We should also mention AE PsA, which was a suspected Blažko star with a period 5.78 d (SF07). Frequency analysis exposed a peak with $f = 2.0027$ c/d corresponding to a 5.78-day period, but this could probably be a false peak, because it appears close to a one-year alias of $f = 2$ c/d.

Stars suspected of multiple/irregular modulation and IK Hya

In the bottom part of Table 4.4 there are six stars that we suspect of some peculiarity in their modulations. All these stars showed additional peaks around f_0 , probably related to an additional modulation component. This behavior was described, for instance, in XZ Cyg (LaCluyzé et al., 2004), UZ UMa (Sódor et al., 2006), CZ Lac (Sódor et al., 2011), or more recently in V445 Lyr (Guggenberger et al., 2012). We also identified expected peaks around $2f_0$, which was a necessary condition to mark the stars as multiply modulated. Unfortunately, except for SU Col, these peaks had low amplitude under the confidence limit $S/N > 4$. Prewhitened frequency spectra of these stars in the vicinity of f_0 and $2f_0$ with identification of the peaks are plotted in fig. 4.9. There are also phase-plots corresponding to suspected modulation periods in fig. 4.9.

SF07 identified SU Col as a star with triple modulation. Peaks corresponding to periods 65 and 89 d (see fig. 4.9) were easily identified. Our analysis did not show any sign of the suspected 29.5-day period (the positions of peaks referring to this period are marked by an arrow in fig. 4.9). Residuals around additional peaks seem to be quite high, which could indicate that more peaks can be present, but undetectable in the dataset. This, along with the absence of the 29.5-day peak, could suggest that the Blažko modulation of SU Col is irregular and changing.

A very interesting case of a possible multiple/irregularly-modulated star is IK Hya (fig. 4.10). Its frequency spectra are somewhat confusing. There are two strong triplets (f_{m1l}, f_0, f_{m1r} and f_{m2l}, f_0, f_{m2r} , where indexes ‘l’ and ‘r’ mean ‘left’ and ‘right’, $f_{m1r} = f_0 + f_{m1}$, $f_{m1l} = f_0 - f_{m1}$ and similarly for f_{m2l} and f_{m2r}). Frequency f_{m1} corresponds to a 71.81-day known period, f_{m2} holds for the newly determined period of 1403 d. The spacing of the closer triplet was almost identical; i.e., $\Delta f = (f_{m2r} - f_0) - (f_0 - f_{m2l}) = 4 \cdot 10^{-5}$, while the offsets of wider peaks from f_0 were approximate matches only ($\Delta f = 6.9 \cdot 10^{-4}$). This discrepancy resulted in an inequality of the first modulation period based on the left peak (75.57 d) and the right peak (71.81 d). Thus, these peaks might indicate two independent periods or limiting values of a changing modulation period.

This is supported by the identification of symmetric counterparts of f_{m1l} and f_{m1r} with respect to f_0 that we found in the frequency spectrum, but which had amplitudes close to $S/N = 4$. The difference between the right-hand-side peaks f_{m1r} and f_{m2r} nearly equals $f_0 - f_{m1l}$, in other words $75.57^{-1} \cong 71.81^{-1} + 1403^{-1}$. This means that we actually observed one narrow triplet f_{m2l}, f_0, f_{m2r} and two doublets (one on each side of f_0) with spacing corresponding to a 1403-d period. This could indicate a 1403-day long-term cycle, during which the Blažko and pulsation characteristics are changing similarly to the four-year cycle of RR Lyr (Detre & Szeidl, 1973; Stellingwerf et al., 2013). A very interesting and possibly important thing is that the long period (1403 d) is very close to half of the beating period of 75.57 d and 71.81 d periods, which is 2886 days.

In the SuperWASP data of IK Hya only one slightly asymmetric triplet (Blažko effect with period 73.2 d) was identified. This period would support the theory of a changing Blažko effect of IK Hya rather than a compound modulation with three periods. With the ASAS and SuperWASP data, it is impossible to perform a more detailed analysis.

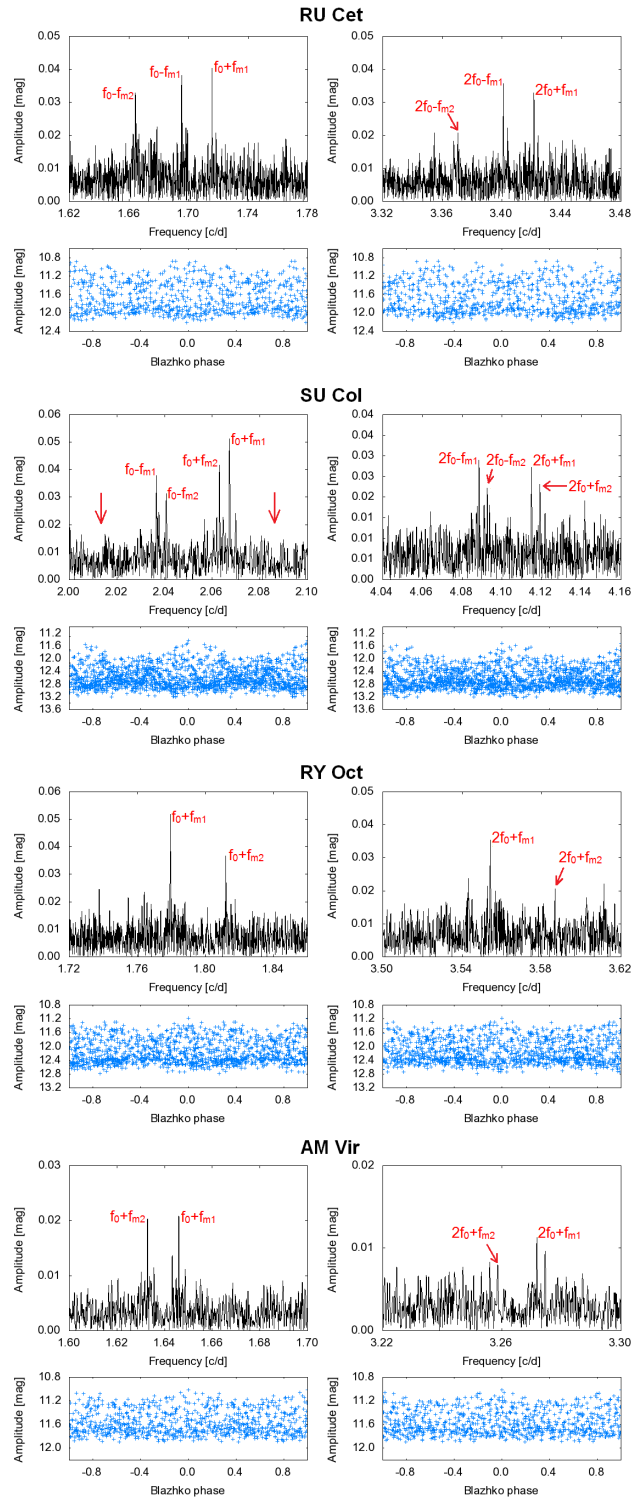


Figure 4.9: Four stars from our ASAS sample with double/irregular modulation. The first column depicts Fourier transform in the vicinity of f_0 after prewhitening with the main pulsation components and data phased with period corresponding to f_{m1} . The second column shows the vicinity of $2f_0$ and phase plot according to the second modulation period (related to f_{m2}).

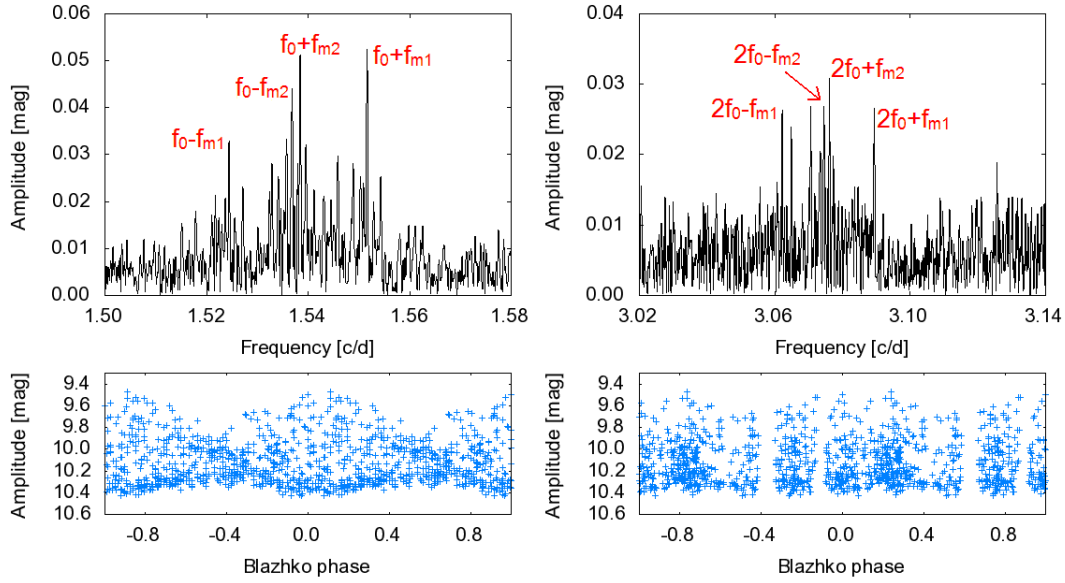


Figure 4.10: IK Hya. The vicinity of f_0 , $2f_0$ and light curves constructed with periods 71.81 d (bottom left) and 1403 d (bottom right). The frequency f_{m1r} corresponds to 71.81 d, f_{m1r} to 75.57 d, and f_{m2} to 1403 d.

New Blažko stars

There are 19 new Blažko stars in Table 4.5 which were not identified by WS05 or by SF07. Only two of the newly revealed Blažko variables showed a triplet structure, which is probably the consequence of a weak manifestation of the Blažko effect. V784 Oph is actually not a new Blažko star, because we discovered the modulation at the same time as de Pontiere et al. (2013), who identified its multiple modulation (our analysis showed only simple modulation).

Table 4.5: New Blažko stars from our ASAS sample

Star	Epoch HJD	P_{puls} [d]	P_{BL} [d]	A_- [mag]	A_+ [mag]	A_+/A_-	n	TS [d]
EL Aps	2451870.4229	0.5797216(5)	25.96(2)	-	0.019	-	849	3275
HH Aqr	2451889.5259	0.574434(1)	3360(270)	-	0.057	-	395	3274
LS Boo	2453103.7768	0.552704(2)	42.28(9)	-	-	-	359	2371
UY Boo	2454289.5426	0.650902(2)	171.8(2)	-	0.038	-	312	2907
V595 Cen	2453835.6569	0.691035(1)	107.5(6)	-	0.025	-	656	3188
RW Hyi	2454150.5160	0.555791(1)	135.2(6)	0.048	0.036	0.75	654	3296
AO Lep	2453767.6882	0.5600866(7)	93.0(1)	0.048	0.044	0.92	570	3296
XZ Mic	2452757.8704	0.4491584(4)	85.7(3)	-	-	-	595	3238
V784 Oph	2452775.7903	0.603359(1)	25.61(2)	-	0.044	-	352	2884
ASAS173154-1653.1	2453864.7477	0.602590(1)	52.41(8)	-	0.014	-	453	3145
CY Peg	2453337.5595	0.647939(2)	464(5)	0.071	-	-	238	2349
RU Scl	2452141.8678	0.4933549(2)	23.91(2)	-	0.010	-	338	3262
AE Scl	2452213.5875	0.5501123(9)	46.2(2)	-	0.046	-	497	3243
V Sex	2454633.4803	0.487372(1)	118.5(4)	-	0.061	-	317	2570
SS Tau	2453046.5674	0.3699068(7)	123.3(4)	-	0.057	-	320	3220
HH Tel	2451963.8028	0.4820925(5)	143(2)	-	-	-	518	3166
FS Vel	2454618.5425	0.4757576(5)	59.29(7)	-	0.040	-	618	3300
UV Vir	2451887.0160	0.5870842(7)	103.9(3)	-	0.027	-	365	3163
AF Vir	2454678.5669	0.483747(1)	42.15(5)	-	0.041	-	340	2915

In the case of LS Boo, XZ Mic, and HH Tel, their modulation periods are based on side peaks with a S/N slightly lower than 4, but their Blažko phased light curves clearly show the Blažko effect

(fig. 4.11). Comparing the Blažko periods of HH Tel and of XZ Mic with values taken from the SuperWASP data (Table 4.7), we see that they are indeed present and nearly have the same value. This raises the question if the significance condition $S/N > 4$ should not be lowered⁷. HH Aqr have a somewhat uncertain Blažko period, because it is longer than the time span of the data.

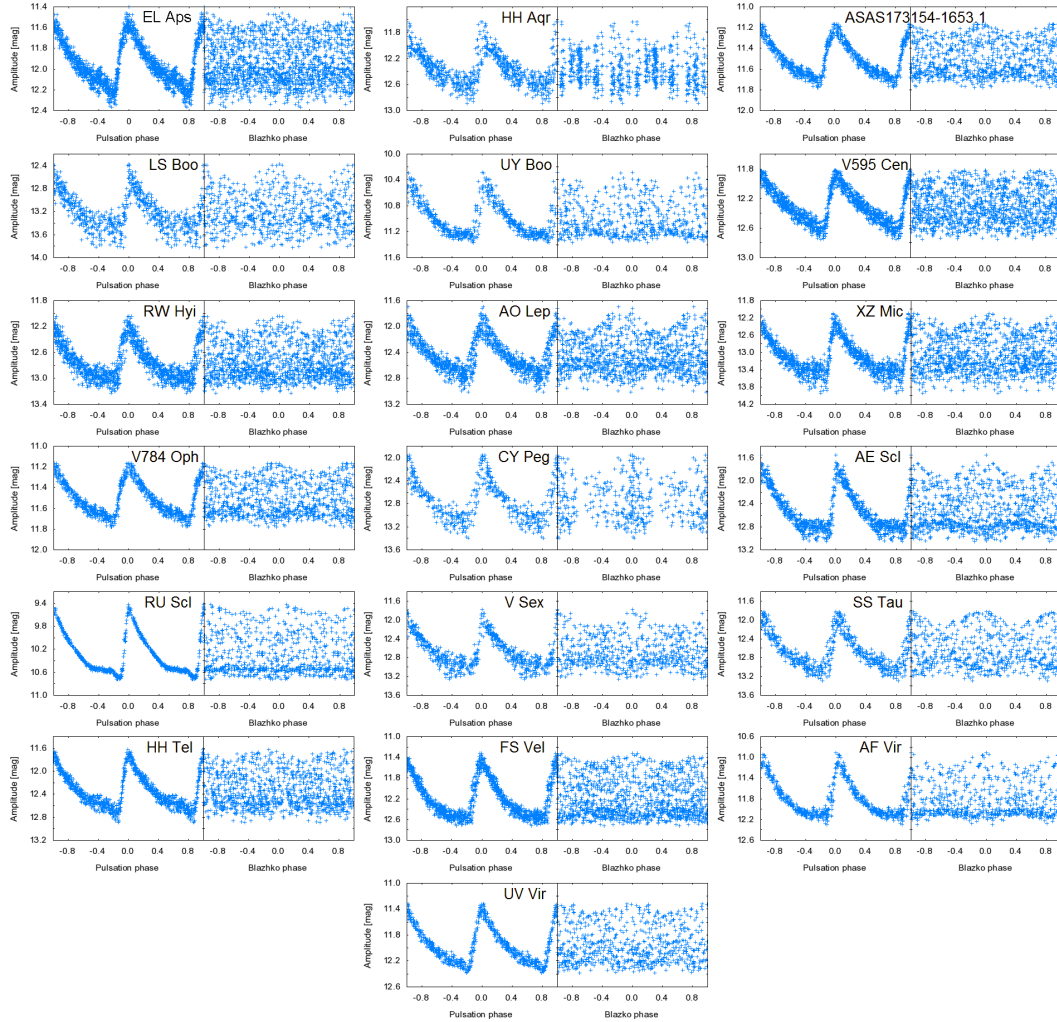


Figure 4.11: New Blažko stars from ASAS database. Data are phased with respect to ephemerides given in tab. 4.5.

Table 4.6: Stars suspected of the Blažko effect.

Star	Epoch HJD	P_{puls} [d]	n	TS [d]
BK Ant	2454911.6407	0.5165704(6)	602	3169
DN Aqr	2452471.8336	0.6337573(4)	400	3219
V444 Cen	2452144.6919	0.5141328(6)	537	3194
V1344 Cen	2453890.5987	0.4182563(4)	594	3187
WZ Hya	2454838.7787	0.5377193(3)	628	3300
AE Leo	2452630.7110	0.626673(2)	421	2400
VX Scl	2451916.0250	0.637066(1)	552	3295
CS Ser	2453896.6210	0.5267982(8)	472	3168

A frequency analysis of UY Boo showed, except for the modulation side peak, an additional peak which corresponds to the period 1976 d. This is probably the consequence of its peculiar period changes (Le Borgne et al., 2007).

The Blažko effect of stars in Table 4.6 is somewhat ambiguous. These eight stars are candidate Blažko variables. They show scattering around maxima (fig. 4.12), but not necessarily due to modulation – it could simply be the consequence of scattering. There were peaks with $S/N < 4$ iden-

⁷The significance limit was lowered for example by Kolenberg et al. (2006), who used criterion $S/N = 3.5$ for modulation peaks.

tified in the Fourier spectrum of CS Ser, which could be caused by the Blažko effect with a period of 118.3 d. Similar to the aforementioned cases of HH Tel and XZ Mic with the same characteristics, these peaks probably are real manifestations of modulation. AE Leo was later confirmed as a modulated star by Bramich et al. (2014).

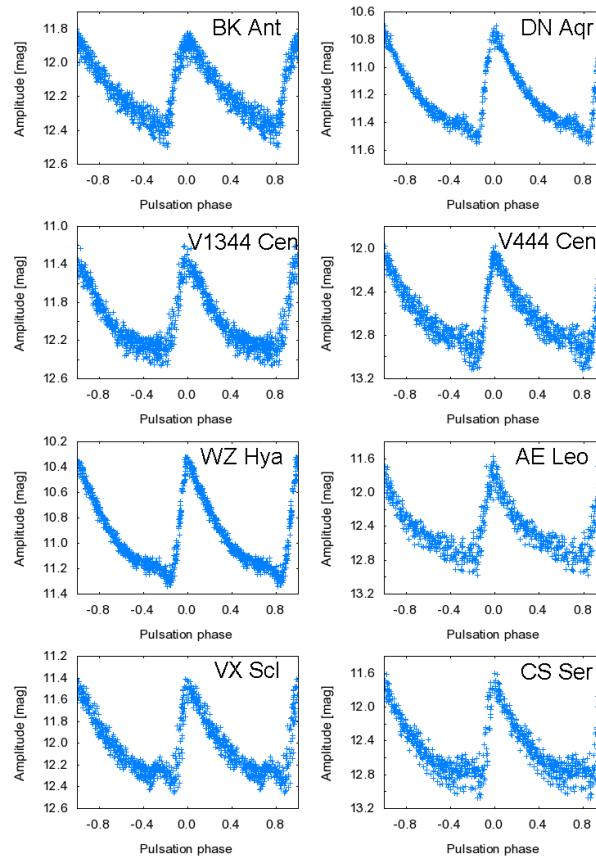


Figure 4.12: Possible Blažko stars. Data are phased with respect to ephemerides given in Table 4.6.

4.2.5 Blažko stars from SuperWASP

Known Blažko stars

After a pre-selection of 243 RR Lyraes from SuperWASP data we obtained 106 stars for further analysis. Twenty-eight objects were proposed to show the Blažko effect. For six of them (SW And, OV And, RY Com, V Ind, AR Per, and U Tri), no significant indication of modulation was found. In the case of RY Com and AR Per, this was due to the limited precision of the data used, because their modulation was confirmed independently (Jurcsik et al., 2009; Watson et al., 2006).

Twenty-two remaining stars with known modulation are listed in Table 4.7. The fifth column gives the modulation period based on frequency analysis (P_{BL}^F), and the sixth (P_{BL}^M) gives the Blažko period based on the Mag_{max} vs. T_{max} analysis. The last column provides modulation periods obtained from literature. Other columns correspond with those in Table 4.4. An asterisk in the first column (if present) indicates that the data were also available in the ASAS survey. The times T_{max} and magnitudes Mag_{max} of maxima (Table 4.8) are given as supplementary information on the enclosed CD or at the CDS portal.

Frequency spectra of almost all SuperWASP stars were affected by artificial effects, such as small shifts in the data from different nights or by gaps between observations, which resulted in

Table 4.7: Known Blažko stars from our SuperWASP sample.

Star	Epoch HJD	P_{puls} [d]	P_{BL}^F [d]	P_{BL}^M	A_- [mag]	A_+ [mag]	A_+/A_-	n	TS [d]	$P_{\text{BL}}^{\text{Lit}}$
DR And	2454334.5942	0.563112(6)	58.11(2)	58.2(3)	0.052	0.066	1.27	4536	705	57.5 ⁽¹⁾
U Cae*	2453996.5377	0.41978515(5)	22.77(2)	22.7(5)	0.025	-	-	5252	491	22.8 ⁽²⁾
AH Cam	2454362.6540	0.368721(4)	10.772(6)	10.65(6)	0.034	0.075	2.21	1783	1227	10.83 ⁽²⁾
SS Cnc*	2454167.5509	0.367341(1)	5.419(9)	5.42(3)	0.012	-	-	3554	116	5.309 ⁽³⁾
Z Cvn	2456078.3420	0.653684(9)	22.48(2)	-	0.042	0.044	1.04	2086	121	22.98 ⁽²⁾
SS CVn	2453140.6137	0.4785195(2)	94.19(2)	94.26(9)	0.062	0.099	1.54	8811	1476	93.72 ⁽²⁾
RY Col*	2454423.3675	0.4788302(2)	82.35(2)	82.4(2)	0.027	0.074	2.74	9478	516	82.08 ⁽²⁾
DM Cyg	2454344.4237	0.4198639(8)	10.38(1)	10.7(1)	-	0.009	-	1940	473	10.57 ⁽⁴⁾
XZ Dra	2454686.4674	0.4765587(5)	-	75(1)	-	-	-	5807	83	73–77 ⁽⁵⁾
SS For*	2453997.4793	0.4954351(5)	34.73(1)	34.66(7)	0.03	0.059	1.97	8684	654	34.94 ⁽⁶⁾
RT Gru*	2454246.6550	0.5121845(6)	86.7(2)	87.8(3)	0.025	0.037	1.48	10238	537	87 ⁽⁷⁾
SV Hya*	2454528.4773	0.478546(2)	62.8(3)	63(2)	-	0.025	-	5374	131	63.29 ⁽⁸⁾
IK Hya*	2454155.5952	0.650247(4)	73.18(3)	73.2(3)	0.032	0.061	1.91	12856	754	67.5 ⁽²⁾
V559 Hya*	2454199.5359	0.4479571(2)	26.454(2)	26.47(2)	0.093	0.12	1.29	10055	754	26.6 ⁽⁷⁾
FU Lup	2454594.3086	0.3821526(3)	42.81(1)	42.74(9)	0.034	0.107	3.15	8300	752	42.49 ⁽⁸⁾
V1645 Sgr*	2454307.315	0.552955(3)	-	-	-	-	-	11310	754	1331.74 ⁽⁸⁾
BR Tau*	2454143.386	0.390600(1)	-	18.14	-	-	-	2063	139	19.3 ⁽⁹⁾
CD Vel*	2454151.3312	0.5735080(7)	66.34(4)	66.38(26)	0.016	0.023	1.44	14501	735	66.35 ⁽⁸⁾
Stars suspected of multiple modulation										
RS Boo	2453132.5463	0.3773210(2)	41.3(2), 62.5(2)	64(3)	0.006, 0.006	0.010, 0.007	1.66, 1.16	3737	133	532.48 ⁽²⁾
RW Cnc	2454118.5843	0.547191(6)	29.14(8), 21.9(1)	30.0(3), 21.9(5)	0.021	0.012, 0.014	0.57	3513	129	87 ⁽¹⁰⁾
RX Col*	2454106.4342	0.593743(1)	134.3(1), 79.7(2)	135.7(7), 81(2)	0.014	0.050, 0.011	3.57	11003	677	134.77 ⁽²⁾
RW Dra	2454655.5652	0.4429239(4)	41.42(1), 72.6(2)	41.49(5), 72.3(3)	0.055, 0.018	0.090, 0.013	1.64, 0.72	17386	492	41.42 ⁽²⁾

(1) Lee & Schmidt (2001); (2) Le Borgne et al. (2012); (3) Jurcsik et al. (2006); (4) Jurcsik et al. (2009b) (5) Jurcsik et al. (2002); (6) Kolenberg & Bagnulo (2009); (7) WS05; (8) SF07; (9) Jurcsik et al. (2009); (10) Smith (1995).

additional peaks near f_0 with no clear interpretation. In addition, peaks corresponding to the time span of the data occurred frequently.

Table 4.8: Times and magnitudes of maximum light of 35 stars from the SuperWASP survey, which is enclosed on the CD. It is also available as a supplementary material of Skarka (2014a).

Star	HJD T_{Max}	err _{HJD}	Max [mag]	err _{Max}
DR And	2454325.5842	4	11.972	4
	2454330.6559	9	11.832	12
...

In XZ Dra and BR Tau, the Blažko effect was not detected in their frequency spectra, but it was noted in the change in maximum magnitude. V1645 Sgr surely show modulation, but SuperWASP data were in this case insufficient for determining the Blažko period.

SuperWASP stars suspected of multiple/irregular modulation

Four known Blažko variables in our SuperWASP sample were identified as stars with multiple modulation (the bottom part of Table 4.7, fig. 4.13). RS Boo, RW Cnc and RW Dra were suspected of such behaviour in the past; RX Col is a newly discovered multiple modulated star (it was known as a single-modulated star).

The Blažko period of ~ 533 d of RS Boo has been known for a long time (Oosterhoff, 1946), but there have been some indications of additional periodicity. Kanyo (1980) reported another period in the range of 58–62 days, but it was not observed by Nagy (1998). There was no indication of a 533 d period in the SuperWASP data – probably due to the time span of only 133 d. During

the analysis we revealed a period of 62.5 d, which is close to the period noted by Kanyo (1980). Except for this period we also noted obvious indications of a period of 41.3 d.

Balazs & Detre (1950) reported RW Cnc to be a double-modulated star with modulation periods of 29.95 and 91.1 d. The first modulation period was determined as 29.14 d (30.0 d from maxima analysis), and the second period as 21.9 d from both frequency and maxima analysis. No indications of a 91-day cycle were found. The 87-day period given by Smith (1995) was also not observed.

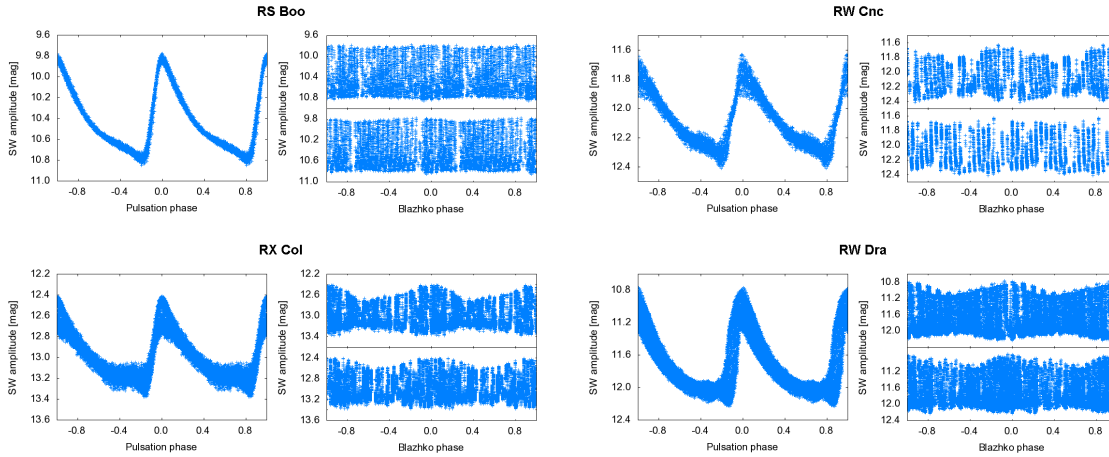


Figure 4.13: Known Blažko stars with more than one modulation period. In the left panel of each star the data are folded with respect to the basic pulsation period. On the left, panels are data-phased with modulation periods.

RW Dra was found to be multiple-modulated by Balazs & Detre (1952). A Blažko period of 41.61 d was accompanied by a period of 124 d and two other periods with lengths in the order of years. We noted the Blažko period of 41.42 d and only one secondary modulation period of 72.6 d.

These four stars have a very interesting feature – the modulation periods are very close to a resonance with small integers: $(P_{m2}/P_{m1})_{RS\ Boo} = 1.513 \cong 3:2$; $(P_{m1}/P_{m2})_{RW\ Cnc} = 1.331 \cong 4:3$; $(P_{m1}/P_{m2})_{RX\ Col} = 1.685 \cong 5:3$ and $(P_{m2}/P_{m1})_{RW\ Dra} = 1.753 \cong 7:4$. In the ASAS stars only the modulation periods of SU Col approximate the resonance 4:3 ($P_{m2}/P_{m1} = 1.369$). It is very likely that this discrepancy between ASAS and SuperWASP stars is due to the bad sampling of ASAS data. Very recently, Benkő et al. (2014) found that resonances with small integers observed by Sódor et al. (2011) in CZ Lac occur almost in all multiple modulated stars observed in the *Kepler* field.

New Blažko stars from SuperWASP

Nine new, previously unknown single-modulated Blažko stars were identified in our SuperWASP sample (Table 4.9, fig. 4.14). For six of these stars (marked by an asterisk) ASAS data were also available. Three stars showed double modulation or some peculiarity in their Blažko effect.

Table 4.9: New Blažko stars from our SuperWASP sample.

Star	Epoch HJD	P_{puls} [d]	P_{BL}^F [d]	P_{BL}^M	A_- [mag]	A_+ [mag]	A_+/A_-	n	TS [d]
XX Boo	2454267.5088	0.5813995(3)	105.9(1)	105.6(3)	0.012	0.015	1.25	8707	1150
V595 Cen*	2454239.2256	0.6910344(5)	107.41(9)	107.6(2)	0.004	0.019	4.75	15709	754
GY Her	2454619.5950	0.524244(6)	49.6(2)	49.1(9)	0.049	0.053	1.08	8065	108
XZ Mic*	2453964.2968	0.4491569(6)	85.8(2)	85.7(5)	0.034	0.035	1.03	8591	537
TU Per	2454438.5346	0.6070469(4)	59.0(3)	-	0.021	0.015	0.71	2383	108
RU Scl*	2454364.4311	0.493368(1)	23.6(1)	24.0(3)	0.003	0.008	2.67	3725	103
V4424 Sgr	2453881.6352	0.4245024(2)	29.28(4)	27.62(8)	0.005	0.004	0.80	8778	528
HH Tel*	2454347.2643	0.482056(5)	-	133(9)	-	-	-	2761	93
FS Vel*	2454201.2979	0.4757597(2)	59.48(4)	59.1(2)	0.020	0.026	1.30	9677	713
Stars suspected of multiple/irregular modulation									
RZ CVn	2454263.4059	0.567418(-)	33.35-33.26	29.6-33.36	0.007	0.017	2.43	7148	1136
AG Her	2454669.4418	0.6494465(3)	79.69(7), 47.93(7)	79.58(7), 47.96(2)	0.010, 0.014	0.030, 0.020	3, 1.43	22362	1552
AE Scl*	2453920.5919	0.550116(2)	46.07(2), 104.7(2)	46.04(4)	0.019, 0.019	0.044, 0.015	2.32, 0.79	8179	563

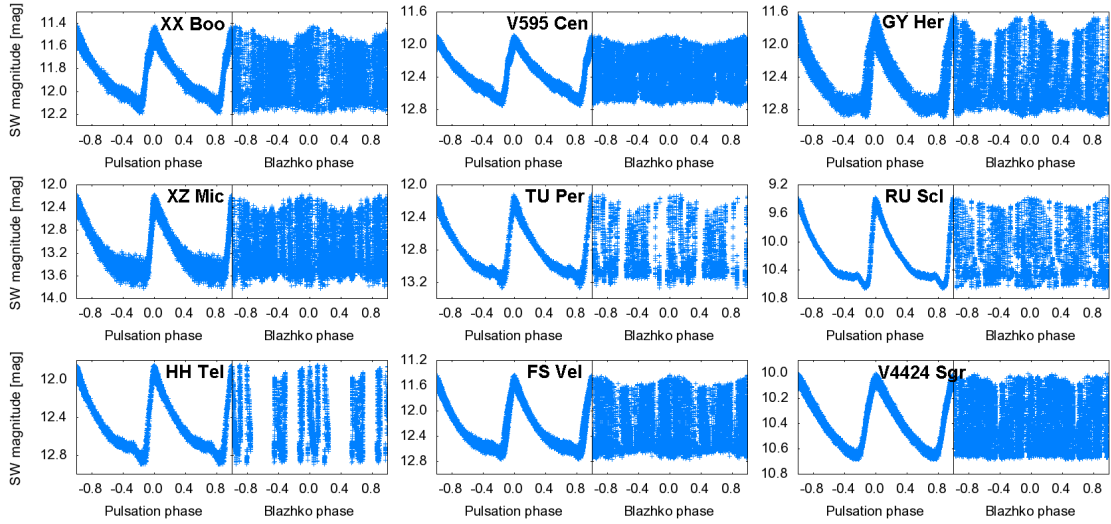


Figure 4.14: New Blažko stars from SuperWASP database. Light curves are constructed according to the ephemerides listed in Table 4.9.

RZ Cvn (fig. 4.15) seemed to change its Blažko period. For the first part of the data sample (between HJD 2453130 and 2453249), the Blažko period was 33.35 d (29.6 d on the basis of maxima analysis), the amplitude of the modulation was 0.104 mag (peak to peak) and $A_1 = 0.339$ mag, while between HJD 2454135 and 2454266, the Blažko cycle lasted 33.26 d (33.4 d based on maxima analysis). The amplitude of the modulation was almost twice as big as in the first part (0.192 mag) and $A_1 = 0.363$ mag. The basic pulsation period also changed slightly (0.567411 vs. 0.567418 d). For example, similar behaviour is known in XZ Dra (Jurcsik et al., 2002) or RV UMA

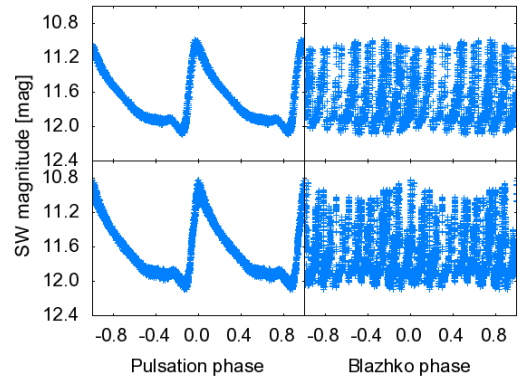


Figure 4.15: RZ CVn in different seasons.

(Hurta et al., 2008). It is worth noting that in the case of RZ CVn the Blažko periods determined on the basis of maxima analysis offer better confidence.

The second multiple-modulated star, AG Her (fig. 4.16), shows possible resonances of its modulation periods $(P_{m1}/P_{m2})_{AG\ Her} = 1.659 \cong 5:3$ similar to RX Col and the other three stars discussed in previous section. AE Scl was identified as single-modulated in the ASAS data set.

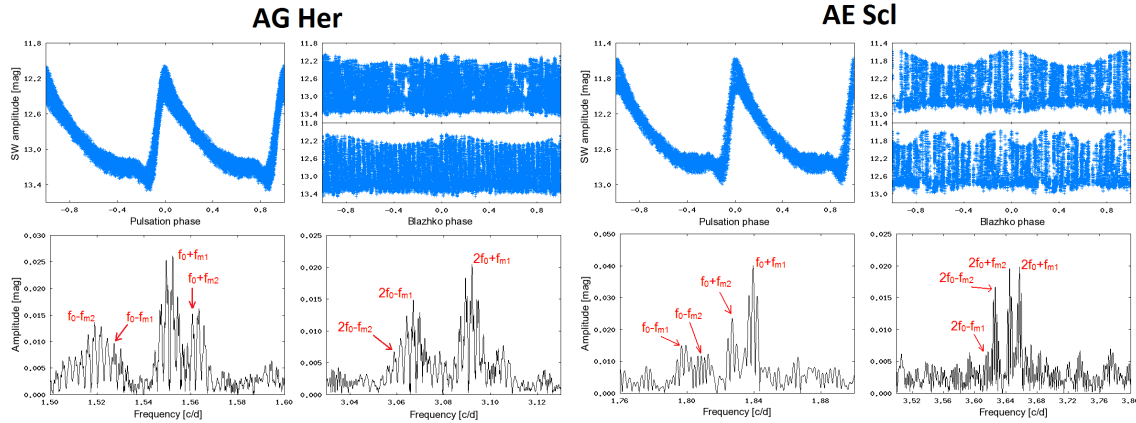


Figure 4.16: Data of AG Her and AE Scl folded with elements given in Table 4.9 and with their frequency spectra in the vicinity of f_0 and $2f_0$. In Blažko phased data of AE Scl it is apparent that the second modulation period should be $104.7/2$ instead of 104.7 d, but the frequency spectra indicated a period of 104.7 d.

4.2.6 Statistics of the Blažko variables in the ASAS and SuperWASP sample

From the sample containing 321 RRab type stars, one hundred objects were identified as modulated stars. This means that the incidence rate of Blažko stars among RRab sample stars was 31 %. If we include certain Blažko variables, whose modulation was not detectable (5), this percentage would grow to almost 33 %. If Blažko candidates (8) are also taken into account, this rate would be 35 %. Finally, if all suspected stars are included (18 instead of 5), the percentage would be 39 %. In addition, it is likely for this number to be slightly higher, because the modulation of a number of stars with low modulation amplitude might have remained uncovered.

Compared to incidences of 5.1 % (SF07) and 4.3 % (Wils et al., 2006), our percentage is significantly higher and roughly approximates the percentage based on precise measurements – 48 % (Benkš et al., 2011) based on *Kepler* data, or 47 % (Jurcsik et al., 2009), when precise ground-base observations were utilized. Our incidence is higher than in the LMC, SMC and GB (see sec. 2.4).

About 60 % of confirmed Blažko variables were of the BL2 type. Considering ASAS and SuperWASP surveys separately, this rate was 48 % (ASAS) and 76 % (SuperWASP). Several stars in the SuperWASP sample turned out to be of the BL2 type, while in ASAS they were of the BL1 type. This finding clearly shows that the classification of stars based on their side-peak distribution strongly depends on data quality and should not be used when analysing low-quality data, which is known (Alcock et al., 2003). In addition, ultra-precise space measurements showed that almost every modulated star⁸ has peaks on both sides. Our recommendation is also supported by the fact that the percentage of stars which show $A_+/A_- > 1$, was about 89 % in our ASAS sample contrary to 51% given by SF07.

⁸V2178 and V354 Lyr are possibly of the BL1 type (Nemec et al., 2013).

Twelve stars in our sample turned out to be multiple-modulated and/or with changing modulation, which is 12 % of all studied Blažko stars. Only a few stars have been known to show such behaviour based on a ground-based observations until today. It is very likely that compound modulation is more common than astronomers thought and that the number of known multiple-modulated stars will increase in future analyses. This is supported by a recent study of Benkő et al. (2014).

4.3 Characteristics of bright ab-type RR Lyrae stars from the ASAS and SuperWASP surveys

In this section we describe a deeper analysis of light curves of fundamental mode RR Lyrae stars with data from the ASAS and SuperWASP surveys. It is a direct continuation of the analysis introduced in previous sections. The main goal is to investigate the differences of Fourier parameters (eq. 1.8 and 1.9) and physical characteristics (their derivation is described in sec. 1.3.3) between ordinary and modulated stars. As an extension we also compiled and utilized available data of stars from globular clusters, the LMC, SMC and GB and compared their light-curve parameters with those from our basic data set.

4.3.1 Data sets

ASAS and SuperWASP data

We initially started with a sample of 321 RRab Lyraes with well defined light curves (see sec. 4.2.2). After additional visual examination, we discarded stars with sparse and uneven light curves and stars for which we could not decide whether they are modulated or not. That left us with 268 objects (176 stable stars and 92 Blažko stars). From this sample, 99 stars had high-density, high-precision data in the SuperWASP survey containing typically a few thousands data points per star, which span from several tens of days to about three years. Compared to ASAS light curves, which had typically only few hundreds of points spread out over several years, SuperWASP data were of significantly better quality with a magnitude-order lower scatter than ASAS light curves.

To be at least reasonably objective, we applied a slightly modified approach introduced by Kovács (2005) (eq. 1.12) for the determination of the degree of fit (eq. 1.7) for ASAS light curves. Firstly a sixth order fit was applied to each light curve. Subsequently parameter m^* was calculated:

$$m^* = \text{ROUND} \left[\frac{A_1 \sqrt{n^*}}{20\sigma} \right]. \quad (4.2)$$

In the above equation A_1 is the first-component amplitude, σ is the uncertainty of the 6th order fit and n^* is the number of points in the particular light curve. Since we worked with about double the amount of data that Kovács used, his constant 10 (in the denominator of eq. 1.12) was changed to 20 and his function INT was changed to ROUND. For $m^* < 4$ and $4 < m^* < 10$ a fit with $n = 4$ and $n = m^*$ components was used, respectively. If $m^* > 10$ than $n = 10$. Nevertheless, in several tens of stars, the degree of the fit was changed by visual inspection to get a better model of the light curve. The noted conditions were used to avoid over-fitting of noisy light curves and under-fitting of well defined ones as was already discussed by Kovács. In the case of SuperWASP data, observations were always fitted with ten components. Since SuperWASP data were more dense and more numerous than those from ASAS, uncertainties of parameters based on SuperWASP data were in the order of a few thousandths, while uncertainties of parameters derived from ASAS data were of a magnitude larger.

Calibrations of SuperWASP to ASAS

The vast majority of relationships between Fourier parameters and physical characteristics (sec. 1.3.3) use Fourier coefficients based on V -light curve decomposition. ASAS measurements are in the V filter, and offsets of light-curve parameters from ASAS and those based on the standard V Johnson filter are known (table 3 in Kovács, 2005)). Since we utilized only data from SuperWASP and ASAS, the consistency between parameters from these two surveys was more important than precise calibration to the standard Johnson V filter. Thus we decided to transform SuperWASP broad-band light-curve parameters to that of ASAS using 24 stars common to both datasets. Subsequently, values were shifted using Kovács's offsets.

When we compared SuperWASP Fourier coefficients with those from ASAS, it was found that offsets are very scattered (examples in fig. 4.17). Therefore, we assumed a linear relation between SuperWASP and ASAS parameters rather than simple shifts. The dependences were iteratively fitted using the weighted least-squares method, and outliers deviating more than 3σ were removed in each iteration. The resulting fits showing almost 1:1 relations are in fig. 4.18, and final parameters of the fits can be found in Table 4.10.

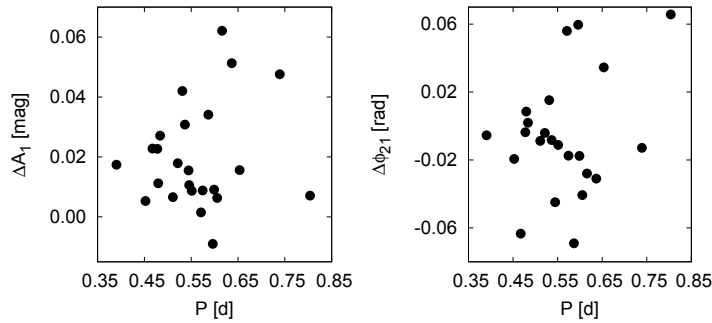


Figure 4.17: Offsets between SuperWASP and ASAS in amplitude A_1 (left panel) and parameter ϕ_{21} (right panel).

Despite the fact that the conversion from the SuperWASP to ASAS system significantly increases the uncertainties, parameters based on SuperWASP are given in the cases when the stars had both SuperWASP and ASAS data available, because SuperWASP light curves are much better defined. Derived Fourier parameters, converted to the standard system, together with physical characteristics and other properties of light curves, are given in table 4.11.

Globular cluster RRab stars

Since many of RR Lyrae stars located in GC's have been studied in detail in the past two decades, a relatively large sample of their accurate Fourier coefficients

Table 4.10: Parameters of the linear fit in the form $X_{ASAS} = a * X_{SuperWASP} + b$. The third column gives the standard deviation of the fit. The errors in the final digits are given in parenthesis.

ID	a	b	σ
A_1	1.001(37)	0.015(13)	0.013
A_2	1.003(30)	0.005(5)	0.005
A_3	1.033(28)	0.001(3)	0.004
A_4	0.979(26)	0.004(2)	0.003
R_{21}	0.981(58)	0.004(28)	0.009
R_{31}	0.988(72)	0.002(24)	0.008
R_{41}	0.975(39)	0.003(8)	0.005
ϕ_{21}	0.960(31)	0.086(74)	0.016
ϕ_{31}	0.986(24)	0.052(118)	0.019
A_{tot}	1.027(33)	0.006(30)	0.034
RT	1.032(94)	0.005(15)	0.013

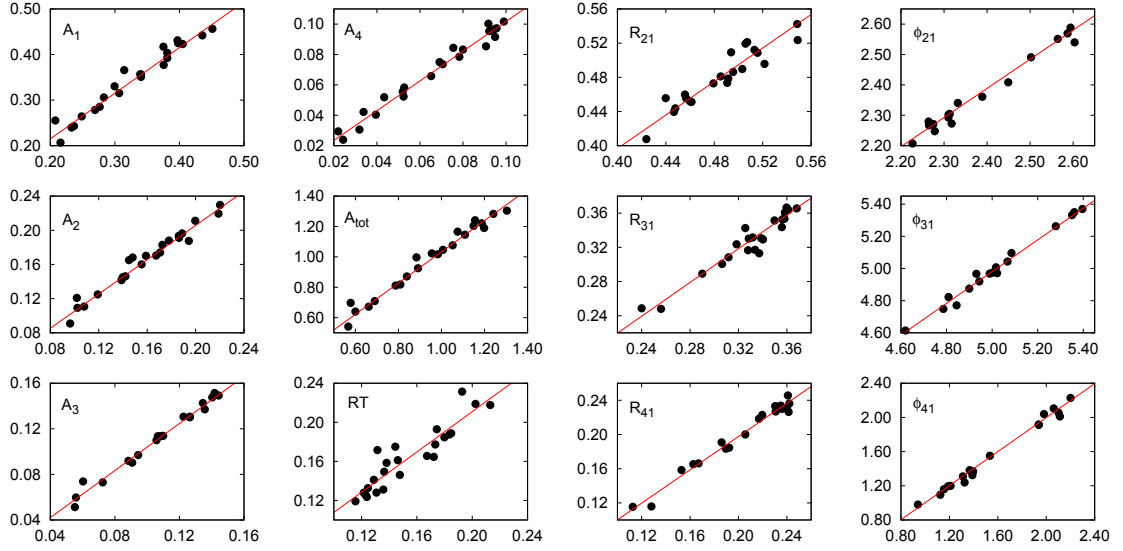


Figure 4.18: Weighted linear least square fits of various light-curve parameters. The SuperWASP value is on the abscissa, while the ASAS value is on the ordinate. The corresponding parameter is labelled in the top left corner of each sub-plot. Outliers located more than 3σ from the fit were iteratively removed. Amplitudes are in magnitudes, ϕ_{i1} in radians and rise time (RT) in the part of the pulsation cycle. Parameters of each fit are in table 4.10.

Table 4.11: Parameters of sample stars. In the second column ‘a’ and ‘w’ mean that parameters are based on ASAS and SuperWASP data, respectively. The last column gives information about modulation. The errors in the final digits of the corresponding parameter are given in parenthesis. The full table is available on the enclosed CD or as a supplementary material of Skarka (2014c).

ID	n	p [d]	A_1 [mag]	R_{21}	R_{31}	ϕ_{21} [rad]	ϕ_{31} [rad]	A_{tot} [mag]	RT [phase]	$[Fe/H]_{CG}$	M_V [mag]	T_{eff} [K]	$(B-V)_0$	\mathcal{M} [M_\odot]	BL
SW And	w	0.4422605(8)	0.3212(3)	0.545(1)	0.325(1)	2.615(3)	5.441(4)	0.94	0.18	-0.11(4)	0.81(11)	6745(18)	0.320(3)	0.48(2)	-
...

is available. Unfortunately, in many of these RR Lyrae stars it is not possible to find information about their modulation, which reduces the number of suitable objects for our purpose.

Kovács & Walker (2001) compiled an extensive list of almost four hundred cluster RR Lyrae stars with Fourier decomposition. We scanned the literature (ω Cen (Jurcsik et al, 2001), M53 (Dékány & Kovács, 2009; Arellano Ferro et al., 2011), M5 (Jurcsik et al., 2011), M3 (Jurcsik et al., 2012), M9 (Arellano Ferro et al., 2013), M62 (Contreras et al., 2010), NGC5466 (Arellano Ferro et al., 2008), NGC1851 (Walker, 1998), NGC6171 (Clement & Shelton, 1997), and IC4499 (Walker & Nemeč, 1996)) to get information about the modulation of stars in the set of Kovács & Walker (2001), and to extend and enhance this list.

Contreras et al. (2010) provides only information about a deviation parameter D_m of stars in M62. Usually, non-modulated stars are considered to have $D_m < 3$. However, as already mentioned in sec. 1.3.1, Cacciari et al. (2005) showed that D_m is effectively unable to distinguish between Blažko and non-Blažko stars down to $D_m \leq 2$. Therefore, only stars in M62 with $D_m < 2$ were included in our list and were considered as stable stars. The final sample of GC RRab Lyraes that we used Skarka (table 4.12, available on the enclosed CD or as a supplementary material of 2014c)), contains 188 stars with stable light curves and 86 modulated stars.

Table 4.12: Fourier parameters of Fundamental mode RR Lyrae variables located in globular clusters. The second column gives information about the modulation of the star. The complete table is only available on the enclosed CD or as a supplementary material of Skarka (2014c).

ID	BL	p [d]	A_1	R_{21}	R_{31}	ϕ_{21}	ϕ_{31}	ref.
M53 V1	-	0.6098	0.365	0.4904	0.3479	2.333	5.045	1
M3 V3	+	0.5582	0.408	0.4975	0.3358	2.307	4.968	2
...

References: (1) Clement & Shelton (1997), (2) Walker (1998), (3) Kovács & Walker (2001), (4) Arellano Ferro et al. (2008), (5) Arellano Ferro et al. (2011), (6) Arellano Ferro et al. (2013), (7) Jurcsik et al. (2011), (8) Dékány & Kovács (2009), (9) Contreras et al. (2010).

Fourier parameters of RR Lyrae stars located in the LMC, SMC and GB

Fourier coefficients of RRab Lyraes observed in the framework of the OGLE-III survey (Udalski et al., 1997; Szymański, 2005) were gathered through the WWW interface⁹ for comparison of field stars with stars in the GB (11 371 stars, Soszyński et al., 2011), LMC (16 941, Soszyński et al., 2009) and SMC (1 863, Soszyński et al., 2010). In the case of LMC stars we also used data of modulated stars (731 objects, Alcock et al., 2003).

Since Fourier decomposition of the OGLE data were available for the I passband, and were based on the cosine-series, they were transformed to V filter to match our results using equations 1.10 and 1.11, and relations introduced by Morgan et al. (1998).

4.3.2 Physical parameters determination

Physical parameters were calculated using formulas discussed in sec. 1.3.3. As already mentioned, Fourier techniques can be used for stable stars as well as for stars with the Blažko effect that have uniformly and properly sampled light curves (e.g. Kovács, 2005; Smolec, 2005; Jurcsik et al., 2009)). In the case of modulated stars, Nemeč et al. (2013) utilized new high-dispersion spectroscopic measurements and precise photometric data from the *Kepler* space telescope and recommend to determine $[\text{Fe}/\text{H}]$ as an average of metallicity during the Blažko cycle, rather than to use a mean light-curve fit, which gives slightly inferior results.

Since we used ground-based data, which are often sparse (and therefore inappropriate for determination of parameters during a modulation cycle), and with much poorer quality than data from space, our physical parameters were based on a mean-light-curve fit. In addition, the goal of this study is to compare Blažko stars with stable stars, not to precisely determine physical parameters. Therefore the use of a mean light curve should be of sufficient accuracy for our purpose.

For metallicity determination we used relation 1.14. Although authors warned that this relation could give higher metallicity at the low abundance level, this discrepancy is not conspicuous in our $[\text{Fe}/\text{H}]_{\text{spec}}$ vs. $[\text{Fe}/\text{H}]_{\text{phot}}$ plot (fig. 4.19). Spectroscopic metallicity is taken from Layden (1994) in the Zinn & West (1984) scale. Photometric metallicity based on equation 1.14, which is on the Carretta & Gratton (1997) scale, was transformed via eq. 1.18.

From fig. 4.19 it is apparent that our photometric metallicities agree very well with the spectroscopic ones. The solid line represents the line of equality, dotted lines above and below the diagonal line show the 3σ limit of eq. 1.14 taken from Jurcsik & Kovács (1996). Except for 13 outliers (5 Blažko and 8 non-modulated stars), the remaining 161 stars are concentrated within this zone.

⁹<http://ogledb.astrouw.edu.pl/~ogle/CVS/>

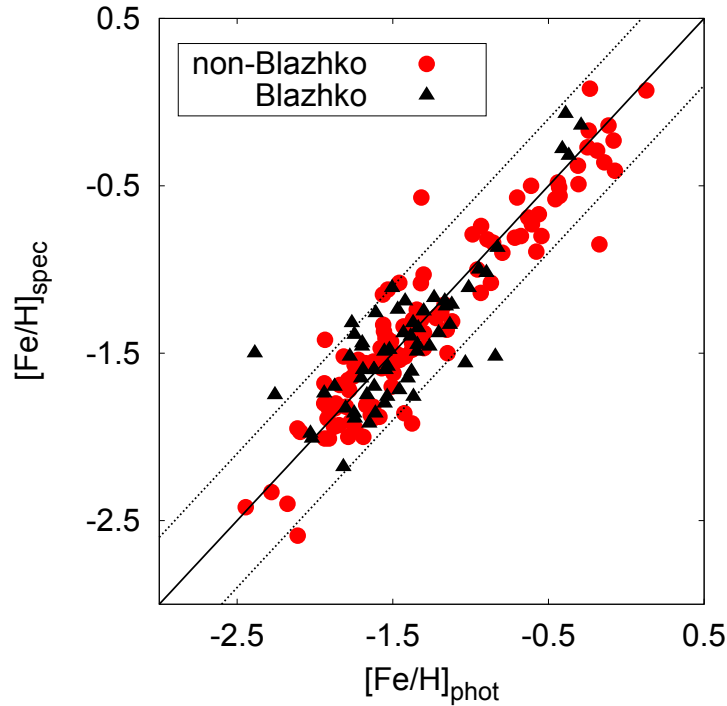


Figure 4.19: Spectroscopic (Layden, 1994) versus photometric (this study) metallicities on the ZW scale. The solid line is 1:1 relation, dotted lines denote 3σ limit. For details see the text.

Absolute magnitude was estimated using eq. 1.24. The value was subsequently decreased by 0.2 mag according to discussions in Nemeč et al. (2013) and Lee et al. (2014). Effective temperature was estimated via eq. 1.28, extinction-free $(B - V)_0$ via eq. 1.25 and mass was determined through eq. 1.30.

It is worth noting again that the goal of this study is a comparison between Blažko and regular stars, not the precise determination of their parameters. In addition, comparison of different calibrations, which give slightly different results, and searching for the most reliable equations is outside the scope of this thesis. An extensive discussion and comparison of different calibrations can be found, for example, in Nemeč et al. (2011). Derived parameters are listed in tab. 4.11.

4.3.3 Light-curve properties of regular and modulated RRab stars

In general, there are a few differences between the light curves of Blažko and non-Blažko stars, as can be logically expected. These were already discussed in sec. 2.5. As was noted by Szeidl (1988), who used a period-amplitude diagram, Blažko stars gain a similar amplitude as modulation-free stars only during their maximum Blažko phase. In other modulation phases their light changes are smaller. This means that the mean light curves of Blažko stars have typically smaller amplitudes than stars with stable light changes.

As a direct consequence of the lower amplitudes (at constant period), average light curves of modulated stars are more symmetrical than light curves of modulation-free stars. This further means a longer rise time and lower amplitudes of higher components of Fourier fits for modulated stars, as also noted by Alcock et al. (2003) and Smolec (2005).

Amplitudes

Figure 4.20 shows the distribution of the observed total LC amplitude A_{tot} (difference between maximum and minimum light) and the first three Fourier amplitudes as a function of pulsation period of a star. The formerly noted facts are easily resolvable: Blažko stars tend to have lower amplitudes than modulation-free stars. There is no distinct difference in the first Fourier amplitude A_1 (average values 0.342(6) and 0.331(7) for modulation-free and Blažko stars, respectively), while higher-order amplitudes differ significantly ($A_{2,\text{ave}} = 0.171(3)$ and $A_{3,\text{ave}} = 0.113(3)$ for non-modulated stars and $A_{2,\text{ave}} = 0.148(4)$ and $A_{3,\text{ave}} = 0.088(3)$ for Blažko stars). This means that the reduction in total amplitudes of modulated stars is caused by higher-order Fourier amplitudes. However, this is to be expected, because the light curves of modulated stars have more symmetric shape. From Table 4.13, it is apparent that the trend of lower amplitudes for modulated stars is period-independent. For comparison, there are also GC stars plotted in fig. 4.20 (empty symbols). No apparent difference between GC and field stars was found.

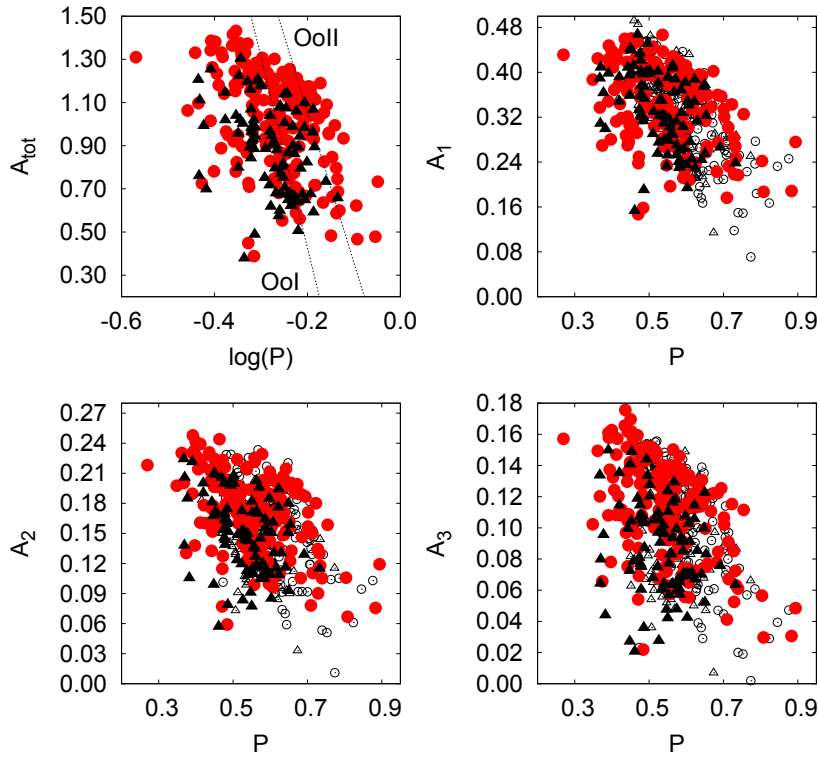


Figure 4.20: Period-amplitude diagrams for field RR Lyrae stars (filled symbols) and their counterparts in GCs (open symbols). Blažko stars are depicted as triangles, while stable stars are plotted with circles. Pulsation period on the abscissa is in days, while amplitudes are in magnitudes.

The top left panel of fig. 4.20 shows a classical Bailey diagram, which is usually used for distinguishing between RR Lyrae types, as well as for investigation of membership to any of the Oosterhoff groups (sec. 1.3.2). Except for sec. 4.3.4, we do not deal with the Oosterhoff phenomenon, because our sample is very limited and spread over the whole sky. For those who are interested in this topic, we refer to the studies of Szczygieł et al. (2009) and Kinemuchi et al. (2006), which were based on much wider samples of stars observed in the ASAS and NSVS surveys.

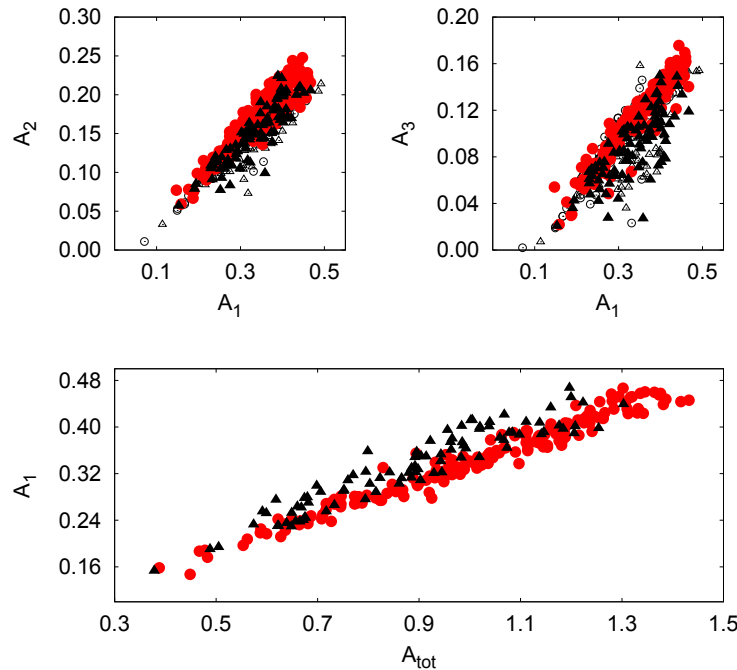
Nevertheless, it is worth mentioning that Blažko stars probably do not prefer any of the Oosterhoff groups, as apparent from the top left panel of fig. 4.20 where the two dotted lines illustrate

Table 4.13: Average amplitudes for different period intervals. Values in parentheses are standard errors of the means. ‘S’ means stable stars and ‘BL’ modulated stars, respectively.

	$P \leq 0.5$		$P \in (0.5, 0.6)$		$P \geq 0.6$	
	S	BL	S	BL	S	BL
A_1	0.370(9)	0.369(12)	0.342(8)	0.316(9)	0.306(10)	0.294(15)
A_2	0.192(5)	0.167(7)	0.166(4)	0.139(6)	0.150(6)	0.135(8)
A_3	0.127(4)	0.095(6)	0.113(4)	0.084(4)	0.096(5)	0.082(6)

empirical loci of Oosterhoff groups according to Szczygieł et al. (2009). From the same part of fig. 4.20, it is obvious that Blažko stars have smaller total mean amplitudes ($A_{\text{totBL}} = 0.89 \pm 0.02$ mag) than their regular counterparts ($A_{\text{totSTABIL}} = 1.01 \pm 0.02$ mag).

If A_2 and A_3 are plotted as a function of A_1 we obtain the plots showed in the top panels of fig. 4.21. Again, Blažko stars tend to have lower Fourier amplitudes. Below the limit of $A_1 \sim 0.2$ it seems that modulated stars follow the trend of stable stars fairly well. Similar behaviour was noticed in GB stars by Smolec (2005) for I -band light curves. However, this statement is based only on three modulated field stars and two GC stars. In the bottom panel A_1 is plotted against the total amplitude A_{tot} of a star. A fleeting glance indicates that Blažko stars are well separated from regular stars, which is not surprising, because A_1 is the dominant component of the total amplitude of Blažko stars. With the unprecedented precise measurements of the *Kepler* satellite, Nemeč et al. (2011) found this dependence likely to be cubic.


 Figure 4.21: Correlations between Fourier amplitudes (in magnitudes). The top panels shows dependencies of higher-order amplitudes on A_1 , while A_1 is plotted against the total amplitude of light changes in the bottom panel. Symbols are the same as in fig. 4.20.

From fig. 4.20 it is also apparent that the range of possible amplitudes decreases when the period increases for both Blažko and ordinary stars. However, this does not mean that stars with a longer period automatically have a smaller amplitude (fig. 2 and discussion in Nemeč et al., 2011).

Fourier parameters R_{21} and R_{31}

All differences in Fourier amplitudes get more evident when R_{31} is plotted as a function of R_{21} (fig. 4.22). In this figure, the dependence has the shape of a bent pin, where stars accumulate along the diagonal stem and around the horizontal pinhead. For comparison, modulation-free RR Lyrae stars from the LMC, SMC, and GB are plotted in this figure.

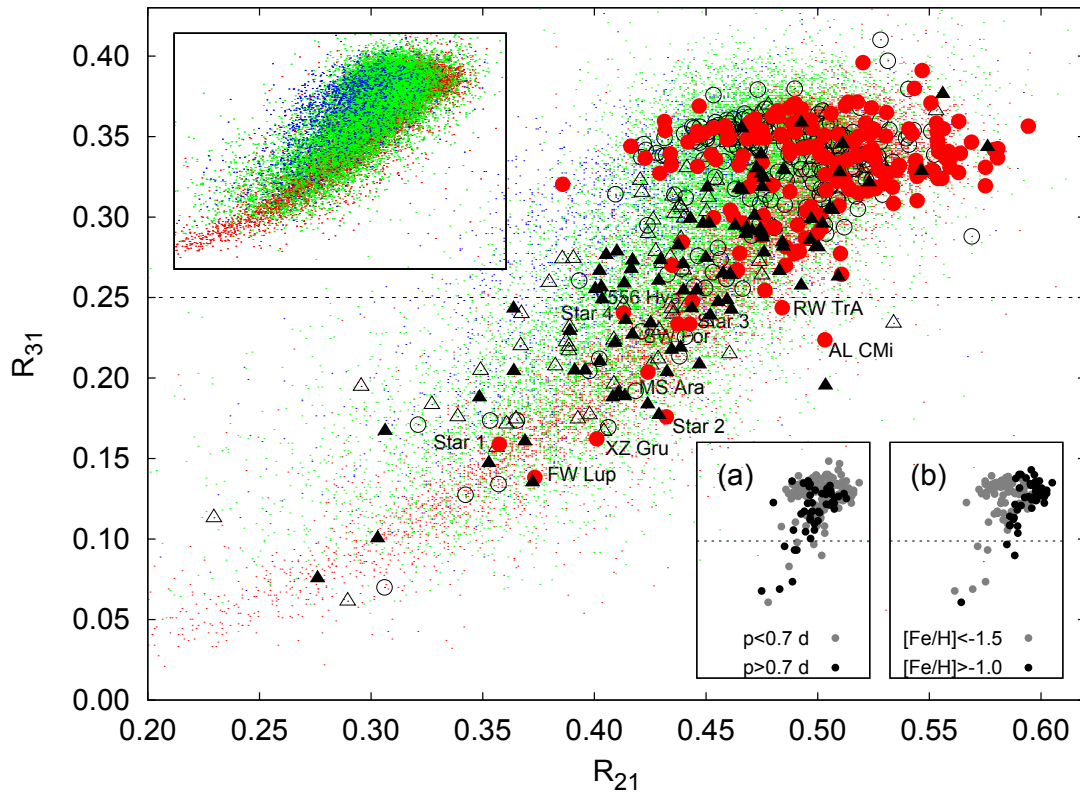


Figure 4.22: The correlation between R_{31} and R_{21} . In the main plot, as well as in the top-left detail, there are LMC (green dots), SMC (blue dots) and GB (red dots) plotted together with field and GC stars (the same symbols as in fig. 4.20, for greater clarity see the electronic version of the thesis). The dotted line represents the 0.25-limit below which Blažko stars constitute the majority of the RRab population. For information about labelled stars see the text. Star 1 corresponds to ASAS 134046+1749.2, Star 2 is ASAS083412-6836.1, Star 3 is ASAS 165126-2434.9 and Star 4 corresponds to ASAS160332-7053.4. In the bottom-right panel (a), modulation-free stars are distinguished with respect to their periods. Panel (b) shows regular stars drawn with different symbols for different metallicity. The same scale is used for all the plots.

Evidently, Blažko stars are located along the stem and regular stars prefer the pinhead around $R_{31} \approx 0.34$ (average of all stable stars is 0.326(3)). This is also apparent from the right-hand panel of fig. 4.23 where the distribution of stars according to their R_{21} and R_{31} are plotted. Below $R_{31} = 0.3$ about 69 % of the stars are Blažko stars. Similarly for $R_{31} < 0.25$ only 6 % of the stars are stable stars. These 11 outlier-stars are labelled in fig. 4.22. Either they are long period RR Lyrae

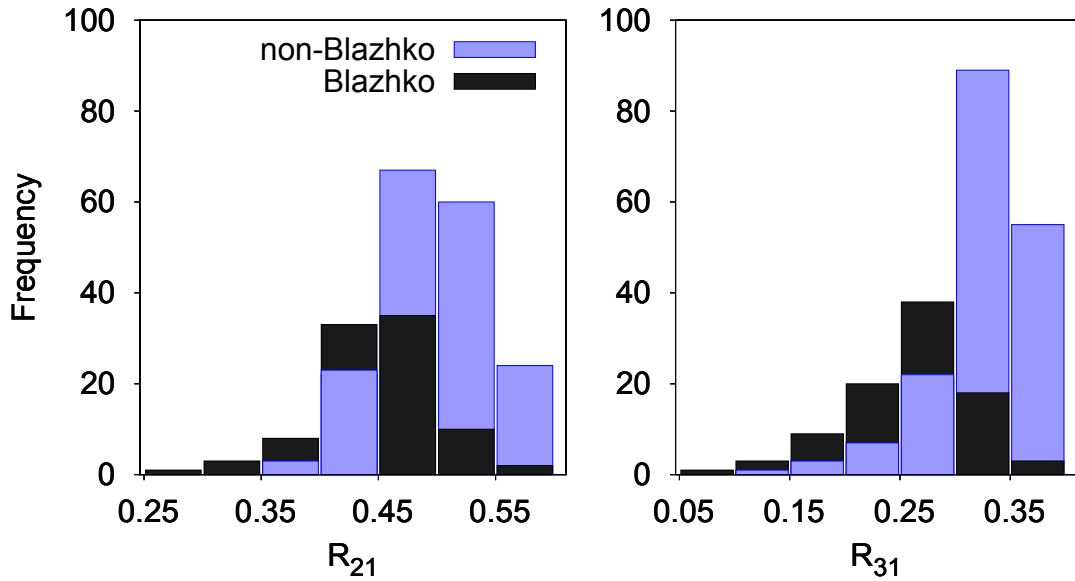


Figure 4.23: The distribution of Fourier amplitudes R_{21} and R_{31} for the studied stars. In the left-hand panel a significant drop in the stable-star population is apparent below $R_{31} \approx 0.3$.

stars ($P > 0.7$ d) or are somehow peculiar. AL CMi¹⁰, RW TrA and FW Lup have unusually high photometric metallicity exceeding $[\text{Fe}/\text{H}]_{\text{ZW}} = 0.0$, or even higher. However, this would probably not be the cause of their location, because there are also GC stars with a variety of metallicities located in this region. MS Ara, AL CMi and V556 Hya show some scatter in their light curves, but they are considered as stars with stable light variations. The bottom-left detail (a) in fig. 4.22 depicts stable stars with respect to their periods. It is clear that the long-period variables prefer the diagonal stem rather than the pinhead.

The top left close-up of fig. 4.22 shows only data for the GB, LMC and SMC for greater clarity. When looking carefully, it is apparent that the dependences are slightly different and shifted. LMC (green dots) and SMC points (blue dots) are more scattered and shifted to the left, while data of stars located in the GB (red dots) are sharply defined on the right edge of the plot. It is very probable that this feature correlates mainly with metallicity. Stars with higher metallicity tend to be more to the right in this plot. SMC stars with the lowest average metallicity of about $[\text{Fe}/\text{H}]_{\text{ZW}} \approx -1.72$ (Kapakos & Hatzidimitriou, 2012) are mostly to the left, LMC RR Lyrae stars with $[\text{Fe}/\text{H}]_{\text{ZW}} \approx -1.48$ in the middle, and GB stars with $[\text{Fe}/\text{H}]_{\text{ZW}} \approx -1.23$ (both from Smolec, 2005) are mostly to the right.

The metallicity assumption is supported by the appearance of the bottom-right (b) panel of fig. 4.22, and also by theoretical models. Nemeč et al. (2011) presented predicted Fourier parameters calculated with the Warsaw convective-pulsation codes (Smolec & Moskalik, 2008). Since they studied stars observed by the *Kepler* satellite, they obtained a similar dependence as in the upper part of fig. 4.22. Nevertheless, the situation is not simply just metallicity-dependent, because the position in the R_{31} versus R_{21} plot depends also mainly on the luminosity and mass of a star (see fig. 14 and 15 of Nemeč et al., 2011).

¹⁰AL CMi has a spectroscopic metallicity much lower than photometric metallicity ($[\text{Fe}/\text{H}]_{\text{ZW}} = -0.81$, Layden, 1994).

Fourier phases ϕ_{21} and ϕ_{31}

In fig. 4.24 it can be seen that the relationship between ϕ_{21} and ϕ_{31} is nearly linear, which was also observed in the *Kepler*-field stars, but this dependence was not so pronounced in synthetic diagrams (Nemec et al., 2011). Noted discrepancies between observation and theory need to be investigated more closely.

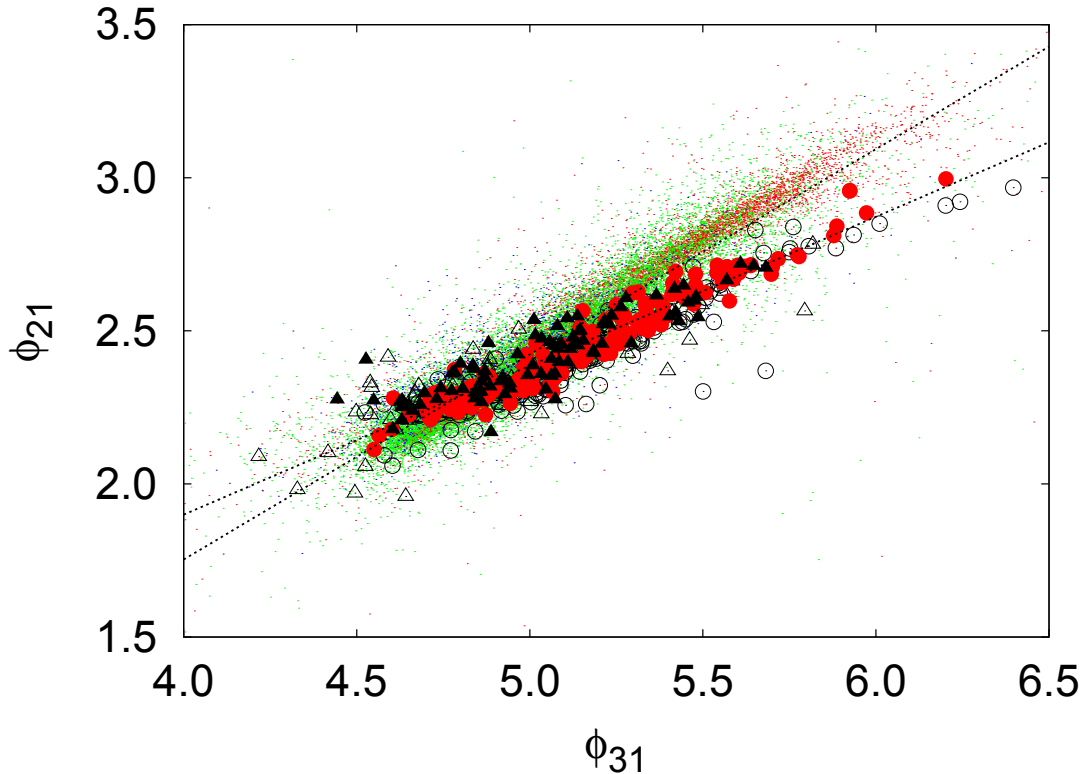


Figure 4.24: Fourier phase ϕ_{21} as a function of ϕ_{31} . Symbols are as in fig. 4.20. The dotted lines highlight the difference in inclination of the dependence for field and GC RR Lyrae stars, and for LMC, SMC and GB stars.

From fig. 4.24 it is evident that the slope of field and GC stars is different than the slope of the dependence for stars from the LMC, SMC and GB (both dependences are highlighted by dotted lines, which are based on linear fits). The reason for this property is apparent in the details of fig. 4.25. Since the dependences of ϕ_{21} and ϕ_{31} for field and GC stars are linear and parallel in the whole range of periods, the vast majority of stars in the LMC and GB stars follow the dependence, which curves to higher values at the point of about $P = 0.55$ d. The reason for this phenomenon is not clear. Evolutionary effects are suspected to be responsible for this interesting behaviour. As a consequence, linear P – $[\text{Fe}/\text{H}]$ – ϕ_{31} calibrations based on field and GC stars would very likely give incorrect results for LMC, SMC and GB RR Lyrae stars.

The bottom panel of fig. 4.25 shows the traditional result that at a constant period more metal-abundant stars have a higher ϕ_{31} , which is consistent with theoretical predictions when keeping mass and luminosity constant (see the bottom left panel of fig. 15 in Nemec et al., 2011). Nemec et al. (2011) also suggested that the stars with the lowest luminosity are expected to have a low ϕ_{21} , and that Blažko stars should prefer a higher metallicity (due to a lower A_{tot} and higher ϕ_{31}). Our

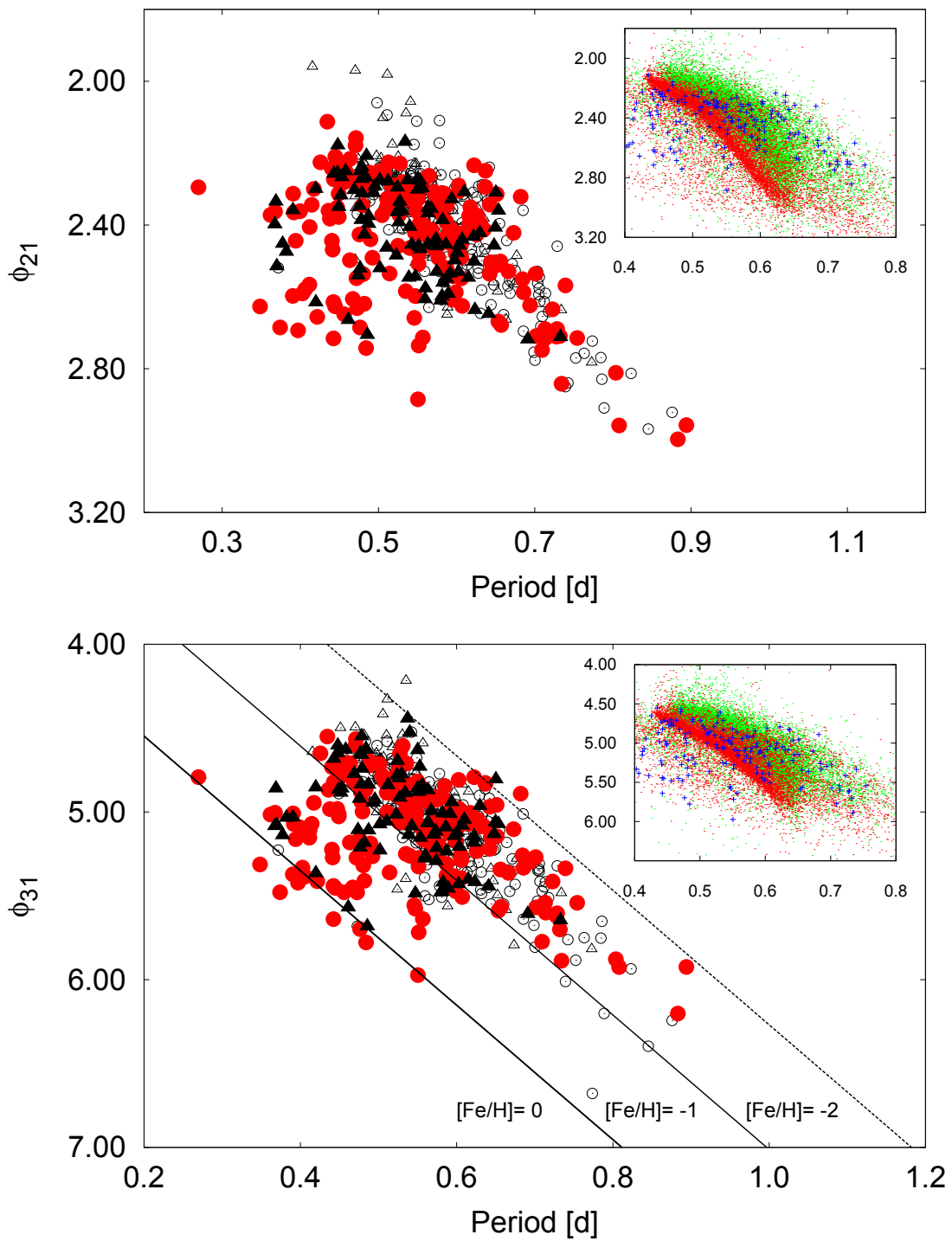


Figure 4.25: Distribution of Fourier phases according to period (in days) of a star. Symbols are the same as in fig. 4.20. For comparison, there are stable field stars (blue crosses), LMC (green dots) and GB stars (red dots) in the details of each plot. For a better representation see the electronic version. The lines in the bottom panel show points with the same metallicity ($[\text{Fe}/\text{H}]_{\text{CG}} = 0; -1; \text{ and } -2$ according to eq. 1.14).

results contradict this statement, because many of the low-luminous RR Lyraes have a high ϕ_{21} , and Blažko stars have on average a lower ϕ_{31} than regular RR Lyrae stars. This indicates that results on several RRab stars in the *Kepler* field can not be extrapolated to the wider sample. Low-luminous stars form a separated sequence in ϕ_{21} and ϕ_{31} vs. P diagrams ($\phi_{21} \geq 2.5$, $\phi_{31} \geq 5$ and $P < 0.6$ d), and correspond to metal-strong Oosterhoff I stars (see sec. 4.3.4).

The differences in the average values of ϕ_{21} and ϕ_{31} for modulated and non-modulated stars over the same period interval are very small. We obtain $\phi_{21\text{ave}} = 2.45(2)$ and $\phi_{21\text{ave}} = 2.42(2)$ for stable and modulated stars over the whole period interval, respectively. The situation is similar for ϕ_{31} , where regular RR Lyrae stars have $\phi_{31\text{ave}} = 5.14(3)$, while Blažko stars have $\phi_{31\text{ave}} = 5.03(2)$. From table 4.14 we see that between the periods 0.5 and 0.6 days the averages of ϕ_{21} and ϕ_{31} are almost the same. Over other period ranges the differences are slightly more pronounced.

Table 4.14: Average ϕ_{21} , ϕ_{31} and RT values for different period ranges. Numbers in parentheses are the standard errors of the means. ‘S’ denotes stable stars and ‘BL’ modulated stars, respectively.

	$p \leq 0.5$		$p \in (0.5, 0.6)$		$p \geq 0.6$	
	S	BL	S	BL	S	BL
ϕ_{21}	2.41(2)	2.37(3)	2.41(2)	2.43(2)	2.55(3)	2.49(3)
ϕ_{31}	5.08(4)	4.93(5)	5.08(4)	5.03(4)	5.32(5)	5.22(6)
RT	0.152(4)	0.225(12)	0.159(4)	0.227(12)	0.176(5)	0.200(8)

Rise time

Figure 4.26 shows how rise time correlates with some light-curve characteristics. It is seen that stable stars follow roughly linear trends, while RT s of modulated stars are very scattered and with typically higher values than for non-modulated stars. From these plots RT appears to be a powerful indicator predicting which stars are Blažko-modulated. It appears that 1/3 of stars ($RT > 0.24$) can be clearly separated from stable stars.

When looking carefully, the top left panel of fig. 4.26 is, after reversing the vertical axis, very similar to dependencies in fig. 4.25 for stable stars. This means that RT can also be used for metallicity determination (Sandage, 2004). Nevertheless, the RT -metallicity equation can be used only for modulation-free

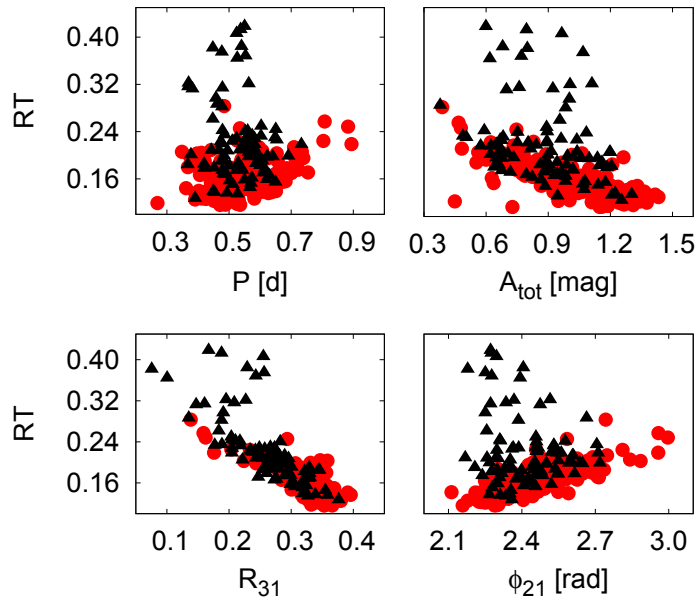


Figure 4.26: Rise time as a function of various light-curve parameters. Non-modulated stars are, as in other figures, plotted with red circles, modulated stars are drawn with black triangles.

stars, because Blažko stars do not behave linearly and results for these stars would be completely wrong or at least systematically shifted.

In Table 4.14, it can be found how average RT behaves in different period ranges. As can be expected, a longer period means a higher rise time. For stars with regular light curves, the average rise time is $RT_{\text{ave}} = 0.161(3)$ over the whole period interval, while for modulated stars it is $RT_{\text{ave}} = 0.221(7)$.

4.3.4 Discussion on physical parameters

In our analysis we assume that the equations in sec. 1.3.3 work for both stable and Blažko stars. This implies that different coefficients for modulated RR Lyrae stars would result in different physical parameters. However, we can not rule out the possibility that slightly different or additional physics occurs inside Blažko stars. In such a case, although Blažko and stable stars would share the same physical parameters, their light-curve parameters would be different. Since at this moment no signs of different physics are apparent, we assume that different light-curve parameters mean different physical parameters.

Remarks on period distribution

The period-range of our 268 sample stars is between 0.27 and 0.89 days, which is also the range for our regular RR Lyrae stars. Periods of modulated stars range from 0.36 to 0.73 days. To test if the two samples come from the same distribution the Kolmogorov-Smirnov test was performed. The p-value 0.321 implies that they are consistent. The largest difference between the distributions (shown in the bottom panel of fig. 4.27) is at $P = 0.65$ d and exceeds $D = 0.121$. The appearance of the cumulative plot together with the histogram in fig. 4.27 point out the weak lack of Blažko stars in the long-period part of the distribution.

In sec. 2.5 we saw that Blažko stars probably prefer shorter periods. Jurcsik et al. (2011) proposed the occurrence rate of modulated stars in M5 with period shorter than 0.55 d as about 60 %. In our sample, the percentage of Blažko stars below and above this limit is almost identical (34.8 % and 33.9 %, respectively). The mean period of our sample RRab stars is 0.542(6) d, while the average period of Blažko stars is only slightly lower (within the errors equal to 0.532(8) d). Thus we see, that although the tendency of modulated stars to have shorter periods is obvious for M5 and the LMC, the difference for field stars is not conclusive. To solve this problem, a more numerous sample would be needed. In addition the reanalysis of LMC stars (comprising new measurements since 2003) could shed some light on this matter.

Metallicity of non-modulated and Blažko stars

Although the Kolmogorov-Smirnov test showed the Blažko sample to be consistent with the regular-stars sample ($p = 0.333$, $D = 0.120$ at $[\text{Fe}/\text{H}]_{\text{ZW}} = -0.94$), from the cumulative distribution function and histogram in fig. 4.28, it seems that Blažko stars could subtly prefer lower metallicity. The incidence rate of Blažko stars with $[\text{Fe}/\text{H}]_{\text{ZW}} < -1$ is about 38 %, while among stars with $[\text{Fe}/\text{H}]_{\text{ZW}} > -1$ it is only 23 %. Average values of metallicity are $[\text{Fe}/\text{H}]_{\text{ZWave}} = -1.40(5)$ for modulated stars, and $[\text{Fe}/\text{H}]_{\text{ZWave}} = -1.32(5)$ for variables with a stable light curve, respectively. These numbers are similar and can be considered as equal according to their errors. Therefore, our average values prefer the metallicity-independent scenario found by Smolec (2005).

Nevertheless, all these statistics can be affected by selection effects. It is probable that some metal-rich modulated stars could remain undisclosed, because of the possible small modulation amplitude of these stars. For example, DM Cyg, SS Cnc and RS Boo (all with $[\text{Fe}/\text{H}]_{\text{ZW}} > -0.5$,

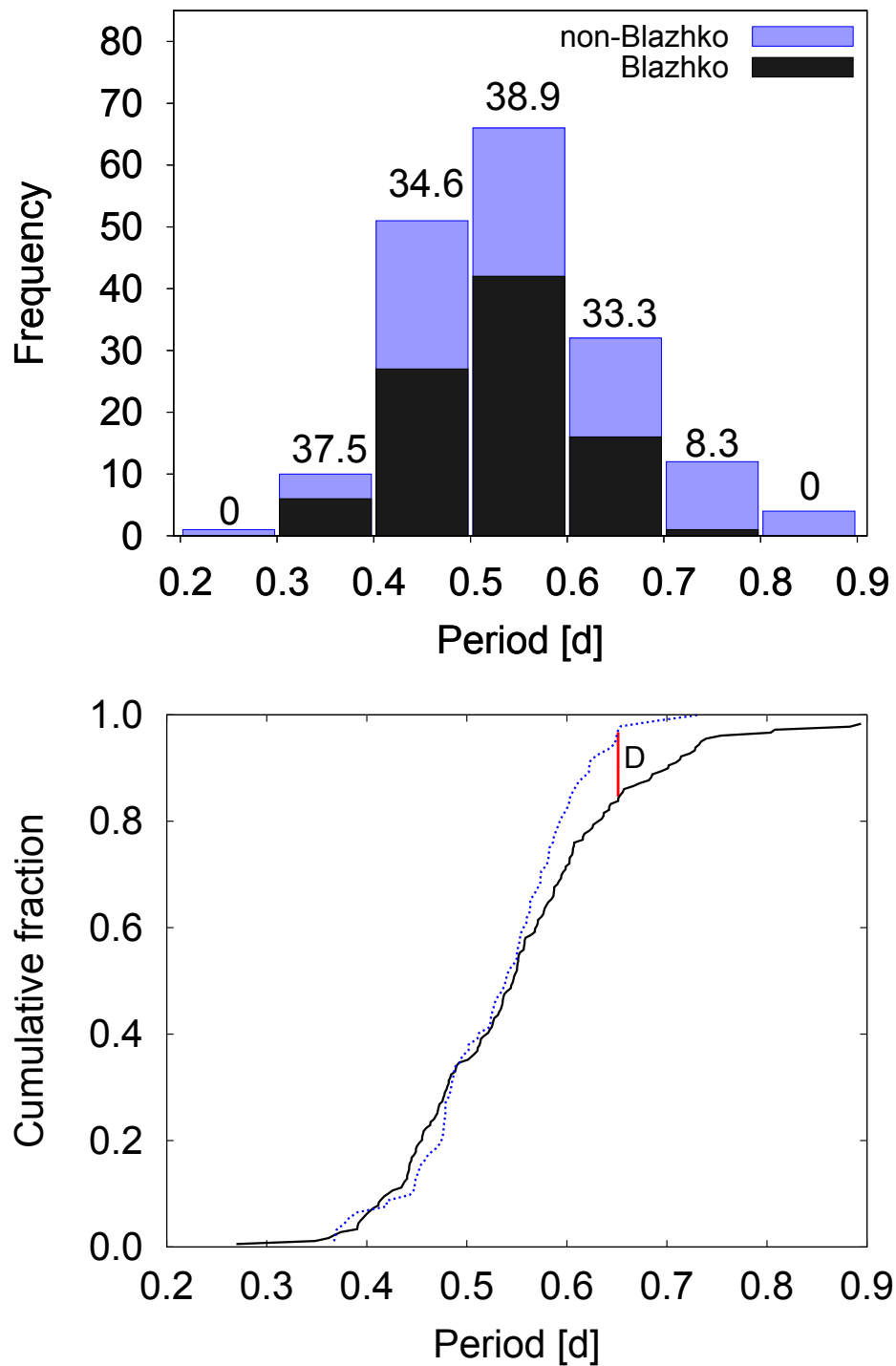


Figure 4.27: Distribution of sample stars according to their period (top panel) and their cumulative plots (bottom panel, the continuous black line is for regular stars, dotted for modulated stars). Numbers above each bin in the top panel give information about the percentage of Blažko stars in each bin. Parameter D in the bottom panel shows the largest difference between the two populations.

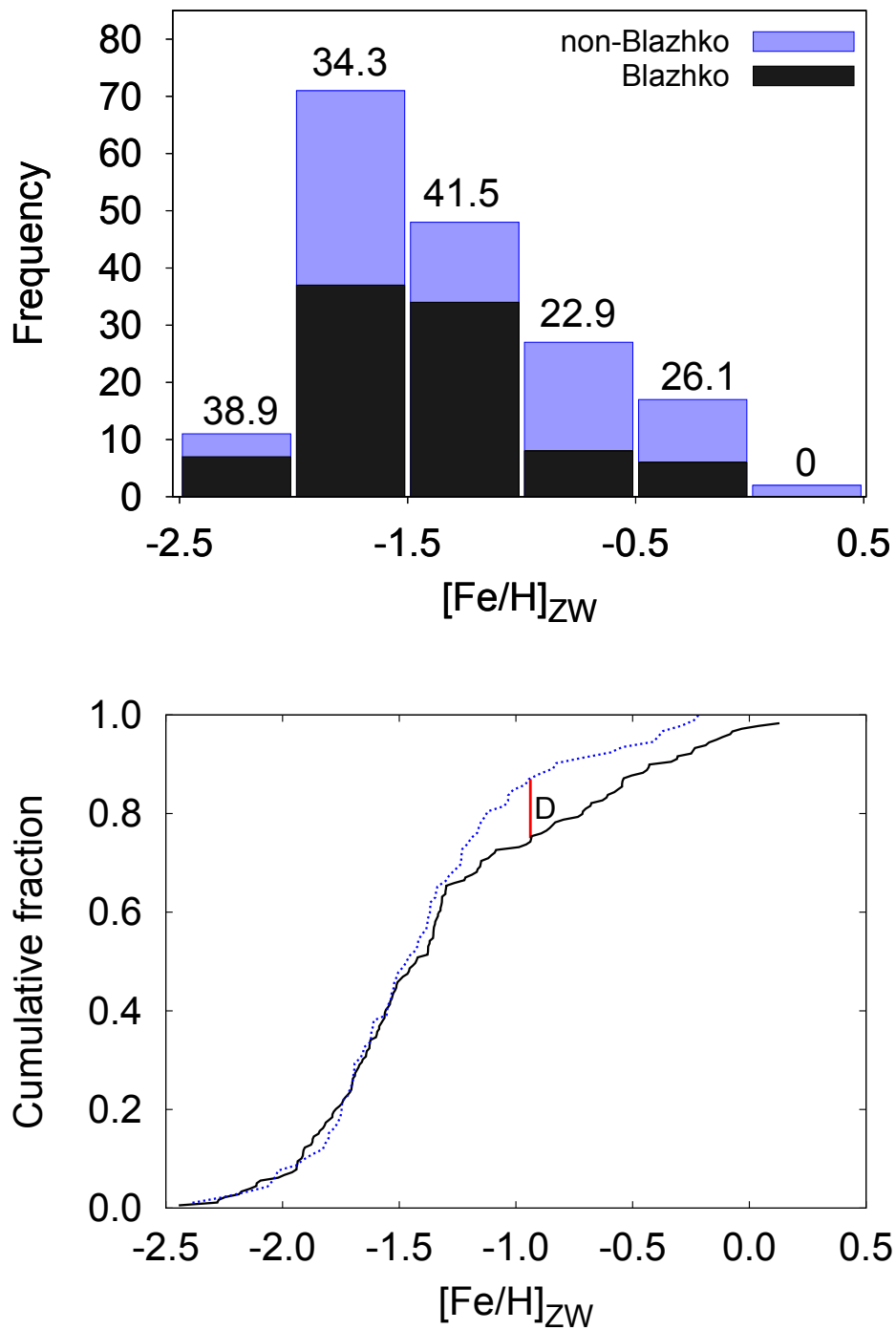


Figure 4.28: Distribution of sample stars according to their metallicity (top panel) and their cumulative plot (bottom panel, the black solid line is for regular stars, dotted for modulated stars). Numbers above each bin in the top panel and parameter D in the bottom panel have the same meaning as in fig. 4.27.

Layden, 1994) have modulation amplitudes of only about 0.1 mag. As in the case of basic pulsation periods, our analysis can not conclusively confirm metallicity dependence as an indicator of the occurrence rate of Blažko stars.

Absolute magnitude and mean colours

The well-known linear dependence of absolute magnitude vs. metallicity is shown in fig. 4.29. The blue line represents a linear fit of stable stars. When the slope of this dependence is considered to be the same for modulated stars, the zero-point shift with $\Delta M_V = 0.03$ mag appears. Very similar behaviour, based on directly observed properties of RR Lyrae variables, was noted in M5, where the difference between stable and modulated stars was found as $\Delta M_V = 0.05$ mag (Jurcsik et al., 2011). Therefore, lower luminosity can be a general property of Blažko variables and not only due to selection bias.

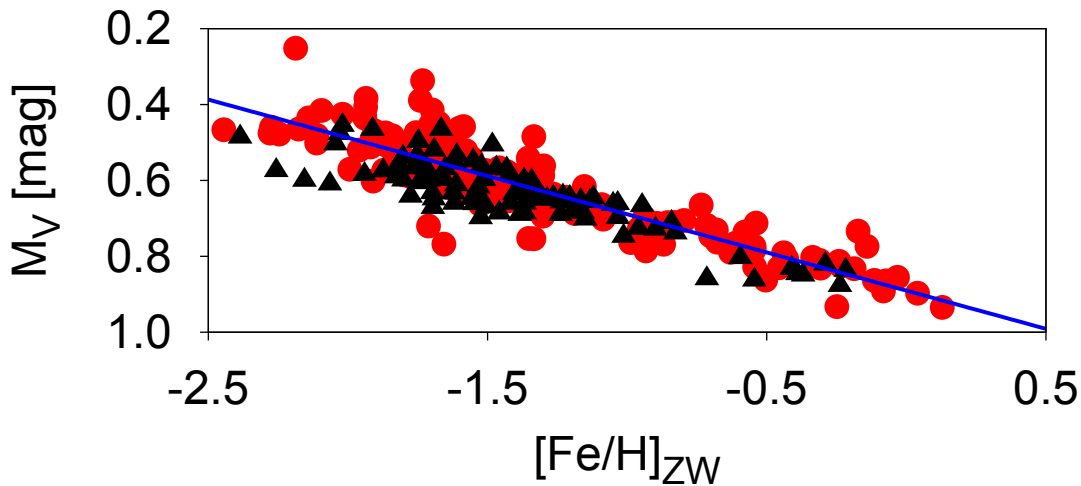


Figure 4.29: Metallicity dependence of absolute V -magnitude. The blue continuous line shows the linear fit of regular RR Lyrae stars. Notation in the top panel is the same as in fig. 4.19.

To map the colour distribution of Blažko stars among regular stars we constructed colour-magnitude (fig. 4.30) and colour-temperature diagrams (fig. 4.31). To be more conclusive, stars with different metallicity are plotted with different symbols in these plots. It is apparent that modulated stars with similar metallicity are uniformly spread out over the whole width of the dependence in fig. 4.30. In agreement with Arellano Ferro et al. (2012), no apparent tendency of Blažko stars to be bluer than regular stars at any $[\text{Fe}/\text{H}]$ is seen (both groups have the average $(B - V)_0 = 0.333(2)$). On the other hand, this is contrary to the finding of Jurcsik et al. (2011), who proposed modulated stars in M5 to be bluer than the average. This property also needs to be investigated more closely in other stellar systems, because it seems that results on limited sample stars in M5 alone could be misleading.

For instance, lines of constant period for mean-evolved stars (equation 7 from Sandage (2010)) are plotted with dotted lines in fig. 4.30. When looking carefully, stars with $M_V < 0.6$ mag suggest a different dependency (different slope) than above this limit. Since metallicity correlates with absolute magnitude as well as period, a similar linear dependence can be found for $[\text{Fe}/\text{H}]$ vs. $(B - V)_0$ and also for $[\text{Fe}/\text{H}]$ vs. period. This agrees well with figs. 1-4 of Sandage (2006).

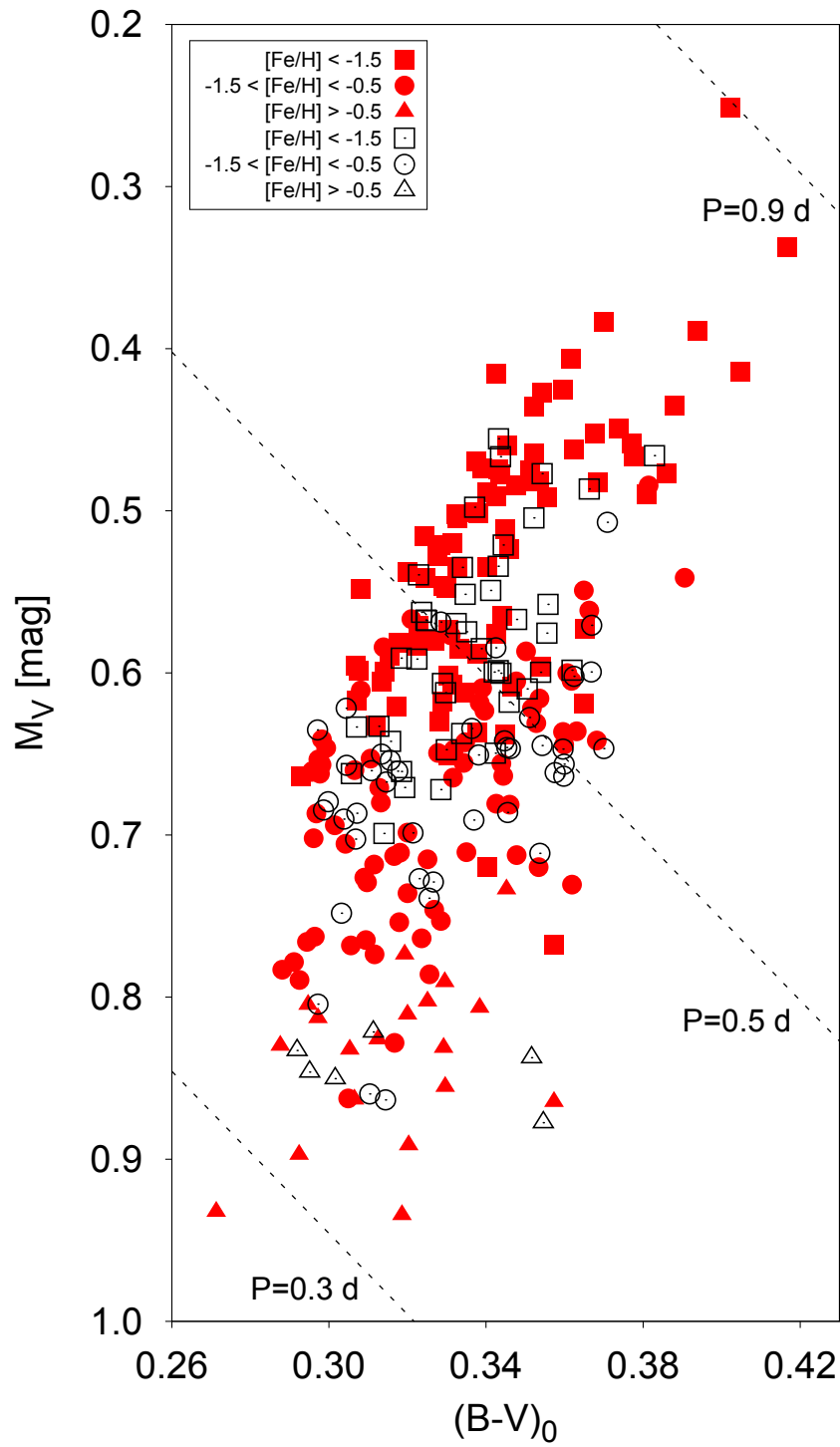


Figure 4.30: Colour dependence of absolute V-magnitude. Filled symbols denote RR Lyrae stars with stable light curves, while empty symbols relate to modulated stars. Dotted lines show places with constant period (labelled at each line). For more details see the text.

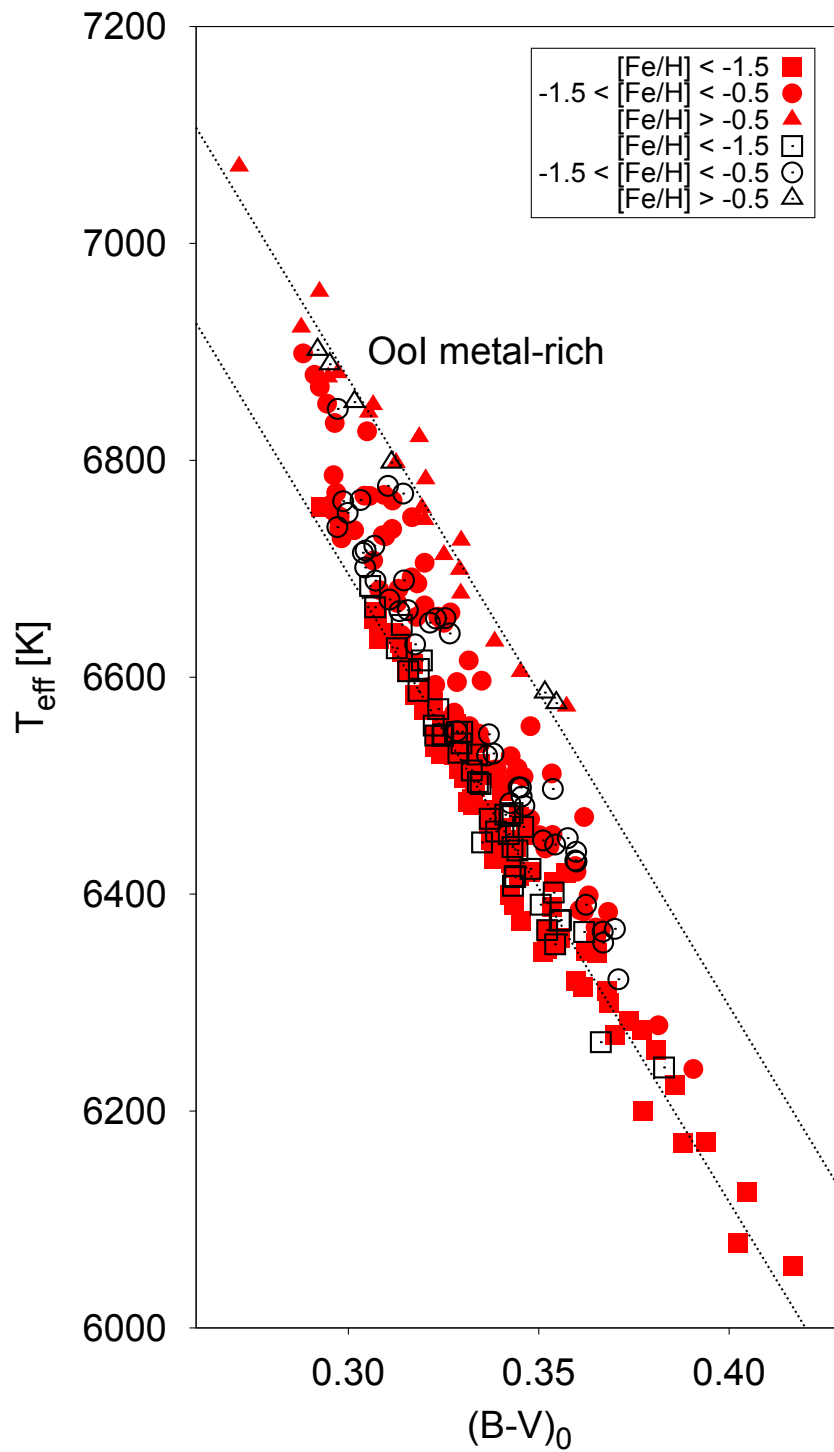


Figure 4.31: Effective-temperature dependence on colour index $(B - V)_0$. The bottom line represents the fit to stars with $[\text{Fe}/\text{H}]_{\text{ZW}} < -1.5$. The top line is the fit with the same slope for stars with $[\text{Fe}/\text{H}]_{\text{ZW}} > -0.5$. The zero-point difference between these two lines is 180 K. Symbols are the same as in fig. 4.30.

The plot in fig. 4.30 is very illustrative, and many properties of RR Lyrae variables can easily be extracted from this plot. Firstly, the horizontal branch comprises horizontal layers (constant M_V) with similar metallicity. The lower the metallicity, the more luminous the star at constant $(B - V)_0$. McNamara & Barnes (2014) assigned an average absolute magnitude $M_V = 0.43$ mag to metal-poor stars from the OoII group and $M_V = 0.61$ mag to the stars from the OoI group that are more metal-rich. This corresponds well with the appearance of our fig. 4.30. When a star evolves blueward, its period gets shorter and vice versa. Stars with similar period, but with different colour, have different metallicity.

Short-period metal-rich variables

When effective temperature is plotted against mean $(B - V)_0$ (fig. 4.31), an interesting split is observed. The dependence forms two well defined sequences shifted by 180 K with continuous transition between them. From this picture it is apparent that the branches roughly follow the metal content of the stars, e.g. stars with high metallicity have higher temperature than stars with lower metallicity at a constant $(B - V)_0$. However, it is not a strict rule: a metal-strong sequence is at its blue part contaminated with a few lower-metal-abundant variables.

The upper sequence depicted in fig. 4.31 comprises short-period, metal-rich stars, which were mentioned in sec. 4.3.3 (fig. 4.25) to form an isolated branch in the ϕ_{21} - P and ϕ_{31} - P plots. These stars were marked as OoIb stars by Szczygieł et al. (2009) and were very recently discussed by McNamara & Barnes (2014), who linked them with metal-strong, short-period stars belonging to Oosterhoff group I (OoI), which are not observed in GCs. They assumed them to be Blažko stars with $M_{\text{aveV}} = 0.89$ mag. This value corresponds very well with the appearance of fig. 4.30. Nevertheless, our findings clearly show that the metal-strong branch is formed mainly by stars with stable light curves, which contradicts their assumption that this sequence is populated by modulated stars. McNamara & Barnes (2014) proposed the temperature-difference between OoI and OoII stars to be 270 K, but no such split or broadening is observed in our sample.

Fig. 4.32 is analogous with fig. 2 of McNamara & Barnes (2014). In this plot, OoI metal-rich stars constitute the left most sequence, while the other two branches correspond to OoI and OoII stars. The dotted lines in this plot are drawn to roughly define different Oosterhoff groups. The separation of stars into different branches in fig. 4.32 approximately corresponds to sequences, which are also visible in fig. 4.20, where the most metal-rich stars occur in the left part of the plot.

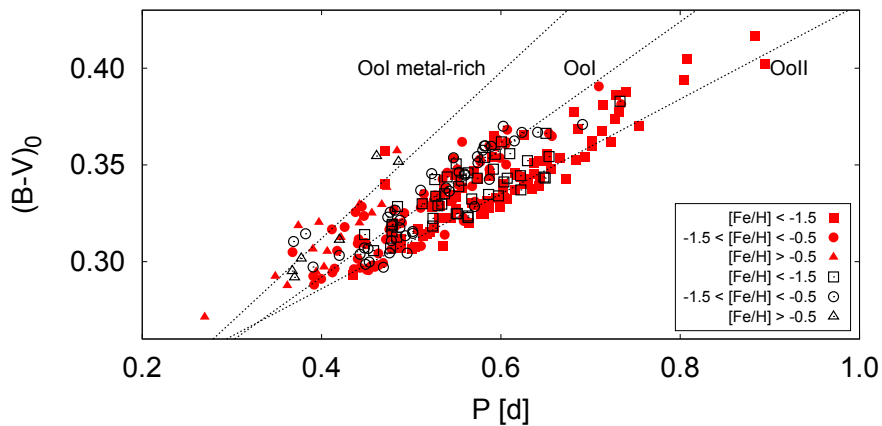


Figure 4.32: $(B - V)_0$ vs. P plot. Lines are only for illustration and roughly define Oosterhoff groups. For details see the text. Symbols are the same as in fig. 4.30.

Higher temperature and lower luminosity of OoI metal-strong stars imply that they should have significantly smaller diameters than their more luminous counterparts. If the mass-metallicity dependence (eq. 1.30) is assumed to be continuous, a jump in periods should be observed, because a lower diameter would result in a higher density which, according to pulsation equation, would lead to shorter periods. Such jump in periods is really observed in fig. 4.32. This new, metal-rich subclass of RR Lyrae variables is very interesting and deserves appropriate attention.

Summary and conclusions

This thesis has two basic goals. Firstly a short overview of current knowledge on RR Lyrae type pulsating stars, and mainly in the still mysterious Blažko phenomenon, is given. Secondly this work presents an extensive study of the photometric characteristics of fundamental mode RR Lyrae stars and an attempt to find some differences between ordinary and modulated stars.

The first third of the thesis (chapters 1 and 2) provides a brief overview of the current knowledge of RR Lyrae stars and of the Blažko effect. Pulsation and physical characteristics, evolution of RR Lyrae type stars, and the connection of physical parameters with the light curve parameters are discussed in the first chapter. The second chapter provides an introduction to the Blažko effect. Mathematical description, observed properties, incidence rates of modulated stars in various stellar systems, known differences between regular and modulated stars are given in this chapter. In addition, models proposed for the explanation of the Blažko effect are discussed.

Chapters 3, 4 constitute the core of the thesis. Section 3.1 focuses on the photometric study of an RRc star, TV Boo. Based on data in the SuperWASP archive (almost 9000 points in 205 nights) it was found that this star undergoes parallel modulation with periods 9.737(5) d and 21.5(2) d that causes long-term changes in the shape of the light curve (Skarka & Zejda, 2013). At the time of publication it was the first field RRc star showing such behaviour. Compound modulation of TV Boo was independently confirmed by Hajdu et al. (2012). The basic pulsation period of the star changes with an amplitude of 21 minutes during the modulation cycle.

About 2500 points in each of BVR_c filters were gathered at the Masaryk University Observatory during years 2009-2011. The data, which were calibrated to the standard Johnson system, allowed us to estimate the basic physical characteristics through the empirical relations using Fourier coefficients. Since our light curve is well covered, physical parameters of good reliability were gained. It was found that TV Boo has $[Fe/H] = -1.89(14)$ which is much higher than previously published values. This discrepancy, together with the change in metallicity during the Blažko cycle, was discussed in detail in sec. 3.1.3.

The light curve of TV Boo shows some minor indications that it could possibly experience some sort of long-term cyclic changes similar to the four-year cycle of RR Lyrae. This assumption raises from the observation of a bump during the seasons 2010 and 2011 in MUO data and in 2004 in SuperWASP data. The assumption is supported by the fact that the asymmetry parameter Q_A turned from positive to negative for the second modulation component during seasons. However, more observations are needed to confirm this behaviour. Results of the study of TV Boo were published in Skarka & Zejda (2013).

The *Czech RR Lyrae Stars Observation Project* is introduced in sec. 3.2. The motivation for founding this project was induced by the lack of precise multicolour observations of RR Lyrae stars. To be able to get as many measurements as possible in a short time, the project is designed to incorporate amateur observers with appropriate CCD equipment (7 members in summer of 2014). The choice of targets are constrained by the location of the Czech Republic and the apertures of telescopes used. Thus we concentrate on RR Lyrae brighter than 12.5 mag in maximum light and

with a declination typically greater than $+20^\circ$. Introduction of the project was published in Skarka et al. (2013).

The main goal is to obtain well-covered light curves in standard BVR_cI_c filters, which are subsequently further analysed to determine ephemerides, periods, and light curve characteristics. The first results of the project are described in sections 3.2.2 and 3.2.3. CN Cam was found to be a Blažko star with a modulation period of 48.25 d (Skarka et al., 2013). In addition, two other stars were identified as modulated stars (Skarka & Cagaš, 2013).

At the beginning of chapter 4 the BlaSGalF database is introduced (Skarka, 2013, 2014b). It is a regularly updated on-line database that comprises known galactic RR Lyrae stars showing modulation. Currently the list provides basic information about 338 stars (coordinates, pulsation type, magnitude range, pulsation and modulation periods, references). The BlaSGalF database represents a powerful tool for statistics on Blažko stars. From this sample the vast majority consists of fundamental mode pulsators (84 %). Thirty two stars show multiple modulation (10.5 %), and six stars show a changing Blažko effect. In addition, when modulation period is plotted against pulsation period, RRc and RRab stars are clearly separated, and areas where they are located can be defined (Skarka, 2014b). Assuming that the characteristics of this plot are not the result of observation bias, it allows us to identify interesting objects that behave abnormally.

The data from the ASAS and SuperWASP surveys were analysed to identify and describe modulation in bright RRab stars - the details are described in sec. 4.2. After careful cleaning and inspection of each light curve, 321 of the original 557 stars remained for detailed analysis. To identify possible modulation we performed frequency spectra and maximum amplitude and maximum timings analysis. This study revealed 25 objects that show modulation and that were previously known as RRab stars with regular light changes. Eight stars turned out to be objects with parallel modulation that was previously unknown. Compared to a previous study based on ASAS data, a surprisingly high percentage of modulated stars was observed (at least 31 %). In addition, it was revealed that a significant number of modulated stars shows multiple modulation or some peculiarity in their modulation. In many of these targets the modulation period ratio was a small integer ratio Skarka (2014a). The same was observed in data from the *Kepler* telescope (Benkó et al., 2014). We also discussed the difficulties to identify modulation in poor quality data. It was clearly demonstrated that statistics derived from the appearance of frequency spectra are of poor reliability. However, it was confirmed that the vast majority of modulated stars have a side peak related to the modulation frequency with higher amplitude at the right-hand side of f_0 . RZ CVn and IK Hya were highlighted, because they show interesting frequency spectra and change their modulation dramatically. Results on RR Lyrae stars from the ASAS and SuperWASP surveys were published in Skarka (2014a).

As a direct continuation of the analysis of light curves of RRab stars from the ASAS and SuperWASP surveys, we proceeded with the determination of the Fourier coefficients and other light curve characteristics of 268 stars with well defined, well sampled light curves (sec. 4.3, Skarka, 2014c). The goal was to test whether the light curve parameters and physical parameters, that were determined via empirical relations using Fourier coefficients, differ for regular and modulated RRab stars. In addition, characteristics of stars from the Galactic bulge, LMC, SMC and globular clusters were used to extend our small sample.

Firstly, it was necessary to stitch parameters from ASAS and SuperWASP surveys, because they observe in different passbands. This was done using 24 stars common in both surveys. Subsequent comparison of parameters confirmed that Blažko stars have lower total amplitudes and longer rise times than regular stars. While amplitudes A_1 were the same for stable and modulated stars, higher order amplitudes were lower for Blažko stars. The reason for this behaviour should be obvious, because regular stars have more skewed light curves than modulated stars.

Rise time appeared to be a powerful indicator of modulation, because almost all stars with $RT > 0.24$ were modulated. In addition, it was found that empirical relations that use RT have limited plausibility only for ordinary RRab Lyrae stars Skarka (2014c). It was found that the shape of the graph of the R_{31} vs. R_{21} dependence resembles the bent pin. Whereas stable stars prefer the pin-head with values around $R_{31} \sim 0.34$, modulated and long period stars condense mainly in the stem. In addition, the R_{31} vs. R_{21} plot appears to be strongly metallicity dependent - variables with high metallicity were mostly found to the left, while metal deficient stars settles more to the right Skarka (2014c).

When ϕ_{31} is plotted against ϕ_{21} the dependence is linear. It is very interesting that the slope of the dependence for field and globular cluster stars differs from the slope for stars from the Galactic bulge and that of the Large and Small Magellanic clouds. The difference is also seen in ϕ_{i1} vs. pulsation period plots. It has a very important implication that empirical relations that use ϕ_{i1} , which were determined on the basis of field and globular cluster stars, give wrong, or at least systematically shifted results for stars in the GB or beyond the Milky Way galaxy Skarka (2014c).

Although our analysis showed that modulated stars have a weak preference for shorter periods and lower metallicity, the results were not convincing (Skarka, 2014c). More precise measurements of more stars would probably be needed to obtain a reliable answer onto this question, because almost all studies differ. However, it could be an intrinsic property of Blažko stars, since in their case shorter periods are generally observed.

Similar to what is observed in the globular cluster M5, stars showing the Blažko effect appeared to be slightly less luminous than their regular counterparts (Skarka, 2014c). However, the difference of only 0.03 mag is very small and needs to be independently confirmed in other stellar systems. When absolute magnitude was plotted as a function of $(B - V)_0$, no evident preference for Blažko stars was observed. During our analysis we easily identified metal-rich short-period stars which were discovered only recently. These stars clearly form separate sequences in the T_{eff} vs. $(B - V)_0$ and $(B - V)_0$ vs. P plots. It was found that this group is populated by both modulated and ordinary RRab Lyrae stars, and that they are about 180 K hotter than the rest of the RRab stars (Skarka, 2014c).

Hopefully all the research efforts of this thesis spread over the past four years, will help to solve the mysterious Blažko phenomenon. However, like in the case of other studies, many new questions raised. From the one point of view this could be annoying, but on the other hand it is also encouraging, because new photometric and spectroscopic measurements are still highly needed. Therefore there is no need to be discouraged, because there is a lot of work ahead!

References

- Alcock, C., Allsman, R., Alves, D. R., et al. 2000, *ApJ*, 542, 257
- Alcock, C., Alves, D. R., Becker, A., et al. 2003, *ApJ*, 598, 597
- Alonso-García, J., Catelan, M., Amigo, P., et al. 2013, *Memorie della Societa Astronomica Italiana*, 84, 63
- Alsubai, K. A., Parley, N. R., Bramich, D. M., et al. 2013, *Acta Astron.*, 63, 465
- Arellano Ferro, A., Rojas López, V., Giridhar, S., & Bramich, D. M. 2008, *MNRAS*, 384, 1444
- Arellano Ferro, A., Figuera Jaimes, R., Giridhar, S., et al. 2011, *MNRAS*, 416, 2265
- Arellano Ferro, A., Bramich, D. M., Figuera Jaimes, R., Giridhar, S., & Kuppuswamy, K. 2012, *MNRAS*, 420, 1333
- Arellano Ferro, A., Bramich, D. M., Figuera Jaimes, R., et al. 2013, *MNRAS*, 434, 1220
- Bailey, S. I., & Leland, E. F. 1899, *ApJ*, 10, 255
- Bailey, S. I. 1902, *Annals of Harvard College Observatory*, 38, 1
- Baker, N., & Kippenhahn, R. 1962, *Zeitschrift für Astrophysik*, 54, 114
- Balazs, J., & Detre, L. 1950, *Communications of the Konkoly Observatory Hungary*, 23, 1
- Balazs, J., & Detre, L. 1952, *Communications of the Konkoly Observatory Hungary*, 27, 1
- Benkő, J. M., Kolenberg, K., Szabó, R., et al. 2010, *MNRAS*, 409, 1585
- Benkő, J. M., Szabó, R., & Paparó, M. 2011, *MNRAS*, 417, 974
- Benkő, J. M., Plachy, E., Szabó, R., Molnár, L., & Kolláth, Z. 2014, *arXiv:1406.5864*
- Bezdeneshnyi, V. P. 1988, *Information Bulletin on Variable Stars*, 3141, 1
- Blažko, S. 1907, *Astronomische Nachrichten*, 175, 325
- Bono, G., Caputo, F., & Di Criscienzo, M. 2007, *A&A*, 476, 779
- Borkowski, K. J. 1980, *Acta Astron.*, 30, 393
- Bramich, D. M., Alsubai, K. A., Arellano Ferro, A., et al. 2014, *Information Bulletin on Variable Stars*, 6106, 1
- Breger M. et al., 1993, *A&A*, 271, 482

- Bryant, P. H. 2014, *ApJL*, 783, L15
- Bryant, P. H. 2014, arXiv:1408.0263
- Buchler, J. R., & Kolláth, Z. 2011, *ApJ*, 731, 24
- Butler D., 1975, *ApJ*, 200, 68
- Butler, D., Manduca, A., Bell, R. A., & Deming, D. 1982, *AJ*, 87, 640
- Butters O.W. et al., 2010, *A&A*, 520, 10
- Cacciari, C., Corwin, T. M., & Carney, B. W. 2005, *AJ*, 129, 267
- Cagaš, P., & Pejcha, O. 2012, *A&A*, 544, L3
- Campos-Cucarella, F., Nomen-Torres, J., Gomez-Forrellad, J. M., & Garcia-Melendo, E. 1996, *Information Bulletin on Variable Stars*, 4323, 1
- Carretta, E., & Gratton, R. G. 1997, *A&AS*, 121, 95
- Cassisi, S., Castellani, M., Caputo, F., & Castellani, V. 2004, *A&A*, 426, 641
- Catelan, M. 2009, *Astrophysics and Space Science*, 320, 261
- Catelan, M., & Cortés, C. 2008, *ApJL*, 676, L135
- Chadid, M., Wade, G. A., Shorlin, S. L. S., & Landstreet, J. D. 2004, *A&A*, 413, 1087
- Chadid, M., Benkő, J. M., Szabó, R., et al. 2010, *A&A*, 510, A39
- Christy, R. F. 1966, *ApJ*, 144, 108
- Clement, C. M., & Shelton, I. 1997, *AJ*, 113, 1711
- Clementini, G., Gratton, R., Bragaglia, A., et al. 2003, *AJ*, 125, 1309
- Contreras, R., Catelan, M., Smith, H. A., et al. 2010, *AJ*, 140, 1766
- Cox, J. P., Cox, A. N., Olsen, K. H., King, D. S., & Eilers, D. D. 1966, *ApJ*, 144, 1038
- Cutri, R. M., Skrutskie, M. F., van Dyk, S., et al. 2003, *VizieR Online Data Catalog*, 2246, 0
- Dékány, I., & Kovács, G. 2009, *A&A*, 507, 803
- Demarque, P., Zinn, R., Lee, Y.-W., & Yi, S. 2000, *AJ*, 119, 1398
- de Ponthiere, P., Hamsch, F.-J., Krajci, T., & Menzies, K. 2013, *Journal of the American Association of Variable Star Observers (JAAVSO)*, 41, 214
- Detre L., 1965, *Astron. Abh. Leipzig*, p. 621
- Detre L., Szeidl N., 1973, *Information Bulletin on Variable Stars*, 764, 1
- Dorman, B. 1993, *The Globular Cluster-Galaxy Connection*, *Astronomical Society of the Pacific Conference Series*, 48, 198
- Drake, A. J., Catelan, M., Djorgovski, S. G., et al. 2013, *ApJ*, 763, 32

- Dziembowski, W. A., & Mizerski, T. 2004, *Acta Astron.*, 54, 363
- Eddington, A. S. 1926, *The Internal Constitution of the Stars*, Cambridge: Cambridge University Press, 1926. ISBN 9780521337083.
- Feast M.W. et al., 2008, *MNRAS*, 386, 2115
- Fernley J. et al., 1998, *MNRAS*, 293, 61
- Firmanjuk B.N., 1974, *Astronomicheskii Tsirkulyar*, 863, 7
- Fitch, W. S. 1967, *ApJ*, 148, 481
- Fitch, W. S., Wisniewski, W. Z., & Johnson, H. L. 1966, *Communications of the Lunar and Planetary Laboratory*, 5, 3
- For, B.-Q., Preston, G. W., & Sneden, C. 2011, *ApJS*, 194, 38
- Gillet, D. 2013, *A&A*, 554, A46
- Gillet, D., & Crowe, R. A. 1988, *A&A*, 199, 242
- Gillet, D., Fabas, N., & Lèbre, A. 2013, *A&A*, 553, A59
- Goranskij, V., Clement, C. M., & Thompson, M. 2010, *The Pulsation Mode Changes of the RR Lyrae Type Variable Star V79 in the Globular Cluster M3*, in proceedings of Variable stars, the Galactic halo and Galaxy Formation
- Groebel, R. 2013, arXiv:1307.6454
- Guggenberger, E., Kolenberg, K., Nemeč, J. M., et al. 2012, *MNRAS*, 424, 649
- Gutnick P., Prager R. 1926, *Astronomische Nachrichten*, 228, 353
- Hajdu, G., Jurcsik, J., Sódor, Á., et al. 2012, *Astronomische Nachrichten*, 333, 1074
- Hurta Zs. et al., 2008, *AJ*, 135, 957
- Iben, I., Jr., & Rood, R. T. 1970, *ApJ*, 161, 587
- Iben, I., Jr. 1971, *Publications of the Astronomical Society of the Pacific*, 83, 697
- Jerzykiewicz, M. 1995, *Astrophysical Applications of Powerful New Databases*, General Assembly of the I.A.U., 78, 265
- Jurcsik, J. 1998, *A&A*, 333, 571
- Jurcsik, J., & Kovács, G. 1996, *A&A*, 312, 111
- Jurcsik, J., Clement, C., Geyer, E. H., & Domsa, I. 2001, *AJ*, 121, 951
- Jurcsik, J., Benkő, J. M., & Szeidl, B. 2002, *A&A*, 396, 539
- Jurcsik, J., Szeidl, B., Nagy, A., & Sodor, A. 2005a, *Acta Astron.*, 55, 303
- Jurcsik, J., Sódor, Á., Váradi, M., et al. 2005b, *A&A*, 430, 1049
- Jurcsik, J., Sódor, Á., & Váradi, M. 2005c, *Information Bulletin on Variable Stars*, 5666, 1

- Jurcsik, J., Szeidl, B., Sódor, Á., et al. 2006, *AJ*, 132, 61
- Jurcsik, J., Sódor, Á., Hurta, Z., et al. 2008, *MNRAS*, 391, 164
- Jurcsik, J., Sódor, Á., Szeidl, B., et al. 2009, *MNRAS*, 400, 1006
- Jurcsik, J., Hurta, Z., Sódor, Á., et al. 2009b, *MNRAS*, 397, 350
- Jurcsik, J., Szeidl, B., Clement, C., Hurta, Z., & Lovas, M. 2011, *MNRAS*, 411, 1763
- Jurcsik, J., Hajdu, G., Szeidl, B., et al. 2012, *MNRAS*, 419, 2173
- Kanyo, S. 1980, *Information Bulletin on Variable Stars*, 1832, 1
- Kapakos, E., & Hatzidimitriou, D. 2012, *MNRAS*, 426, 2063
- Kapteyn, J. C. 1890, *Astronomische Nachrichten*, 125, 165
- Kiess, C. C. 1912, *Publications of the Astronomical Society of the Pacific*, 24, 186
- King, D. S., & Cox, J. P. 1968, *Publications of the Astronomical Society of the Pacific*, 80, 365
- Kinemuchi, K., Smith, H. A., Woźniak, P. R., McKay, T. A., & ROTSE Collaboration 2006, *AJ*, 132, 1202
- Kinman, T. D., & Carretta, E. 1992, *Publications of the Astronomical Society of the Pacific*, 104, 111
- Kinman, T. D., Harmer, D. L., Saha, A., & Willmarth, D. W. 2007, *Information Bulletin on Variable Stars*, 5805, 1
- Kiss, L. L., & Szatmáry, K. 2002, *A&A*, 390, 585
- Klotz, A., Vachier, F., & Boër, M. 2008, *Astronomische Nachrichten*, 329, 275
- Klotz, A., Boër, M., Atteia, J. L., & Gendre, B. 2009, *AJ*, 137, 4100
- Kluyver, H. A. 1936, *Bull. Astron. Inst. Netherlands*, 7, 313
- Kolláth, Z., Molnár, L., Szabó, R. 2011, *MNRAS*, 414, 1111
- Kolenberg, K. 2005, “*The Blazhko Project: Joint Efforts in Solving a Century-old Problem*”, *The Light-Time Effect in Astrophysics: Causes and cures of the O-C diagram*, *Astronomical Society of the Pacific*, 335, 95
- Kolenberg, K. 2007, “*The Blazhko Project: Unravelling the Mysteries of Amplitude Modulation*”, *ASPC series, Solar and Stellar Physics Through Eclipses*, 370, 294
- Kolenberg, K., Smith, H. A., Gazeas, K. D., et al. 2006, *A&A*, 459, 577
- Kolenberg, K., & Bagnulo, S. 2009, *A&A*, 498, 543
- Kolenberg, K., Szabó, R., Kurtz, D. W., et al. 2010, *ApJL*, 713, L198
- Kolenberg, K., Bryson, S., Szabó, R., et al. 2011, *MNRAS*, 411, 878
- Kolenberg, K., Kurucz, R. L., Stellingwerf, R., et al. 2014, “*RR Lyrae studies with Kepler: showcasing RR Lyr*”, *IAU Symposium*, 301, 257

- Koopmann, R. A., Lee, Y.-W., Demarque, P., & Howard, J. M. 1994, *ApJ*, 423, 380
- Kovács, G., & Zsoldos, E. 1995, *A&A*, 293, L57
- Kovács, G., & Jurcsik, J. 1996, *ApJL*, 466, L17
- Kovács, G., & Kanbur, S. M. 1998, *MNRAS*, 295, 834
- Kovács, G., & Walker, A. R. 2001, *A&A*, 371, 579
- Kovács, G. 2005, *A&A*, 438, 227
- Kraft, R. P., & Ivans, I. I. 2003, *Publications of the Astronomical Society of the Pacific*, 115, 143
- LaCluyzé A. et al., 2004, *AJ*, 127, 1653
- Landolt, A. U. 1992, *AJ*, 104, 340
- Layden, A. C. 1994, *AJ*, 108, 1016
- Le Borgne, J. F., Paschke, A., Vandebroere, J., et al. 2007, *A&A*, 476, 307
- Le Borgne, J.-F., Klotz, A., Poretti, E., et al. 2012, *AJ*, 144, 39
- Le Borgne, J. F., Poretti, E., Klotz, A., et al. 2014, *MNRAS*, 441, 1435
- Lee, Y.-W. 1989, Ph.D. thesis, Yale University
- Lee, Y.-W., & Demarque, P. 1990, *ApJS*, 73, 709
- Lee, Y.-W., Demarque, P., & Zinn, R. 1990, *ApJ*, 350, 155
- Lee, J.-W., & Carney, B. W. 1999, *AJ*, 118, 1373
- Lee, K. M., & Schmidt, E. G. 2001, *Publications of the Astronomical Society of the Pacific*, 113, 1140
- Lee, J.-W., López-Morales, M., Hong, K., et al. 2014, *ApJS*, 210, 6
- Lenz P., Breger M., 2004, *Comm. Ast.*, 146, 53
- Liu T., Janes K.A., 1990, *AJ*, 354, 273
- Lub, J. 1977, *A&AS*, 29, 345
- Maintz, G. 2012, *BAV Rundbrief - Mitteilungsblatt der Berliner Arbeits-gemeinschaft fuer Veraenderliche Sterne*, 61, 83
- Martin, W. C. 1938, *Annalen van de Sterrewacht te Leiden*, 17, 1
- McNamara, D. H., & Barnes, J. 2014, *AJ*, 147, 31
- Metcalf, T. S., Brown, T. M., & Christensen-Dalsgaard, J. 2004, *SOHO 14 Helio- and Asteroseis-mology: Towards a Golden Future*, 559, 567
- Miceli, A., Rest, A., Stubbs, C. W., et al. 2008, *ApJ*, 678, 865
- Mizerski, T. 2003, *Acta Astron.*, 53, 307

- Molnár, L., & Szabados, L. 2014, MNRAS, 442, 3222
- Molnár, L., Benkő, J. M., Szabó, R., & Kolláth, Z. 2014b, “*Kepler RR Lyrae stars: beyond period doubling*”, IAU Symposium, 301, 459
- Morgan, S. M., Simet, M., & Bargerquast, S. 1998, Acta Astron., 48, 341
- Morgan, S. M., Wahl, J. N., & Wieckhorst, R. M. 2007, MNRAS, 374, 1421
- Moskalik, P. 1986, Acta Astron., 36, 333
- Moskalik, P. 2013, “*Multi-periodic Oscillations in Cepheids and RR Lyrae-Type Stars*”, Stellar Pulsations: Impact of New Instrumentation and New Insights, 31, 103 (arXiv:1208.4246)
- Moskalik, P. 2014, “*Multi-mode oscillations in classical Cepheids and RR Lyrae-type stars*”, IAU Symposium, 301, 249
- Moskalik, P., & Buchler, J. R. 1990, ApJ, 355, 590
- Moskalik, P., & Poretti, E. 2003, A&A, 398, 213
- Moskalik, P., Smolec, R., Kolenberg, K., et al. 2013, in: J.C. Suárez, R. Garrido, L.A. Balona, & J. Christensen-Dalsgaard (eds.), “*Discovery of Peculiar Double-Mode Pulsations and Period Doubling in KEPLER RRc Variables*”, Stellar Pulsations: Impact of New instrumentation and New Insights, Astrophysics and Space Sci. Proc., Vol. 31 (Berlin, heidelberg: Springer-Verlag), Poster No. 34 (arXiv:1208.4251)
- Motl, D. 2009, C-MuniPack, <http://c-munipack.sourceforge.net/>
- Mucciarelli, A., Lovisi, L., Lanzoni, B., & Ferraro, F. R. 2014, ApJ, 786, 14
- Nagy, A. 1998, A&A, 339, 440
- Nemec, J. M. 2004, AJ, 127, 2185
- Nemec, J. M., Smolec, R., Benkő, J. M., et al. 2011, MNRAS, 417, 1022
- Nemec, J. M., Cohen, J. G., Ripepi, V., et al. 2013, ApJ, 773, 181
- Olech, A., Kaluzny, J., Thompson, I. B., et al. 1999, AJ, 118, 442
- Olech, A., & Moskalik, P. 2009, a&A, 494, L17
- Oosterhoff, P. T. 1939, The Observatory, 62, 104
- Oosterhoff, P. T. 1944, Bulletin of the Astronomical Institutes of the Netherlands, 10, 55
- Oosterhoff, P. T. 1946, Bulletin of the Astronomical Institutes of the Netherlands, 10, 101
- Peña, J. H., Arellano Ferro, A., Peña Miller, R., Sareyan, J. P., & Álvarez, M. 2009, Revista Mexicana de Astronomía y Astrofísica, 45, 191
- Petersen, J. O. 1984, A&A, 139, 496
- Pickering, E. C., & Bailey, S. I. 1895, ApJ, 2, 321
- Pickering, E. C. 1901, Astronomische Nachrichten, 154, 423

- Pietrinferni, A., Cassisi, S., Salaris, M., & Castelli, F. 2004, ApJ, 612, 168
- Pietrinferni, A., Cassisi, S., Salaris, M., & Castelli, F. 2006, ApJ, 642, 797
- Pojmanski, G. 1997, Acta Astron., 47, 467
- Pojmanski, G. 2001, “*The All Sky Automated Survey (ASAS-3) System - Its Operation and Preliminary Data*”, IAU Colloq. 183: Small Telescope Astronomy on Global Scales, 246, 53
- Pojmanski, G. 2002, Acta Astron., 52, 397
- Pollacco, D. L., Skillen, I., Collier Cameron, A., et al. 2006, Publications of the Astronomical Society of the Pacific, 118, 1407
- Preston, G.W., 1959, ApJ, 130, 507
- Preston, G. W., Krzeminski, W., Smak, J., & Williams, J. A. 1963, ApJ, 137, 401
- Reimers, D. 1975, Memoires of the Societe Royale des Sciences de Liege, 8, 369
- Renzini, A. 1983, MmSAI, 54, 335
- Ritter, A. 1879, Ann. Phys. Chem. Neue Folge, 8, 157
- Samus N. N. et al., 2012, CDS, B/gcvs (ver. Feb. 2012)
- Sandage, A. 1990, ApJ, 350, 603
- Sandage, A. 1993, AJ, 106, 687
- Sandage, A., Katem, B., & Sandage, M. 1981, ApJS, 46, 41
- Sandage, A. 1981, ApJ, 248, 161
- Sandage, A. 2004, AJ, 128, 858
- Sandage, A. 2006, AJ, 131, 1750
- Sandage, A. 2010, ApJ, 722, 79
- Sandage, A., & Cacciari, C. 1990, ApJ, 350, 645
- Schlegel, D. J., Finkbeiner, D. P., & Davis, M. 1998, ApJ, 500, 525
- Schwarzenberg-Czerny, 1996, ApJ, 460, L107
- Schwarzschild, M. 1940, Harvard College Observatory Circular, 437, 1
- Shapley, H. 1914, ApJ, 40, 448
- Shapley, H. 1916, ApJ, 43, 217
- Searle, L., & Zinn, R. 1978, ApJ, 225, 357
- Shibahashi, H. 2000, “*The Oblique Pulsator Model for the Blazhko Effect in RR Lyrae Stars. Theory of Amplitude Modulation I.*”, IAU Colloq. 176: The Impact of Large-Scale Surveys on Pulsating Star Research, 203, 299

- Simon, N. R. 1988, ApJ, 328, 747
- Simon, N. R., & Lee, A. S. 1981, ApJ, 248, 291
- Simon, N. R., & Teays, T. J. 1982, ApJ, 261, 586
- Simon, N. R., & Aikawa, T. 1986, ApJ, 304, 249
- Simon, N. R., Clement, C. M. 1993, ApJ, 410, 526
- Skarka, M. 2013, A&A, 549, AA101
- Skarka, M. 2014a, A&A, 562, AA90
- Skarka, M. 2014b, “*The BlaSGalF database*”, Precision Asteroseismology, Proceedings of the International Astronomical Union, IAU Symposium, 301, 485
- Skarka, M. 2014c, MNRAS, 445, 1584
- Skarka, M., & Zejda, M. 2013, MNRAS, 428, 1442
- Skarka, M., & Cagaš, P. 2013, Information Bulletin on Variable Stars, 6068, 1
- Skarka, M., Hoňková, K., & Juryšek, J. 2013, Information Bulletin on Variable Stars, 6051, 1
- Smith, H. A. 1995, “*RR Lyrae stars*”, Cambridge Astrophysics Series, 27, Cambridge University Press
- Smith, H. A. 2013, arXiv:1310.0533
- Smith, H. A., Catelan, M., & Kuehn, C. 2011, “*RR Lyrae Period-Amplitude Diagrams: From Bailey to Today*”, RR Lyrae Stars, Metal-Poor Stars, and the Galaxy, 17
- Smolec, R. 2005, Acta Astron., 55, 59
- Smolec, R., & Moskalik, P. 2008, Acta Astron., 58, 193
- Smolec, R., Moskalik, P., Kolenberg, K., et al. 2011, MNRAS, 414, 2950
- Smolec, R., Soszyński, I., Moskalik, P., et al. 2013, “*First Detection of Period Doubling in a BL Herculis Type Star: Observations and Theoretical Models*”, Stellar Pulsations: Impact of New Instrumentation and New Insights, 31, 85
- Sódor, Á. 2007b, Astronomische Nachrichten, 328, 829
- Sódor, Á., & Jurcsik, J. 2005, Information Bulletin on Variable Stars, 5641, 1
- Sódor, Á., & Wils, P. 2005, Information Bulletin on Variable Stars, 5655
- Sódor, Á., Vida, K., Jurcsik, J., et al. 2006, Information Bulletin on Variable Stars, 5705, 1
- Sódor, Á., Szeidl, B., & Jurcsik, J. 2007, A&A, 469, 1033
- Sódor, Á., Jurcsik, J., Szeidl, B., et al. 2011, MNRAS, 411, 1585
- Sódor, Á., Jurcsik, J., Molnár, L., et al. 2012, “*First Results of the Konkoly Blazhko Survey II*”, Progress in Solar/Stellar Physics with Helio- and Asteroseismology, 462, 228

- Soszyński, I., Udalski, A., Szymański, M., et al. 2003, *Acta Astron.*, 53, 93
- Soszyński, I., Udalski, A., Szymański, M. K., et al. 2009, *Acta Astron.*, 59, 1
- Soszyński, I., Udalski, A., Szymański, M. K., et al. 2010, *Acta Astron.*, 60, 165
- Soszyński, I., Dziembowski, W. A., Udalski, A., et al. 2011, *Acta Astron.*, 61, 1
- Soszyński, I., Dziembowski, W. A., Udalski, A., et al. 2014, *Acta Astron.*, 64, 1
- Srdoc, G., & Bernhard, K. 2012, *BAV Rundbrief - Mitteilungsblatt der Berliner Arbeitsgemeinschaft fuer Veraenderliche Sterne*, 61, 29
- Stellingwerf, R. F., Nemeč, J. M., & Moskalik, P. 2013, “*The Kepler RR Lyrae SC data set: Period variation and Blazhko effect*”, in *proceedings to 40 Years of Variable Stars: A celebration of contributions by horace A. Smith*, online book, arXiv:1310.0543
- Stetson, P. B. 1987, *Publications of the Astronomical Society of the Pacific*, 99, 191
- Stothers, R. 1980, *Publications of the Astronomical Society of the Pacific*, 92, 475
- Stothers, R. B. 2006, *ApJ*, 652, 643
- Stothers, R. B. 2010, *Publications of the Astronomical Society of the Pacific*, 122, 536
- Strohmeier, W., & Knigge, R. 1961, *Astronomische Nachrichten*, 286, 133
- Suntzeff, N. B., Kraft, R. P., & Kinman, T. D. 1994, *ApJS*, 93, 271
- Sweigart, A. V., & Renzini, A. 1979, *A&A*, 71, 66
- Sweigart, A. V. 1987, *ApJS*, 65, 95
- Szabó, R., Kolláth, Z., & Buchler, J. R. 2004, *A&A*, 425, 627
- Szabó, R., Kolláth, Z., Molnár, L., et al. 2010, *MNRAS*, 409, 1244
- Szabó, R., Benkő, J. M., Paparó, M., et al. 2014, arXiv:1408.0653
- Szczygieł, D. M., & Fabrycky, D. C. 2007, *MNRAS*, 377, 1263
- Szczygieł, D. M., Pojmański, G., & Pilecki, B. 2009, *Acta Astron.*, 59, 137
- Szeidl, B. 1976, “*Multiple Periodic RR Lyrae Stars: Observational Review*”, *IAU Colloq. 29: Multiple Periodic Variable Stars*, 60, 133
- Szeidl, B. 1988, *Multimode Stellar Pulsations*, 45
- Szeidl, B., & Jurcsik, J. 2009, *Communications in Asteroseismology*, 160, 17
- Szeidl, B., Hurta, Z., Jurcsik, J., Clement, C., & Lovas, M. 2011, *MNRAS*, 411, 1744
- Szymański, M. 2005, *Acta Astron.*, 55, 43
- Udalski, A., Kubiak, M., & Szymański, M. 1997, *Acta Astron.*, 47, 319
- van Albada, T. S., & Baker, N. 1973, *ApJ*, 185, 477

- Vanderbroere, J., Le Borgne, J.-F., & Boninsegna, R. 2014, GEOS circular on RR Type variable, 53, http://www.micosmos.net/geos/circ/RR_53.pdf
- Walker, A. R. 1998, AJ, 116, 220
- Walker, A. R., & Nemec, J. M. 1996, AJ, 112, 2026
- Warner, B. D. 2007, Minor Planet Bulletin, 34, 113
- Watson, C. L., Henden, A. A., & Price, A. 2006, “*The International Variable Star Index (VSX)*”, 25th Annual Symposium, The Society for Astronomical Sciences, 47W
- Wils, P., & Sódor, Á. 2005, Information Bulletin on Variable Stars, 5655, 1
- Wils, P., Lloyd, C., & Bernhard, K. 2006, MNRAS, 368, 1757
- Wils P. et al., 2008, MNRAS, 387, 783
- Wozniak P.R. et al., 2004, AJ, 127, 2436
- Wunder, E. 1990, BAV Rundbrief - Mitteilungsblatt der Berliner Arbeits-gemeinschaft fuer Ver-aenderliche Sterne, 39, 9
- Zhevakin, S. A. 1953, Russ. Astron. J. 30, 161
- Zinn, R., & West, M. J. 1984, ApJS, 55, 45

List of publications

Refereed papers

- Skarka, M. 2013, *Known Galactic field Blazhko stars*, A&A, 549, A101
- Skarka, M., & Zejda, M. 2013, *Photometric study of the star with changing Blazhko effect: TV Bootis*, MNRAS, 428, 1442
- Skarka, M., Hoňková, K., & Juryšek, J. 2013, *First result of the Czech RR Lyrae Stars Observation Project - a new Blazhko star CN Cam*, Information Bulletin on Variable Stars, 6051, 1
- Skarka, M., & Cagaš, P. 2013, *CzeV283 and CzeV397 - new RR Lyrae stars showing Blazhko effect*, Information Bulletin on Variable Stars, 6068, 1
- Krtička, J., Janík, J., Marková, H., Mikulášek, Z., Zverko, J., Prvák, M., Skarka, M. 2013, *Ultraviolet and visual flux and line variations of one of the least variable Bp stars HD 64740*, A&A, 556, A18
- Liška, J., & Skarka, M. 2013, *Discovery of a new periodic variable star CzeV 503*, Information Bulletin on Variable Stars, 6077, 1
- Skarka, M. 2014, *Bright Blazhko RRab Lyrae stars observed by ASAS and the SuperWASP surveys*, A&A, 562, A90
- Paunzen, E., Skarka, M., Holdsworth, D. L., Smalley, B., & West, R. G. 2014, *HD 54272, a classical lambda Bootis star and gamma Doradus pulsator*, MNRAS, 440, 1020
- Skarka, M. 2014, *Characteristics of bright ab-type RR Lyrae stars from the ASAS and WASP surveys*, MNRAS, 445, 1584

Conference proceedings and unrefereed papers

- Brát, L., Šmelcer, L., Kučáková, H., et al. 2008, *B.R.N.O. Times of minima*, Open European Journal on Variable Stars, 94, 1
- Wolf, M., Zejda, M., Mikulášek, Z. et al. 2010, *NSVS 0165 3195 Ser: A New Low-Mass Binary*, in proceedings of the conference Binaries - Key to Comprehension of the Universe, Astronomical Society of the Pacific, 435, 441
- Skarka, M. 2011, *Blazhko effect - a century old challenge*, in Proceedings of the 42nd Conference on Variable Stars Research, Open European Journal on Variable Stars, 139, 4

- Skarka, M. 2012, *Blazhko effect and RR Lyrae type stars - light curve analysis*, in Proceedings of the 43rd Conference on Variable Stars Research, Open European Journal on Variable Stars, 154, 1
- Skarka, M. 2013, *Physical parameters of RR Lyrae type stars DH Peg and UY Cam*, in Proceedings to Stellar pulsation: New instrumentation and new insights, vol. 31. 2013 (poster)
- Skarka, M. 2014, *The BlaSGalF database*, IAU Symposium, 301, 485 (poster)
- Hladík, B., Skarka, M., Liška, J. 2014, *A new delta scuti variable CzeV616 Cyg*, Open European Journal on Variable Stars, 166, 1
- Skarka, M., Liška, J., Šmelcer, L., Brát, L. 2014, *Variable star and exoplanet section of the Czech astronomical society*, in proceedings of the conference Living together: Planets, Host stars and Binaries, submitted (poster)
- Skarka, M., Liška, J., Dřevěný, R., Auer, R. F. 2014, *Observing RR Lyrae stars*, in proceedings of the 46th conference on Variable Stars Research, submitted
- Skarka, M. 2014, *Blazhko effect at the time of Kepler*, in proceedings of the 46th conference on Variable Stars Research, submitted

List of abbreviations

2MASS	Two Micron All Sky Survey
AM	amplitude modulation
ASAS	All Sky Automated Survey
BlaSGalF	Blazhko Stars of Galactic Field
CDS	Centre de Données astronomiques de Strasbourg
CG	Caretta-Gratton scale
CRRLSOP	Czech RR Lyrae Observation Project
FM	frequency modulation
GB	Galactic bulge
GC	globular cluster
GCVS	General Catalogue of Variable Stars
GEOS	Groupe Européen d'Observations Stellaires
GSC	Guide Star Catalogue
HB	horizontal branch
HIF	half-integer frequency
HJD	heliocentric Julian date
HRD	Hertzprung-Russel diagram
IS	instability strip
KIC	Kepler Input Catalogue
LC	light curve
LINEAR	Lincoln Near-Earth Asteroid research
LMC	Large Magellanic Cloud
MACHO	MAssive Compact Halo Objects
MORP	Magnetic Obligue Rotator/Pulsator
MUO	Masaryk University Observatory
NRRP	non-radial resonant rotator
NSVS	North Sky Variability Survey
OGLE	Optical Gravitational Lensing Experiment
OoI,II,III	Oosterhoff I,II,III group
PD	period doubling
PM	phase modulation
RGB	red giant branch
RT	rise time
SMC	Small Magellanic Cloud
S/N	signal to noise ratio
SuperWASP	Super Wide Angle Search for Planets
TAROT	Télescopes à Action Rapide pour les Objets Transitoires
USNO	US Naval Observatory
VSX	Variable Star indeX
ZAHB	zero age horizontal branch
ZW	Zinn-West scale

